SIGNIFICANT CONTRIBUTION ASSESSMENT OF HEAVY METAL CONTAMINATED RIVER SEDIMENT DUE TO HEAVY METAL MIGRATION BY SOIL EROSION IN A REMOTE WATERSHED

Mr. Komsoon Somprasong

A Dissertation Submitted in Partial Fulfillment of the Requirements

for the Degree of Doctor of Philosophy Program in Environmental Management

(Interdisciplinary Program)

Graduate School

Chulalongkorn University

Academic Year 2014

การประเมินนัยสำคัญของปัจจัยที่มีต่อการปนเปื้อนโลหะหนักในตะกอนลำน้ำอันเนื่องจากการกัดเซาะผิวดินสำหรับพื้นที่ลุ่มน้ำที่ยากแก่การเข้าถึง

นายคมสูรย์ สมประสงค์

Thesis Title	SIGNIFICANT CONTRIBUTION ASSESSMENT OF HEAVY METAL CONTAMINATED RIVER SEDIMENT DUE TO HEAVY METAL MIGRATION BY SOIL EROSION IN A REMOTE WATERSHED
By	Mr. Komsoon Somprasong
Field of Study	Environmental Management
Thesis Advisor	Dr.Pichet Chaiwiwatworakul, Ph.D.
Thesis Co-Advisor	Dr.Thongthit Chayakula, Ph.D.
	Assistant Professor Dr. Srilert Chotpantarat, Ph.D.

Accepted by the Graduate School, Chulalongkorn University in Partial Fulfillment of the Requirements for the Doctoral Degree

-------------------------------- Dean of the Graduate School
(Associate Professor Ph.D. Sunait Chutintaranond)

THESIS COMMITTEE

-------------------------------- Chairman
(Assistant Professor Ph. D. Chantra Tongcumpou)

-------------------------------- Thesis Advisor
(Dr.Pichet Chaiwiwatworakul, Ph.D.)

-------------------------------- Thesis Co-Advisor
(Dr.Thongthit Chayakula, Ph.D.)

-------------------------------- Thesis Co-Advisor
(Assistant Professor Dr. Srilert Chotpantarat, Ph.D.)

-------------------------------- Examiner
(Associate Professor Dr.. Chakkaphan Sutthirat, Ph.D.)

-------------------------------- Examiner
(Associate Professor Dr. Pisut Painmanakul, Ph.D.)

-------------------------------- External Examiner
(Dr. Somchai Chonwattana, Ph.D.)

คมสูรย์ สมประสงค์ : การประเมินนัยสำคัญของปัจจัยที่มีต่อการปนเปื้อนโลหะหนักในตะกอนลำน้ำอัน
เนื่องจากการกัดเซาะผิวดินสำหรับพื้นที่ลุ่มน้ำที่ยากแก่การเข้าถึง (SIGNIFICANT CONTRIBUTION
ASSESSMENT OF HEAVY METAL CONTAMINATED RIVER SEDIMENT DUE TO HEAVY
METAL MIGRATION BY SOIL EROSION IN A REMOTE WATERSHED) อ.ที่ปรึกษาวิทยานิพนธ์
หลัก: อ. ดร.พิเชฐ ชัยวิวัฒน์วรกุล, อ.ที่ปรึกษาวิทยานิพนธ์ร่วม: อ. ดร.ธงทิศ ฉายากุล, ผศ. ดร. ศรีเลิศ โชติ
พันธรัตน์, หน้า.

ลุ่มน้ำแม่ตาวเป็นลุ่มน้ำขนาดเล็ก มีที่ตั้งอยู่ในเขต อำเภอแม่สอด ประเทศไทย โดยมีลำน้ำแม่ตาว ซึ่งมีต้น
กำเนิด ณ ดอยแม่ตาว และดอยไร่ผาเป็นลำน้ำสายหลัก ลำน้ำแม่ตาวมีทิศทางการไหลผ่านบริเวณเหมืองแร่สังกะสี และที่
พักอาศัย โดยลำน้ำถูกระบุว่ามีการปนเปื้อนของโลหะหนัก จำพวกแคดเมียมโดยจากการตรวจสอบพบว่า มีค่าปนเปื้อน
ของโลหะแคดเมียม เกินกว่าระดับมาตรฐานที่ 5 มิลลิกรัมต่อลิตร อย่างไรก็ดี โดยธรรมชาติทางธรณีวิทยาของลุ่มแม่น้ำแม่
ตาว ยังมีศักยภาพในการเป็นต้นกำเนิดของการปนเปื้อนในลำน้ำแม่ตาวจากแร่ประกอบสังกะสีและแคดเมียมซึ่งจะเกิด
ร่วมกันในสายแร่ตามธรรมชาติได้ เพื่อเป็นการศึกษาเกี่ยวกับความเป็นไปได้ของการเป็นปัจจัยที่มีนัยสำคัญต่อการ
ปนเปื้อนจากธรรมชาติ จึงได้มีการออกแบบการศึกษาครั้งนี้ขึ้น โดยอาศัยการผสมผสานวิธีการประเมินเชิง
ประจักษ์ (Empirical estimation) ด้วยสมการการกัดเซาะ Revised Universal Soil Loss Equation (RUSLE) เข้ากับ
วิธีการประเมิน เชิงสมมติ (Hypothetical estimation) โดยอาศัยแบบจำลองทางชลศาสตร์ ด้วยโปรแกรม MIKE ซึ่งความ
เหมาะสมในการสร้างแบบจำลองคณิตศาสตร์ของการเคลื่อนที่ของตะกอนลำน้ำ และปริมาณน้ำหลากระหว่างการชะล้าง
หน้าดินได้ ในส่วนของการประเมินปริมาณตะกอนและสารปนเปื้อนจากน้ำหลากบริเวณหน้าดินของลุ่มน้ำแม่ตาว ได้จัด
ให้มีการสร้างแบบจำลองส่วนขยายเพิ่มเติมของการเคลื่อนที่ของตะกอนที่เกิดจากน้ำหลากผิวดินภายใต้ชื่อ Overland flow
Sediment Transport module (OfSET) ขึ้น โดยส่วนต่อขยายดังกล่าวมีความสามารถในการคำนวณปริมาณตะกอนที่เกิด
จากการกัดเซาะโดยน้ำหลากได้ ในการศึกษาครั้งนี้ จะใช้ค่านำเข้าในแบบจำลอง ทั้งแบบปฐมภูมิและทุติยภูมิ โดยค่าปฐม
ภูมิจะได้จากการวัดค่าจากพื้นที่ที่สามารถปฏิบัติงานได้โดยตรง สำหรับค่าทุติยภูมิจะได้จากการรวบรวมข้อมูลจากงานวิจัย
ที่เกี่ยวข้องและนำมาใช้งาน ผลการศึกษาในส่วนของการประเมินเชิงประจักษ์ แสดงให้เห็นว่าพื้นที่เหมืองแร่มี
ความสามารถสูงที่สุดในการปลดปล่อยแคดเมียม เท่ากับ 1.854 ± 0.088 ตันต่อเฮคเตอร์ต่อปี ในขณะที่การประเมินเชิง
สมมติพบว่าโลหะแคดเมียมที่พัดพากับตะกอนตามลำน้ำแม่ตาวมีค่าเท่ากับ 21.93 กิโลกรัมและ 0.51 กิโลกรัม ในฤดูน้ำ
หลากและฤดูฝนตามลำดับ ในขณะเดียวกันสำหรับตะกอนแคดเมียมที่ถูกพัดพามากับน้ำหลากผิวดิน มีค่าเท่ากับ 8.36
กิโลกรัม ในฤดูน้ำหลาก และ 0.08 กิโลกรัม ซึ่งค่าการประเมินดังกล่าวแสดงให้เห็นว่า แหล่งแร่ธรรมชาติในบริเวณลุ่มน้ำ
แม่ตาวเป็นปัจจัยที่มีนัยสำคัญต่อปริมาณการปนเปื้อนของโลหะหนักในลำน้ำโดยเฉพาะอย่างยิ่งในฤดูน้ำหลากที่มีค่า
ประเมินของสัดส่วนแคดเมียมจากการกัดเซาะผิวดิน เท่ากับ 38.12%

สาขาวิชา การจัดการสิ่งแวดล้อม	ลายมือชื่อนิสิต ....
ปีการศึกษา 2557	ลายมือชื่อ อ.ที่ปรึกษาหลัก ....
	ลายมือชื่อ อ.ที่ปรึกษาร่วม ....
	ลายมือชื่อ อ.ที่ปรึกษาร่วม ....

5387758120 : MAJOR ENVIRONMENTAL MANAGEMENT

KEYWORDS: CADMIUM / CONTAMINATION / SOIL EROSION / HYDROLOGY MODEL

KOMSOON SOMPRASONG: SIGNIFICANT CONTRIBUTION ASSESSMENT OF HEAVY METAL CONTAMINATED RIVER SEDIMENT DUE TO HEAVY METAL MIGRATION BY SOIL EROSION IN A REMOTE WATERSHED. ADVISOR: DR.PICHET CHAIWIWATWORAKUL, Ph.D., CO-ADVISOR: DR.THONGTHIT CHAYAKULA, Ph.D., ASST. PROF. DR. SRILERT CHOTPANTARAT, Ph.D., pp.

The Mae Tao Basin is a small basin located in Mae Sot, Thailand. The Mae Tao Creeks is a main branch belongs to the basin, originates at Doi Mae Tao and Doi Rei Pha. The Creeks has the flow direction pass through the mining production area and residential area. The Creeks has been claimed as a cadmium contamination site, which is certified to be higher than the acceptable level at 5.0 mg/L in water. Due to the geological characteristic of the area that is the deposition area of zinc-composite mineral, there are some possibilities that the natural erosion by the flood during the wet season can wash down the small particles with high concentration of zinc and cadmium into the Mae Tao Creeks. According to this information, the study has been set up and aimed to clarify the possibility that geological characteristic of the basin can contribute to the concentration of cadmium. The study has been set up by applying the combination between empirical study based on Revised Universal Soil Loss Equation (RUSLE) and a hypothetical estimation using hydrological model name as MIKE which has a capability to simulate the phenomena of the water especially overland flow in basin scale and the remote sensing technique. In order to evaluate the potential of geological characteristic of the area as a contributor for contaminated particles and sediments, new external modules named as Overland flow Sediment Transport module (OfSET) was developed. This development can enhance the capability of the program from simulating only the sediment transport via channel flow, to be capable to simulation the migration of cohesive contaminated particles through the overland flow over the surface area of the Mae Tao Basin. The model input, applied in this study come from both primary and secondary sources. Direct field observations were conduct in the available area of the basin, while some in the remote area were represented by the secondary value from literatures review. As a result of empirical estimation, mining production area demonstrates the highest potential in releasing cadmium contamination flux due to erosion at 1.854 ± 0.088 t/ha/y. For the hypothetical estimation, total cadmium flux in stream sediment, transported by the Mae Tao Creeks, is equal to 21.93 kg and 0.51 kg during wet and dry season of 2012-2013 respectively. Additionally, cadmium transported via overland sediment are equal to 8.36 kg and 0.08 kg in wet and dry season. These simulated values indicate that the natural zinc- cadmium deposition in the Mae Tao Basin is one of the contributions of cadmium contamination in the Mae Tao Creeks with the highest contribution at 38.12% in wet season.

Field of Study: Environmental Management   Student's Signature ....

Academic Year: 2014   Advisor's Signature ....

                                                Co-Advisor's Signature ....

                                                Co-Advisor's Signature ....

ACKNOWLEDGEMENTS

CONTENTS

List of Tables

List of Figures

CHAPTER 1

Introduction

1.1 Introduction

Cadmium, a hazardous heavy metal, has been concerned in terms of its toxicity affecting to the environment. It mainly exists inform of cadmium sulfide in association with zinc especially in zinc treatment processes (National Toxicology Program, 2011). Its toxicity can accumulate in plants and transfer from plant to animal or human, consuming those contaminated plants.

Cadmium, as one of heavy metals, can be transported though environmental phases by trapping with sediments and bound back into water system, and their accumulation are dominated by physical-chemical properties of the sediment. The solubility of heavy metal into water phase is depended on water chemical properties such as pH, chelating agents, redox conditions and, salinity (Arnason J. G. and Fletcher B. A., 2003; Jain C.K., 2014; Chen C.W. et al., 2007; Yunus K., 2011).

In addition, cadmium is very fatal to humans due to its longevity and accumulation. Long term exposure of cadmium via contaminated food can cause chronic known as Itai-Itai with a form of osteomalacia and proximal tubular renal dysfunction Acute effects can cause edema, headaches, nausea, vomiting, chills, weakness, and diarrhea (Nogawa K. and Kido T., 1993).

The Mae Tao Basin, Thailand's largest zinc deposit is located in Mae Sot district, Tak province. Zinc mines in this area have been continuously operated by several companies over the past 30 years (Tharathammathigorn W., 2010). As a byproduct in zinc industries, cadmium contamination can be occurred in the production area for example, drilling material transfer, disposal of mine tailings and drainage (Unhalekhaka U. and Kositanont C., 2008). During 1998-2003, the International Water Management Institute and Department of Agricultural (DOA) reported the high value of cadmium levels in paddy fields and rice at Ban Pateh and Ban Mae Tao Mai, Pratat Padaeng sub-district, Mae Tao district Tak province (Simmons R.W. et al., 2005). (Akkajit P. and Tongcumpou C., 2010; Phaenark C. et al., 2009)

For agricultural area, 95% of rice was found to contaminate with cadmium which the levels exceeding the standard of Codex Committee on Food Additives and Contaminants; CCFAC, 1972 (Codex Alimentarius Commission 2002). For the cadmium concentrations of soil samples utilizing water via irrigation from the Mae Tao Creek, were in the range of 61-207 mg/kg which exceeded the soil standard of European Economic Community (3 mg/kg).

The cadmium transport and the contamination level in the Mae Tao Creeks, a single water resource of the Mae Tao Basin have been studied. As, cadmium has gradually accumulated in stream sediment and the community's public irrigation system uses water from the creeks, the distribution of the contaminant has spread through all the rice fields (Nichanon K., 2005). Moreover, the natural pH of the water in the study area is about 7.91-8.44 (Karoonmakphol P. and Chaiwiwatworakul P., 2010; Maneewong P., 2005; Tharathammathigorn W., 2010) that means cadmium is not in a soluble form.

Although the studies involving the contamination status of the Mae Tao Basin has been continuously accomplished but few of them concerned and investigated the potential of the natural zinc deposit as one of the contributors of cadmium in the Mae Tao Basin. According to those studies, they can be implied that some of cadmium contaminants are exposed from the cadmium deposited in association with zinc in natural deposition by surface runoff and contaminated the creeks as the suspended sediment.

Erosion due to rainfall upstream of the creeks was found to be one of the major mechanics that make cadmium available for transport to the downstream. However, mining procedures and the mine area management have also been blamed for contributing to the problem (Pollution Control Department (PCD), 2009).

Erosion associated with overland flow from highlands may be the intermediate transport mechanism that reinforces the spread of hazardous substances leaching into area soil. Therefore, the erosion rate of the basin was estimated to determine its cadmium contribution potential in the study area.

For many years, environmentalists try to create the best explanation for the erosion and sediment transport over the soil surface, in order to provide the appropriate management and policy. Various method and equation (such as fractionation, C-14 detection) has been applied to demonstrate the behavior of the sediment. However,

most contaminated areas contain some difficulties in both field observation and sampling procedure and some of them are unreachable area which can caused unpleasant conditions in simulation. Besides, some difficulties in the simulation of sediment transport over the soil surface or overland flow are occurred when the analyst take an effort to proof the source of heavy metal over the inspected area.

According to those difficulties and limitations in the assessment of heavy metal-contaminated sediment transport in the overland flow, some integrated techniques should be applied to enhance the capability of field observation and simulation. This study aims to provide the alternative procedure to diminish those difficulties in contaminated-sediment transport assessment.

This study aims to determine the possibility and the potential of natural zinc deposit as one of the main contributors of cadmium contamination in the Mae Tao basin. To determine this possibility of the geological characteristic of the area as the contributors of the cadmium contamination in the Mae Tao Basin, remote sensing technique was assigned in order to gather necessary information from the area. Information, obtained from the area, was sent to the GIS program and hydrological program named as MIKE-SHE to create the module for simulating the migration of cadmium by the activity of the overland flow phenomena in the Mae Tao Basin.

1.2 Objective

- To provide the heavy metal assessment method for remote watershed, that can be applied to other similar heavy metal contaminated area.

1.2.1 Sub-objectives:

- o Create the soil profile of the study area using integrated GIS method.
- o Create the erosion potential map for contaminated- remote area based on empirical erosion model.
- o Develop the integrated hydrologic model which is applicable for the monitoring of cohesive sediment particles and suspended sediment in overland flow.
- o Develop the assessment frame work for the study area.

1.3 Hypothesis

Geological characteristic of the area which is the natural-deposition of zinc-composite mineral has been one of the contributors of cadmium- contamination in the pilot area.

1.4 Scope of the study

- The estimation of erosion by overland flow during raining incidents of the Mae Tao Basin Thailand.
    - Estimation of the erosion potential of the Mae Tao basin, which is based on empirical model named as Revised Universal Soil Loss Equation (RUSLE).
    - Estimation of the erosion potential of the Mae Tao Basin which is based on the hypothetical model named as Overland flow Sediment Transport Module (OfSET).
- The estimation, using Revised Universal Soil Loss Equation (RUSLE), is operated by retrieving required parameters (Rainfall intensity (R), Supported land practice (P), Soil erodibility (K), Cover practice (P), Slope and steepness (LS) in form of secondary data from government sectors, private sector and literature review from both online articles and documents.
- The satellite photo from LANDSATS(TM) is analyzed by NDVI analysis for pre calculation of K factor in RUSLE estimation.
- Geographic Information System (GIS) are applied as the main tool in calculating RUSLE and potential flux from erosion layer.
- MIKE11 and MIKE SHE are used as based software in hypothetical model estimation.
    - MIKE11 is used to simulate the hydrodynamic property and the sediment transport of the Mae Tao Creeks.
    - MIKE SHE is used to simulate the flow incident of water in the Mae Tao Basin.
- Topography, metrological data, properties of the saturated zone and unsaturated zone data for model were reviewed from the government sectors.

- Bed load and suspended sediment samples were collected and analyzed to determine the characteristic of the sediment from both the wet and dry seasons.

- The bed load and suspended sediment were collected by compositing and analyzed triplicate at the laboratory.

- The analysis focuses on total cadmium accumulated in bed load and suspended sediment.

- Station MT 01 was assigned as downstream boundary condition.

- The water level at station MT 04 had been record daily recorded for model verification

- Overland flow depth and Overland flow in X and Y directions from MIKE SHE simulation were used as the input in OfSET

- The Cadmium fluxes from the simulations were analyzed to retrieve the final result.

1.5 Expected Outcome

1. The empirical result of potential cadmium flux from erosion of the Mae Tao Basin area.

2. The accumulate cadmium transfer values due to the cohesive sediment transport in the overland flow over the Mae Tao Basin are quantified.

3. The accumulate cadmium transfer values due to sediment transport in the Mae Tao creeks are quantified.

4. The significant contributor of the cadmium contamination is assessed based on the result from the sediment transportation simulation.

CHAPTER 2

Literature review

2.1 Study area

2.1.1 Boundary

The Mae Tao Basin is located in Mae Sot district, Tak province. Mae Sot consists of 10 sub-districts, namely, Mae Sot, Mae Ku, Phawo, Mae Tao, Mae Kasa, Tha Sai Luat, Mahawan, Dan Mae La Mao, and Pratat Padaeng. The basin covers 59.61 km^2, from 47N 457000 1839000 to 47N 458000 184800 (WGS 1984 UTM Zone 47N). The basin contains mining production areas, crop fields, and residential areas. The active mine is operated by Padaeng Industry Public Company Limited while the abandoned mine is the property of Tak Mining Company Limited (Karoonmakphol P, 2009).The location of the Mae Tao Basin is demonstrated in Figure 2-1 . The studied area is in the western part of Tak province. This area has a high rainfalls potential because of the monsoon. Tak's climates consist of 3 seasons: summer (February to mid-May), rainy (mid-May to October), and winter (October to February) (Pollution Control Department (PCD), 2011)
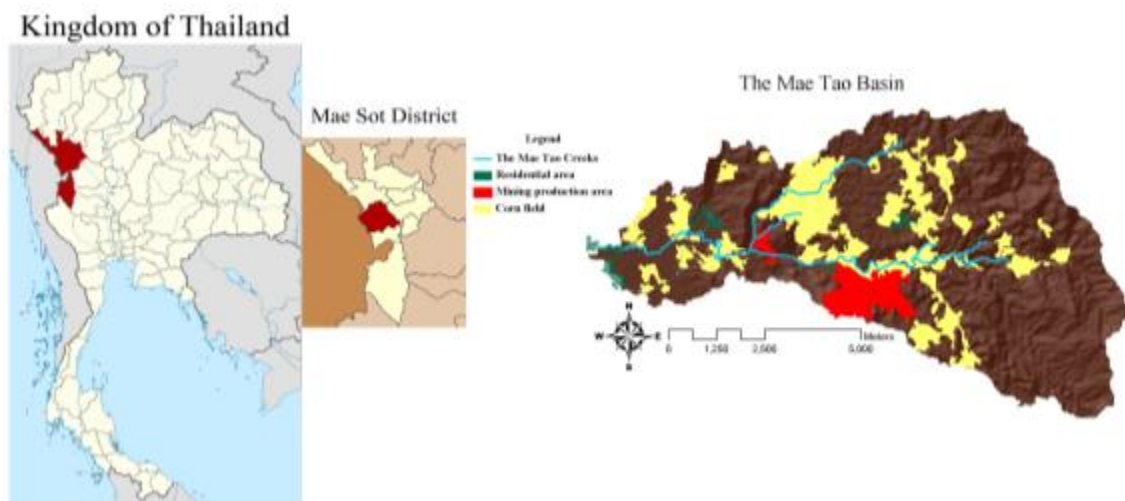
Figure 2-1 The location of the Mae Tao Basin, Mae Sot district, Tak province, Thailand

2.1.2 Hydrology and Climates

The Mae Tao Creeks consists of three main branches which are the Main Mae Tao, the Mae Tao Right and the Mae Tao Left. The creek is a stream with continued flow in the self-formed dendritic pattern throughout the year; however: it contains low rate of water flow and is shallow in some sections during the dry season. The flow direction is from east to west passing through zinc deposits area with a total distance of 33 kilometers of the riverhead to Moei River. The grain size particle in water is classified as gravelly sand. The stream has a height bank about 1.5 to 2.0 meters and an average width about 3.0 to 4.0 meters. The depth of Mae Tao Creek is about 0.15 to 0.20 meters in the dry season, and 1.0 to 1.2 meters in the wet season. Average amount of water is 16.3 million cubic meters per year. The lowest average minimum flow is about 7,499 cubic meters in December while the average maximum flow is about 5.6 million cubic meters in August (Mahidol University, 2006)

2.1.3 Land utilization

According to the Department of Primary Industries and Mines, under the Ministry of Industry, the land use of Mae Sot can be classified into five major categories (Department of Primary Industries and Mines (DPIM), 2009).

2.1.3.1 Deciduous forest area:

is located in the north-eastern and eastern part of the study area. Most of the area is belong to the national forest area. The area is covered with mixed deciduous forest and underlain by sandy loams or lateritic soil with low fertility, resulting in the existence of dwarfed trees. Several areas are encroached that resulting in deforestation and some remediated area.

2.1.3.2 Agricultural area:

is abundantly located in the western area of the Mae Tao Basin which is the largest type of land use in the area. Most of the agricultural area is rice paddy field and these filed utilized the water from rainfall and the Mae Tao Creek for

irrigation. Furthermore other economic plant, such as soybeans and corn, are substituted during dry season.

2.1.3.3 Urban and residential area:

There are some Karen's residential area, locating at in Ban Mae Tao Mai (western part), Ban Thum Suea (north part), Ban Nong Khiao (southeast part), Ban Pateh (northwest part), and a few area of Ban Mae Ku Nuea (southwest part).

2.1.3.4 Public area:

Roads, creeks and reservoirs. The roads are divided into concrete roads, laterite roads and local ground road.

2.1.3.5 Mining production area:

The mining production area consists of zinc mine and its derivative operation including ore processing area and discharge area.

Table 2-1 Land use around zinc mines area (Thamjesda T., 2012)

Land use	Area (m^2)				
	Zone A	Zone B	Zone C	Zone D	
	within 0-5 kilometers downstream mining	within 5-10 kilometers downstream mining	greater than 10 kilometers downstream mining	upstream and within mining	Total
Forest	2,907,743	749,060	3,320,631	13,516,819	20,494,253
Agriculture	18,763,074	21,004,936	8,689,164	7,369,610	55,826,784
Residential area	2,288,958	2,874,886	1,269,381	46,141	6,479,366
Public land	336,100	300,298	982,095	145,492	1,763,985
Mine	-	-	-	3,921,938	3,921,938
Industry	704,126	70,820	738,729	-	1,513,675

2.2 Background of the study area

During 1940s, the Department of Mineral Resources discovered the outcrop and of zinc resource at Doi Padaeng, Mae Tao Sub-district, Mae Sot district, Tak province. In 1969-1975, Thai Zinc Company Limited surveyed and developed the zinc mine, obtaining about 150,000 tons of zinc ore, and shut down at a later time. The area had been abandoned for 6 years and was taken over by Padaeng Industry Public Company Limited in 1981. In 1985, Tak Mining Company Limited was granted the concession for mining in a relative area until now. (Pollution Control Department (PCD), 2011)

Padaeng Industry Public Company Limited has obtained the rights for 6 concession blocks from the Department of Mineral Resources since 1982. Four of these were expired and the other 2 concession blocks are still in operation, which will be expired in 2017 and 2023 (Department of Primary Industries and Mines (DPIM), 2009)

Tak mining Company Limited has been granted 5 concession blocks in both surface and underground mining operations. Even though Tak Mining Company Limited has shut down mining activities since 2003, the company still operates to take out zinc ore from the rock gaps and sell it to Padaeng Industry Public Company Limited (Department of Primary Industries and Mines (DPIM), 2009) For the environment impact assessment, Padaeng Industry Public Company Limited conducts and submits report to the office of Natural Resources and Environmental Policy and Planning (ONEP) and other agencies every 6 months. Tak Mining Company Limited chose to stop mining activities so the conduction of the environmental impact assessment report has not been continued. However, environmental management of Tak Mining Company Limited was not sufficient during the non-production period that might affect the environment due to the abandonment of mining pit and sediment pounds. According to the study, three major causes of contamination could be identified as: (1) rainfall flowing through mining area, (2) settling ponds near the creek, and (3) flooding of erosive mine drifts (Pollution Control Department (PCD), 2011).

2.3 Mineralogy of Zinc and cadmium composite

 2.3.1 Zinc

  2.3.1.1 Zinc and its properties

   Zinc is a chemical element with symbol Zn. This element is commonly found as zinc ore such as sphalerite , smithsonite , hemimorphite , wurtzite (another zinc sulfide), and hydrozincite. Zinc is a bluish-white, lustrous, and has less dense than iron. It has a hexagonal crystal structure; with a distorted form of hexagonal close packing.

   Zinc is normally occurred in association with other base metals such as copper and lead in ores due to geologic condition. This element is a chalcophile, which refers to the element that has a low affinity for oxides and prefers to bond with sulfides. Chalcophiles formed as the crust solidified under the reducing conditions of the early Earth's atmosphere.

   Zinc naturally occurs in air, water and soil, but the raising of zinc concentrations are depended on the addition of zinc through human activities. Most zinc concentration has been increased during industrial activities, such as mining, coal and waste combustion and steel processing. Some soils in the zinc mining production area are heavily contaminated with zinc. Additionally zinc can be detected in the sewage sludge from industrial areas and fertilizer.

   Most zinc is utilized in galvanizing with other metals, such as iron in order to prevent rusting. Galvanized steel is used for car bodies, street lamp posts, safety barriers and suspension bridges. Large quantities of zinc are material in die-castings, which are important in the automobile, electrical and hardware industries. Zinc also takes and important role in alloy manufacturing such as brass, nickel silver and aluminum solder. Zinc oxide is widely used in the manufacture of many products such as paints, rubber, cosmetics, pharmaceuticals, plastics, and electrical equipment

2.3.2 Cadmium

2.3.2.1 Cadmium and its properties

Cadmium (Cd) is a soft, ductile, silver-white metal that associated with zinc and copper, and lead ores. It has the low melting (320.9 ºC) and boiling (765 ºC) points and high vapor pressure. This element cannot be found independently the nature, but it associated with the sulfide ores of zinc, lead and copper. Some of them are byproducts and tailing from the zinc industry (WHO, 2014) .

Cadmium naturally presents in the environment in association with zinc ore. Utilization of cadmium using was firstly in paint pigment, dental amalgams, and substitute for tin after discovering in 1817. Nevertheless, most of the utilization have been applied in nickel-cadmium batteries, pigments, alloy electroplating and coating, and stabilizers in plastics(IARC, 1993; National Toxicology Program, 2011; T.O., 1994).

Cadmium has an ability to accumulate in plants, animal and human, but can create the poisonous effect only in animal and human due to longevity and organ accumulation after eating plants. The chronic effect in human from long term contamination of cadmium is known as Itai-Itai. This disease is a form of osteomalacia and proximal tubular renal dysfunction (Honda R. , 2010). The acute effect produced them suffering from pulmonary edema, headaches, nausea, vomiting, chills, weakness, and diarrhea (Nogawa K. and Kido T., 1993). Cadmium exists in nature in various inorganic forms. In air, cadmium vapor is instantly oxidized to be cadmium oxide. Cadmium vapor is produced to be another compound such as cadmium carbonate, cadmium hydroxide, cadmium sulfite, cadmium sulfate and cadmium chloride when reacts to carbon dioxide, water vapor, sulfur dioxide, sulfur trioxide and hydrogen chloride, respectively. Moreover, the transform compounds can be accumulated and discharged to the environment. In water, cadmium consists of two forms that are water-soluble form (Cd^{2+}) and water-insoluble form (cadmium sulfide, cadmium carbonate, cadmium oxide). However, cadmium in insoluble form can be changed to a soluble form when water quality in nature changes such as water pH (Thamjesda T., 2012).

2.3.2.2 Cadmium contamination source

Cadmium can be exposed to environment from 2 sources which are natural sources and anthropogenic sources (International Cadmium Association (ICDA), 2009).

2.3.2.2.1 Natural sources

The primary natural source of cadmium is volcanic eruption and continuous low-level activity. The amount of natural cadmium accumulation is different attributable to the origin of mineral composite and rock formation (International Programme on Chemistry Safety (IPCS) 1992) .

2.3.2.2.2 Anthropogenic sources

Human activities are the greater source of cadmium contamination. Anthropogenic sources consist of many activities such as industry activity, fossil fuel combustion, fertilizer application, sewage sludge, municipal incineration, landfill, traffic and transport. In relation to industrial activity, cadmium sources can be divided into 3 sources (Oil Spill Prevention Administration and Response (OSPAR) Commission 2002) which are

- Primary production sources: metallurgic process such as non-ferrous industry (mining, smelting and refining of zinc, lead and copper ores), meting and pouring of cadmium element, and iron and steel industry.

- Secondary production sources: manufacture and disposal of cadmium containing products such as nickel-cadmium battery, solar cell, alloy and electronic compound, pigment and coloring agent, stabilizer, coating.

- Recycling production sources: cadmium recycling plants.

2.3.3 Cadmium contamination and distribution in the environment

According to previous section, human activities are claimed to be the major source of cadmium contaminations in the environment; especially the emission from manufacturing of industry, mining overflow and mineral gangue, disposal of cadmium containing wastes. These give the emphasis to the distribution of cadmium into the environment soil to water, water to atmosphere, atmosphere to soil, soil to atmosphere and etc. Using of wastes or contaminated byproducts can directly and widely raise the impacts. A cycle of cadmium distribution is shown in Figure 2-2.
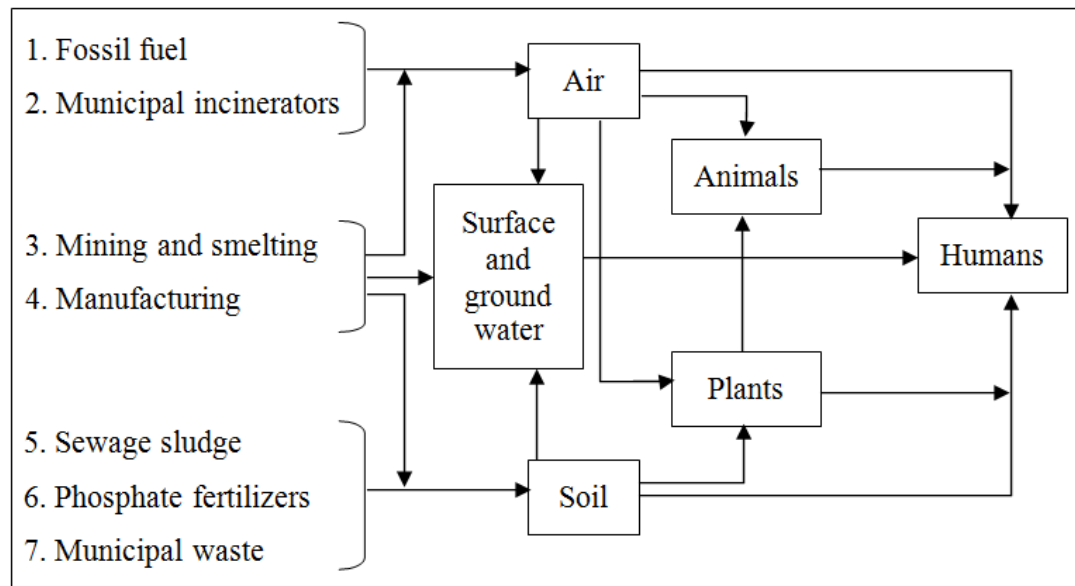
Figure 2-2 Cadmium contamination cycle and its distribution (Thamjesda T., 2012)

2.3.4 Cadmium and regulation

Cadmium can be detected in every environmental phases. The standards of cadmium concentration in nature are established by various organizations as shown in Table 2-2 to Table 2-3. Cadmium concentrations in air, water and soil are under the Hazardous Substances Acts of B.E. 2535 (1992). Furthermore, European Economic Community (European Economic Commission (EEC)) established the soil quality standard. Maximum levels for cadmium in water are complied with in the surface water quality standard and groundwater quality standard according to the Notification of the National Environmental Board No. 8, B.E. 2537 (1994) and the Notification of the National Environmental Board No. 20, B.E. 2543 (2000), respectively (Pollution Control Department (PCD), 2009). For the standard of cadmium concentration in food, the standard issued by the Codex Committee on Food Additives and Contaminants (Codex Alimentarius Commission 2002) and the joint FAO/WHO Expert Committee on Food Additives (Joint FAO/WHO Expert Committee on Food Additives (JECFA) 2003) are applied.

Table 2-2 Standard of cadmium concentration in the environment

Substances	Cadmium Concentration Permission	References
Air Quality Standards		
- Air emission	1 mg/m^3	PCD, 1998
- Dust in working area	0.2 mg/m^3	
- Dust in working area (maximum level)	0.6 mg/m^3	
- Fume in working area	0.1 mg/m^3	
- Fume in working area (maximum level)	3 mg/m^3	
- Emission from infected waste incinerator	0.05 mg/m^3	PCD, 2009
Water Quality Standards		
- Surface water: Hardness ≤ 100 mg/L of CaCo$_3$	0.005 mg/L	PCD, 2009
: Hardness > 100 mg/L of CaCo$_3$	0.05 mg/L	
- Groundwater	0.003 mg/L	
- Groundwater for drinking purposes	0-10 mg/m^3	
- Drinking water	0-10 mg/m^3	
- Bottled drinking water	5 mg/m^3	
- Water for aquatic living	1 mg/m^3	
- Industrial effluent	0.03 mg/m^3	
- Discharged water into irrigation system	30 mg/m^3	
- Discharged water into deep wells	100 mg/m^3	
- Zinc smelter effluent	100 mg/m^3	PCD, 1998
Soil Quality Standards		
- Soil for habitat and agriculture	37 mg/kg	PCD, 2009
- Soil for other purposes	810 mg/kg	
- Sludge amended soil for agriculture	1.0-3.0 mg/kg	EEC, 1986
- Agricultural soil	3.0 mg/kg	NEPC, 1999

(Pollution Control Department (PCD), 2011; Pollution Control Department (PCD), 2009),(European Economic Commission (EEC), 1986),(NEPC, 1999)

Table 2-3 Standard of cadmium concentration in the environment (continued)

Substances	Cadmium Concentration Permission	References
- Agricultural soil	1.4 mg/kg	Canadian Council of Ministers of the Environment, 2002
- Agricultural soil (Vietnam standard)	2.0 mg/kg	Simmons *et al.*, 2008
Food Quality Standards		
- Rice grain	0.2 mg/kg	CCFAC, 2002
- Milled Rice (Codex & Japanese)	0.4 mg/kg	JECFA, 2005
Aquatic animal Quality Standards		
- Fish and fishery: CAC, WHO/FAO	1.00 mg/kg	PCD, 2011
: TPHR, Australia	5.50 mg/kg	
: NHMRC, Australia	2.00 mg/kg	
: FDA, USA	2.00 mg/kg	
: EU	0.10-1.00 mg/kg	
: Japan	1.00 mg/kg	
: India	3.00 mg/kg	
- Sea fish (Czech Republic)	0.20 mg/kg	
- Fresh water fish (Czech Republic)	0.10 mg/kg	
- Molluscs (Czech Republic)	1.00 mg/kg	
- Crustaceans and gastropods (Czech Republic)	0.50 mg/kg	
Health Perspective		
- Provisional Tolerable Weekly Intake (PTWI)	7 µg/kg body weight/week	JECFA, 2003

(Pollution Control Department (PCD), 2011; Pollution Control Department (PCD), 2009), (Simmons R.W. et al., 2008; CCME, 2002), (Joint FAO/WHO Expert Committee on Food Additives (JECFA) 2005; Joint FAO/WHO Expert Committee on Food Additives (JECFA) 2003; Codex Alimentarius Commission 2002)

Cadmium is classified as the third category of hazardous substances by Hazardous Substances Acts of B.E. 2535 (1992). The regulation and allowances standard are presented in Table 2-4.

Table 2-4 Cadmium concentration in Water and Soil Quality Standards under Thai environmental regulations (Pollution Control Department (PCD), 2009), (Thamjesda T., 2012)

Circumstances	Cadmium Standard Value	Unit
Surface Water Quality Standards		
• Hardness $\leq$ 100 mg/L of CaCo$_3$	5	mg/m^3
• Hardness > 100 mg/L of CaCo$_3$	50	mg/m^3
Coastal Water Quality Standards	5	mg/m^3
Groundwater Quality Standards	3	mg/m^3
Groundwater Quality Standards for Drinking Purposes	0-10	mg/m^3
Drinking Water Quality Standards	0-10	mg/m^3
Bottled Drinking Water Quality Standards	5	mg/m^3
Appropriated Water Quality Criteria for Aquatic Living	1	mg/m^3
Industrial Effluent Standards	30	mg/m^3
Water Characteristics Discharged into Irrigation System	30	mg/m^3
Water Characteristics Discharged into Deep Wells	100	mg/m^3
Soil Quality Standards for Habitat and Agriculture	37	mg/kg
Soil Quality Standards for Other Purposes	810	mg/kg

Cadmium contamination in Mae Tao creek where people are used for agricultural activities caused health effects in four dimensions. Impact on health, about 6,000 people living in eight villages of Phra That Pha Daeng and Mae Tao consumed the cadmium contaminated rice for a long time so the accumulation of cadmium is high in body and cause Itai-Itai (Nichanon K., 2005).

Impact on mental health, people with a high amount of cadmium accumulation suffered from cadmium disease, and worry about sending their children in high school because of non-occupation support (Thamjesda T., 2012). Impact on social, the prohibition of rice field changed the traditional of local people so this cultural traditional will disappear. Impact on spiritual experience, people is confident that the mining caused the health and environmental problem.

2.3.5 Mineralogy of Zinc and cadmium composite

Zinc and cadmium are naturally born in association with each other. In some mineral vein lead and other heavy metal can be found in a small proportion. The occurrence of zinc and cadmium deposition in the Mae Tao Basin can be separated into to two types which are

2.3.5.1 Primary Deposition

Primary deposition is the mineral deposition which is naturally occurred by the geological process under the earth crust. The mineral composite, mostly found in form of sulfite mineral such as Sphalerite (ZnS) and Galena (Pbs) are born naturally with associated mineral, contains other heavy metal such as Cadmium (Cd) Antimony (Presbitero A.L.) and Silver Julien P.Y. et al. (1995). Primary deposition can be narrowed down into two type of occurrence.

▪ **Vein-Type Deposits**: occurs when the hydrothermal fluids move through the surface from cooling intrusive rocks (magma charged with water, various acids, and metals in small amounts) via fractures, faults, brecciated rocks, porous layers and other channels (i.e. like a plumbing system) and chemically react with the country rock. The formation of new mineral take place when the fluids are directed through a structure where the temperature, pressure and other chemical conditions are favorable for the precipitation and deposition.

▪ **Replacement Deposits**: occurs when the excess hydrothermal fluids moves into the lenses or porosity of existing ore as a layer.

2.3.5.2 Secondary Deposition

Secondary deposition is the mineral deposition which is occurred near the soil surface due to the activity of groundwater. The leaching and oxidizing reaction near the mineral vein can produce new form of mineral especially oxide silicate and carbonate composite.

According to the report from Thai Pollution Control department, the zinc composite, mostly founded and operated in the Mae Tao basin is Hemimorephite $[Zn_4(Si_2O_7)(OH)_2 \cdot 2H_2O]$ and Zn_2SiO_4 which is a zinc-silicate mineral. However from the observation the existence of independent cadmium composite cannot be founded in both mining production area and the area nearby.

2.4 Contamination in the study area

According to the location of the two mine and flow direction, The Mae Tao Basin, together with the Mae Tao Creeks, has been reported on the situation of being contaminated by cadmium as show in Table 2-5 to Table 2-10.

Table 2-5 Summary of cadmium contamination in the Mae Tao Creeks

Institute/Researcher and study year	Study area/ Sample	Result of cadmium contamination
Padaeng Industry Public Company Limited, 1992–2002 and 2008-2009 (Padaeng Industry Public Company Limited, 2009)	During 1992-2002: The Mae Tao Creek: 5 stations located before entering zinc mine area to Mae Tao Mai During 2008-2009: - The Mae Tao Creek: 11 stations, Mae Ku Creek: 4 stations - Both dry and wet season	Most stations in the Mae Tao Creek exhibited that cadmium concentration in surface water were lower than 0.003 to 0.005 mg/L. In contrast, cadmium at releasing location of zinc mine was determined in the range of 0.05-0.10 mg/L **The Mae Tao Creek:** pH values of the water were slightly alkali, ranged from 6.94 to 8.37 in dry season and 7.33 to 8.56 in wet season. Observed cadmium concentrations from surface water were lower than 0.0001-0.0029 mg/L in dry season, and lower than 0.0001-0.0278 mg/L in wet season. **The Mae Ku Creek:** pH values were slightly, between 7.33 to 8.50 in dry season and 6.61to 8.40 in wet season. Total cadmium values were lower than 0.0001-0.0006 mg/L in dry season and lower than 0.0001-0.0046 mg/L in wet season. The results showed that all stations in the project area contained lower cadmium levels than the surface water quality standard.
Mahidol University, 2004 (Mahidol University, 2006)	The Mae Tao Creek: 8 stations, Mae Ku Creek: 2 stations, Mae Sot Creek: 1 control station Both dry (April 2004) and wet season (September 2004	pH value of the water ranged from 6.9 to 8.6 in the Mae Tao Creeks and the Mae Ku Creek, and 7.0-7.2 at the Mae Sot Creek. Cadmium concentrations from the first two crease ranged from 0.004 to 0.006 mg/L in dry season, and 0.0241 to 0.0318 mg/L in wet season. At the Mae Sot Creek, cadmium levels were 0.006 and 0.0241 in dry and wet season, respectively. Cadmium was less than the surface water quality standard in all stations. Cadmium in surface water may be influenced by fertilizer using, which may distribute cadmium into agricultural area and leach into water and became higher in its concentration during the wet season.

Table 2-6 Summary of cadmium contamination in the Mae Tao Creeks (cont.)

Institute/Researcher and study year	Study area/ Sample	Result of cadmium contamination
Maneewong, 2005 (Maneewong P., 2005)	The Mae Tao Creek, the Mae Ku Creek, and Nong Khiao Creek (control station)	Surface water's pH varied in a range of 7 to 8.5. Cadmium level was very low and complied with the surface water quality standard (less than 0.005 mg/L).
Krissanakriangkrai, 2006 (Krissanakriangkrai O., 2007)	The Mae Tao Creek: 9 stations at upstream to downstream of mining area for 10 km. - Both dry and wet season	Average cadmium concentration was0.5 µg/L and 2.16 µg/L in dry and wet season, respectively. For dry season, cadmium contamination did not exhibit the differences for sampling stations at upstream and downstream of mining area, while in the wet season, the cadmium-distributions was significantly higher than the dry season, but still less than the standard.
Padaeng Industry Public Company Limited, 1992-2002 and 2008-2009 (Padaeng Industry Public Company Limited, 2009)	During 1999: shallow wells: 3 stations During 2008-2009 (dry and wet season): shallow and deep wells - Around mining area - At mining area: before and after tailing storage basin, discharge of tailing storage basin	During 1999, pH values ranged from 7.2 to 7.6, and the total cadmium values ranged from lower than 0.001 to 0.001 mg/L. At mining area, the water pH values were between 6.74-7.67 in dry season and 6.87 to 7.78 in wet season. The cadmium level were lower than 0.0001-0.0034 mg/L in dry season and lower than 0.0001-0.0310 mg/L in wet season. Cadmium in wet season was higher than groundwater quality standard for drinking.

Table 2-7 Summary of cadmium contamination in the Mae Tao Creeks (cont.)

Institute/Researcher and study year	Study area/ Sample	Result of cadmium contamination
IWMI-DOA, 1998-2000 and 2001-2003 (Simmons R.W. et al., 2005)	(Somboon P., 1999) - During 1998-2003: paddy field area near Ban Pateh (154 plots) - During 2001-2003: paddy field near Mae Tao Creek (434 plots)	Total cadmium concentrations in soil were determined to be higher than EU standard (3 mg/kg) for 94 times and 72 times during 1998-2002 and 2001-2003, respectively.
Somboon, 1999 Somboon P., 1999)	Upstream and downstream areas located in the same watershed with zinc mine, and nearby area outside the watershed boundary	Total cadmium was exhibited at 50.84 mg/kg, which was higher than that in the upstream and the area nearby. The cadmium concentration exeeded the soil quality standard in downstream while the other two study areas were lower. The average cadmium concentrations at 3 study area differed from the soil quality standard at the statistically significantly level of 0.05.
Simmons, 2001-2003 (Simmons et al., 2008)	Pratat Padaeng and Mae Tao Mai sub-districts - During 2001-2002: 308 soil samples at 0-20 cm. depth levels During 2003:20 fields	During 2001-2002, cadmium concentration observed from soil samples were verified at the range of 0.59 to 217 mg/kg with the average of 26.2 mg/kg and 89% of total soil samples exceeded the standard of 3.0 mg/kg. Comparing with the Thai Investigation Level of cadmium, 0.15 mg/kg (Zarcinas, 2004), total soil exceeded this standard. During 2003, cadmium concentrations in 20 soil sampleswere detected at the average of 36.7 mg/kg. Only 2 samples complied with the soil quality standard of EU.

Table 2-8 Literature reviews of cadmium contamination in the Mae Tao Creeks (cont.)

Institute/Researcher and study year	Study area/ Sample	Result of cadmium contamination
Department of Primary Industries and Mines, 2003-2004 (DPIM, 2006)	Pratat Padaeng, Mae Tao and Mae Ku sub-district - soil sampling at every depth levels of 20 cm. for 1-2 m.	Soil contained cadmium lower than 1-9 mg/kg at depth level of 1 m. A high terrain and colluviums on western region contained the cadmium concentration ranged from 1 to 430 mg/kg. The samples from agricultural area on the western region contained cadmium between 1 to 101 mg/kg.
Mahidol University, 2004 (Mahidol University, 2006)	Soil samples at depth level of 0-30 cm (10 stations): 8 stations at impact area and 2 stations at near zinc deposit area.	pH values of the soil ranged from 6.2 to 8.0. The concentration of cadmium were detected to be between no detection (ND) to 136.13 mg/kg except the downstream of discharge point of Padaeng Industry Public Company Limited was higher than 37.0 mg/kg.
Department of Mineral Resources, 2004-2005 (Pollution Control Department (PCD), 2011)	The Mae Tao Creek and TheMae Ku Creek: 184 stations	Shallow soil samples contained cadmium concentrations between 0.3to 192.3 mg/kg while the soil samples around road contained high cadmium concentrations between 159 to 1,027 mg/kg.
Sriprachot, 2006 (Sriprachot A., 2006)	Shallow soil: every 200 m. for 1 km2 at Ban Pateh - deep soil: at lowland/highland of Mae Tao Creek (right/left side) - control soil: at paddy field for 7 km. from northern of Ban Pateh	Soil contained cadmium concentration between 23 to 27 mg/kg. The results of soil analysis exhibited that soil, received water from the Mae Tao Creek and contained higher concentration of cadmium than the others. The cadmium contaminated was low at more depth levels of soil and was highest at depth levels of 0-20 centimeters by immediately decreasing at depth levels of 20-40 cm.

Table 2-9 Summary of cadmium contamination in the Mae Tao Creeks (cont.)

Institute/Researcher and study year	Study area/ Sample	Result of cadmium contamination
Phaenark, 2006-2007 (Phaenark, 2009)	Padaeng Industry Public Company Limited and Ban Pateh - tailing pond area, open pit area, stockpile area, forest area, and cadmium contaminated rice field.	Soil pH values were between 7.1 to 7.6. Total cadmium concentrations were in the range of 64-1,458 mg/kg. The total cadmium concentrations at each station were 596 mg/kg in tailing pond area, 543 in mg/kg open pit area, 894 mg/kg in stockpile area, 1,458 mg/kg in forest area, and 64 mg/kg in cadmium contaminated rice field.
Akkajit, 2007 (Akkajit and Tongcumpou, 2010)	Downstream of Padaeng Industry Public Company Limited - 81 soil samples at 30 cm depth level	Cadmium concentrations, detected in soil sample were in the range of 0.73 to 172.7 mg/kg, with the average concentration of 15.14 mg/kg. In comparison with the soil quality standard for sludge-amended soil of European Union (0.3 mg/kg) 50% of 81 soil samples complied with the standard.
Pollution Control Department, 2010 (PCD, 2011)	Soil in agricultural area that received water from Mae Tao Creek and Mae Ku Creek - 16,500 samples at depth levels of 0-30 cm., and 481 samples at depth level of 30-60, 60-120, 120-180 cm.	Cadmium concentration level in soil at 0-30 cm. was ranged between 0.5 to 338 mg/kg. 25 sample from agricultural area, where were not received water from the Mae Tao Creek and the Mae Ku Creek, contained cadmium concentrations between 0.5 to 3.96 mg/kg. 8 The highest cadmium concentrations in soil obtained from Ban Mae Ku Nuea and the Mae Ku Creek for 32 mg/kg and 21 mg/kg, respectively. 93% of 161 soil samples at 60-120 cm. depth level contained cadmium concentrations lower than 0.05 mg/kg.

Table 2-10 Summary of cadmium contamination in the Mae Tao Creeks (cont.)

Institute/Researcher and study year	Study area/ Sample	Result of cadmium contamination
Pollution Control Department, 2010 (PCD, 2011)	Mae Tao Creek, Mae Ku, Nong Nam Kaew, Huay Muang, drain block of Padaeng Industry Public Company Limited - 220 stations with 224 samples: 220 shallow sediment, 4 deep sediment at 30 cm depth level	The cadmium concentrations in sediment were the average of 5.71 mg/kg. At the Mae Tao Creek, cadmium concentration was lower than 1 mg/kg at upstream far from the mine, and was 13.9 mg/kg from tailing storage basin of Padaeng Industry Public Company Limited to Moei river. At the Mae Ku Creek, the cadmium concentration at east before the mining boundary was determined to be less than 1 mg/kg while at south of mine contained higher concentration within the range of 2.6 to 9.8 mg/kg. At small hill at east of Ban Mae Ku Nuea contained the cadmium level with 52.8 mg/kg and came down at downstream of the Mae Ku Creek as 0.7 mg/kg.
Thamjesda T. ,2012	Mae Tao Creek - 10 stations with suspended sediment and bed load samples - Both dry (April) and wet season (October)	Cadmium contaminated of the sediment transportation in the Mae Tao Creek is mainly generated in the wet season, and was dominated by suspended sediment transport. The amount of cadmium transported out of the Mae Tao Creek was approximately 16.33 kg in the wet season with 16.20 kg and in the dry season with 0.13 kg

According to the studies, related to the study area, cadmium contamination in the nearby area of the Mae Tao Creeks has been reported, but the detail of the study are almost related to the condition of the area such as the contamination level of suspended sediment and bed load or the contamination state of the agricultural area and soil which were exceed the acceptable for the standard, related to cadmium allowance. The summary of the cadmium contamination, compared to Thai and existing standard, are listed in Table 2-11.

Table 2-11 Summary of cadmium contaminated assessment from literature review

Sample	Cadmium concentration	Existing standards
Water	0.0001-0.1 mg/L	≤ 0.05 mg/L (Thai Water quality Standard)
Soil	0.1-1,458 mg/kg	≤ 37 mg/kg (Thai Soil Quality Standard for Residential and Agricultural area)
Sediment	<1-1,350 mg/kg	≤ 3.5 mg/kg (Probable Effect Levels standard: Canada)
Rice	0.02-7.75 mg/kg	≤ 0.2 kg/kg (Codex Standard)

2.5 Microwave digestion (EPA 3015A, 3051A and 3052)

Microwave sample preparation provides an efficient and clean sample preparation for multi-element analytical techniques such as ICP-OES and ICP-MS. This method is the most versatile and has been well proven. It allows variations in reagents and methodology, making it ideal for a variety of matrices and elements.

This method is provided as a rapid multi-element, microwave assisted acid digestion prior to analysis protocol so that decisions can be made about the site or material. Digests and alternative procedures produced by the method are suitable for analysis by flame atomic absorption spectrometry (FLAA), cold vapor atomic absorption spectrometry (CVAA), graphite furnace atomic absorption spectrometry (GFAA), inductively coupled plasma atomic emission spectrometry (ICPAES),

coupled plasma mass spectrometry (ICP-MS) and other analytical elemental analysis techniques where applicable.

Due to the rapid advances in microwave technology, consult your manufacturer's recommended instructions for guidance on their microwave digestion system and refer to this manual's "Disclaimer" when conducting analyses using Method 3015A, 3051A and 3052.

Table 2-12 Comparison between EPA's microwave disgestion method

Method	3015A	3051A	3052
Title	Microwave assisted acid digestion of aqueous samples and extracts	Microwave assisted acid digestion of sediments, sludge, soils, and oils	Microwave assisted acid digestion of siliceous and organically based matrices
Result	Perform extraction using microwave heating with nitric acid, or alternatively, nitric acid and hydrochloric acid. This method is not intended to accomplish total decomposition of the sample.	Perform extraction using microwave heating with nitric acid, or alternatively, nitric acid and hydrochloric acid. This method is not intended to accomplish total decomposition of the sample.	Total sample decomposition for general use with judicious choice of acid combinations.
Typical Samples	Aqueous samples, drinking water, mobility-procedure extracts, wastes that contain suspended solids	Sediments, sludge, soils and oils	Ashes, biological tissues, oils, oil contaminated soils, sediments, sludge and soils
Elements	Ag, Al, As, B, Ba, Be, Ca, Cd, Co, Cr, Cu, Fe, Hg, K, Mg, Mn, Mo, Na, Ni, Pb, Sb, Se, Sr, Tl, V, Zn		

2.6 Atomic spectroscopy analysis

Atomic spectroscopy is the technique for determining the elemental composition of an analyte by its electromagnetic or mass spectrum. Several analytical techniques are available, and selecting the most appropriate one is the key to achieving accurate real-world results. Proper selection requires a basic understanding of each technique due to its individual strengths and limitations. Atomic spectroscopy can be divided by atomization source and spectroscopy type.

In this study, Grafite Furnace Atomic Absorbtion Spectroscopy (GFAAS) and Flame Atomic Absorbtion Spectrometry (FLAAS) were applied as the analyser for sediment and bed load sample.

2.6.1 Graphite furnace atomic absorption spectrometry

Graphite furnace atomic absorption spectrometry is a type of spectrometry utilizing a graphite-coated furnace to vaporize the sample. Theoritically, the technique is based on the circumstance that free atoms will absorb light at unique frequencies or wavelengths of interested element.Within the limited capability, the amount of light absorbed can be linearly correlated to the concentration of analyte present. Free atoms of most elements can be produced from samples by the application of high temperatures.

In GFAAS, samples are held in small graphite or pyrolytic carbon coated graphite tube, and then be heated to vaporize and atomize the analyte. It can raise the temperatures as high as 3000 °C, and then the heated graphite furnace provides thermal energy to break chemical bonds within the sample and produce free ground-state atoms. The atoms absorb ultraviolet or visible light and make transitions to higher electronic energy levels. Ground-state atoms are capable of absorbing energy and are elevated to an excited state. The amount of light energy absorbed increases as the concentration of the selected element increases Concentration measurements are usually determined from a working curve after calibrating the instrument with standards of known concentration. Figure 2-3 demonstrates a simplr diagram of the GFASS' working components.
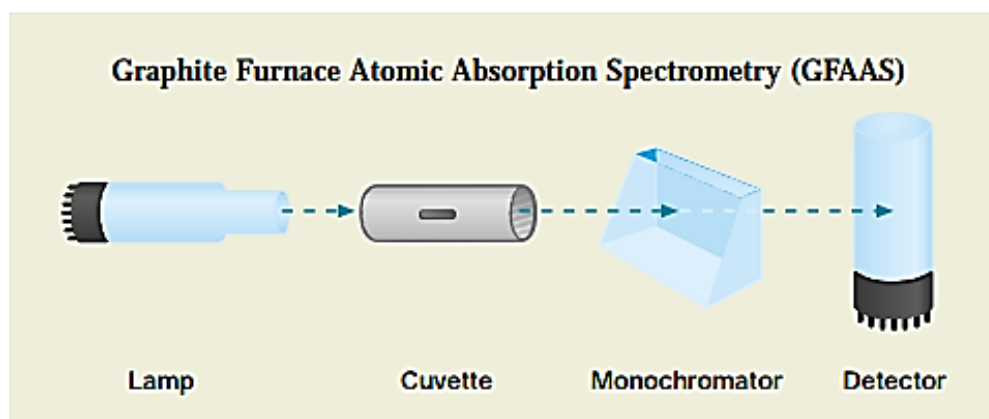
Figure 2-3 Basic components of GFAAS

2.6.2 Flame atomic absorption spectrometry (FLAAS)

Flame atomic absorption spectrometry is a quantitative analytical method based on measuring the light absorption of free, ground state atoms. The ground state atoms are excited by electromagnetic radiation (light), while absorbing photons having equivalent wavelength with the excitation energy. The absorption spectrum of atoms (similarly to emission spectrum) is line spectrum. The lines are present at exactly determined wavelengthes and they have a very small, approximately 0,001 nm FWHM (full widht at half maximum).

This type of absorption spectrum of atoms gives the high selectivity of atomic absorption spectrometry. At the best line of a given element the probability of absorption of other elements is very low thus complex systems containing several elements can be analyzed without the separation of elements. This procedure has great adventage to molecule absorption spectrometry methods where there is a higher probabilty of optical interfering effect due to the band absorption and usually the analysis of complex systems is possible only after the application of separation techniques. Figure 2-4 demonstrates the simple components of FLAAS.
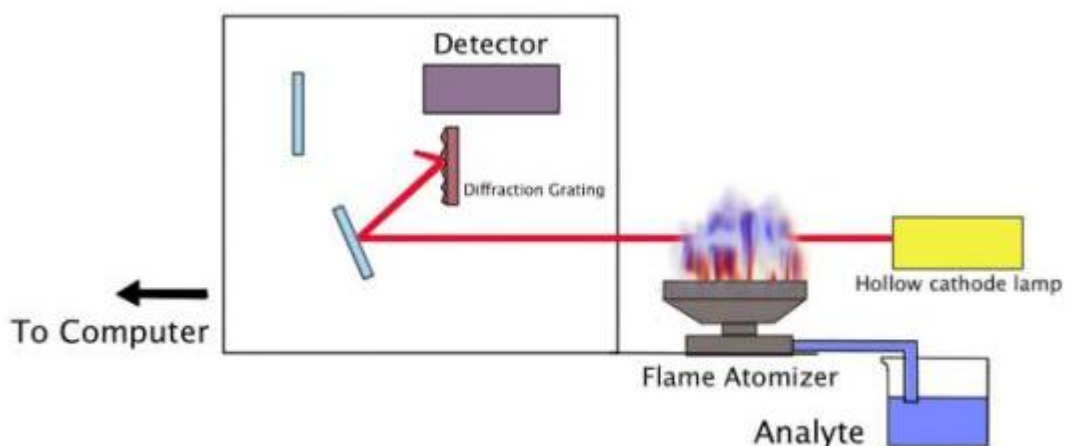
Figure 2-4 Basic components of FLAAS (Bryan G., 2012)

2.7 Erosion

Erosion geologically refers to the loss of mass from one location to another location upon the Earth's surface by exogenic processes (such as water flow or wind as a media). Despite the fact that erosion is a natural process, human activities can raise the erosion rate by 10-40 times at which erosion is occurring.

Water and wind are the two primary causes of erosion. Intensive agriculture, deforestation, roads, anthropogenic climate change and urban sprawl are the significant human activities which reinforce the number of erosion globally. However, there are many prevention and remediation practices that can curtail or limit erosion of vulnerable soils.

2.7.1 Erosion in the study area

Erosion due to rainfall upstream of the creeks was found to be one of the major mechanics that make cadmium available for transport to the downstream. However, mining procedures and the mine area management have also been blamed for contributing to the problem (Pollution Control Department (PCD), 2009). As cadmium has gradually accumulated in stream sediment and the community's public irrigation system uses water from the creeks, the distribution of the contaminant has spread through all the rice fields (Nichanon K., 2005).

Erosion associated with overland flow from highlands may be the intermediate transport mechanism that reinforces the spread of hazardous substances leaching into area soil. Therefore, the erosion rate of the basin was estimated to determine its cadmium contribution potential in the study area**.**

2.7.2 Soil erosion

Soil loss or soil erosion, represent the amount of soil moved from one particular area to another in the form of sediments yield. This phenomenon depends on the relationship between raindrops, runoff and the erodibility of the certain area.

The science of predicting soil erosion and sediment delivery has continued to be refined to reflect the importance of different factors on soil erosion and runoff. Enhancing the accuracy in estimating erosion and sediment delivery is also the advantages in minimizing pollution by sediments and the chemicals carried by those particles.

Revised Universal Soil Loss Equation (RUSLE) is a science-based equation, extended Universal Soil Loss Equation (USLE) has been developed over the last several years, and this equation provides an estimate of the severity of erosion in the form of quantifiable results by extending the term of cover management and support practice into the equation.

Since the result of the study area are almost related to the condition of the contamination among the Area of the Mae Tao Basin, the RUSLE will be assigned to use as the tool for predicting and simulating the incident, occurred by the runoff in this study. RUSLE is demonstrated in equation 2-1.

$$A = R \times K \times Ls \times C \times P \qquad (2\text{-}1)$$

Where:

A	=	Average annual soil loss in tons per acre per year
R	=	Rainfall/runoff erosivity
K	=	Soil erodibility
LS	=	Hill slope length and steepness
C	=	Cover-management
P	=	Support practice

The R factor is an expression of the erosivity of rainfall and runoff at a particular location. The value of "R" increases as the amount and intensity of rainfall increase.

The K factor is an expression of the inherent erodibility of the soil or surface material at a particular site under standard experimental conditions. This term is a function of the particle-size distribution, organic-matter content, structure, and permeability of the soil or surface material.

The LS factor is the term representing the effect of topography, specifically hillslope's length and steepness, on rates of soil loss at a particular site. This value increases when the value of hillslope's length and steepness increase, under the specific assumption that the runoff accumulates and accelerates in the downslope direction.

The C factor is an expression for the effects of surface covers and roughness, soil biomass, and soil-disturbing activities on rates of soil loss at a particular site. The value of "C" decreases when surface cover and soil biomass rose.

"C" refers to the effects of plants, soil cover, soil biomass, and soil disturbing activities on erosion. RUSLE uses a subfactor method to compute soil loss ratios, which are the ratios at any given time in a cover management sequence to soil loss from the unit plot. Soil loss ratios differ by time as canopy, ground cover, roughness, soil biomass and consolidation change. A "C" factor value is an average soil loss ratio weighted according to the distribution of R during the year.

Surface cover is material in contact with the soil surface that intercepts raindrops and slows surface runoff. The total percent of the surface covered is the characteristic used by RUSLE to compute how surface cover affects erosion.()

Roughness is, accounted in C value, reduced in RUSLE as a function of cumulative rainfall after the last tillage operation. Roughness also indicates the degree of clodiness and the likelihood that the surface will seal, producing increased runoff and soil erodibility. Accounting for roughness, such as with the plow plant tillage system, is one reason some C values are lower with RUSLE.

If a C factor of 0.15 represents the specified cropping management system, it signifies that the erosion will be reduced to 15 percent of the amount that would have occured under continuous fallow conditions.

The P factor refers of the effects of supporting conservation practices, such as contouring and buffer strips of cover vegetation on soil loss at a particular site. The value of "P" decreases with the installation of these practices because the reduction of

runoff volume and velocity and encourage the deposition of sediment on the hillslope surface.

Figure 2-5 exhibits the source of the data and observation practice that will be count into RUSLE's term and calculation.
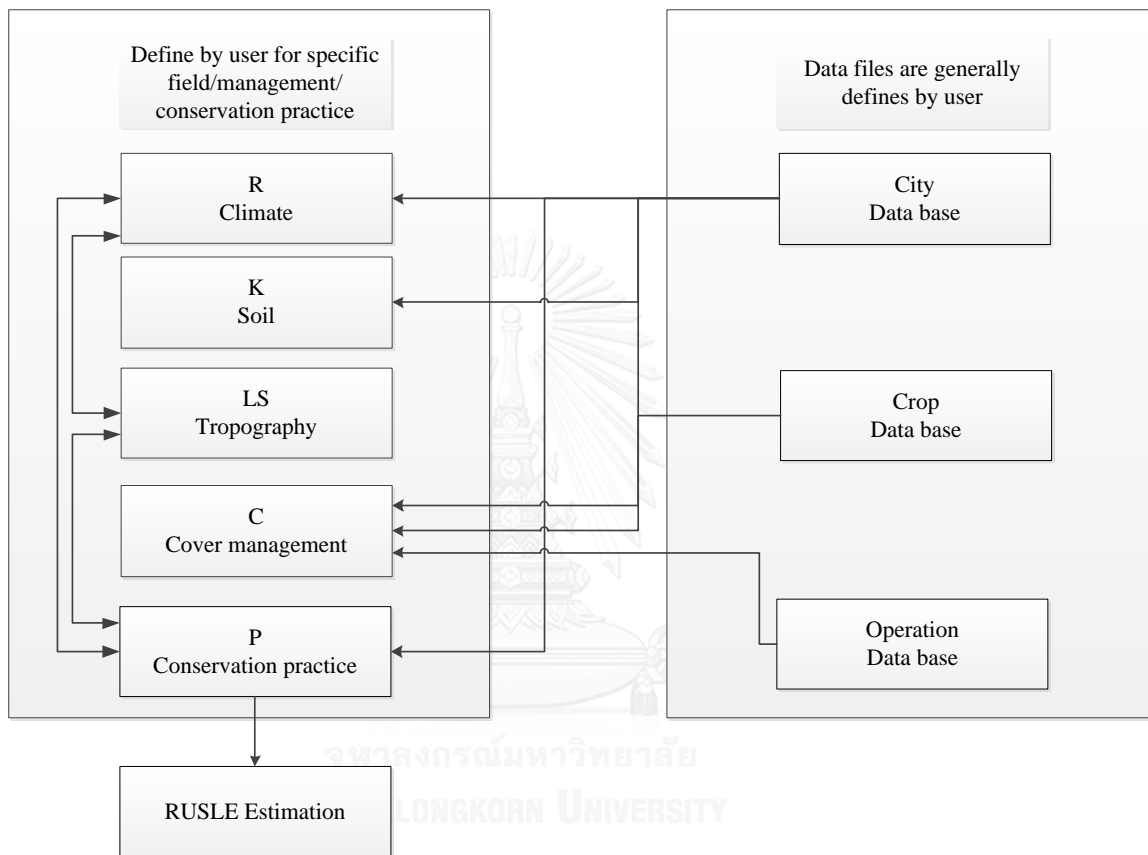
Figure 2-5 Flowcharts of the sources of RUSLE's parameter (Joe R. Galetovic, 1999)

2.7.2.1 Literature review on the study of RUSLE

D. Warren (Steven D. Warren, 2005) and his team conducted a study on three U.S. military training areas using Unit Stream Power Erosion and Deposition (USPED) model, a 3-dimensional enhancement to the Universal Soil Loss combined with remote sensing technique and found that the applications of the USLE consistently and significantly overestimated soil erosion.

Soo Huey Teh (Soo H.T., 2011)successfully predicted the soil loss from the upper catchment area of Cameron Highlands, Malaysia by using RUSLE

estimation. The study processes perform the example that the achievement in RUSLE practice can be accomplished if the required parameters are provided.

Sadeghi S.H. (2004) predicted the erosion of The Amameh catchment and found that runoff is a better indicator than rainfall for sediment prediction. Sufficient number of the storms occurring during the different conditions with a wide range of variation should be considered for calibration and development of equations and can give satisfactory results. The result shows that Remote Sensing and GIS are useful tools for modeling soil erosion, evaluating various disturbance alternative and spatial optimizations of conservation measures.

2.8 GIS and Remote sensing technique

2.8.1 Geographic information system (GIS)

A geographic information system (GIS) is a computer-based tool and application, enabling the user to create mapping and analyzing spatial data. This technology integrates common database operations such as query and statistical analysis with the unique visualization and geographic analysis on the map. GIS store information and statistic data in form of thematic layers, which can be merged and linked together by geography. These abilities distinguish GIS from other information systems and become the most important technology, widely use in both public and private activities (Whitlock W. and Rumpus A., 2010)

2.8.2 GIS concept and operation

Geographic information contains both explicit geographic reference such as a latitude and longitude or national grid coordinate (Whitlock W. and Rumpus A., 2010), and the implicit reference such as forest stand identifier, road name, even a soil profile of the interesting area. The automated process called geocoding is applied to create explicit geographic references (in form of locations) from implicit references (regular data such as address or vegetation type). These geographic references cannot be used to locate features and events, such the business impact after earthquake, on the Earth's surface for analysis. The principal of georeference is demonstrated in Figure 2-6. The convention of GIS consists of six main tasks which are data input,

map creation, data manipulation, file management, query and analysis and virtualization of the result.
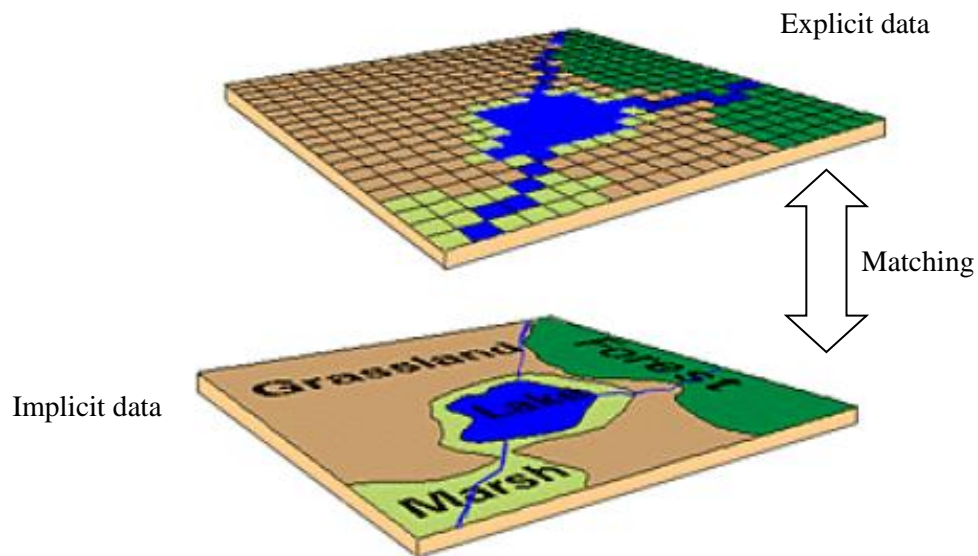
Figure 2-6 Principal concept of georeference (ESRI, 2015)

2.8.3 Remote sensing technique

Remote sensing is the technique to acquire the information of an object or phenomenon without making physical contact with the object. At present, the term remote sensing inclusively refers to the utilization of aerial sensor technologies to detect and classify objects on Earth (both on the surface, and in the atmosphere and oceans) by means of propagated signals (e.g. electromagnetic radiation).

Passive sensors such as film photography, infrared, charge-coupled devices and radiometer acquire natural radiation which is reflected by the object or surroundings. Reflected sunlight is the most common source of radiation measured by passive sensors. Alternatively, active collection emits energy to scan objects and areas whereupon a sensor then detects and measures the radiation that is reflected or backscattered from the target.

2.8.3.1 Landsat5

Landsat 5 is the fifth satellite of the Landsat program. It was launched on March 1, 1984, with the primary goal of providing a global archive of satellite photos (U.S. Geological Survey (USSG), 2012). This Program is managed by United States Geological Survey (USGS), and data from the satellite is collected and distributed from the USGS's Center for Earth Resources Observation and Science. The specification of Landsat5are described in Table 2-13 below.

Table 2-13 Landsat5 specification

Specification	
Diameter	1.8 m
Weight	2000 kg
Altitude	705 km
Regime	sun-synchronous, near-polar
Inclination	98.2°
Equatorial crossing time	9:45 AM +/- 15 minutes
Repeat interval	16 days
Image recorder	Multispectral Scanner(MSS) and Thermatic Mapper (TM)
Interval time	99 minutes
Swath width	185 km
Resolution	80 m(MSS), 30 m (TM)

According to the satellite's image recorder, the Thermatic Mapper recorder can produce 7 bands of satellite image and each band can be used in specific area of study which is demonstrated in Table 2-14 (U.S. Geological Survey (USSG), 2012).

Table 2-14 Landsat5 band utilization

Band	Spectral Bands	Wavelength(μm)	Utility
1	Blue, Green	0.45-0.52	Useful for bathymetric mapping and distinguishing soil from vegetation and deciduous from coniferous vegetation.
2	Green	0.52-0.60	Emphasizes peak vegetation, which is useful for assessing plant vigor.
3	Red	0.63-0.69	Discriminates vegetation slopes.
4	Reflected Infrared	0.76-0.901	Emphasizes biomass content and shorelines.
5	Reflected Infrared	1.55-1.75	Discriminates moisture content of soil and vegetation; penetrates thin clouds.
6	Thermal Infrared	10.40-12.50	Useful for thermal mapping and estimated soil moisture.
7	Reflected Infrared	2.08-2.35	Useful for mapping hydrothermally altered rocks associated with mineral deposits.

2.8.3.2 Vegetation classification using Landsat5

Vegetation classification is an important component in the management and planning of natural resources especially in the hazard management. Remote sensing, with spectral data of satellite's bands which are obtained from Landsat5, integrated with topographic variables from through fieldwork and DEM (digital elevation model), take and important role as tool in classifying vegetation.

Since the improvement in remote sensing technology, vegetation inventories for large regions in a short period of time can be monitored and detected for changes in vegetation using thematic mapper techniques. Vegetation classification through remote sensing requires two important conditions for its' use; the interpreter must have the ability to understand the basic criteria of vegetation classification and unit delineation in satellite imagery and the satellite sensor must have the ability to act as a surrogate for the terrain interest points.

Landsat5's spectral data derived from TM proved to be an improvement in the separation of non-forested upland classes and should be integrated into multispectral classification of mountainous regions. It collects images that have higher spatial, spectral and radiometric resolution and discriminates between

vegetation type and vigor, plant and soil moisture requirements and differentiates between clouds and snow.

Permana (Jaideep KM et al., 2006) and his team had chosen Yonezawa region of Japan vegetation classification. It has been found that the overall accuracy of around 85% is achieved using combination of two components of bands. 1, 2, 7 and three selected raw TM band data (band 3, 4, 5) data in contrast to accuracies derived using another transformed image combination. By using this combination, the classification accuracy is significantly higher for cedar and red pine, indicating better discrimination between the vegetation classes. From this experiment, we can conclude that the proposed method is useful for vegetation classification of Landsat-5 TM data.

2.8.3.3 NDVI Analysis

The significant method for vegetation area identification and change detection in remotely sensing analysis is through vegetation indices (Deering D. W. and Haas R.H., 1980) . Vegetation indices are algorithms aimed at simplifying data from multiple reflectance bands to a single value correlating to physical vegetation parameters (Tucker C.J., 1979). These vegetation indices are referenced by the well-documented unique spectral characteristics of healthy green vegetation over the visible to infrared wavelengths.

The normalized difference vegetation index (NDVI) is one of the various spectral vegetation indices (Rouse J.W. et al., 1974)). NDVI is conducted by researchers for extracting vegetation abundance from remotely sensed data (Tucker C.J., 1979). According to Figure 2-7, the reaction to the differences wave lengths of green pigments in plant is specific, so dividing the difference between reflectance values in the visible red and near-infrared wavelengths by the overall reflectance in those wavelengths can give an estimate of green vegetation abundance (Tucker C.J., 1979).In essence, the algorithm isolates the dramatic increase in reflectance over the visible red to near infrared wavelengths, and normalizes it by dividing by the overall brightness of each pixel in those wavelengths. The computation of NDVI is demonstrated in Equation 2-2

$$NDVI = \frac{NIR - VIS}{NIR + VIS} \qquad (2\text{-}2)$$

Where

NIR	=	reflectance in the near infrared band (Band4)
VIS	=	reflectance in the red (visible) band (Band3)

Theoretically, NDVI should range between -1.0 and +1.0, but in practice, the measurements generally range between -0.1 and +0.7. Environmental effect such as rain and clouds can initiate negative NDVI values. Bare soils and other background materials produce NDVI values between -0.1 and +0.1. Larger NDVI values occur as the amount of green vegetation in the observed area increases.

NDVI has been integrated to various type of vegetation cover characteristics measurement especially crop assessment studies (Asrar G. et al., 1984; Benefetti et al., 1993; Deering D. W. and Haas R.H., 1980; Rouse J.W. et al., 1974; Wanjura D.F. and Hatfield J.L., 1987) . Some of them provide weekly vegetation maps, monitor crops over large regions, monitor vegetation change in much of the tropics, and estimate biomass. Dymond (Dymond J.R. et al., 1992) used NDVI to estimate rangeland degradation with a high accuracy result. As therefore, NDVI, applied in this study will be generated and used for vegetation classification.
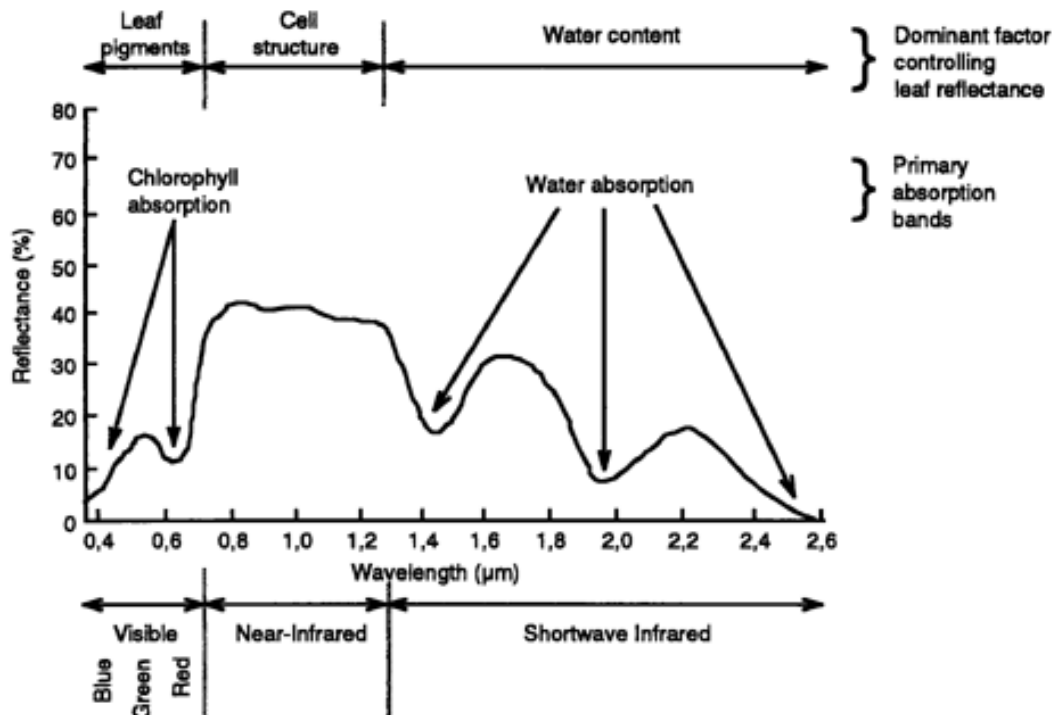
Figure 2-7 Typical spectral response characteristics of green vegetation
(Hoffer R.M., 1998)

2.8.3.4 Integrated-study for soil mapping

During the recent decade, remote sensing techniques have been continuously developed; however, the limitation in derivation of soil type from this procedure is still unsatisfied. This makes many researcher developed the integration between remote sensing and GIS techniques together in order to enhance the capability for the remote sensing operation especially for soil profile surveying.

Zhang M., Rudi G., & L Daels (1993) mentioned in their study of soil mapping in the rolling hills area of China that

1. For integration procedure the algorithm and threshold parameter use in the analysis can significantly influence the result of soil classification.

2. GIS is the powerful tool to improve the accuracy of remote sensing data.

3. The accuracy for main unit of soil typed can be acceptable while for the sub unit the soil profile exhibit the opposite side of the result. Zhang M. et al. (1993)

(Demattê* J.A.M. et al., 2009) estimated soil attributes by laboratory and orbital sensors and compare these results with soil classification. A sampling grid of 100 by 100 m was established and the exact position of each point was georeferenced, and sent to traditional (wet) laboratory analyses. The results encourage the applying of quantitative evaluation of spectral reflectance permits the acquisition of Fe_2O_3 and clay data as a basis for soil mapping and classification.

2.9 Cadmium transportation study in the Mae Tao Basin

The cadmium contamination via sediment transport has been inclusively studied in the Mae Tao Creek, Mae Sot district, Tak province since 2009 (Karoonmakphol P, 2009). The simulated result indicates that the cadmium contaminated sediment transport via bed load in the Mae Tao creek. The report stated the utilization of the MIKE SHE coupled with MIKE 11 to simulate the hydrodynamic results which were daily time series of water depth and water discharge, and sediment transport using the Meyer-Peter and Muller model in 2009. The size distribution of the bed load in studied area was studied and the results indicated that sand particles were the significant size.

The accumulated sediment transport at the downstream of the Mae Tao Creek in 2009 was computed to 24.522 m^3, whereas 99.77 % of sediment transport occurred in the wet season. The cadmium transport occurred in the Mae Tao Creeks were estimated as 1.599 kg. The results revealed that higher rate of cadmium transport and distribution can be detected during wet season. However there was some level of uncertainty in the results due to insufficient information (Thamjesda T., 2012). Tharathammathigorn (2010) assessed the cadmium transport in the Mae Tao Creek due to sediment transport from May 2010 to February 2011.

The study separated sediment transport into bed load and suspended sediment. MIKE 11 was applied to investigate the channel flow, and sediment transport based on Van Rijn model. The simulated results indicated a significant difference between

the dry and wet seasons. The total of accumulated sediment transport at the downstream of the Mae Tao Creek was approximately 760.17 m^3 and 78.46% of sediment transport took place in wet season. Additionally, 86.86% of sediment that transport was suspended sediment and can be concluded that the suspended sediment was a dominant transport of cadmium transport in the creek. The cadmium was allocated out from the Mae Tao creek for 20.74 kg during May 2010 to February 2011. However the over prediction may be occurred due to model limitations such as neglecting in hydraulic structure.

Thamjesda (2012) studied the effect of land use and the hydraulic structure in the Mae Tao Basin. The study indicated that the distribution of cadmium contaminated via sediment was mainly generated in the wet season. According to high transport capacity of suspended sediment, the cadmium transport was dominant by suspended sediment transport. During the study period from May 2011 to February 2012, 16.33 kg of cadmium was transported out of the Mae Tao Creek and most of the cadmium was transported during the wet season.

Conversion of rice in current agricultural land use to sugarcane plantation to compare the cadmium distribution, demonstrates a decreasing on accumulated sediment both suspended sediment and bed load. For the study on the effect of a hydraulic structure, with the hydraulic structure at downstream of the Mae Tao Creek presented a decreasing of accumulated sediment transport both suspended sediment and bed load after passing the weir, contribution to a lowering in cadmium transport. The result shows that when applying a hydraulic structure operation as 12.86 kg.

2.10 Cohesive Sediment transportation process

2.10.1 Cohesive Sediment

Cohesive sediments are primarily consisted of clay-sized material with strong inter-particle forces due to their surface ionic charges. When the particle size of cohesive sediment decreases, its surface area per unit volume (i.e. specific surface area) increases, and the inter-particle forces, not the gravitational force, dominate the behavior of sediment.

The boundary between cohesive sediment and non-cohesive sediment is indistinct and the definition is usually depended on the monitoring site. Generally, finer particles are more cohesive. Sediments, smaller than 2 pm, are generally considered to be cohesive sediment. Sediment of size greater than 60 pm is coarse non-cohesive sediment. Silt (2pm -60pm) is considered to be between cohesive and non-cohesive sediment.

Certainly, the cohesive properties of silt are primarily due to the existence of clay. Therefore in engineering practice, silt and clay are both considered to be cohesive sediment. Cohesive sediments consist of clay minerals (e.g. silica, alumina, montmorillonite, illite, and kaolinite) and organic material (Hayter E.J., 1983) They are concerned in many waterways and closely linked to water quality.

Many pollutants, such as heavy metals, pesticides, and nutrients preferentially adsorb to cohesive sediments. Besides, the contaminants adsorbed to the sediments, the sediments themselves are sometimes a water quality concern. The turbidity, occurred by sediment particles, can restrict the penetration of sunlight and decrease food availability, thus affecting aquatic life.

2.10.2 Deposition

Deposition occurs when the bottom shear stress is less than the critical shear stress. Only aggregates with sufficient shear strengths to withstand the highly disruptive shear stresses in the near bed region will deposit and adhere to the bed. In 1973 Metha and Parthen provided laboratory studies on the deposition-behavior of cohesive sediment and reported that deposition condition is controlled

1. Bed shear stress,
2. Turbulence processes in the zone near the bed
3. Settling velocity,
4. Depth of flow,
5. Suspension characteristic such as concentration and ionic constitution of the suspending fluid (Hayter E.J. et al., 1999)

Krone (Krone R.B., 1962) theorized the equation for Deposition for cohesive sediment transport as shown in Equation 2-3

$$Q_d = P_d \omega C \qquad (2\text{-}3)$$

Where

Q_d = Deposition rate (m^3/s)

ω = Settling velocity (m/s)

P_d = Deposition probability.

C = Sediment concentration

The term P_d refers to the probability of particles permanently stick to the bed and not being back to the flow by any flow activity. The probability of deposition is given by

$$P_d = 1 - \frac{\tau}{\tau_{df}}; \tau < \tau_{df} \qquad (2\text{-}4)$$

Where

τ = Bottom shear stress

τ_{df} = Critical shear stress for full deposition

According to the real condition of deposition, full deposition has a small possibility occurring in the overland flow so the partition deposition has been established. Partial deposition exists when the bed shear stress is greater than the critical shear stress for full deposition but smaller than the critical shear stress for partial deposition. At this range of bed shear stress, relatively strong flocs are deposited and relatively weak flocs remain in suspension. The partial deposition formulation is written as

$$Q_d = P_d \omega (c - c_{eq}); \tau_{df} < \tau < \tau_{dp} \qquad (2\text{-}5)$$

Where

c_{eq} = Equilibrium sediment concentration.

The equilibrium sediment concentration is the concentration of relatively weak particle which insufficiently strong bonds. These particles will be broken down before reaching the bed or will be eroded after being deposited. The probability of deposition is given by

$$P_d = 1 - \frac{\tau}{\tau_{dp}}; \tau_{df} < \tau < \tau_{dp} \tag{2-6}$$

In the other hands, deposition will not be occurred, when the bed shear stress is larger than the critical shear stress for partial deposition. The deposition rate is zero.

$$P_d = 0; \tau \geq \tau_{dp} \tag{2-7}$$

2.10.3 Erosion

Erosion for cohesive sediment refer to the phenomena that individual particles or small aggregates are removed from the soil mass by hydrodynamic forces such as drag and lift (Millar and Quick, 1998) Mass erosion occurs when the yield strength is exceeded the resistance power of the particle or bed of substance such as a slip failure of a stream bank or when large flakes or chunks of soil are eroded from the streambed.

Due to the complexity of erosion phenomena, no comprehensive theory regarding the erosion of cohesive soils the equations presented are empirical formula for the surface erosion rate was presented by Ariathurai (Ariathurai R . and Arulanandan K. , 1978) based on fitting the experimental plots of erosion rate versus applied shear stress by Partheniades (Partheniades E., 1962).

$$Q_{se} = \begin{cases} M_{se} \dfrac{\tau - \tau_{se}^c}{\tau_{se}^c}; \tau \geq \tau_{se}^c \\ 0; \tau < \tau_{se}^c \end{cases} \tag{2-8}$$

Where

Q_{se}	=	Surface erosion rate (m³/s)
τ, τ_{se}^c	=	Bed shear stress and critical surface erosion shear stress, respectively
M_{se}	=	Surface erosion rate constant.

The critical erosion shear stress depends on a number of factors including sediment composition, bed structure, chemical compositions of the pore and eroding fluids, deposition history, and the organic matter and its state of oxidation.

Although direct measurement of cohesive soil properties provides the best possible results for determining erosion and deposition - parameters, it is not always practical, especially for critical shear stress. In order to decrease this problem, many studies have been performed linking mechanical soil properties to erosion phenomena.

Hwang and Mehta performed erosion experiments to determine the critical shear stress and the erosion rate for surface and mass erosion using an annular flume with sediment and eroding fluid from Lake Okeechobee, Florida. By obtaining erosion rates and critical shear stress values for various wet bulk densities (Hwang K.N. and Mehta A.J., 1989)

Van Rijn (1993) compiled data relating critical shear stress to dry bulk density, as the result the equation for estimating the critical shear stress from dry bulk density is exhibited in equation 2-9.

$$\tau_{se}^{c} = j(\rho_{b})^{k} \qquad (2-9)$$

Where

τ_{se}^{c} =   Critical surface erosion shear stress

j and k =   Coefficients determined by experiment.

ρ_{b} =   Bulk density (kg/m^{3})

The coefficient k was found to be in the range of 1 to 2.5 (Van Rijn L.C., 1993) Thorn and Parsons found k = 2.3 for mud from the Brisbane River, Australia, Grange mouth Estuary, Scotland and Belawan, Indonesia. Burt determined that k = 1.5 for mud from Cardiff Bay, England (Burt T. N., 1990).Van Rijn did not mention of any values for j in the literature. Table 2-15 provides shear stress data from (Van Rijn L.C., 1993) and others related to the dry bulk density.

Table 2-15 Shear strength data and dry bulk density from the study of Van Rijn (Van Rijn L.C., 1993)

Soil type	Sand (%)	Organic (%)	Critical shear stress for surface erosion (Pa)				
			Bulk density (kg/m3)				
			100	150	200	250	300
Kaolinite (Saline water)	0	0	No data	0.05-0.10	0.30-0.40	No data	No data
Kaolinite (Distrilled water)	0	0	No data	0.05-0.10	0.15-0.20	0.20-0.25	0.25-0.30
Holland Diep1 (Lake)	9	10	0.15-0.25	0.30-0.40	0.40-0.50	0.60-0.80	No data
Holland Diep2 (Lake)	23	9	0.10-0.20	0.30-0.40	0.40-0.50	0.80-1.00	No data
Ketelmeer (Lake)	7	12	0.20-0.25	0.20-0.25	0.25-0.35	0.50-0.70	No data
Biesbosch (Lake)	8	8	0.15-0.30	0.25-0.30	0.30-0.35	0.50-0.70	No data
Maas (River)	36	8	0.15-0.25	0.30-0.40	0.40-0.50	0.80-0.10	No data
Bresken Habour (Estaury)	27	5	0.05-0.15	0.25-0.35	0.35-0.45	0.60-0.80	No data
Delfzijl Habour (Estaury)	60	2	0.20-0.30	0.15-0.20	0.20-0.25	0.40-0.60	No data
Loswal Noord (Sea)	69	2	0.20-0.32	0.30-0.35	0.35-0.45	0.60-0.80	No data
Brisbane, Grangemouth and Belawan	0	No data	0.20-0.30	0.40-0.60	0.80-1.0	No data	No data
Loire	No data	No data	0.10-0.15	0.15-0.20	0.20-0.30	0.30-0.40	0.80-1.20
Cardiff Bay	No data	No data	0.20-0.35	0.40-0.50	0.60-0.70	0.70-0.90	No data

2.11 Mathematical Model

MIKE SHE and MIKE 11, developed and extended by DHI Group, were chosen as a tool to simulate the overland flow depth, overland flow direction and sediment transport in the Mae Tao Creeks. The simulate results, operated in association with a private module based on CASC2D which is the freeware from Colorado State University, are applied in order to retrieve the final result of the study.

2.11.1 MIKE SHE

MIKE SHE, a distributed and physically based model system, provides the simulation for the hydrological cycle. It includes overland flow (OL), evapotranspiration (ET), unsaturated flow (UZ), saturated flow (SZ) and river and lake (channel flow, OC), as illustrated in Figure 2-6. Related water quality modules are consisted of advection-dispersion, particle tracking, sorption and degradation, geochemistry, biodegradation, crop yield, and nitrogen consumption (DHI, 2010). Each process can be specified in various levels of spatial distribution and complexity corresponding to desired outputs, availability of input data, and user's preference (Butt M. B. et al., 2004) MIKE SHE contains wide range of the application for the analysis, planning and management of a broad range of water resources and environmental and ecological problems related to surface water and groundwater, for example impact of land use change and anthropogenic effects (A. and Kjelds J., 2001; Refsgaard J.C., 1998)

Refsgaard and Kjelds (2001) selected MIKE SHE to be the best modeling system to simulate groundwater-surface water related issues. Additionally, MIKE SHE can provide the best and most comprehensive description interaction with a full dynamic coupled description of the hydrological processes. (A. and Kjelds J., 2001; Refsgaard J.C., 1998)

2.11.2 MIKE 11

MIKE 11 is capable for simulating the channel flow, water quality and sediment transport. MIKE 11 contains comprehensive modules to model complex channel networks, lakes and reservoirs, and river structures, such as gates, sluices, and weirs. The hydrodynamic (HD) module is the core of MIKE 11; furthermore,

MIKE 11 includes the add-on modules for hydrology, advection-dispersion, models for various aspects of water quality, cohesive sediment transport, and non-co cohesive sediment transport (DHI Water Environment Health, 2011a; DHI Water Environment Health, 2011b; DHI Water Environment Health, 2011c)
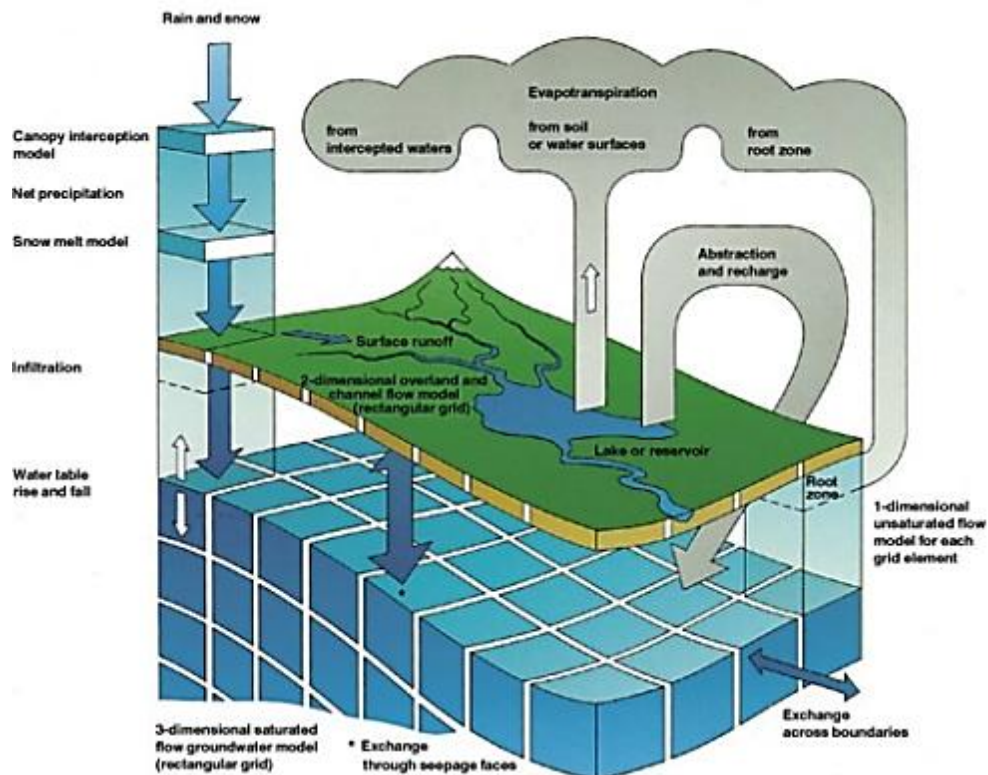
Figure 2-8 Hydrological processes in MIKE SHE (DHI, 2011 a)

The hydrodynamic (HD) module composed of an implicit, finite difference computation of unsteady flows in rivers. The module is suitable for the unsteady flows in branched and looped river networks, and quasi two-dimensional flows in floodplains. The module solves the equations of conservation of continuity and momentum (the 'Saint Venant' equations) (DHI, 2010). The solutions to the equations are based on four assumptions. Firstly, the water is incompressible and homogeneous. Secondly, the small of bottom slope caused the cosine of the angle it makes with the horizontal could be equaled to 1. Thirdly, the wave lengths are greater than the water depth by assuming the flow can be to flow parallel to the bottom everywhere. Finally, the flow is sub-critical when actual water depth is higher than critical depth. (Kamel A.H., 2008).

The sediment transport in channel system can be retrieved from the simulation of two main modules. Firstly, advection-dispersion module (AD) is suitable for cohesive sediment such as silts and clays. Secondly, sediment transport module (ST) is proper for non-cohesive sediment such as gravels and sands.

2.11.3 CASC2D

CASC2D (Rosalía R.S., 2002) was developed in order to define the runoff hydrograph generated from any temporally-spatially varied rainfall event. The erosion and sedimentation module of CASC2D contain a capability to predict the sediment transportation rates any location. In CASC2D, the routed of overland flow into channels is based on diffusive wave approximation in two dimensions. In channels, the water routed is calculated by a 1-D diffusive wave equation. The modified Kilinc-Richardson equation (Julien P.Y. et al., 1995) is applied in CASC2D-SED to define the upland sediment transport by grain size (silt, clay, and sand) from one cell into the next one in two orthogonal directions. CASC2D solves the equations of conservation of mass, energy and linear momentum to estimate watershed runoff for a given rainfall input. The overland flow routing formulation is based on an explicit 2-D finite difference (FD) technique. The channel formulation is based on an explicit 1-D FD technique.

2.12 Summary of the study concept

From the previous studies, related to the contamination instance in the Mae Tao Basin area, most of the studies are aime to monitor the cadmium contamination level of the cadmium in environmental phases, including soil, water, crop and some livestock.

Moreover, some of the studies can describe only contamination status at a significant location without studying the effect of potential sources of cadmium in the basin, so that the phenomena of cadmium transport in the study area still unrevealed. Since, more than a half of the Mae Tao Basin is a remote area with a lot of obstacles in direcfield observation, the contamination level in some area of the basin are undercovered.

Since, more than a half of the Mae Tao Basin is a remote area with a lot of obstracles in direcfield observation, the contamination level in some area of the basin are undercovered. In order to extend the effectiveness of those studies to gain more understanding in the contamination level of cadmium over the basin remote sensing technique which is the indirect field observation methos were applied to dispose of the limitation in the direct field observation.

The Mae Tao Basin has been determined to be the largest deposition of zinc composite mineral, in which cadmium can be detected. With this statement, the natural can be one of the main contributors of cadmium in the Mae Tao Basin area. According to the previous studies, stream sediment transport is one of the media that convey the cadmium contamination to the downstream of the Mae Tao Creek, but the effect of overland sediment transport which can transport the contamination into the creek are not mentioned.

With the purpose of complementing this gap in understanding of cadmium contamination phenomena in the Mae Tao Basin, the study on the sediment transport by the overland flow of the basin and the Mae Tao Creek were conduct. This study aims to determine the possibility and the potential of natural zinc deposit as one of the main contributors of cadmium contamination in the Mae Tao basin. To determine this possibility of the geological characteristic of the area as the contributors of the cadmium contamination in the Mae Tao Basin, remote sensing technique was assigned in order to gather necessary information from the area. Information, obtained from the area, was sent to the GIS program and hydrological program named as MIKE-SHE to create the module for simulating the migration of cadmium by the activity of the overland flow phenomena in the Mae Tao Basin.

CHAPTER 3
Methodology

This study aims to determine the possibility that the geological characteristic of the area which is naturally rich in zinc and cadmium can become one of the contributors of the cadmium contamination in the Mae Tao Basin. Since cadmium and zinc are naturally born in association with each other, the source of cadmium contamination in the Mae Tao Creeks can possibly be natural. In order to accomplish the determination, the integrated techniques between GIS, Remotes sensing and Hydrologic model application were set up. The study on potential of the natural source as one of the main cadmium contributor is consisted of 5 main parts which are:

1. Data collection: the land usage, topography and meteorology were obtained from the government departments. The leaf area index which used to identify the vegetation type in land usage was reviewed from the literature.

2. Field observation: suspended sediment and bed load were collected to estimate the cadmium concentration during the dry and wet seasons. In addition to bed load, the grain size distribution and soil classification were also determined. At station MT 01 and MT 04 was measured the water depth daily to verify model. Hydraulic structure existence between station MT 02 and MT 03 was measured the parameter to estimate its effect on cadmium transport. In addition ten monitoring check dams were installed to monitor the erosion in which occurred in the Mae Tao Basin. The stations were installed at the location where the significant levels of the potential cadmium were detected.

3. NDVI Analysis: the satellite photo of the Mae Tao Basin, captured by LANSAT5 (TM), and Satellite image interpreter application was analyzed based on NDVI technique to separate the vegetation area and the bare soil area out of the Mae Tao Basin. This part of the study is a preliminary observation before the RUSLE application is applied.

4. RUSLE estimation: five required parameters were retrieved from literature and calculation. The operation of the parameters was based on GIS application. The results from the estimation were integrated with cadmium concentration profile which is analyzed based on Klinging Method to calculate the potential cadmium flux from erosion in the Mae Tao Basin.

6. Model simulation: once the required information were collected and analyzed, mathematic model was applied from MIKE SHE and MIKE 11. Simulation processes were divided into hydrodynamic simulation and sediment transport simulation. The hydrodynamic part was firstly simulated applying MIKE SHE

coupled with MIKE 11 and calibrated by daily water level at station MT 04. The sediment transport was later computed with inputting the simulated hydrodynamic result into MIKE 11.

7. OfSET module development: once the simulation from MIKE SHE had been accomplished, the simulated overland flow depth and direction were exported to use as the input in the private module named as Overland flow Sediment transport module. The module has a capability to estimate the mass of cohesive sediment transport via rain fall erosion. Three scenarios including wet season, dry season and raining incident were monitored to compare the result of potential of the area as cadmium contributor.

8. Cadmium transport estimation: cadmium transport in the Mae Tao Creek and the Mae Tao basin were calculated from observed cadmium concentration and simulated sediment transport. The results from each part of the simulation were compared so as to appraisal the potential of the area source for being one of a main contributor of cadmium in the Mae Tao Basin.

The methodology scope of the study is demonstrated in Figure 3-1.

3.1 Data collection

3.1.1 Simulation input data

Input data required for MIKE SHE and OfSET module were obtained from the government departments, field observation, and literature.

3.1.1.1 Topography

The Mae Tao sub catchment was obtained from the map sheet 4742III of series L7018, edition 1-RTSD with a scale of 1:50,000 (Appendix A). Elevation in the study area ranged from 200-950 m, as shown in Figure 3-2.

3.1.1.2 Meteorological data

Evaporation and precipitation rate data in year 2010-February 2012 (presented in Appendix B) were collected from the Thai Meteorological Department (TMD). Mae Sot meteorological station located at Tha Sai Luat Sub district, Mae Sot district, UTM Easting: 457098, UTM Northing: 1841791.
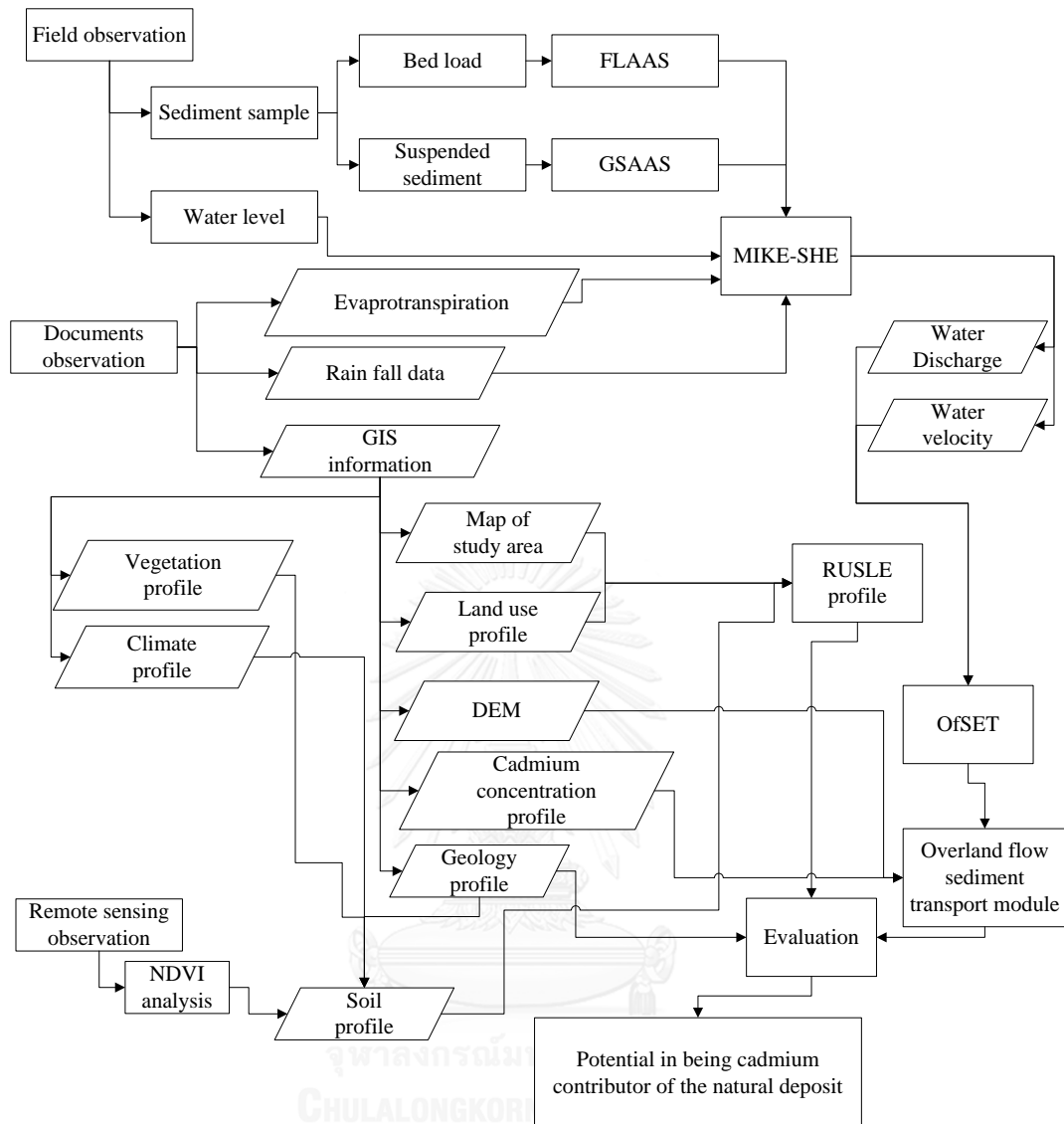
Figure 3-1 Methodology framework of this study

3.2 Field observation

(a)

(b)
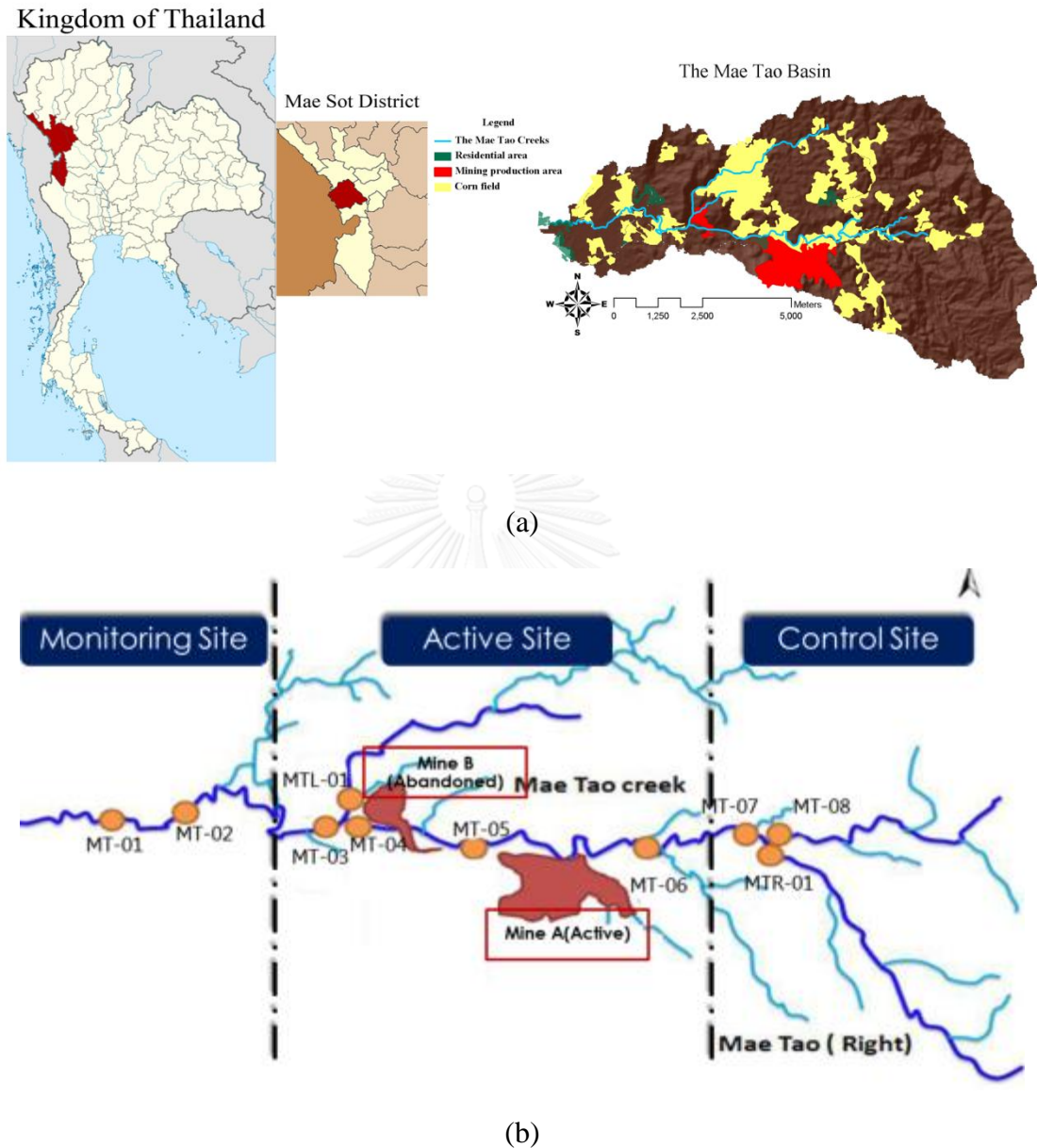
Figure 3-2 (a) Map of The Mae Tao Creek and the locations of the ten observation stations

(b) Location of ten monitoring station for cadmium concentration

Ten observations along Mae Tao Creek stations have been placed at upstream locations, junctions, and the outlet of the catchment, as presented in Figure 3-2 (b) and Table 3-1 to Table 3-2. At each station, the observation must include the pH, dissolved oxygen, conductivity of water, water temperature, sediment properties (cadmium concentration in sediment and grain size distribution), and hydraulic structure parameter.

Table 3-1 Location of sediment monitoring station along the Mae Tao Creeks

Station	Easting	Northing	Description	Field observation
MT 01	457998	1843017	- Village area - Location at downstream of Mae Tao subcatchment - Observation station of water level	
MT 02	459400	1843330	- Village area	
MT 03	461274	1843034	- Connection between station MT 04 and station MTL 01 - Receiving converged water from station MT 04	
MT 04	461374	1843110	- Downstream pass through Tak mining Company Limited's mine - Observation station of water level	
MTL 01	461438	1843286	- Mae Tao Left - Receiving converged water from Mae Tao Left	

Table 3-2 Location of sediment monitoring station along the Mae Tao Creeks

Station	Easting	Northing	Description	Field observation
MT 05	462046	1842870	Location between Tak Mining and Padaeng	
MT 06	465638	1842718	Location above two zinc mines	
MT 07	466937	1842750	- Conjunction between station MTR 01 and station MT 08 - Receiving water from station MTR 01 and station MT 08	
MTR 01	467228	1842559	Mae Tao Right	
MT 08	467088	1842736	Upstream of the main Mae Tao Creek	

For monitoring check dam, ten observation stations were installed during July 2014 to October 2014 at the locations that the significant erosion rates were indicated. At each station, the sediments from rainfall erosion were collect. The physical properties of the sediment including mass and grain size distribution were monitored. The location of the check dam station and the description of the location were listed in Table 3-3. Figure 3- 3 represent the location of the monitoring check dam on the Mae Tao basin.

Table 3-3 Location of the monitoring check dam over the study area

Station	UTM		Location
	Easting	Northing	
SED_OB1	459400	1843330	Downstream (MT02)
SED_OB2	463430	1842304	Heavy Equipment plant
SED_OB3	464087	1847923	Active Mining zone
SED_OB4	465266	1842053	Bench (Overburden Dump site 3)
SED_OB5	464285	1841898	Green Mining zone
SED_OB6	464667	1841792	Water Management HQ office
SED_OB7	465259	1842050	Overburden Dump Site
SED_OB8	464279	1841892	Bench (Overburden Dump site 1)
SED_OB9	465642	1841200	Sediment Pawn (E1)
SED_OB10	466937	1842750	Upstream (MT07)
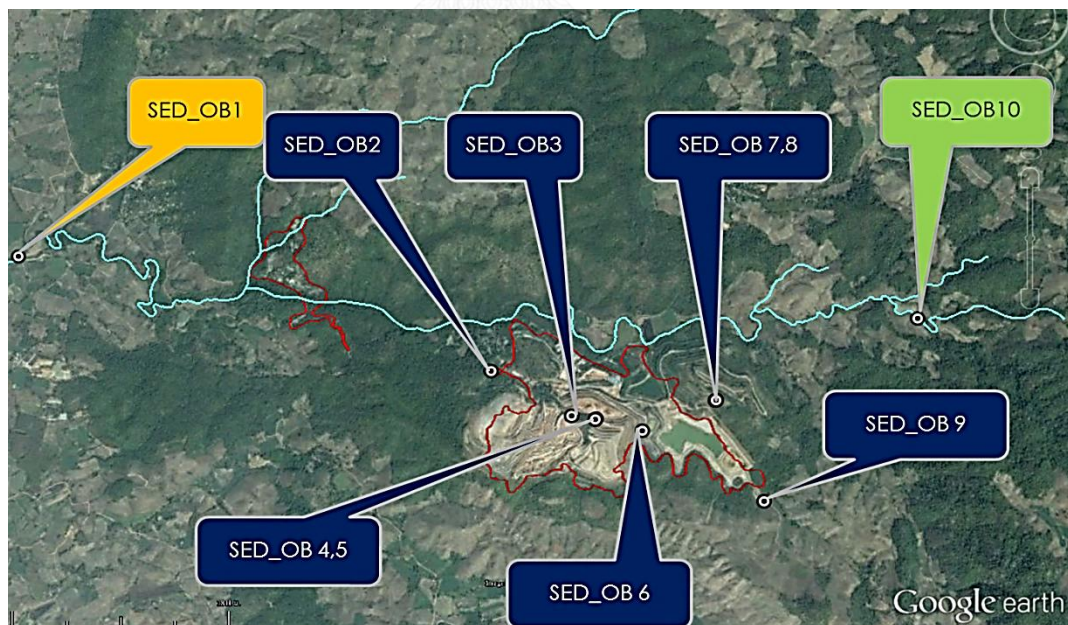
Figure 3-3 Check dam monitoring site in the Mae Tao Basin

3.3 Physical properties of sediment

3.3.1 Sample collection and preparation

For sediment monitoring station, suspended sediment and bed load were obtained and analyzed for their composition during the dry and wet seasons. The suspended sediments were collected in order to estimate the total cadmium concentration, while bed load samples were collected for analyzing the grain size distribution, soil classification, total cadmium concentration and the distribution of cadmium concentration. Moreover the sediments from monitoring check dam were collect for estimating the grain size distribution, cadmium concentration flux, cadmium distribution in size fraction of the sediments and mass erosion of the significant potential area during the monitoring period.

Suspended sediment

- At the center of the stream, two liters of water were collected to take suspended sediment by using a polyethylene container.
- The collected water was filter with a pre-weighed filter paper (GFC WATTMAN) by coupling with the vacuumed pump. The filter paper with retained sediment was placed in a Petri dish.
- The suspended sediment on the filter paper was dehydrated in an oven at 60°C for 24 hours and weighted.

Bed load

- About 2 kg of bed load were collected at the top layer of sediment (0-5 cm) and contained in a polyethylene container.
- The bed load was dehydrated at 105°C for 24 hours in an oven, and allowed to cool at room temperature.
- A ring mill was used to grind the bed load samples before analyzing of grain size distribution, soil classification and cadmium concentration. The cadmium and zinc distribution was investigated from various size of bed load which were sieved with sieve No. 65, 100, 150 and 200 (0.231- mm, 0.150- mm, 0.100- mm and 0.075- mm mesh openings respectively).

3.3.2 Grain size distribution

The bed load was analyzed grain size distribution by following ASTM C136-06, the "Standard Test Method for Sieve Analysis of Fine and Coarse Aggregates" and ASTM D422-63, the "Standard Test Method for Particle-Size Analysis of Soils".

A) Instruments

- Sieves (No. 3/4'', 3/8'', 4, 10, 20, 35, 65, 100, 150, and 200)
- Weighing apparatus
- Cleaning implements

B) Methods
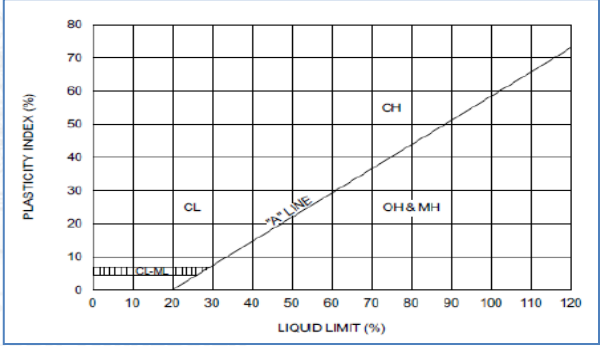
- The grinded bed load of each station and each select sieve were weighed.

- The sieves were set up by ranking from the smallest sieve (no. 200) at the bottom to the largest sieve (no. 3/4'') at the top of the sieve set.

- The bed load was added to the top of sieve set and sieved for around 30 minutes.

- Each sieve which contained the bed load was weighed.

Note: The grain size analysis should be repeated if the sample loses more than 2% of its weight. Moreover, the hydrometer analysis is recommended if there is more than 10% of sample passing sieve No. 200.

3.3.3 Soil Classification

Both of the sediment from the creeks and check dams were classified by following the Unified Soil Classification System (USCS) (ASTM D2487).

Table 3-4 Soil classification method

% sample passing sieve No.200	Classification	Equation
Less than 50%	Coarse-grained particles - Gravel (G) - Sand (S)	$CF = \dfrac{C}{F} = \dfrac{\text{\% coarser than 4-mesh sieve}}{\text{\% coarser than 200-mesh sieve}}$ (3.1) - If the CF (coarse fraction) is less than 50%, the sample will be classified as sand (S). - If the CF is greater than 50%, the sample will be classified as gravel (G).
More than 50%	Fine-grained particles - Inorganic silt (M) - Inorganic clay (C) - Organic silt or clay (O) - Peat (Pt)	$PI = 0.73\,(LL-20)$ (3.2) (PI= plasticity index, LL= liquid limit) **Figure 3-4** Plasticity chart and the A line (ASTM D 2487) - If the ratio between LL and PI is under the A-line, the sample is classified as inorganic silt (M) or organic silt or clay (O). - If the ratio between LL and PI is above A-line, the sample is classified as inorganic clay (C).

(International, 2009a; International, 2009b)

3.3.4 Measurement of cadmium concentration

1) Suspended sediment (EPA method 3050 B)

A) *Instruments*

- Hot plate
- Whatman disc filter paper No.41
- Graphite furnace atomic absorption spectrometry (GFAAS)
- GFAAS sample vessels
- Polyethylene bottles
- Weighing apparatus
- Glassware and others

B) *Materials*

- 65% Nitric acid
- Hydrochloric acid
- 30% Hydrogen peroxide
- Standard cadmium concentration
- Standard zinc concentration
- Deionized water

C) *Methods*

- Before analyzing, the laboratory glassware and plastic ware were cleaned with deionized water and 10% nitric acid for 2 hours, and rinsed with deionized water.
- The sample on filtered paper was weighed and heated to 95±5°C with 10 ml of 1:1 nitric acid for 10 to 15 minutes without boiling (covering with a watch glass).
- Nitric acid was added to the cooling solution about 5 ml and refluxed for 30 minutes. (The replicate of this step must be done when the brown fumes are occurred.)
- The solution was heated at 95±5°C without boiling for 2 hours.
- 2 ml of water and 3 ml of 30% hydrogen peroxide mixed along with 1 ml of 30% hydrogen peroxide were added to the cooling solution until being of unchanged solution.

- The solution was heated at 95±5°C without boiling for 2 hours.

- Each sample was filtrated with Whatman disc filter paper No. 41 and adjusted the volume to 50 ml before placing into a polyethylene bottle.

- The filtered solutions were analyzed by graphite furnace atomic absorption spectrometry. Detection limit for GFAAS is 0.0001 ng/mL for cadmium measurement and 0.00005 ng/mL for zinc measurement.

Note: The cadmium and zinc concentration used the t-distribution to estimate a standard deviation at the 80% confidence level.

2) Bed load (EPA method 3051)

A) Instruments

- Microwave digestion system: Mileston Ethos SEL
- Whatman disc filter paper No. 5
- PTFE vessels and covers
- Polyethylene bottles
- Sieve No. 65, 100, 150, 200
- Weighing apparatus
- Flame atomic absorption spectroscopy (FLAAS)
- FLAAS sample vessels
- Glassware and others

B) Materials

- 65% Nitric acid
- Hydrochloric acid
- Standard cadmium concentration
- Standard zinc concentration
- Deionized water

C) Methods

- Before analyzing, the laboratory glassware and plasticware were cleaned with deionized water and 10% nitric acid for 2 hours, and rinsed with deionized water.

- The sieving sediment from each sieve (No. 65, 100, 150, 200) was weighted around 0.5 g and placed in each PTFE vessels.

- Each PTFE vessels were added 9 ml of 65% nitric acid and 3 ml of hydrochloric acid.

- Each PTFE vessels were placed into a microwave system at 170±5 ℃ for 8 minutes and remain at 170 ℃ for 7 minutes, and allowed them cool down to the room temperature.

- Each cooled sample was filtrated with Whatman disc filter paper No. 5 and adjusted the volume to 50 ml before placing into a polyethylene bottle.

- The filtered samples were analyzed by flame atomic absorption spectroscopy. Detection limit for FLAAS is 1 ng/mL for cadmium measurement and 2ng/mL for zinc measurement.

Note: The cadmium and zinc concentration used the t-distribution to estimate a standard deviation at the 80% confidence level.

3.4 NDVI analysis

Seven bands of LANDSAT 5's satellite images, recorded by a Thermic Mapper (TM), were retrieved from "Geo-Informatics and Space Technology Development Agency (GISTDA).The analysis was conducted based on equation 3-1 by a raster calculation in GIS application. By selecting the visible band (Band 3) and near infrared band to be calculated, the result of NDVI analysis was obtained as a raster data set. The operation on NDVI analysis is demonstrated in Figure 3-5.
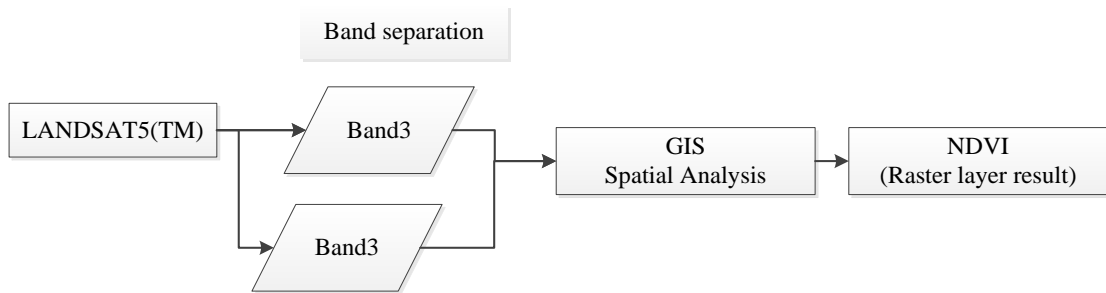
Figure 3-5 NDVI analysis operation on GIS application

3.5 RUSLE estimation

3.5.1 Parameter determinations

3.5.1.1 R-factor calculation

In view of the fact that there are many available equations to estimate the rainfall runoff value or RUSLE R factor, the calculation method must be able to specifically and appropriately represent the rainfall runoff factor of the Mae Tao Basin. Shamshad (*et al.* 2008) developed an equation using the Fourier relationship of rainfall data, which is appropriate for calculating the R value of a small area when there has been a short monitoring period. These proposed sets of equations were also used in R-factor calculations in Laos, which shares a similar climate with Thailand, Eq. 3-1 through Eq.3-3 are

$$Fi_x = \frac{M_x^2}{P_y} \qquad (3\text{-}1)$$

$$Ei_{30,x} = kFi_x^{0.584} \qquad (3\text{-}2)$$

$$R = \frac{1}{n}\sum_{x=1}^{n} Ei_{30,x} \qquad (3\text{-}3)$$

Where

Fi_X	=	Fourier index of rainfall in month x (mm).
M_X	=	Rainfall precipitation during month x (mm)
P_y	=	Amount of yearly precipitation (mm).

$$k \quad = \quad 227 \ (\text{MJ ha}^{-1} \ \text{h}^{-1})$$

$$Ei_{30,x} \quad = \quad \text{Maximum intensity rainfall energy of month } x$$
$$(\text{MJ mm ha}^{-1} \ \text{h}^{-1}).$$

3.5.1.2 C- and P-factor identification

Because of the characteristics of the Mae Tao Basin is a remote area, which is geographically inaccessible, direct field observation was hardly achieved. To overwhelm this limitation, secondary data collection (e.g., land use observation data from the Land Development Department of Thailand) was applied to obtain the required values by existing studies and directly input into GIS layer.

3.5.1.3 K-factor evaluation

The results from the NDVI analysis were compared to the satellite images to classify into vegetation types based on the vegetation index and field observation data to create the vegetation profiles. Afterward, the estimated vegetation data was received in the form of raster data on the vegetation types in the Mae Tao Basin. This data was utilized with the specific secondary data on soil properties, soil taxonomy, and Thai local soil data series to evaluate the K values of the study area base on the record, mentioned in the study of Supakij et.al (2012). The K-factor values were later assigned in the attribute data in GIS to create a raster calculation file for the K-factor value.

3.5.1.4 LS-factor calculation

LS-factor calculation schemes have been continuously improved and utilized for both direct field observation techniques and digital analysis techniques (José L G.R. and Martín C. GS., 2010). As a digital analysis tool, GIS can compute the LS factor from DEM alone. There are many equations and their derivations that have been utilized up until now.

Three different LS calculation method were studied in order to compare the results of soil erosion over the basin. These three methods are the (1) conservative method, (2) derivative method, and (3) applied method. They were used

in the area of the Mae Tao Basin that had the highest likelihood of experiencing soil erosion. These three equations are provided as Eq. 3-4 to Eq. 3-6. Equation 3 - 4 is widely used for LS-factor calculation using GIS (Mitasova H. et al., 1999)

$$LS = (\frac{Flowacc \times resolution}{22.13})^{0.6} (\frac{Sin(slope \times 0.01745)}{0.09})^{1.3} \qquad (3\text{-}4)$$

Eq. 3-5 is a derivative from Eq. 3-4 and uses sin θ to calculate the slope of the area of interest (Presbitero A.L. , 2003)

$$LS = (\frac{Flowacc \times resolution}{22.13})^{m} (65.41 \sin^2 \theta + 4.56 \sin \theta + 0.0654) \qquad (3\text{-}5)$$

Eq.3-6 is an equation used by Bizuwerk et al. (2008) to calculate the LS factor by applying the slope gradient to the calculation. This equation was used to calculate erosion potential by Soo (2011). (Bizuwerk A. et al., 2008)

$$LS = (\frac{Flowacc \times resolution}{22.13})^{m} (0.065 + 0.045s + 0.0065s^2) \qquad (3\text{-}6)$$

The LS factor characterizes the surface terrain of the basin and can be regained in both percent and gradient type. Furthermore, the slope gradient of the study area was calculated and analyzed by the spatial analysis. The term Flowacc refers to "Flow accumulation" which can be calculated by GIS application. The value of m, referred to a coefficient related to the ratio of rill to inter-rill erosion, was varied from 0.2-0.5, depending on the slope gradient and m, defined previously, was equivalent to 0.5 for s> 5%, 0.4 for   3% < s ≤ 5%, 0.3 for 1% < s ≤ 3%, and 0.2 for s ≤ 1%.

In order to calculate the Flow accumulation, a DEM (30 x 30 m resolution) of the basin from the Royal Thai Survey Department (RTSD) was filled to avoid any discontinuity in the flow simulation, which can occur when water is trapped in a cell surrounded by cells of higher elevation. Then, the flow direction was generated from these filled grids. Flow accumulation was calculated based on the direction acquired from the flow direction analysis. This procedure was applied to identify the quantity of surface flow accumulation in each cell. As a final step, the

raster calculation was applied to determine the LS factor. Detail of calculation command in GIS application is described in Appendix and the process used to retrieve the LS factor is illustrated in Figure 3-6.
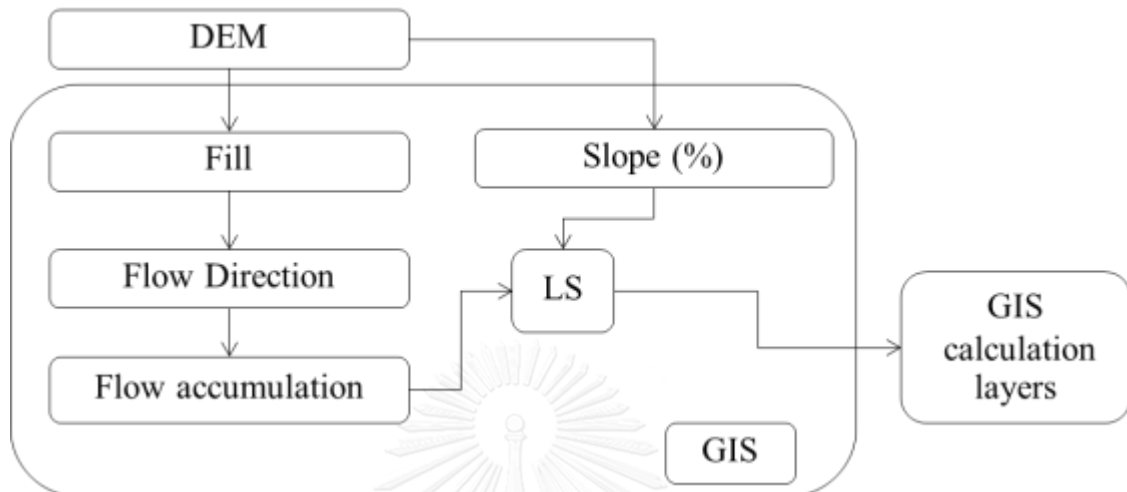
Figure 3-6 LS-factor calculation process

3.5.2 Cadmium concentration profile estimation

Information from Thai Pollution Control Department (Pollution Control Department (PCD), 2009) reported the extent of cadmium contamination in the Mae Tao Basin. The PCD's observation results were integrated and digitized using Kriging method to establish the cadmium concentration contours for the calculation of the potential cadmium flux from erosion. This method is a popular interpolation used in many fields, such as mining, geographical mapping, and environmental assessment offsite (Deutsch and Journal, 1998).

3.5.2.1 Kriging method

Kriging is an advanced geostatistical technique that generates an estimated surface from a scattered set of points with z-values (Oliver M.A. and Webster R., 1990) Different from other interpolation, the Kriging method has a capability to comprise an interactive investigation of the spatial behavior of the phenomenon represented by the z-values.

Kriging assumes the distance or direction between sample points as a spatial correlation which can be the explanation of the variation in the surface. The

Kriging method is applicable for a mathematical function with a specified number of points, or all points within a specified radius, to determine the output value for each location.

Kriging weights the surrounding measured values to derive a prediction for an unmeasured location. The general formula is formed as a weighted sum of the data which is demonstrated in Equation 3-7.

$$Z_0^* = \sum_{i=1}^{n} \lambda_i z_i \qquad (3\text{-}7)$$

Where

z_0^* $\quad=\quad$ Interested value at an un-sampled location

λ_i $\quad=\quad$ Weight of the regionalized variable zi at a given location

z_i $\quad=\quad$ Regionalized variable at a given location

The λi values are determined according to three criteria

1. The total weights summation must equal to 1.0
2. The estimation must be unbiased
3. The estimation variance is minimized.

The Kriging system is normally a set of n+1 linear equations containing total n+ 1 unknown. The system of equations is commonly written in terms of covariance and is the result of minimizing the variance. Equation 3-8 demonstrates the calculation for covariance in Kriging method.

$$C_{0i} = \sum_{i=1}^{n} \sum_{j=1}^{n} \lambda_i C_{ij} + \mu \qquad (3\text{-}8)$$

For all i = 1, n. In Equation 3-8, C_{0i} stands for the matrix notation for the covariance between a sample at a given location and the un-sampled location (target), with the same units as for the regionalized variable. C_{ij} is the covariance between two measured samples at surrounding locations, where i and j are the indices of the sample pair and vary between the first and last measurements, with the same units as for the regionalized variable. λi is the undefined weight assigned to a given sample, and for which i is the index of that sample and varies between the first and last measurements while μ is equal to a according to Lagrange multiplier. In matrix shorthand, the formula is written as shown in Equation 3-8, while the equation of Kriging variance is demonstrated in Equation 3-9

$$C\lambda = c \qquad (3\text{-}9)$$

Where

C	=	Covariance matrix constructed from measure sample pairs in a given neighborhood
λ	=	Vector of undetermined weights for measured samples within neighborhood
c	=	Vector of covariance, constructed from measured samples in a given neighborhood to the target location

$$\sigma_k^2 = C_{00} - \sum_{i=1}^{n} \lambda_i C_{0i} + \mu \qquad (3\text{-}10)$$

Where

σ_k^2	=	Kriging variance which its units are in terms of the regionalized variable.
C_{00}	=	Value of the covariance at a lag beyond which the covariance no longer changes (usually a value close to zero)
λ_i	=	Undetermined weight assigned to a given sample and varies between the first and last measurements
C_{0i}	=	Covariance between a sample at a given location and the no-sampled location (target

The estimation variance computed by Kriging method, have a capability to provide the narrowest confidence interval, but only under conditions of multivariate normality. Nevertheless, if the distribution of data values set outs from multivariate normality (a frequent occurrence), the Kriging variance might not be precise and can only represent a measurement of the relative goodness of the estimate.

According to numerous data of cadmium concentration from the report of PCD, the estimation by Kriging method was operated by contour-modeling application. After the contour of cadmium concentration was established, the contour was further digitized into GIS to create contour interval and cadmium profile. (Krige D.G., 1951; Krige D.G. and Assibey-Bonsu W., 1992)

3.5.3 Cadmium contamination assessment

Resembling the raster calculation of RUSLE, the concentration profile of cadmium in the Mae Tao Basin was based on the observation data from the report by Pollution Control Department (2009). The concentration profile was interpolated and digitized into an attribute table before transforming into a raster layer for calculation. The following equation was applied in the raster calculation to estimate the cadmium contamination:

$$Cd_{erosion} = cA \times 10^6 \qquad (3\text{-}11)$$

Where

$Cd_{erosion}$ =   Potential cadmium flux from erosion (t/ha/y)

c =   Cadmium concentration (mg/kg)

A =   Soil erosion from RUSLE (t/ha/y)

3.5.4 Potential cadmium flux from erosion

The estimation of potential cadmium flux from erosion was operated by GIS application. Each calculation layer was transfigured into raster type data. The resolution of these raster data set were transpose and set up at 30 x 30 resolution according to DEM of the study area. The overall calculation process is determined in Figure 3-8.
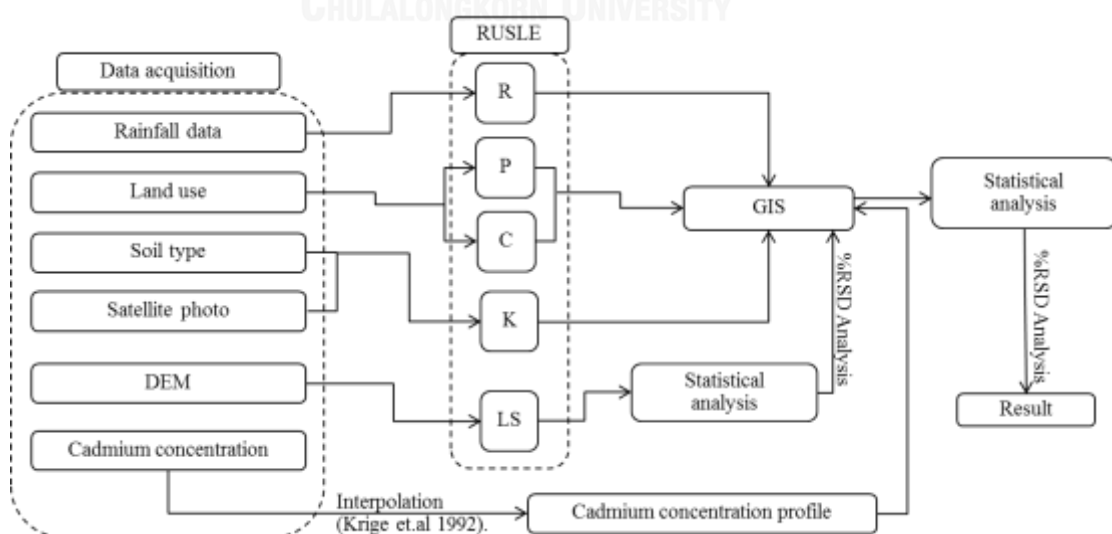
Figure 3-7 Overall process of the estimation of potential cadmium flux from erosion

3.5.5 Relative standard deviation analysis

Meanwhile many secondary data were utilized in this study, precision and repeatability of the result must be concerned. Precision refers to the closeness of concurrence between replicated and independent results under stipulated conditions, while repeatability is the precision of independent test results under the same process (Pryseley et al., 2010)

These two indicators represent consistency and reproducibility of the method by showing how close the method is. With the aim of comparing the precision of potential cadmium fluxes from erosion of these three calculations of LS factors, Relative Standard Deviation (RSD or % RSD) analysis was applied. This analysis is suitable for comparison precision between different methods. Equation 10 demonstrates a calculation method for %RSD. The smaller value of %RSD refers to the more precision in study method.

$$\% RSD = \frac{\sigma}{\bar{x}} \times 100 \qquad (3\text{-}12)$$

σ stands for standard deviation of erosion from each LS calculation method, while $\bar{x}$ represents mean of erosion from each LS calculation method.

3.6 Stream sediment transport simulation

3.6.1 Sediment transport simulation in The Mae Tao Creeks

According to the previous study using MIKE11 and MIKE SHE, the simulation were mostly focus on the sediment transport in the Mae Tao Creeks. In this study, more than the sediment transport in the Mae Tao Creeks, the simulation of these two programs is conducted to retrieve the estimation of overland flow depth and overland flow direction.

3.6.1.1 Land Use module

Land use module in MIKE SHE is capable to define the items on the land surface that affect the hydrology in study area, emphasizing on vegetation distribution. There are two relevant time series parameters: Leaf Area Index (LAI) and Root Depth that are used to define the distribution of vegetation across the model area.

LAI refers to the area of leaves per area of the ground. The role cannot control either leaves control or the significance of this index is photosynthesis, respiration, rain interception. Thus, LAI is an important parameter for many models in characterizing the relationship of vegetation and atmosphere, especially of the water cycles (GCOS. , 2004).

LAI is a dynamic parameter since its value of each crop bases on many factors which are species component, season, stage of development, environment and organization process. According to numerous factors and determination methods, The LAI value is broadly in literature such as range value of 2-4 for annual crops and 6-8 for deciduous forest

LAI can be investigated by two major measurements, one direct and one indirect method, as shown in Table 3-5to Table 3-6 (Breda N.J., 2003; Jonckheere I., 2004)

This study obtained land use map from Land Development Department, 2007. The land use map was converted to a shape file using GIS application and then interpolated in MIKE SHE (see Appendix A, Figure A-2). In MIKE SHE, three vegetation parameters were specified by consisting of LAI, root depth and crop coefficient. The values of these parameters were referenced from MIKE SHE manual (see Appendix D, Table D-2).

Besides, the leaf area index and root depth should be specified at the end of each crop state. The developments of LAI and root depth between the specified values are then interpolated linearly by the model. (Thamjesda T., 2012)

Table 3-5 Summarize of LAI measurement method

Procedure	LAI measurement
Direct method: 1) Leaf collection	There are two methods of leaf collection: harvesting methods and Non-harvest methods. a) <u>Harvesting methods</u>: - *Destructive sampling*: leaves are harvested and removed from a sampling area. - *Model tree method*: destructive sampling is applied for collecting vegetation out of the stand from which the leaf area and vertical distribution of leaf area is estimated leaf by leaf. This method is available for agricultural crop and forest system. b) <u>Non-harvest method</u>: - *Leaf litter collections*: litter traps are predestined box that design to collect the leaves during leaf fall season by non-cover on the top and lateral sides with precluding wind. This approach is applied for deciduous forest.
2) Leaf area determination	Leaf area can be estimated by two techniques: planimetric approach and gravimetric method. - *Planimetric method*: it relies on the relationship between individual leaf area and area, which is covered by the leaf in a horizontal surface. Planimeter is applied for measuring the leaf boundary, and then its area can be calculated. - *Gravimetric method*: it relies on the relationship between dry weight of leaves and leaf area. Leaf mass per area (LMA) is primarily evaluated from a sub sample. -When LMA is completely determined, the whole sample is dehydrated and the leaf area is determined from its dry weight and the sub sample LMA.

Table 3-6 Summarize of LAI measurement method (continued)

Procedure	LAI measurement
Indirect method: a) Indirect contact LAI measurements	- *Inclined point quadrat*: point quadrat is a long thin needle that is used to pierce a leaf canopy with known of elevation and angles, and contact between the needle and green canopy component is counted. LAI is calculated from equations of a radiation penetration model. - *Allometric techniques for forests*: these techniques base on correlation between leaf area and dimensions of woody component, which sustain the green leaf biomass such as stem diameter, height of tree. This correlation depends on species vegetation, site condition, season and canopy structure.
b) Indirect non-contact measurements	Indirect non-contact methods apply the determination of transmission of light trough plant canopies. Instruments have been developed to determine in real time LAI of leaf canopies for 20 years. They consist of two major groups, which are classified on whatever they measure: a first category includes instruments by basing on gap fraction distribution, and a second category includes instruments by basing on gap size distribution.
	- *Gap fraction distribution*: LAI can be determine by using canopy image analysis approach (i.e. Digital Plant Canopy Imager CI 100, MVI), or comparing light measurement above canopy with light measurement below canopy (i.e. Accupar, Demon, Licor LAI-2000 Plant Canopy Analyzer). - *Gap size distribution*: this analysis determines LAI by evaluating the proportions of individual ground area, which are directly illuminated and converting them to the LAI value. The Tracing Radiation and Architecture of Canopies (Phaenark C. et al.) instrument and hemispherical photography are examples of instrument based on this analysis

3.6.1.2 Hydrodynamic

3.6.1.2.1 Water depth

Vertical staff gauge were installed at station MT 01 and station MT 04. At station MT 01, the water depth was daily record three times on the morning, afternoon and evening. At station MT 04, the water depth was record two times on the morning and evening every day.

3.6.1.2.2 Hydraulic structure

The location and hydraulic dimensions of the concrete weir is illustrated in Figure 3-8. These parameters were use as the input in MIKE 11 hydrodynamics simulation.

(a)

(b)
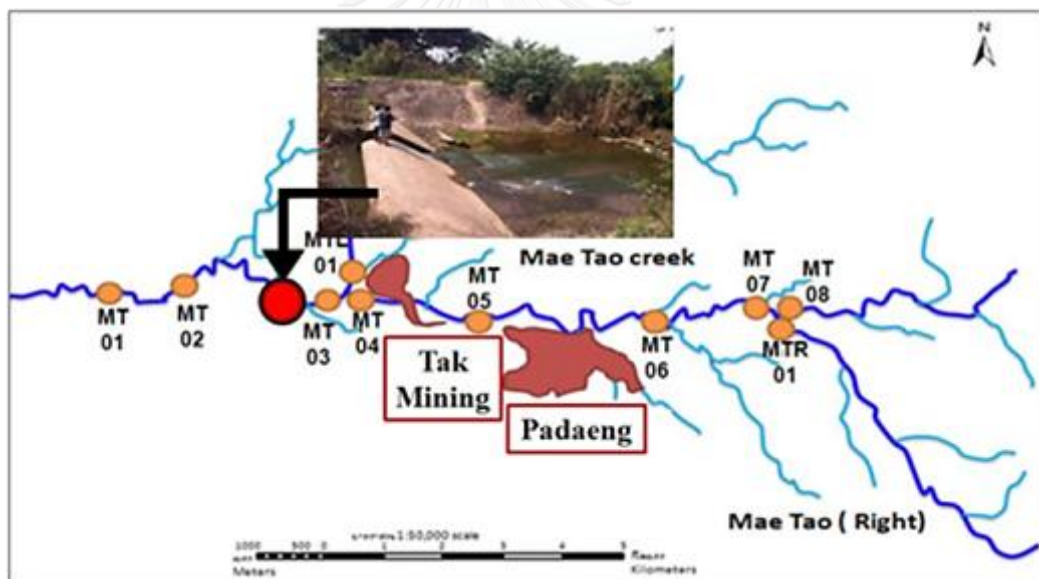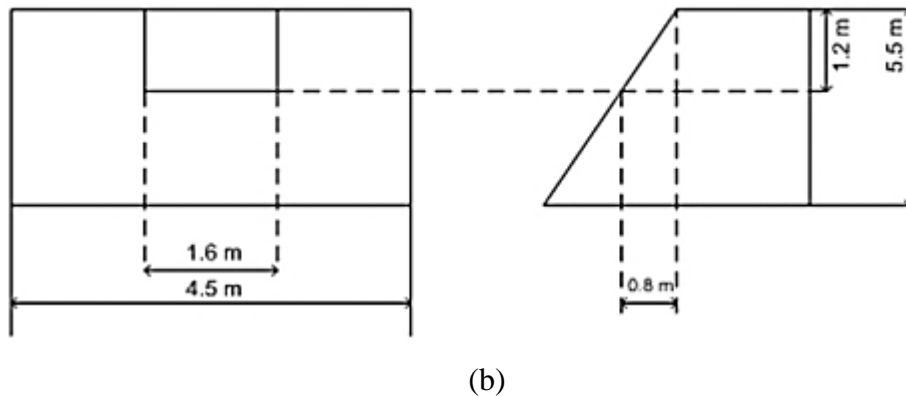
Figure 3-8 (a) Hydraulic structure location (b) Hydraulic structure measurement

3.6.1.3 Hydrodynamic simulation (DHI,2010)

3.6.1.3.1 Overland Flow (OL)

In case that higher precipitation rate than infiltration capacity was found; soil, ponded surface water is generated. It is available as surface runoff to streams. The movement and quantity is depended on topography and the losses from evaporation and infiltration along the flow route.

Overland flow module simulates the movement of ponded surface water across the topography. It can be used for calculating flow on a flood plain or runoff to streams by using the diffusive wave approximation of the Saint Venant equations. The Saint Venant equations are applied for the diffusive wave approximation by reducing momentum losses and lateral inflows perpendicular to the flow direction because of local and convective acceleration. The expression for the two-dimensional diffusive wave approximation to simulate surface runoff, and the velocities and depths relation:

$$uh = K_x \left(-\frac{\partial z}{\partial x} \right)^{\frac{1}{2}} h^{\frac{5}{3}} \tag{3-13}$$

$$vh = K_y \left(-\frac{\partial z}{\partial y} \right)^{\frac{1}{2}} h^{\frac{5}{3}} \tag{3-14}$$

$$z = z_g + h \qquad (3\text{-}15)$$

Where

u	=	flow velocity in x-direction (m/s)
v	=	flow velocity in y-direction (m/s)
K_x	=	Strickler coefficient in x-direction ($m^{1/3}$)
K_y	=	Strickler coefficient in y-direction ($m^{1/3}$)
h	=	flow depth (above ground surface) (m)
z	=	flow depth (referred to datum) (m)
z_g	=	ground surface level (referred to datum) (m)

The Strickler roughness coefficient is equivalent to the Manning M because of the control of surface roughness to the overland flow ratein the simulation. Its inverse is the more conventional Manning's n. The value of n is typicallyin the range 0.01 (smooth channel) to 0.10 (thickly vegetated channel).

$$K = M = \frac{1}{n} \qquad (3\text{-}16)$$

Where

M	=	M ($m^{1/3}$)
n	=	Manning n ($m^{-1/3}$)

The expression for a finite-difference from of the velocity term:

$$\frac{\partial y}{\partial x}(uh) \cong \frac{1}{\Delta x}\left[(uh)_{east} - (uh)_{west}\right] \qquad (3\text{-}17)$$

$$\frac{\partial y}{\partial x}(vh) \cong \frac{1}{\Delta y}\left[(vh)_{north} - (vh)_{south}\right] \qquad (3\text{-}18)$$

Where

$(uh)_{eas}$	=	discharge per unit length across the eastern boundary (m/s)
$(uh)_{west}$	=	discharge per unit length across the western boundary (m/s)
$(vh)_{north}$	=	discharge per unit length across the northern boundary (m$^{1/3}$)
$(vh)_{south}$	=	discharge per unit length across the southern boundary (m$^{1/3}$)
Δx	=	side of length in x-direction (m)
Δy	=	side of length in y-direction (m)

The expression for the flow between grid squares:

$$Q = \frac{K\Delta x}{\Delta x^{\frac{1}{2}}}(Z_U - Z_D)^{\frac{1}{2}} h_u^{\frac{5}{3}} \qquad (3\text{-}19)$$

Where

Q	=	water discharge (m^3/s)
K	=	appropriate Strickler coefficient and water depth (m$^{1/3}$)
Z_U	=	higher depth of the two water levels (referred to datum) (m)
Z_D	=	lower depth of the two water levels (referred to datum) (m)
h_u	=	depth of water that can freely flow into the next cell (m)
x	=	actual water depth minus detention storage

The overland flow equation is calculated from successive over-relaxation (SOR) method to avoid an internal water balance error and divergence of the solution scheme.

$$\sum |Q_{out}| \leq \sum Q_{in} + i\Delta x^2 + \frac{\Delta x^2 h(t)}{\Delta t} \qquad (3\text{-}20)$$

Where

$\sum Q_{out}$	=	sum of outflows (m^3/s)
$\sum Q_{in}$	=	sum of inflows (m^3/s)
i	=	net input to overland flow (net rainfall less infiltration) (m/s)

| $h(t)$ | = | water depth (m) |
| Δt | = | time difference(s) |

3.6.1.3.2 Evapotranspiration (ET)

Total evapotranspiration can be calculated from weather and vegetative data because of canopy interception, drainage from the canopy to the soil surface, canopy evaporation, soil evaporation and transpiration from the vegetation. The primary evapotranspiration model is relied on empirically derived equations that follow a study by Kristensen and Jensen (1975).

3.6.1.3.3 Canopy Interception

Interception is defined as process whereby precipitation is retained on vegetation. The intercepted water directly evaporated no storing to the soil moisture. The interception process is modeled as an interception storage that relies on the vegetation type and its development stage, which is characterized by leaf area index (LAI).

$$I_{\max} = C_{\text{int}} \cdot LAI \qquad (3\text{-}21)$$

Where

I_{max}	=	size of the interception storage capacity (mm)
C_{int}	=	interception coefficient (typical value is about 0.05) (mm)
LAI	=	leaf are index (typical value is between 0 and 7) (-)
		(See Appendix)

3.6.1.3.4 Evaporation from the canopy

The amount of evaporation from the canopy is time-step dependent. The total amount of water stored in the canopy in temperature climates is insignificant correlation to the precipitation, but the semi-arid climates are significant.

$$E_{can} = \min\left(I_{\max}, E_p \Delta t\right) \qquad (3\text{-}22)$$

Where

E_{can} = canopy evaporation (m)

E_p = potential evapotranspiration (m/s)

3.6.1.3.5 Plant Transpiration

The plant transpiration relies on the density of the crop material, the soil moisture content in root zone, and the root density.

$$E_{at} = f_1(LAI) \cdot f_2(\theta) \cdot RDF \cdot E_p \qquad (3\text{-}23)$$

$$f_1(LAI) = C_2 + C_1 \cdot LAI \qquad (3\text{-}24)$$

$$f_2(\theta) = 1 - \left(\frac{\theta_{FC} - \theta}{\theta_{FC} - \theta_w} \right)^{\frac{C_3}{E_p}} \qquad (3\text{-}25)$$

$$RDF_i = \frac{\int_{z_1}^{z_2} R(z)dz}{\int_0^{L_R} R(z)dz} \qquad (3\text{-}26)$$

Where

E_{at} = actual plant transpiration (m³/s)

$f_l(LAI)$ = function based on leaf are index (-)

$f_2(\theta)$ = function based on soil moisture content in root zone(-)

RDF = root distribution function (-)

θ_{FC} = volumetric moisture content at field capacity(-)

θ_w = volumetric moisture content at the wilting point (-)

θ = actual volumetric moisture content (-)

C_1 = empirical evapotranspiration parameter (-)

C_2 = empirical evapotranspiration parameter (-)

C_3 = empirical evapotranspiration parameter(mm/d)

z_1 = depth below the ground surface bounded above layer I (m)

z_2 =   depth below the ground surface bounded above layer I (m)

L_R =   maximum root depth (m)

The roots extraction for transpiration varies over the growing season, and relies on the climatic conditions and the soil moisture conditions.

$$\log R(z) = \log R_0 - AROOT \cdot z \qquad (3\text{-}27)$$

Where

$R(z)$ =   root extraction vary logarithmically with depth (-)

R_0 =   root extraction at the soil surface (-)

$AROOT$=   root mass distribution (-)

z =   depth below ground surface (-)

3.6.1.3.6 Soil Evaporation

The following functions described the soil evaporation:

$$E_S = E_p \cdot f_3(\theta) + \left(E_p - E_{at} - E_p \cdot f_2(\theta)\right) \cdot f_4(\theta) \cdot \left(1 - f_1(LAI)\right) \quad (3\text{-}28)$$

$$f_3(\theta) = \begin{cases} C_2 ; \theta > \theta_W \\ C_2 \dfrac{\theta}{\theta_W} ; \theta_r \leq \theta \leq \theta_W \\ 0 ; \theta < \theta_r \end{cases} \qquad (3\text{-}29)$$

$$f_3(\theta) = \begin{cases} \dfrac{\theta - \dfrac{\theta_W + \theta_{FC}}{2}}{\theta_{FC} - \dfrac{\theta_W + \theta_{FC}}{2}} ; \theta \geq \dfrac{\theta_W + \theta_{FC}}{2} \\ 0 ; \theta < \dfrac{\theta_W + \theta_{FC}}{2} \end{cases} \qquad (3\text{-}30)$$

Where

E_s =   soil evaporation (m/s)

E_{at} =   actual transpiration

C_1 is used in the plant transpiration function, and have and average value of 0.3. C_1 effects the distribution between the soil evaporation and

transpiration: for example; the soil evaporation has a larger relative to the transpiration from a smaller C_1 values in agricultural crop and grass.

C_2; is used in the plant transpiration function, and have and average value of 0.2 for agricultural crops and grass grown on clayey loamy soils. A larger percentage of the actual evapotranspiration will be soil evaporation.

C_3; is used in the plant transpiration and soil moisture function, and is estimated commonly 20 mm/day.

3.6.2 Unsaturated Flow (UZ)

Unsaturated zone is usually heterogeneous and based on cyclic fluctuations in soil moisture that water is replenished with rainfall, eradicated by evapotranspiration and recharge to the ground water table. As a result of the major role during infiltration of gravity, unsaturated flow is primarily vertical. Thus, unsaturated flow in MIKE SHE is calculated only vertically in one-dimension that sufficient on very steep hill slopes with contrasting soil properties in the soil profiles.

A simplified gravity flow is applied to calculate vertical flow in the unsaturated zone. This procedure assumes a uniform vertical gradient and ignores capillary forces. The driving force for water movement in the unsaturated zone is shown as following:

$$h = z + \psi \qquad (3\text{-}31)$$

Where

h	=	hydraulic head (m)
z	=	gravitational head (m)
ψ	=	pressure head (m)

The gravitation head, z (positive upwards) is the elevation of a point above the datum. Atmospheric pressure is defined as reference level for pressure head component (ψ), which is negative under unsaturated conditions due to capillary force and short range adsorption forces between the water molecules and the soil matrix. Nevertheless, the pressure head is not calculated and the driving force is due entirely to gravity in the gravity floe module. So the vertical gradient of the hydraulic head is one.

The volumetric flux is based on Darcy's law:

$$q = -K(\theta)\frac{\partial h}{\partial z}$$ (3-32)

Where

q =   volumetric flux (m^3/s)

$K(\theta)$ =   unsaturated hydraulic conductivity (m/s)

If the soil matrix is incompressible and soil water has a constant density, the continuity equation can be expressed as:

$$\frac{\partial \theta}{\partial t} = -\frac{\partial q}{\partial z} - S(z)$$ (3-33)

Where

θ =   actual volumetric moisture content (-)

S =   root extraction sink term (1/s)

t =   time (s)

3.6.3 Saturated Flow (SZ)

The saturated subsurface flow is calculated from a fully three-dimensional flow in a heterogeneous aquifer by focusing between unconfined and confined conditions. The spatial and temporal variations of the hydraulic head are explained by the three-dimensional Darcy equation.

The three dimensional groundwater-flow is calculated follow by following the 3D finite difference method by the groundwater discharge to the surface water. A three-dimensional saturated porous media is defined the governing flow by:

$$\frac{\partial y}{\partial x}\left(K_{xx}\frac{\partial y}{\partial x}\right) + \frac{\partial y}{\partial x}\left(K_{yy}\frac{\partial y}{\partial x}\right) + \frac{\partial y}{\partial x}\left(K_{zz}\frac{\partial h}{\partial z}\right) - Q = S\frac{\partial h}{\partial t}$$ (3-34)

Where

K_{xx} =   hydraulic conductivity along x axis (m/s)

K_{yy} =   hydraulic conductivity along y axis (m/s)

K_{zz} =   hydraulic conductivity along z axis (m/s)

h =   hydraulic head (m/s)

Q =   source/sink terms (1/s)

S =   specific storage coefficient (1/m)

The potential flow is followed Darcy's law:

$$Q = (\Delta h)C \tag{3-35}$$

Where

Δh =   piezometric head difference (m)

C =   conductance   (m²/s)

Horizontal conductance between node I and i-1:

$$C_{i-\frac{1}{2}} = \frac{KH_{i-1,j,k} KH_{i,j,k} \left(\Delta z_{i-1,j,k} + z_{i,j,k} \right)}{\left(KH_{i-1,j,k} + KH_{i,j,k} \right)} \tag{3-36}$$

Where

$C_{i-\frac{1}{2}}$ =   horizontal conductance (m²/s)

KH =   horizontal hydraulic conductivity (m/s)

Δz =   saturated layer thickness of the cell (m)

The vertical conductance between two cells is calculated from the middle of layer k to the middle of the layer k+1. Thus,

$$C_v = \frac{\Delta x^2}{\dfrac{\Delta z_k}{2K_{z,k}} + \dfrac{\Delta z_{k+1}}{2K_{z,k+1}}} \tag{3-37}$$

Where

C_v =   vertical conductance between two cells (m²/s)

There are two dewatering conditions:

- Dewatered cell below, the actual flow between cell k and $k+1$ will be:

$$q_{k+\frac{1}{2}} = C_{v,k+\frac{1}{2}}\left(z_{top,k+1} - h_k\right) \tag{3-38}$$

- Dewatered cell above, the actual flow from cell k-1 to k will be:

$$q_{k-\frac{1}{2}} = C_{v,k-\frac{1}{2}}\left(h_{k-1} - z_{top,k}\right) \tag{3-39}$$

Where

$\quad q_{k+\frac{1}{2}} \quad = \quad$ the actual flow from cell k to k-1 (m^3/s)

$\quad q_{k-\frac{1}{2}} \quad = \quad$ the actual flow from cell k-1 to k (m^3/s)

The storage capacity is the maximum water content that can be store as ground water in the saturated zone (also known as aquifer) and can be calculated from:

$$\frac{\Delta w}{\Delta t} = \frac{S_2\left(h^n - z_{top}\right) + S_1\left(z_{top} - h^{n-1}\right)}{\Delta t} \tag{3-40}$$

- Confined cells

$$S = \Delta x^2 \Delta z S_{art} \tag{3-41}$$

- Unconfined cells

$$S = \Delta x^2 \Delta z S_{free} \tag{3-42}$$

Where

$\quad \dfrac{\Delta w}{\Delta t} \quad = \quad$ storage capacity (-)

$\quad n \quad = \quad$ time step (-)

$\quad S_1 \quad = \quad$ storage capacity at the start of the iteration at time step (1/m)

$\quad S_2 \quad = \quad$ storage capacity at the last iteration (1/m)

$\quad S \quad = \quad$ storage capacity for the cells (1/m)

3.6.4 Channel Flow

3.6.4.1 Hydrodynamic module

3.6.4.1.1 Continuity equation

$$\frac{\partial A}{\partial t} + \frac{\partial Q}{\partial x} = q \tag{3-43}$$

Where

A	$=$	cross-section area (m^2)
Q	$=$	Discharge (m^3/s)
q	$=$	Lateral inflow per unit width (m^2/s)
x	$=$	distance (m)
t	$=$	time (s)

The continuity equation at grid point j time step $n + \frac{1}{2}$

$$\frac{\partial A}{\partial t} \approx \frac{A_j^{n+1} - A_j^n}{\Delta t} \tag{3-44}$$

$$\frac{\partial Q}{\partial x} \approx \frac{\left(\dfrac{Q_{j+1}^{n+1} + Q_{j+1}^n}{2}\right) - \left(\dfrac{Q_{j-1}^{n+1} + Q_{j-1}^n}{2}\right)}{\Delta x_j + \Delta x_{j+1}} \tag{3-45}$$

Where

Δt	$=$	time difference between time step n and $n + 1$ (s)
Δx	$=$	distance between point j and $j - 1$ (m)

3.6.4.1.2 Momentum equation

$$\frac{\Delta M}{\Delta t} = \frac{\Delta(M \cdot U)}{\Delta x} + \frac{\Delta P}{\Delta x} - \frac{F_f}{\Delta x} + \frac{F_s}{\Delta x} \tag{3-46}$$

Where

$$\frac{\Delta M}{\Delta t} \quad = \quad \text{Mass per unit length} \cdot \text{velocity (representing Momentum)}$$

$$\frac{\Delta(M \cdot U)}{\Delta x} = \quad \text{Momentum} \cdot \text{velocity (representing Momentum flux)}$$

$$\frac{\Delta P}{\Delta x} \quad = \quad \text{Hydrostatic pressure (representing Pressure force)}$$

$$\frac{F_f}{\Delta x} \quad = \quad \text{Force due to bed resistance (representing Friction force)}$$

$$\frac{F_s}{\Delta x} \quad = \quad \text{Contribution in x-direction (representing Gravity force)}$$

Two main momentum equation selections are diffusive wave. Diffusive wave is suitable for relatively steady backwater effects and slowly propagating flood waves. The momentum flux term is ignored because of indifferent tidal flows.

$$\frac{\Delta M}{\Delta t} = \frac{\Delta P}{\Delta x} - \frac{F_f}{\Delta x} + \frac{F_s}{\Delta x} \tag{3-47}$$

3.6.5 Sediment transport simulation

3.6.5.1 Sediment continuity equation

The sediment continuity equation is the sufficient for erosion, deposition, and transport of the non-cohesive sediment to evaluate the bed level changes.

$$\frac{\partial S}{\partial x} + (1-\varepsilon)w \cdot \frac{\partial z}{\partial t} = 0 \tag{3-48}$$

$$s = (q_b + q_s)w \tag{3-49}$$

Where

S	=	sediment transport rate (m^3/s)
t	=	time (s)
w	=	channel width (m)
x	=	longitudinal co-ordinate (m)
z	=	bed level (m)
ε	=	sediment porosity (-)

q_b = bed load transport rate (m³/s)

q_s = suspended sediment transport rate (m³/s)

3.6.5.2 Van Rijn model

According to the Van Rijn model, the sediment is divided into bed load and suspended load by basing on the relative magnitudes of the bed shear velocity and the particle fall velocity.

- Suspended and bed load transport: the velocity of bed shear is more than the particle fall

- Bed load transport: base on rolling and saltation. The rolling occurred when the value of the bed-shear velocity just exceeds the critical value, and saltation is the increasing values of the bed-shear velocity.

- Suspended load transport: base on the depth-integration of the product of the local concentration and flow velocity
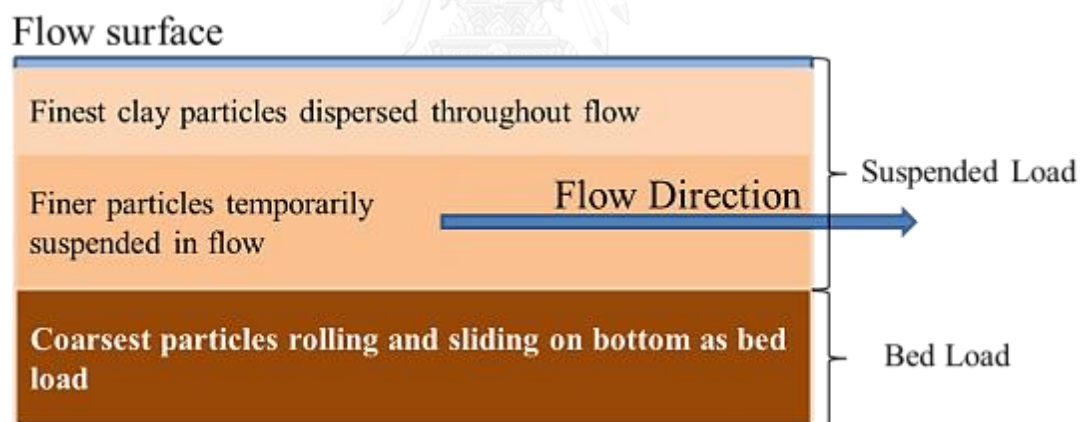
Figure 3-9 Suspended sediment and bed load classification (Pollution Control Department (PCD), 2011)

3.6.5.2.1 Bed load

An expression for bed load transport rate (Van Rijn L.C., 1984a):

$$q_b = u_b \delta_b c_b \qquad (3\text{-}50)$$

Where

q_b =   bed load transport rate (m³/s)
u_{bs} =   the product of particle velocity (m/s)
δ_b =   saltation height (m)
c_b =   Bed load concentration (kg/m³)

The particle velocity and saltation height expressions use the dimension particle diameter and transport stage parameter to express the bed load transport. Saltation is a specific type of particle transport by fluids such as wind or water. It occurs when loose material is removed from a bed and carried by the fluid, before being transported back to the surface which can be calculated by:

$$D_* = d_{50} \left(\frac{s-1}{v^2} g \right)^{\frac{1}{3}} \qquad (3\text{-}51)$$

$$T = \frac{\left(u'_g \right)^2 - \left(u'_{f,cr} \right)^2}{\left(u'_{f,cr} \right)^2} \qquad (3\text{-}52)$$

Where

D_* =   the dimension particle diameter

d_{50} =   the dimension of which 50% are finer (mm)

u'_g =   the bed shear velocity, related to grains (m/s)

$u'_{f,cr}$ =   Shields critical bed shear velocity (m/s)

T =   transport stage parameter

The influence of bed forms is eliminated when drag dose not contribute to bed load transport:

$$u'_g = \frac{\sqrt{g}}{c'} u \qquad (3\text{-}53)$$

$$C' = 10\log\left(\frac{R}{3d_{90}}\right) \tag{3-54}$$

Where

u	=	the mean flow velocity (m/s)
C'	=	Chezy's coefficient related to skin friction (m$^{0.5}$/s)
R	=	the hydraulic radius (or resistance radius) related to the bed (m)
$3d_{90}$	=	considered to be the effective roughness height of the plain bed

An expression for particle velocity and saltation height by solving the equations of motion to a solitary particle:

$$\frac{u_{bs}}{u'_f} = 9 + 2.6\log(D_*) - 8\frac{\theta_c^{0.5}}{\theta} \tag{3-55}$$

$$\frac{u_{bs}}{[(s-1)gd]^{0.5}} = 1.5T^{0.6} \tag{3-56}$$

$$\frac{\delta_b}{d} = 0.3D_*^{0.7}T^{0.5} \tag{3-57}$$

$$C_b = \frac{q_b}{u_{bs}}\delta_b \tag{3-58}$$

Where

u_{bs}	=	particle mobility (m/s)
(δ_b)	=	saltation height (m)
(c_b)	=	bed load concentration

An extensive analysis of flume measurements of bed load transport yielded for the bed load concentration:

$$\frac{c_b}{c_0} = 0.18\frac{T}{D_*} \tag{3-59}$$

Where

  c_0 =   the maximum bed concentration (0.65)

  Combining of an expression for the particle mobility, saltation height, the bed load concentration expresses the bed load transport:

$$\frac{q_b}{\sqrt{(s-1)gd_{50}^{~~3}}} = \frac{0.0537^{2.1}}{D_*^{~0.3}} \qquad (3\text{-}60)$$

$$q_b = \frac{0.0537^{2.1}}{D_*^{~0.3}} \qquad (3\text{-}61)$$

3.6.5.2.2 Suspended load

  The suspended load transport is computed from a reference concentration of bed load transport, expressions, so it expressed by the dimension particle diameter and transport stage parameter (Van Rijn L.C. , 1984b)

$$D_* = d_{50}\left(\frac{(s-1)g}{v^2}\right)^{\frac{1}{3}} \qquad (3\text{-}62)$$

$$T = \frac{\left(u'_g\right)^2 - \left(u'_{f,cr}\right)^2}{\left(u'_{f,cr}\right)^2} \qquad (3\text{-}63)$$

Where

  D_* =   the dimensionless particle diameter

  T =   transport stage parameter

  u'_g =   the bed shear velocity related to the grains (m/s)

  $u'_{f,cr}$ =   the critical bed shear velocity (m/s)

  An expression for a reference level by all sediment transport is bed load:

$$a = 0.5H \qquad (3\text{-}64)$$

Where

a	=	reference level (m)
H	=	the (known) bed from height (m)

$$a = k \qquad (3\text{-}65)$$

Where

k	=	the equivalent sand roughness when the bed from dimensions are unknown or a minimum value of

$$a = 0.01D \qquad (3\text{-}66)$$

Where

D	=	water depth (m)

An expression for the reference concentration:

$$q_b = c_b u_{bs} \delta_b = c_a u_a a \qquad (3\text{-}67)$$

$$u_a = \alpha u_{bs} \qquad (3\text{-}68)$$

Where

c_a	=	reference concentration
c_b	=	the bed concentration
u_{bs}	=	the velocity of bed load particles (m/s)
δ_b	=	the saltation height (m)
u_a	=	the effective velocity at reference level a (m/s)

An expression for combining $\alpha_2 = 2.3$ with the expressions for δ_b and c_b (as functions of D_* and T in Equation 3-51 and 3-52):

$$c_a = 0.0015 \frac{d_{50}}{a} \frac{T^{1.5}}{D_*^{0.3}} \qquad (3\text{-}69)$$

An expression for relating particle size, d_s to the d_{50} and geometric standard deviation, σ_s, of the bed material

$$\frac{d_s}{d_{50}} = 1 + 0.011(\sigma_s - 1)(T - 25); T < 25 \qquad (3\text{-}70)$$

$$\sigma_s = 0.5\frac{d_{84}}{d_{50}} + \frac{d_{50}}{d_{16}} \qquad (3\text{-}71)$$

The expressions for fall velocity by using d_s value:

$$w = \begin{cases} \dfrac{1}{18}\dfrac{(s-1)gd^2}{v}; d < 0.1 \\[2mm] \dfrac{10v}{d}\left\{\left[1 + \dfrac{0.01(s-1)gd^3}{v^2}\right]^{0.5} - 1\right\}; 0.1 \le d \le 1.0 \\[2mm] 1.1[(s-1)gd]^{0.5}; 1.0 < d \end{cases} \qquad (3\text{-}72)$$

The threshold for the initiation of suspension can be determined from the actual flow conditions. Using the overall bed shear stress the criterion implemented in the van Rijn model becomes:

$$\frac{u_f}{w} = \frac{u}{d_s}; 1 < d_s \le 10 \qquad (3\text{-}73)$$

$$\frac{u_f}{w} = 0.4; 10 < d_s \qquad (3\text{-}74)$$

An expression for a suspended parameter Z which expresses the influence of the upward turbulent fluid forces and the downward gravitational forces:

$$Z = \frac{w}{\beta_{Ku'_f}} \qquad (3\text{-}75)$$

$$\beta = 1 + 2\left(\frac{w}{u'_f}\right)^2; 0.1 < \frac{w}{u'_f} < 1 \qquad (3\text{-}76)$$

Where

u_f = the overall bed shear velocity (m/s)

K $\quad=\quad$ von Karman's constant

$\beta \quad=\quad$ a coefficient related to the diffusion of sediment particles

An expression for a modified suspension number Z, which is defined from a single correction factor y:

$$Z' = Z + \psi \tag{3-77}$$

$$\psi = 2.5\left(\frac{w}{u'_f}\right)^{0.8}\left(\frac{c_a}{c_0}\right)^{0.4} \tag{3-78}$$

Where

$c_0 \quad=\quad$ the maximum bed concentration (0.65)

$\psi \quad=\quad$ a function of the main hydraulic parameter

An expression for the suspended load

$$q_s = \int_a^D cudy \tag{3-79}$$

Where

$q_s \quad=\quad$ the suspended load (m^3/s)

$u \quad=\quad$ the current velocity (m/s)

c $\quad=\quad$ the concentration of suspended sediment

$a \quad=\quad$ the thickness of the bed layer which can be approximated by $2d$ model

$D \quad=\quad$ the flow depth (m)

At a distance y above bed level by the logarithmic velocity profile

$$u = 2.5u'_f \ln\left(\frac{30y}{k}\right) \tag{3-80}$$

$$k = 2.5d \tag{3-81}$$

$$c = c_a \left(\frac{D-y}{y} \frac{a}{D-a} \right)^Z \qquad (3\text{-}82)$$

$$Z = \frac{w}{0.4u'_f} \qquad (3\text{-}83)$$

Where

u	=	the current velocity (m/s)
y	=	a distance y (m)
u'_f	=	the friction velocity and the equivalent sand roughness (m/s)
c_a	=	the concentration at the bed
D	=	depth of water (m)
y	=	distance from bed level (m)
Z	=	the Rouse number
w	=	the settling velocity of the suspended material (m/s)

Combining the expression describing the velocity and concentration profiles with the expression for Z and y gives the following expression:

$$q_s = FuDc_a \qquad (3\text{-}84)$$

$$F = \frac{\left(\dfrac{a}{d} \right)^{z'} - \left(\dfrac{a}{D} \right)^{1.2}}{\left(1 - \dfrac{a}{D} \right)^{z'} (1.2 - Z')} \qquad (3\text{-}85)$$

3.6.5.2.3 Additional equations

Relative density or specific gravity of sediment

$$S = \frac{\rho_{sediment}}{\rho_{water}} \qquad (3\text{-}86)$$

Where

S = relative density

$\rho_{sediment}$ = density of sediment (kg/m^3)

ρ_{water} = density of water (kg/m^3)

3.7 Overland flow sediment transport module

The combination of MIKE11 and MIKE SHE give a result for sediment transport for the channel flow of the Mae Tao Creeks, thus the sediment transport via the overland flow over the Mae Tao Basin must be separately calculated due to the limitations of the application.

Overland flow sediment transport (OfSET) has a capability to estimate the amount of cohesive sediment which occurs by the overland flow. The OfSET module contains three main parts which are

- Cohesive sediment erosion calculation
- Deposition and suspension calculation
- Sediment transport direction algorithm

Figure 3-10 illustrated the compatibility between the results from MIKE SHE and OfSET and the overall process of OfSET module calculation and Figure 3-10 demonstrated the summary of OfSET module's calculation.
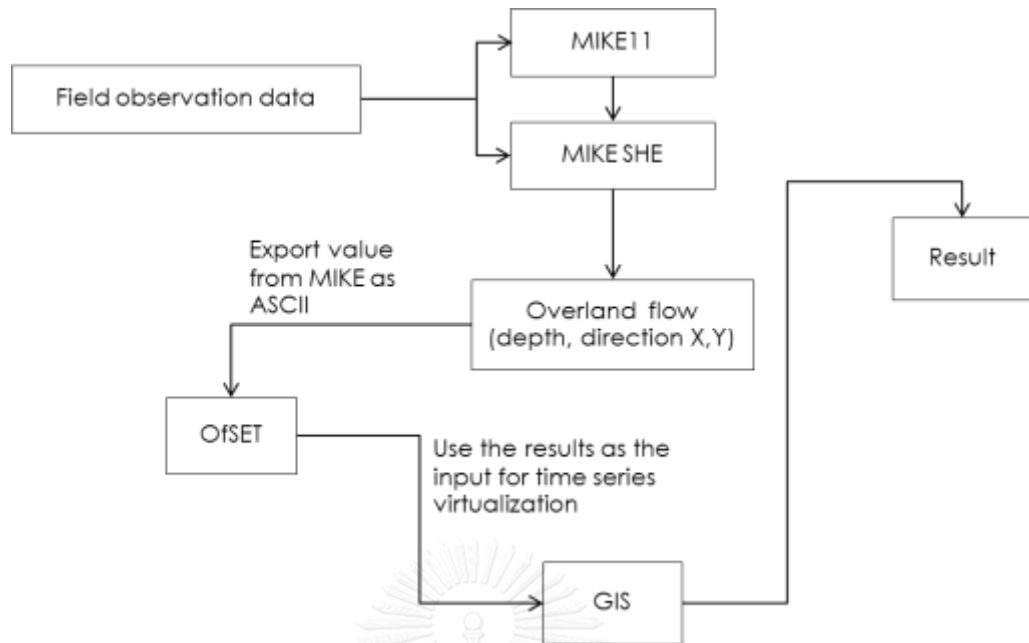
Figure 3-10 Compatibility between MIKE applications and OfSET module
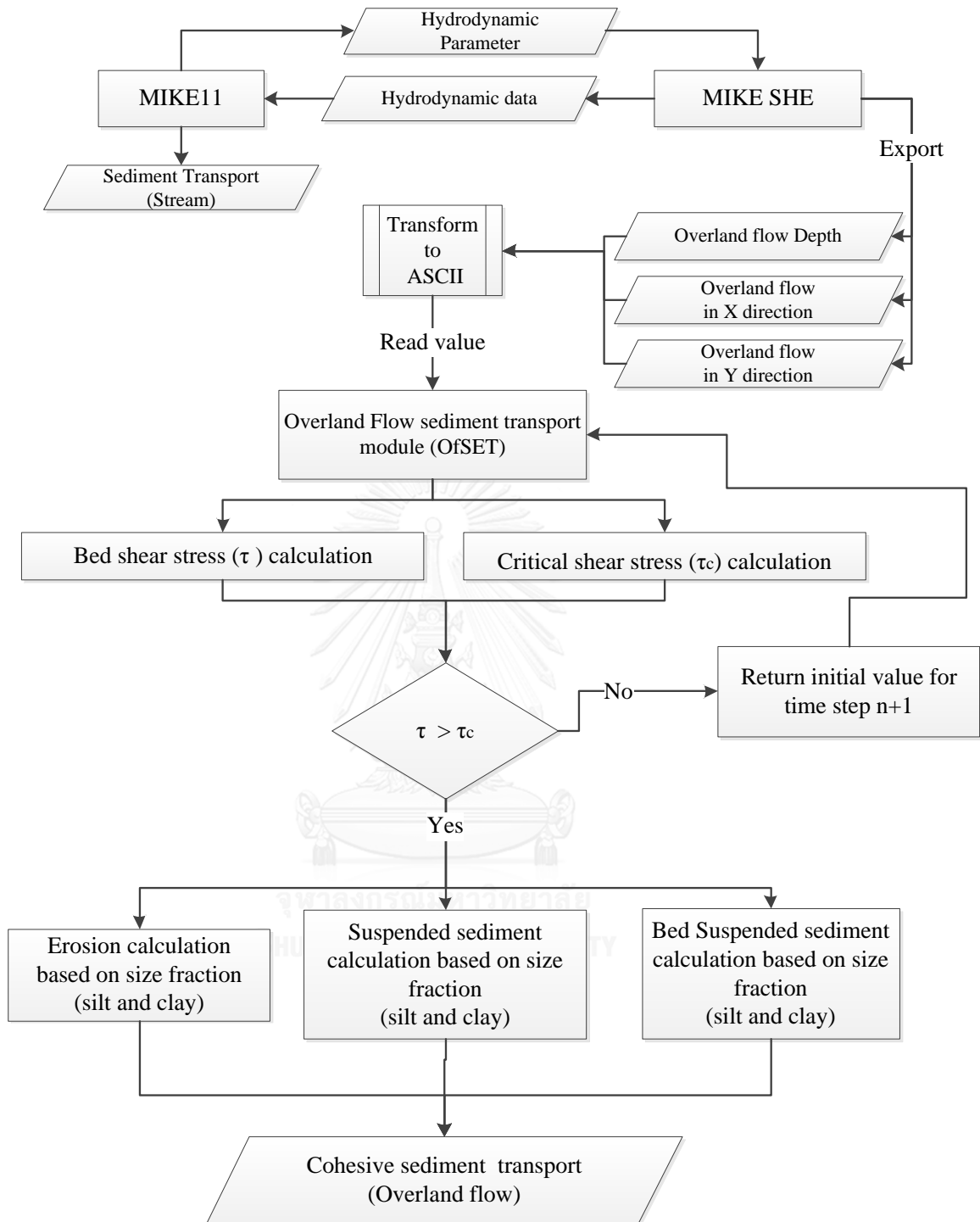
Figure 3-11 Summary of OfSET module's calculation

3.7.1 Cohesive sediment Erosion

The formula for calculating the surface erosion, used in this study, was established by Ariathurai (Ariathurai, 1974) by fitting the experimental plots of erosion rate versus applied shear stress of the overland flow by Partheniades (Partheniades E., 1962).

$$Q_{se} = \begin{cases} M_{se} \dfrac{\tau - \tau_{se}^c}{\tau_{se}^c}; \tau \geq \tau_{se}^c \\ 0; \tau < \tau_{se}^c \end{cases} \qquad (3\text{-}87)$$

$$M_{se} = 0.55 \left(\frac{\rho_b}{100} \right)^3 \qquad (3\text{-}88)$$

Where

     Q_{se} =   Surface erosion rate (kg/m²s)

     τ , τ_{se}^c =   Bed shear stress and critical surface erosion shear stress (Pa)

     M_{se} =   Surface erosion rate constant (kg/m²s)

     ρ_b =   Bulk density of soil (kg/m³)

For applied shear stress at time step n

$$\tau = \gamma D_{of} S_0 \qquad (3\text{-}89)$$

Where

     γ =   Weight density of water (N/ m²)

     D_{Of} =   Depth of the water (m)

     S_0 =   Slope of the water surface

Due to the characteristic of the study area, where contains some unreachable area; so, the field observation for the initial parameter of critical shear stress was not accomplished. The secondary data from Land Development Department of Thailand (LDD) was used to calculate critical shear stress based on the equation of Mitchener (Mitchener H. and Torfs H., 1996) .Equation 3-90 demonstrates the critical shear stress proposed by them.

$$\tau_{se}^c = 0.015(\rho_b - 1000)^{0.84} \qquad (3\text{-}90)$$

The bulk density of soil is related to the land cover practice (C factor) in RUSLE. By literature review the references of bulk density of each type of land cove can be retrieved and directly used as the input for critical shear stress' calculation. The value of bulk density, used in this study is mentioned in Appendix (D-5)

3.7.2 Overland flow sediment transport

The algorithm in OfSET module is developed from the previous study of Rosalía (2002). CASC2D is the base mathematical model for the estimation of overland flow sediment transport which has a capability to simulate the revised upland erosion and sediment routing. In CASC2D, the formula suggested by Julien (*et al.*, 1995), was applied to estimate the total erosion of bare soil. This equation is shown in Equation 3- 91.

$$Q_{usd} = 23210 S_0^{1.66} q^{2.035} \frac{K}{0.15} CP \qquad (3\text{-}91)$$

Where

Q_{usd} = unit sediment discharge (tons/m/s)

q = unit flow discharge (m^2/s)

K = Soil erodibility factor in the RUSLE equation

C = Cover management factor in the RUSLE equation

P = Conservation practice factor in the RUSLE equation

In this study, the cohesive sediment transport was focused so the relationship between Q_{se} and q_s can be derived as shown in Equation 3-92.

$$q_s = \frac{Q_{se} w}{1000} \qquad (3\text{-}92)$$

Where

w = grid cell size (m)

For a grid of cell size, w, and for a time interval, dt, the total volume (in m3) of sediment coming from a cell is calculated as

$$Q_{se\_out} = \frac{0.37Q_{se}w^2dt}{1000} \tag{3-93}$$

In addition for every sediment transport incident, there are some sediment movements, resulting from advection. The rate of mass transport by advection can be estimated by the product of sediment concentration and the velocity component (Julien P.Y. et al., 1995)

$$q_{ADVi} = AVC_i \tag{3-94}$$

Where

q_{ADVi} = size fraction i sediment transport (m^3/ s)

A = flow area (m^2)

V = average flow velocity (m/s)

C_i = suspended size fraction i concentration of particle in water

3.8 Cadmium migration flux estimation

3.8.1 Cadmium migration in stream sediment

The cadmium transport in the stream sediment (mg/season) can be calculated from the following equation

$$Cadmium\,transport = S_{bd}\rho_{bd}[Cd]_{bd} + S_{ss}\rho_{ss}[Cd]_{ss} \tag{3-95}$$

Where

S_{bd} = accumulated bed load transport (m^3/season)

S_{ss} = accumulated suspended sediment transport (m^3/season)

ρ_{ss} = density of suspended sediment (kg/m^3)

ρ_{bd} = density of bed load (kg/m^3)

$[Cd]_{bd}$ = cadmium concentration in bed load (mg/kg)

$[Cd]_{ss}$ = cadmium concentration in suspended sediment (mg/kg)

3.8.2 Cadmium migration in overland flow sediment

The cadmium transport in the overland flow sediment (mg/season) in each particle size distribution can be calculated from the following equation.

$$Cd_{total} = \sum_{i=1}^{3}\left[(Cd_i)(OfVol_i)\right] \qquad (3\text{-}96)$$

Where

Cd_{total}	=	total cadmium transport by overland flow (kg)
Cd_i	=	cadmium concentration in size fraction i
$OfVOL_i$	=	Total suspendedvolume (m^3)

3.9 Statistical Analysis

3.9.1 Sensitivity Analysis

To examine a sensitivity of model parameter which can have the impact on hydrodynamic model, the sensitivity analysis was computed by following the study of Lanhart (2002). Sensitivity index (I) was evaluated for assessing the model parameter sensitivity by expressing a ratio of relative change between model output and model parameter. I can be calculated by Equation (3.77) the sensitivity of model can be classified into four classes as displayed in Table 3-7
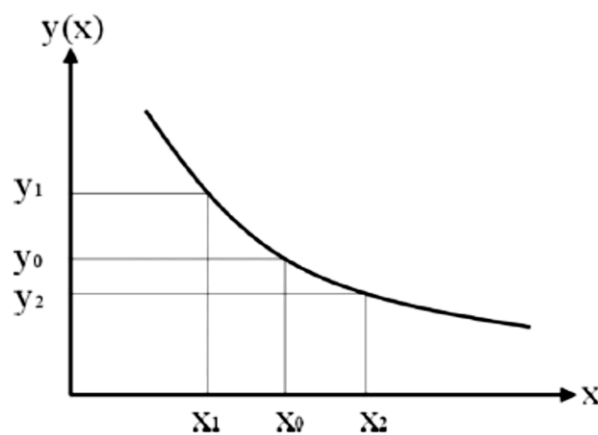
Figure 3-12 Correlation between model output (y) and model parameter (x)

$$I = \dfrac{\dfrac{y_2 - y_1}{y_0}}{\dfrac{2\Delta x}{x_0}} \qquad (3\text{-}97)$$

$$\Delta x = x_0 - x_1 \qquad (3\text{-}98)$$

$$\Delta x = x_2 - x_0 \qquad (3\text{-}99)$$

Where

I	=	sensitivity index (dimensionless),
x_0	=	initial value of parameter x,
y_0	=	model output calculates with x_0,
y_1	=	model output calculates with x_1, and
y_2	=	model output calculates with x_2

Table 3-7 Sensitivity classes

Class	Sensitivity index (*I*)	Sensitivity
I	0.00 - 0.04	Small to negligible
II	0.05 - 0.19	Medium
III	0.20 – 0.99	High
IV	≥ 1.00	Very high

The parameters, which affected in the water discharge and overland flow discharge were analyzed the sensitivity in this study. The parameters (x) that were applied to sensitivity analysis contained overland flow, unsaturated flow and saturated zone parameters (see values in Appendix D, Table D-1). The Δx was determined as a half of parameter x by applying for all parameter. The model output (y_0, y_1, and y_2) are water discharge in Sep 2011 because there was highest precipitation for determining the effect of parameters change to water discharge.

3.9.2 Uncertainty Analysis

Uncertainty is the quantification of ambiguity that exists in the result of any simulation. Each parameter can undermine a simulation result, depending on their sensitivity. Since simulation can never be made under perfect conditions as the real scheme, errors and uncertainties can occur by the most sensitive parameter, resulting in the range of possibility in simulation's result.

According to the study procedure, the observation of suspended sediment can be done one once in dry season and another one during the wet season each year. Due to this limitation, the calculation factor was identified as high uncertainty input for sediment transport simulation.

In addition, concentration of suspended sediment was a significant key to estimate calculation factor in sediment transport module. The calculation factor is applied to compute sediment transport rates as correction factors in sediment transport module. The calculation factor can be calculated from the ratio of measured suspended sediment concentration and simulated suspended sediment, and approximated as 1(Thamjesda 2012).

The concentration profile of suspended sediment is fluctuated with water depth, as displayed in Figure 3-6. Thus, the reference concentration can be estimated from Equation (3.80). For uncertainty analysis, the highest and lowest overland flow depth and ground water depth were used to calculate the calculation factor, which was applied to simulate the possible accumulated sediment transport. Figure 3- 13 demonstrates the process of uncertainty analysis in this study.

$$\frac{c}{c_a} = \left(\frac{a}{d-a}\right)^z \left(\int_a^{0.5d} \left(\frac{d-z}{z}\right)^z \ln\frac{z}{z_0} \, dz + \int_{0.5d}^{d} e^{-4z\left(\frac{z}{d}-0.5\right)} \ln\frac{z}{z_0} dz \right) \quad (3\text{-}100)$$

Where

c	$=$	suspended sediment concentration
c_a	$=$	reference concentration
a	$=$	reference level
d	$=$	depth (m)
z	$=$	vertical coordinate (m)
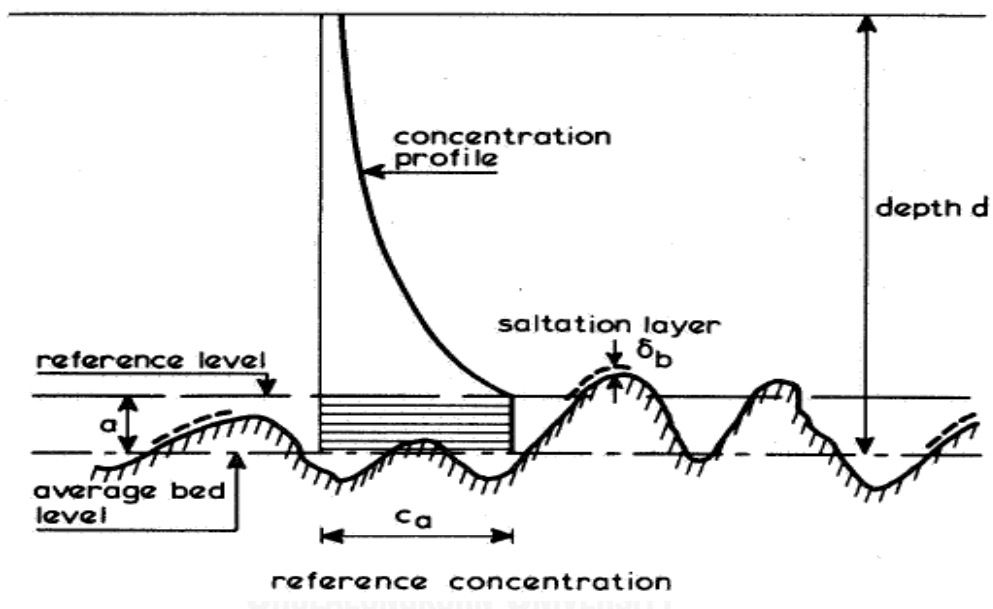
Figure 3-13 Sketch of concentration profile (Van Rijn, 1984b)

The process of uncertainty analysis in this study is based on the calculation for total sediment transport in each season. The sensitive parameters, classified in sensitivity analysis, are used as the input for verifying the uncertainty scenarios. In keeping with, sensitivity analysis' result, the range of simulation results occurs as maximum and minimum total potential sediment transport over the Mae Tao Basin area. From the uncertainty in simulation result, the uncertainty in cadmium transport can be calculated in the same procedure as sediment transport.
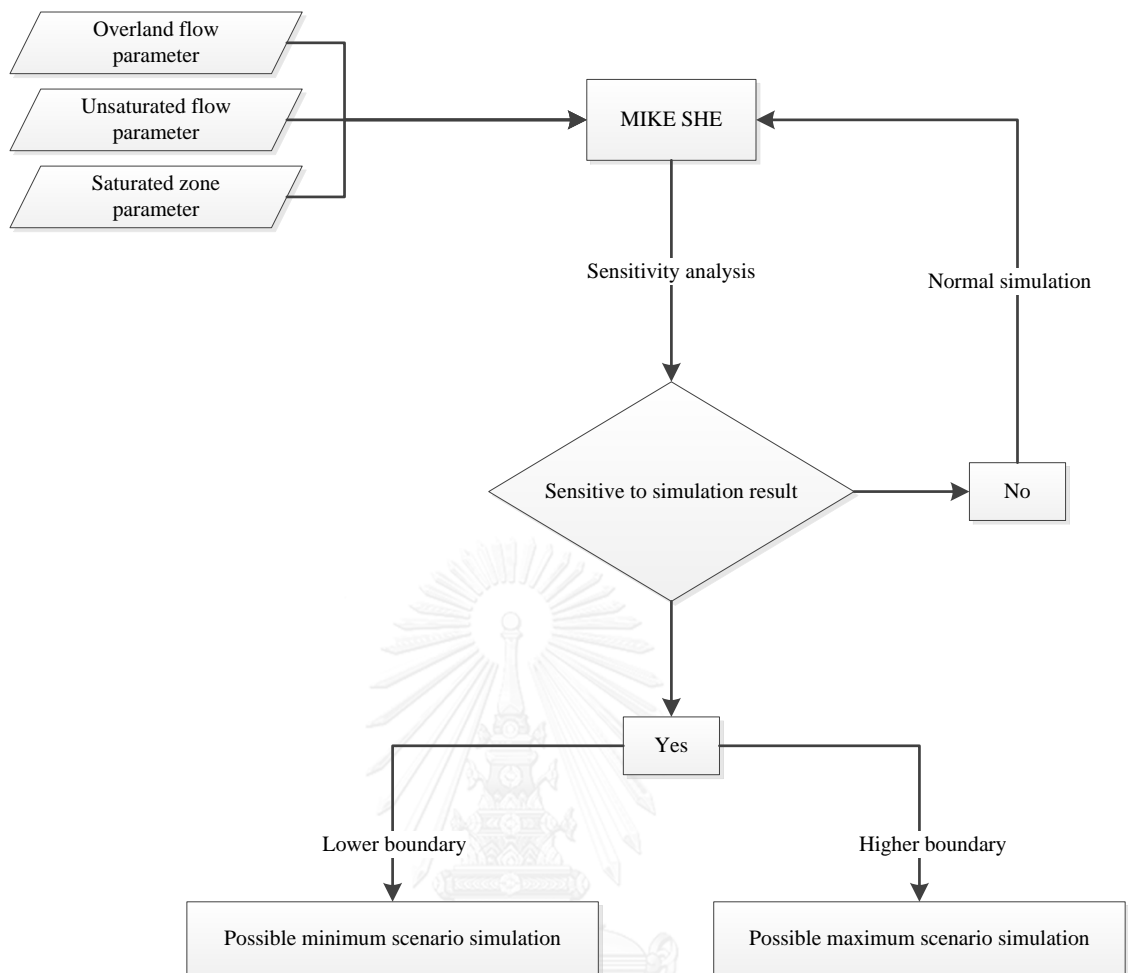
Figure 3-14 Uncertainty analysis process of the study

3.10 Potential cadmium contributor estimation

The estimation of the potential cadmium contributor is based on Eq.3-100. According to the capability of MIKE11and MIKE SHE application, the flux of total sediment, transported by the Mae Tao Creeks, can be simulated as the accumulated sediment during each season. The designation of the potential cadmium contributor can be accomplished by comparison between the fluxes of total cadmium transport over the Mae Tao Basin in the stream sediment and the overland flow sediment from OfSET module

$$J_{Creek}^{C} = J_{Area}^{C} + J_{point\,source}^{C} \qquad (3\text{-}100)$$

While

J_{Creek}^{C} =   Flux of total contaminants, transported into receiving water or a creek in the area (Obtained from MIKE SHE simulation)

J_{Area}^{C} =   Maximum flux of total contaminants, exposed by area source (Obtained from OfSET's simulation)

$J_{Point\,source}^{C}$ =   Flux of total contaminants, exposed by point source

CHAPTER 4

Result and discussion

4.1 Field observation result

4.1.1 pH observation of the water in the Mae Tao Creeks

Table 4-1 demonstrates the field observation data which were obtained from the Mae Tao Creeks during 2012- 2014. The data from both wet and dry seasons were investigated in order to identify the solubility of the water. The results from both seasons indicate the same pattern of water quality. A slightly alkali ranges from 8.07 ±0.00 to 9.19 ±0.17were validated in wet and dry seasons. These pH values refer to an insoluble form of cadmium in the Creeks, influenced by adsorption to sediments (Huynh-Ngoc et al., 1988).

Conductivity refers to water's capability to pass electrical flow. This term is related to the concentration of ions in the water. These conductive ions come from dissolved salts and inorganic materials such as alkalis, chlorides, sulfides and carbonate compounds. According to the observed conductivity, the Mae Tao Creek have more ability to transport soluable ion in dry season.

Dissolved oxygen (DO) in the water is an imperative determinant of water quality. In addition to DO depletion, degradation of organic matter in the sediment results in the release of nutrients and metals, such as ammonium, phosphorus, nitrogen, iron, and manganese, into the water (Gunnison, Chen, and Brannon 1983). Along with the observation results the average dissolved oxygen in the Mae Tao Creek is higher in the wet season.Since, Thai standard of dissolved oxygen in water is preferred to range from 5-8 ppm, so during the dryseason, some area of the Mae Tao Creek demonstrates a low quality of water due to the low flow rate especially at the down stream of the creek (Thamjesda, 2012)

Table 4-1 Observation data from the Mae Tao Creeks during 2012-2013

Station	Field Measurement data					
	Observation Period					
	Dry season			Wet season		
	pH	DO(mg/L)	Conductivity (μS)	pH	DO (mg/L)	Conductivity (μS)
MT01	8.66±0.02	4.85±0.09	456.0±0.1	8.56±0.02	5.62±0.00	340.0±0.0
MT02	8.57±0.01	6.39±0.02	437.6±1.1	8.15±0.00	8.78±0.00	340.0±0.0
MT03	8.93±0.05	9.50±0.05	428.0±0.0	8.95±0.01	7.35±0.00	305.0±0.7
MT04	9.19±0.17	6.29±0.00	442.7±1.2	8.67±0.00	8.61±0.01	322.0±0.0
MTR01	8.56±0.07	4.20±0.00	530.0±0.0	8.93±0.00	7.99±0.00	410.6±0.2
MT05	8.60±0.00	10.10±0.00	456.0±0.0	8.07±0.00	8.41±0.00	210.0±0.0
MT06	8.37±0.00	9.84±0.02	401.5±0.5	8.74±0.03	8.54±0.00	401.0±0.0
MT07	8.58±0.00	5.38±0.01	543.0±0.0	8.77±0.01	4.59±0.01	460.0±0.5
MTL01	8.80±0.00	10.96±0.02	450.9±0.9	8.90±0.00	8.23±0.03	408.4±0.1
MT08	8.75±0.01	5.36±0.00	499.0±0.0	8.24±0.00	7.21±0.20	399.7±0.6

4.2 Laboratory results

4.2.1 Grain size distribution of stream sediments

Bed load samples were examined for the grain size distribution based on ASTM C136-06 and ASTM D422-63. Therefore, the observation results from ten stations are shown in Table 4-2 for dry season and Table 4-3 for wet season.

The Unified Soil Classification System (USCS) method was applied to classify the characteristics of the bed load samples. Following the USCS' method, bed load samples percentage passing sieve No. 200 were less than 50% in all stations, so the bed load is classified as coarse-grained particles. The coarse-grained particles were entirely classified as sand or gravel type by coarse fraction (CF), as shown in Equation (3.1). (Forstner U. and Salomons W.; Groot A.J. et al., 1982; Salomons M., 1980).

Table 4-2 Grain-size distribution of sediment from observation station (dry season 2012-2013)

Sieve	Mesh No.	Sieve Opening (mm)	Mean size (mm)	Weight of sediment (g)									
				Station MT01	Station MT02	Station MT03	Station MT04	Station MTR01	Station MT05	Station MT06	Station MT07	Station MTL01	Station MT10
Weight of sample before sieving				500	500	500	500	1000	500	500	1000	1000	500
1	3/4"	19	19	0	0	0	0	0	0	0	0	0	0
2	3/8"	9.5	14.25	0	0	0	0	0	0	0	0	0	0
3	#4	4.75	7.125	2.8	2.6	51.9	171.1	316.9	4.5	0.5	210.3	542.3	87.1
4	#10	2	3.375	3.4	1.2	102.1	33.8	310.6	8.5	7.2	276.2	160.7	102.3
5	#20	0.85	1.425	1.1	0.7	28.5	5.4	45.2	2.8	11.2	47.7	23.7	19.3
6	#35	0.5	0.675	16.2	18.2	178.8	47.9	180.3	52	127.3	273.4	146.6	149.4
7	#70	0.231	0.366	384.2	288.5	122.9	189.4	90.8	305.8	319.5	181.5	111.3	136.6
8	#100	0.15	0.191	80.9	134.5	13.5	35.4	29.1	96.3	35.4	0	11.2	3.6
9	#150	0.1	0.125	4.1	32.9	3.2	5.5	9.8	20.7	4.7	3.3	3.6	4.6
10	#200	0.075	0.088	5	10.8	0.8	1.6	5.6	6.8	1.4	1.1	1.6	0.9
Receiver		-	0.075	6.1	10.6	1.5	2.2	17.5	7.9	1.1	7.9	3.2	0
Total (g)				503.8	500	503.2	492.3	1005.8	505.3	508.3	1001.4	1004.2	503.8
Loss (g)				-3.8	0	-3.2	7.7	-5.8	-5.3	-8.3	-1.4	-4.2	-3.8
Loss(%)				-0.76	0	-0.64	1.54	-0.58	-1.06	-1.66	-0.14	-0.42	-0.76
%Passing Sieve No.200				1.22	2.12	0.3	0.44	1.75	1.58	0.22	0.79	0.32	0
F = % Coarser than sieve No. 200				98.79	97.88	99.7	99.55	98.26	98.44	99.78	99.21	99.68	100
C = % Coarser than sieve No. 4				0.56	0.52	10.31	34.76	31.51	0.89	0.1	21	54	17.29
CF = Coarse Fraction				0.01	0.01	0.1	0.35	0.32	0.01	0	0.21	0.54	0.17
Stream sediment categorization				SAND	SAND	SAND	SAND	SAND	SAND	SAND	SAND	GRAVEL	SAND

Table 4-3 Grain-size distribution of sediment from observation station (wet season 2012-2013)

Sieve	Mesh No.	Sieve Opening (mm)	Mean size (mm)	Weight of sediment (g)									
				Station MT01	Station MT02	Station MT03	Station MT04	Station MTR01	Station MT05	Station MT06	Station MT07	Station MTL01	Station MT10
Weight of sample before sieving				500	500	500	500	500	500	500	500	500	500
1	3/4"	19	19	0	0	0	0	0	0	0	0	0	0
2	3/8"	9.5	14.25	0	0	0	0	0	0	0	0	0	0
3	#4	4.75	7.125	0	92.75	156	3.2	273.1	76.2	5.2	0.3	222.6	2.2
4	#10	2	3.375	0.6	197.2	115.5	8.4	154.4	58.3	4.2	1.2	69.1	20.4
5	#20	0.85	1.425	0.2	32.1	11.1	8	19	11.4	2.5	0.8	11.5	13.2
6	#35	0.5	0.675	7.9	93.1	68.8	189.7	21.2	79.4	87.7	24.7	70.7	108.4
7	#70	0.231	0.366	359	47.3	82.6	200.2	9.4	184.4	329.3	368.1	76.4	195.2
8	#100	0.15	0.191	110.4	9.5	19.2	67.4	2.2	44	34.2	11.5	18.4	113.1
9	#150	0.1	0.125	18.82	10.6	22.8	7.2	12.8	28.3	19.9	84.1	9.5	37.23
10	#200	0.075	0.088	0.4	1.7	9.3	6.3	12.2	5.8	5.5	4.4	5	9.1
Receiver	-		0.075	3.3	16.3	14.8	18.6	6.3	14.6	14.9	5.2	16	1.7
Total (g)				500.62	500.55	500.1	509	510.6	502.4	503.4	500.3	499.2	500.53
Loss (g)				-0.62	-0.55	-0.1	-9	-10.6	-2.4	-3.4	-0.3	0.8	-0.53
Loss(%)				-0.12	-0.11	-0.02	-1.8	-2.12	-0.48	-0.68	-0.06	0.16	-0.11
%Passing Sieve No.200				0.66	3.26	2.96	3.72	1.26	2.92	2.98	1.04	3.2	0.34
F = % Coarser than sieve No. 200				99.34	96.74	97.04	96.35	98.77	97.09	97.04	98.96	96.79	99.66
C = % Coarser than sieve No. 4				0	18.53	31.19	0.63	53.49	15.17	1.03	0.06	44.59	0.44
CF = Coarse Fraction				0	0.19	0.32	0.01	0.54	0.16	0.01	0	0.46	0
Stream sediment categorization				SAND	SAND	SAND	SAND	GRAVEL	SAND	SAND	SAND	SAND	SAND

The CF factor, calculated from the size distribution result were less than 0.5 almost sampling stations. Consequently, the bed sediment in the Mae Tao Creek could be almost categorized as sand, but classified as gravel in a few station during both the dry and wet season. Figure 4-1 and Figure 4-2 demonstrates the size distribution curve of the bed load samble from dry and wet season respectively.

According to the size distribution curves, the size distributions of the stations are differences in wet and dry season. For exampke, station MTR01 was classified as uniform graded particle, while in wet season, the size distribution at this station turned to be a uniform graded particle. This incident occurs by the effect of the differnces of the flow rate of the between dry and wet season. Since the flow rate of the right branch of the Mae Tao Creek are naturally smaller compare to the main branch especially in the dry season so the movement of bigger particle can be taken place during wet season, resulting in the change of sand particle into gravel as can be seen in Table 4 -2 and 4 -3.
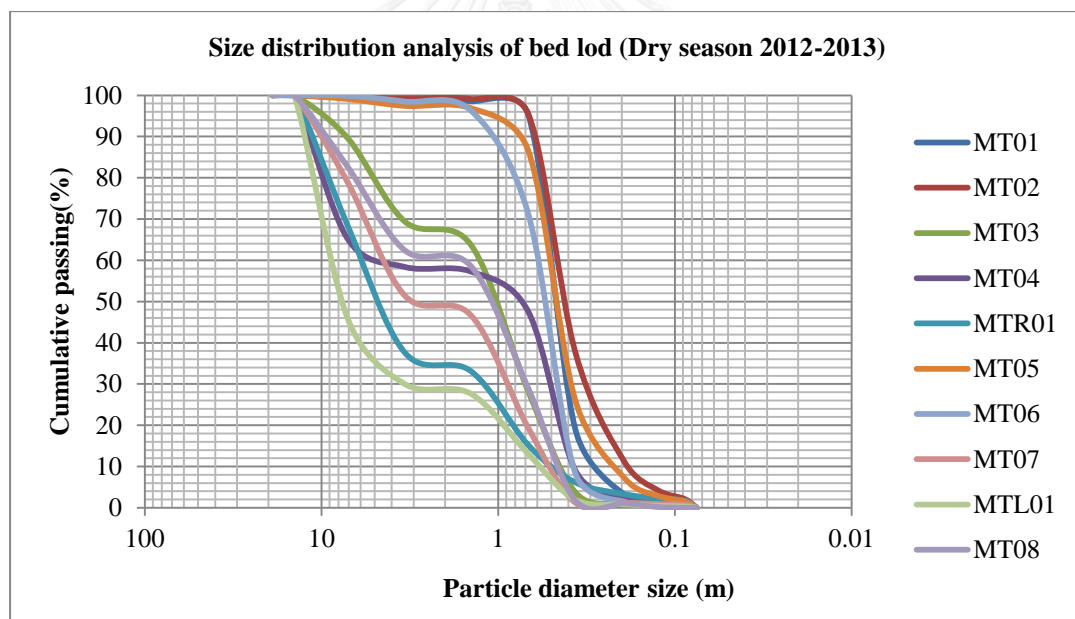
Figure 4-1 Size distribution analysis of bed load (Dry season 2012-2013)
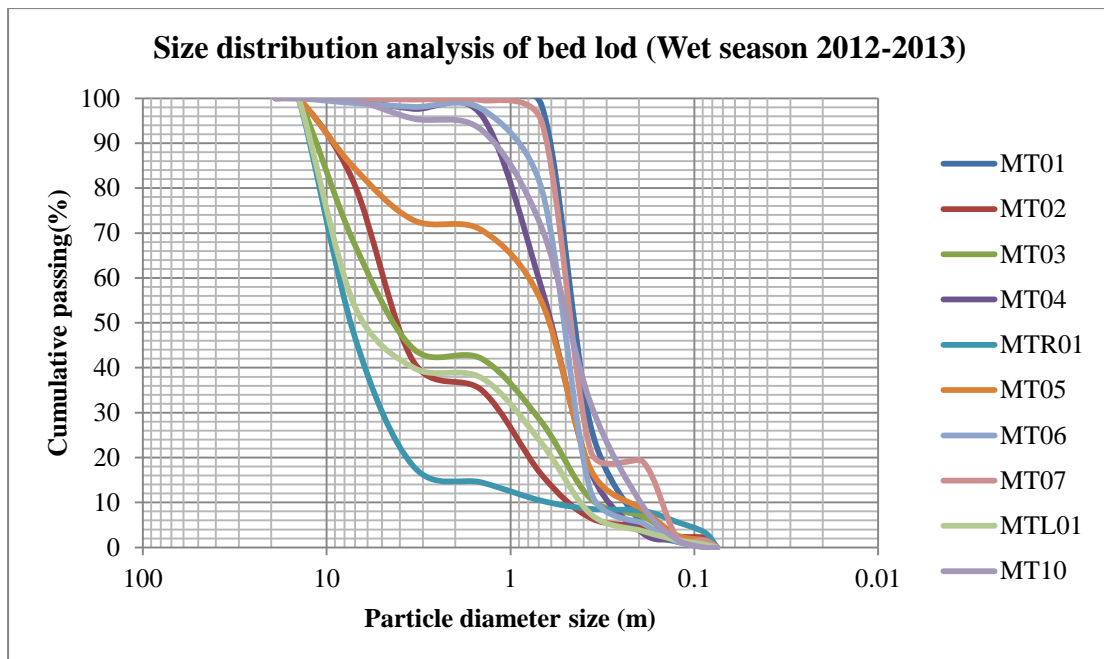
Figure 4-2 Size distribution analysis of bed load (Wet season 2012-2013)

4.2.3 Cadmium distribution in stream sediments

4.2.3.1 Cadmium distribution in suspended sediment

Suspended sediments from ten stations were monitored and analyzed along the Mae Tao Creek by following EPA method 3050A. After that, the total cadmium concentrations were completely analyzed by GFAAS. Figure 4-3 shows the total cadmium concentrations in suspended sediment during the dry and wet seasons of the study period.

The cadmium concentration, observed from the Mae Tao Creeks ranged from 0.58 to 17.50 mg/kg in the dry season and ranged from 0.31 to 65.85 mg/kg in the wet season. High cadmium contaminations were detected at upstream before the creeks entering the mining production area. Station MT06 contains the highest cadmium contamination level among the others.

Thamjesada (2012) detected that high cadmium concentration at the upstream of the Mae Tao Creeks which a highest range from 5.76 mg/kg to 112.4 mg/kg of cadmium concentration. Comparing between these two periods of the study, the high content of precipitation during 2011 to 2012 study period is one of the causes of high contamination of cadmium in the Mae Tao Creeks.

It may be the result from weathering process especially upland erosion and human activities which is resulting as high level of cadmium contamination releasing into environment phases during storm incident. In concurrent with the result

of the RUSLE estimation, It could be described that deforestation for crop plantations especially cornfield, can raise soil and ore erosions due to lack of covering practice in natural ore deposit area (PCD, 2011).

According to the Probable Effect Levels (PELs) standard of the Canadian Environmental Quality Guidelines established by the Canadian Council of Ministers of the Environment was applied to compare the results (PCD, 2011). In comparison with the PELs standard which allowed levels of cadmium contamination lower than 3.5 mg/kg (CCME, 2002), most suspended sediment from upstream station were complied with the standard.

4.2.3.2 Cadmium distribution in size fraction of bed load

Cadmium has high capability on accumulating in small size particles in the sediments)   while the large grain particles usually have low potential on the accumulation of the heavy metal Therefore, cadmium distribution was investigated by bed load sieving with sieve No. 65, 100, 150 and 200 both in dry and wet seasons.

The results for cadmium distribution in each bed load particles size are displayed in Table 4-4 to Table 4-5 for dry season and wet season. The results showed that the cadmium concentrations were distribution in every fraction for both dry and wet season. The smallest size (0.075- mm or 200 mesh opening) of bed load at station MT07 were the highest accumulated cadmium at 61.80 mg/kg.

Despite the fact that heavy metals are naturally occur in the coarse-grained particles such as sand, but the contaminant still contain the highest concentration in the fine-grained particle especially silt and clay both on natural and contamination metals Figure 4-4 demonstrated the total cadmium distribution in the bed load during the study period.
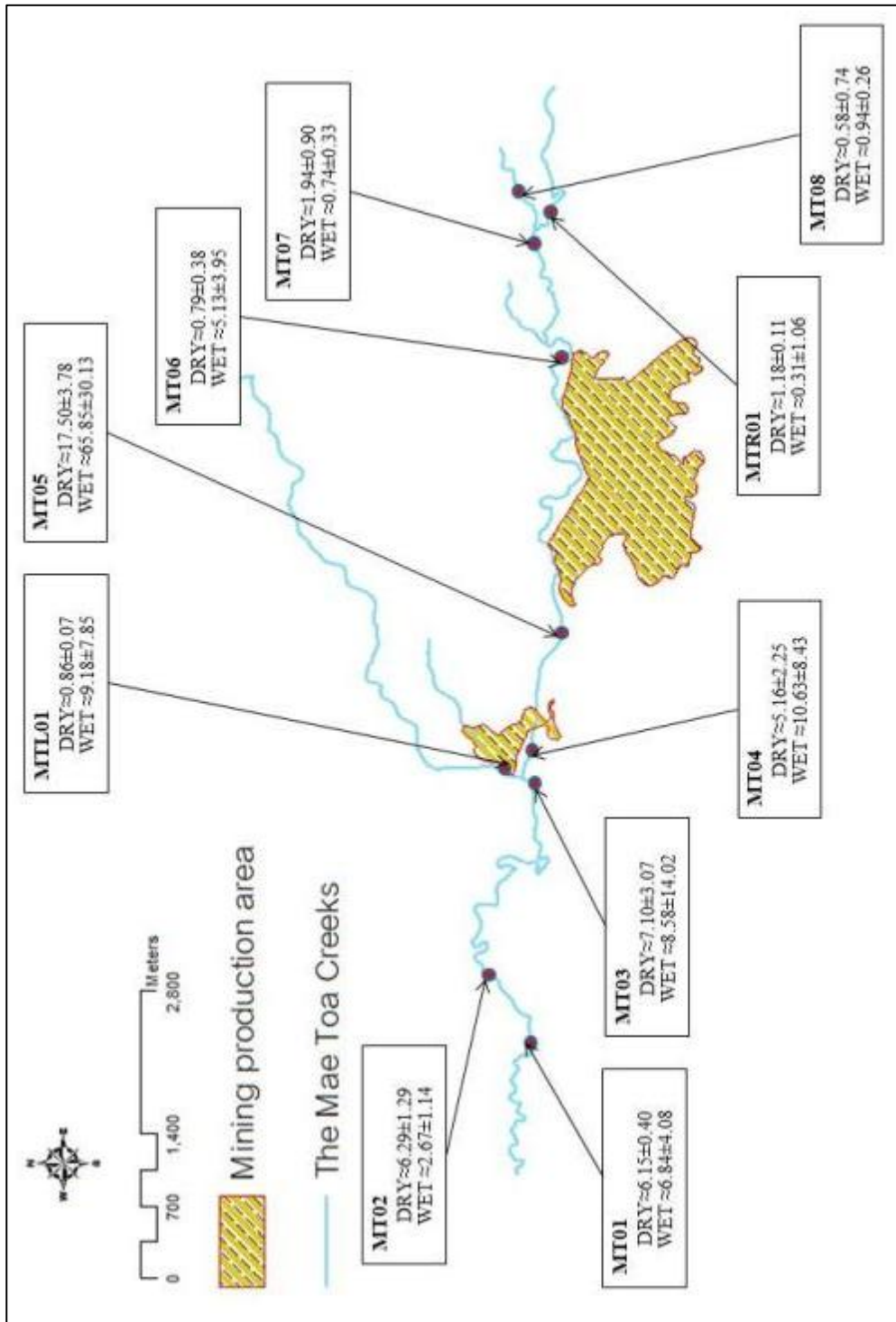
Figure 4-3 Suspended sediment from field observation in the Mae Tao Creeks
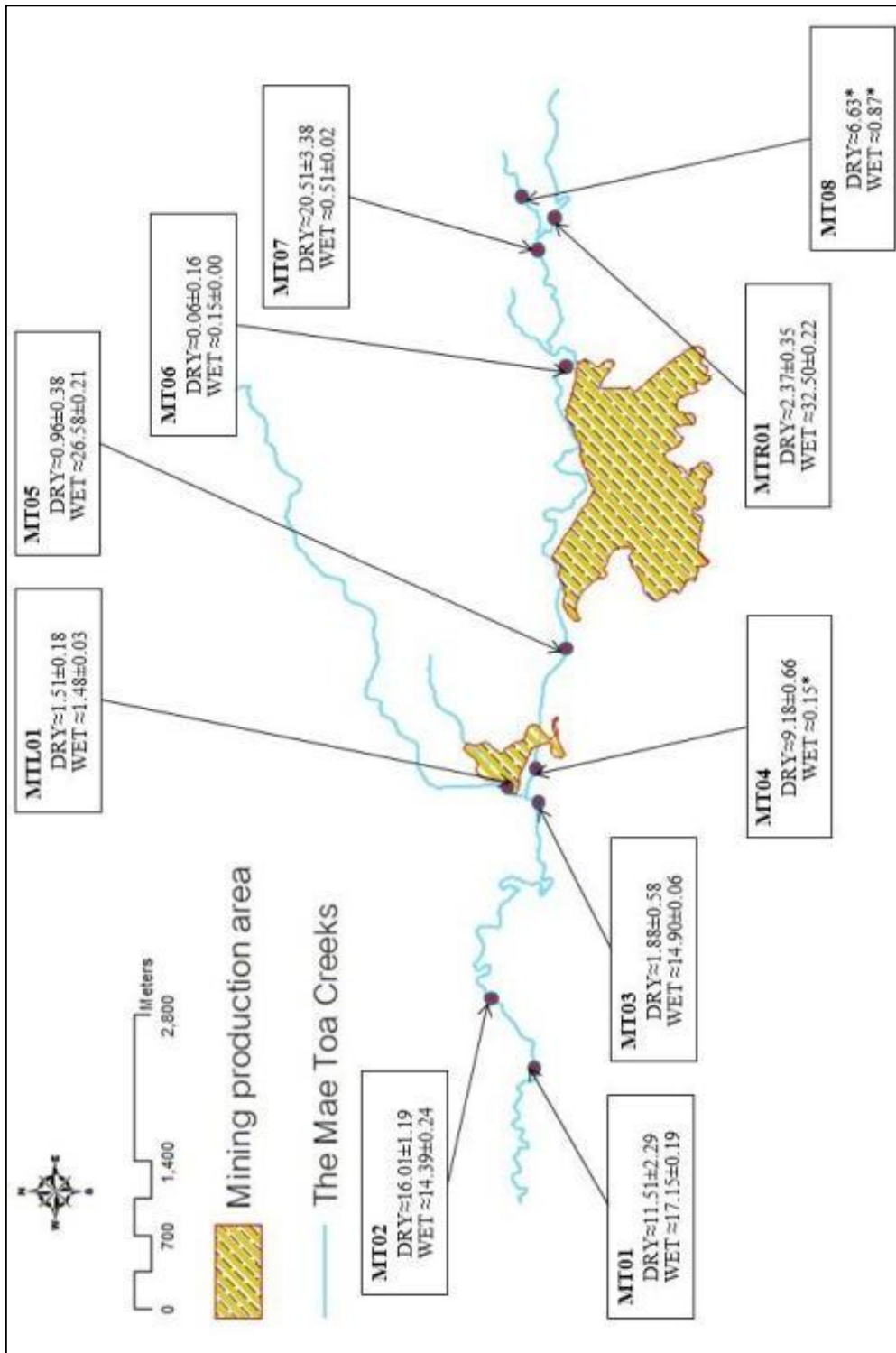
Figure 4-4 Suspended sediment from field observation in the Mae Tao Creeks

Table 4-4 Cadmium concentrations distribute in bed load in dry and wet seasons (2012-2013)

Station	Grain size (mm)	Dry season (mg/kg)	Wet season (mg/kg)
MT 01	#70	10.80±1.20	17.12±0.10
	#100	12.90±1.04	16.9±0.61
	#150	18.73±4.18	19.43±0.05
	#200	37.67±2.75	21.00±0.17
MT 02	#70	18.87±0.78	10.86±0.14
	#100	10.13±0.25	15.03±0.14
	#150	14.5±2.92	27.73±0.41
	#200	17.53±0.82	25.76±0.25
MT 03	#70	1.90±0.54	15.17±0.14
	#100	1.57±0.52	10.50±0.04
	#150	1.70±0.65	17.2±0.00
	#200	4.13±0.62	15.95±0.06
MT 04	#70	9.80±0.64	Insufficient sample
	#100	5.63±0.26	Insufficient sample
	#150	9.63±0.62	2.80±0.00
	#200	13.07±1.11	3.30±0.05
MTL 01	#70	1.27±0.01	0.23±0.00
	#100	2.10±0.00	No data
	#150	1.33±0.01	2.24±0.059
	#200	2.67±0.70	1.97±0.08
MT 05	#70	1.06±0.35	30.14±0.04
	#100	0.67±0.25	19.57±0.18
	#150	1.37±0.63	16.23±0.35
	#200	1.93±0.29	18.43±0.27
MT 06	#70	No data	Insufficient sample
	#100	0.46±0.19	Insufficient sample
	#150	0.70±0.24	2.43±0.01
	#200	1.63±0.19	2.30±0.00
MT 07	#70	19.73±0.95	Insufficient sample
	#100	26.80±0.92	Insufficient sample
	#150	49.43±7.39	2.75±0.03
	#200	61.84±4.25	1.77±0.04

Table 4-5 Cadmium concentrations distribute in bed load in dry and wet seasons (continued)

Station	Grain size (mm)	Dry season (mg/kg)	Wet season (mg/kg)
MTR 01	#70	1.87±0.75	37.73±0.03
	#100	7.34±0.57	23.33±0.19
	#150	3.10±0.10	25.16±0.13
	#200	1.63±0.03	2.31±0.28
MT 08	#70	7.00±0.00	Insufficient sample
	#100	0.80±0.00	Insufficient sample
	#150	1.23±0.71	6.70±0.00
	#200	2.43±0.28	6.73±0.07

4.2.3.3 Total cadmium distribution in stream sediment

The result of the total cadmium concentrations in stream sediments showed a similar trend during the dry and wet seasons as mentioned in Table 4-6. For suspended sediment, the cadmium concentration at station MT05 is the highest value among the other station. However at station MT07, MT08 and MTR01the cadmium concentration can be compiled with the existed standard. According to Thamjesda (2012) the concentration of cadmium contaminant at station MT06 presented the highest value as same as the current study.

Since the precipitation rate of the study period 2012 to 2013 is much lower than the previou study period in 2011, the precipitation rate only is not the dominant cause of high cadmium contamination at this station. In addition, this may be one of the evidences that the cropping area nearby which are mostly corn field can influenced the transportation of contaminated into the Mae Tao Creeks.

Cadmium contribution in bed load before entering the mining production area presented the low concentration except station MTR01 in wet station and MT07 in dry season. This may be caused by the accumulation of sediment from the upland erosion of the Mae Tao Basin.

At the downstream of the Mae Tao Creeks, the results of both sediments type demonstrate the same trend during the whole study period. The total cadmium concentration at station MT 01 to MT04 showed that the Mae Tao Creeks continuously contains high levels of cadmium after passing the mining production area. Thus, the concentrations of cadmium in bed load sediment have higher concentrations than the wet season.

The causes of high cadmium accumulated sediment in the wet season may be surface runoff and rainfall during storm season. Consequently, the most significant sources for cadmium contamination other than precipitation rate are anthropogenic activities especially deforestation and mining activities.

Table 4-6 Total cadmium distribution in stream sediment during the study period

Station	Suspended sediment		Bed load	
	Dry season	Wet season	Dry season	Wet season
	Total Cd concentration (mg/kg)	Total Cd concentration (mg/kg)	Total Cd concentration (mg/kg)	Total Cd concentration (mg/kg)
MT 01	6.15±0.40	6.84±4.08	11.51±2.29	17.15±0.19
MT 02	6.29±1.29	2.67±1.14	16.01±1.19	14.39±0.24
MT 03	7.10±3.07	8.58±14.02	1.88±0.58	14.90±0.06
MT 04	5.16±2.25	10.63±8.43	9.18±0.66	0.15*
MTL 01	0.86±0.07	9.18±7.85	1.51±0.18	1.48±0.03
MT 05	17.50±3.78	65.85±30.13	0.96±0.38	26.58±0.21
MT 06	0.79±0.38	5.13±3.95	0.06±0.16	0.15±0.00
MT 07	1.94±0.90	0.74±0.33	20.51±3.38	0.51±0.02
MTR 01	1.18±0.11	0.31±1.06	2.37±0.35	32.50±0.22
MT 08	0.58±0.74	0.94±0.26	6.63*	0.87*

*insufficient data for calculating standard deviation

4.2.4 Cadmium distribution in overland sediments

4.2.3.1 Cadmium distribution in size fraction of overland sediment

The result from overland stream sediment demonstrated that most of the sediment, smaller than 200 mesh fraction, has the high cadmium concentration. The cadmium concentration ranges from 0.7 mg/kg to 459.5 mg/kg. The highest value of cadmium contamination level was detected at the water management head quarter of the active mine. The water management head quarter is also the area that the run off in the pit move into the sediment dam. Table 4-demonstrates the cadmium distribution in size fraction of the overland sediment from the Mae Tao Basin.

4.2.3.2 Total cadmium distribution in overland sediment

The result of total cadmium indicates the highest value of cadmium concentration at SED_OB 6 which is located mining production area at 303.49±155.59 mg/kg. According to the natural properties of zinc mineral vein, cadmium can occur in association with zinc so that the high significant level of cadmium is ordinary. For the upstream and the downstream area of the Mae Tao Basin, the total overland sediment transport is compiled with PCD's standard (37mg/kg). Table 4-7 to Table 4-9 demonstrates the total cadmium distribution in overland sediment of the Mae Tao Basin.

In keeping with the observation result, the potential cadmium flux from erosion in the area, where incomplicate land utilization located, can give a close value to the empirical estimation based on RUSLE. The potential cadmium flux from erosion at the mining production area, in cluding station SED_OB2 to SED_OB9, is equal to 1.75 t/ha/y while the estimation result from RUSLE is equalt tp 1.854t/ha/y.

The complication in land utilization can cause the effect to the precision of the estimation. This is evidenced by the comparison between tation SED_OB1 and SED_OB10. Station SED_OB1 at the downstream in which many land utilization activity occurs, the value of potential cadmium fluxes from erosion between the field observation and empirical estimation are larger difference than SED_OB10 located in the deciduous forest area.

Table 4-7 Total cadmium distribution in overland sediment of the Mae Tao Basin.

Station	Location	Sieve Size (mesh)	14/7/2014 % Wt	14/7/2014 Cd (mg/kg)	25/7/2014 % Wt	25/7/2014 Cd (mg/kg)	8/8/2014 % Wt	8/8/2014 Cd (mg/kg)	22/8/2014 % Wt	22/8/2014 Cd (mg/kg)	5/9/2014 % Wt	5/9/2014 Cd (mg/kg)
SED_OB1	Downstream (MT02)	70	23.7	1.1			38.5	1.7	24.7	1.4	22.8	1.4
		100	26.4	5.8			17.6	0.8	13.9	0.9	34.1	0.8
		140	11.2	4.5	No Data		13.1	1	11.8	1.9	8.2	0.7
		200	10.2	1.9			12.2	0.9	10.7	1.5	11.1	1.2
		under 200	28.4	3.4			18.6	3.1	38.8	3.7	23.8	5.6
SED_OB2	Heavy Equipment plant	70			10.4	41.3	6.4	41.8	16.9	7.1	17.2	7.4
		100			7.9	13	6.9	9	25.9	1.9	26.7	2.1
		140	No Data		9.8	12.4	12.4	4.9	21.6	2.9	19.6	2.4
		200			9.6	10.4	14.7	5.3	13.6	3.6	13.4	2.9
		under 200			62.4	45.8	59.7	32.4	22.1	34.1	23.1	17.2
SED_OB3	Active Mining zone	70	37.3	104.2	37.2	128.6	31.9	98	59	140.4	28.8	116.3
		100	11.7	67.6	18.9	80.4	24.6	69.7	19.5	102.1	23.3	58
		140	9.1	84.2	14	97.8	16.9	92.5	10.6	144	15.9	72.2
		200	7.9	132.7	10.4	160.3	10.9	145.2	5.3	189.9	9.6	112.3
		under 200	34	428.2	19.6	331.9	15.7	311.9	5.5	356.8	22.5	224.5
SED_OB4	Bench (Overburden Dump site 3)	70			40.6	12.6	5.9	38.4	10.6	40.5	18.4	13.3
		100			5	11.2	7.3	123.1	9.4	37	5.7	9.7
		140	No Data		3.9	12.8	12.9	37.2	10.5	45.1	5.3	11.6
		200			3.8	14.1	12.6	35	9.9	45.1	5.6	14.4
		under 200			46.7	28.8	13.5	49.4	18.8	63.6	64.9	20.2
SED_OB5	Green Mining zone	70	63	49	45.4	43.9	58.3	64.2	44.8	46.8	26.7	29.5
		100	20.5	32.8	21.8	32.8	19	54.4	20.4	37.5	23.8	28.4
		140	7	56.6	12.4	42.1	10.9	84.8	12.4	42.2	15.7	30.2
		200	3.1	108.8	7.2	70.7	4.4	146.5	7.1	58.8	9.8	48.4
		under 200	6.4	330.4	13.2	136.9	7.4	168.1	15.3	69.3	24.1	85.2

Table 4-8 Total cadmium distribution in overland sediment of the Mae Tao Basin(Continued)

Station	Location	Sieve Size (mesh)	14/7/2014 % Wt	14/7/2014 Cd (mg/kg)	25/7/2014 % Wt	25/7/2014 Cd (mg/kg)	8/8/2014 % Wt	8/8/2014 Cd (mg/kg)	22/8/2014 % Wt	22/8/2014 Cd (mg/kg)	5/9/2014 % Wt	5/9/2014 Cd (mg/kg)
SED_OB1	Downstream (MT02)	70	23.7	1.1	No Data	No Data	38.5	1.7	24.7	1.4	22.8	1.4
		100	26.4	5.8			17.6	0.8	13.9	0.9	34.1	0.8
		140	11.2	4.5			13.1	1	11.8	1.9	8.2	0.7
		200	10.2	1.9			12.2	0.9	10.7	1.5	11.1	1.2
		under 200	28.4	3.4			18.6	3.1	38.8	3.7	23.8	5.6
SED_OB2	Heavy Equipment plant	70	No Data	No Data	10.4	41.3	6.4	41.8	16.9	7.1	17.2	7.4
		100			7.9	13	6.9	9	25.9	1.9	26.7	2.1
		140			9.8	12.4	12.4	4.9	21.6	2.9	19.6	2.4
		200			9.6	10.4	14.7	5.3	13.6	3.6	13.4	2.9
		under 200			62.4	45.8	59.7	32.4	22.1	34.1	23.1	17.2
SED_OB3	Active Mining zone	70	37.3	104.2	37.2	128.6	31.9	98	59	140.4	28.8	116.3
		100	11.7	67.6	18.9	80.4	24.6	69.7	19.5	102.1	23.3	58
		140	9.1	84.2	14	97.8	16.9	92.5	10.6	144	15.9	72.2
		200	7.9	132.7	10.4	160.3	10.9	145.2	5.3	189.9	9.6	112.3
		under 200	34	428.2	19.6	331.9	15.7	311.9	5.5	356.8	22.5	224.5
SED_OB4	Bench (Overburden Dump site 3)	70	No Data	No Data	40.6	12.6	5.9	38.4	10.6	40.5	18.4	13.3
		100			5	11.2	7.3	123.1	9.4	37	5.7	9.7
		140			3.9	12.8	12.9	37.2	10.5	45.1	5.3	11.6
		200			3.8	14.1	12.6	35	9.9	45.1	5.6	14.4
		under 200			46.7	28.8	13.5	49.4	18.8	63.6	64.9	20.2
SED_OB5	Green Mining zone	70	63	49	45.4	43.9	58.3	64.2	44.8	46.8	26.7	29.5
		100	20.5	32.8	21.8	32.8	19	54.4	20.4	37.5	23.8	28.4
		140	7	56.6	12.4	42.1	10.9	84.8	12.4	42.2	15.7	30.2
		200	3.1	108.8	7.2	70.7	4.4	146.5	7.1	58.8	9.8	48.4
		under 200	6.4	330.4	13.2	136.9	7.4	168.1	15.3	69.3	24.1	85.2

Table 4-9 Total cadmium distribution in overland sediment

Station	Overland sediment weight (kg)	Total Cd concentration (mg/kg)	Potential cadmium flux from erosion (Field) (t/ha/y)	Potential cadmium flux from erosion (RUSLE) (t/ha/y)
SED_OB1	62.8	2.37±0.67	0.003	0.17
SED_OB2	21.9	15.43±12.98	0.007	1.854
SED_OB3	3580	260.87±200.79	19.425	
SED_OB4	8	18.75±10.28	0.003	
SED_OB5	2500	58.15±11.49	3.024	
SED_OB6	10.35	303.49±155.59	0.065	
SED_OB7	1000	84.12±11.52	1.75	
SED_OB8	34	32.79±29.13	0.023	
SED_OB9	970	3.03±0.71	0.061	
SED_OB10	60.92	7.75±6.62	0.01	0.03

4.3 Result of potential cadmium contamination from erosion estimation

Many parts of the Mae Tao Basin have the potential in releasing cadmium as a result of leaching during soil erosion. This potential, ranging from 0 to 26.80 t/ha/y, depended on the LS factor value. A rundown of each parameter and its calculation results is provided as follows.

4.3.1 R factor calculation result.

Based on Equation 3-1 to 3-3 , the rainfall runoff value of the Mae Tao Basin during the study period (2010 to 2013) was found to be 320 mm/ha/y. The R-factor value was relatively high due to the high precipitation rate in the wet season of 2011.

4.3.2 C- and P-factor mapping results

Land utilization maps were transformed into GIS layer by spatial analysis tool to create a raster file for the calculations. A land use map from the LDD shows that deciduous forest, which was determined to have a high resistance to erosion (low C and P values), covers more than 50% of the study area. The highest values for C and P were found in the mining production area of the basin. The C and P factor results in the form of raster data are respectively revealed in Fig. 4-5 and Fig.4-6. The value of C and P are determined in   Table 4-10 to 4-11.
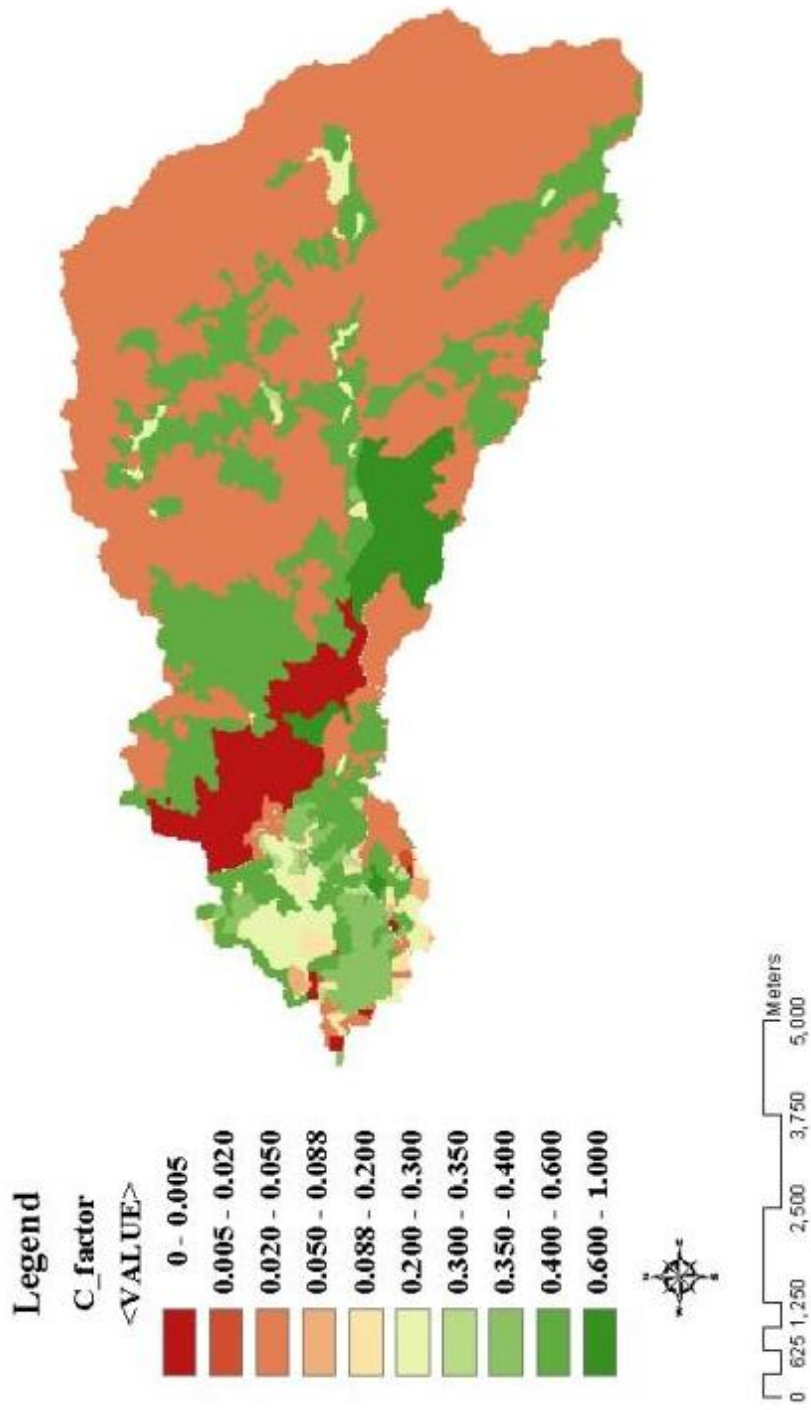
Figure 4-5 C factor calculation raster of the Mae Tao Basin area.

P Factor
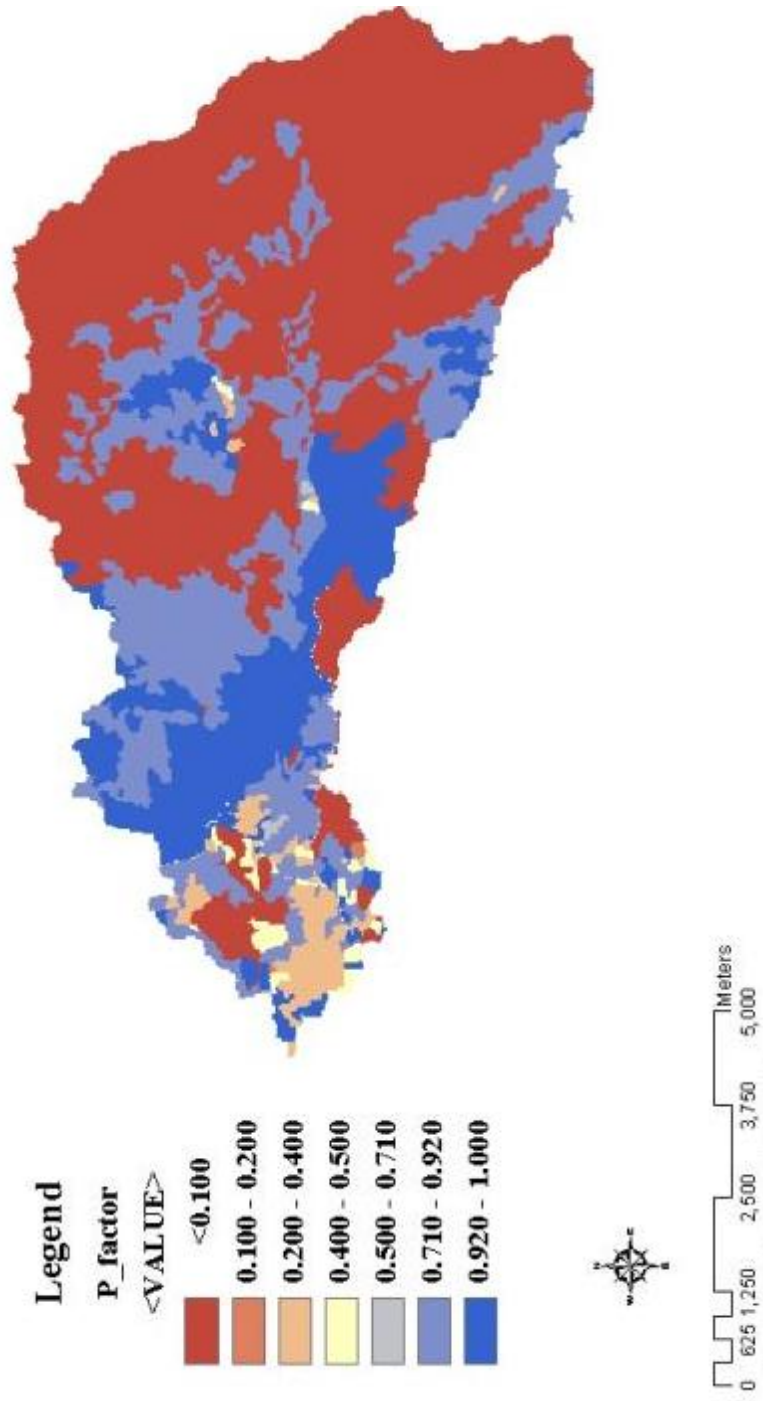
Figure 4-6 P factor calculation raster of the Mae Tao Basin area.

Legend

P_factor
<VALUE>

<0.100
0.100 - 0.200
0.200 - 0.400
0.400 - 0.500
0.500 - 0.710
0.710 - 0.920
0.920 - 1.000

Meters
0 625 1,250   2,500   3,750   5,000

Table 4-10C and P factors used in this study

Land use type	C factor	P factor
Abandoned farm house	0	0.4
Abandoned field crop	0.85	0.45
Active paddy field	0.28	0.1
Active paddy field + corn	0.4025	0.71
Active paddy field + soybean	0.375	0.365
Agro – forest	0.088	1
Bamboo	0.048	1
Banana	0.315	1
Cabbage	0.2	0.4
Cashew	0.15	0.4
Cassava	0.6	0.4
Coconut	0.2	0.5
Corn	0.525	0.92
Corn + mung bean	0.4875	0.4
Dense deciduous forest	0.003	1
Disturbed deciduous forest	0.048	1
Eucalyptus	0.088	1
Eucalyptus/teak	0.088	1
Garbage dump	0	0.7
Landfill	0	0.7
Lateritic pit	1	1
Longan	0.3	0.4
Mango/banana	0.15	0.4
Mango/jackfruit	0.15	0.4
Mine	1	1

Table 4-11 C and P factors used in this study (Continued)

Land use type	C factor	P factor
Papaya	0.3	0.4
Para rubber	0.2	0.4
Para rubber/banana	0.2	0.7
Pasture	0.015	1
Peanut	0.2	0.4
Pomelo	0.3	0.4
Poultry farmhouse	0.005	1
Rose apple	0.3	0.4
Scrub	0.02	0.2
Sugarcane	0.16	0.45
Tamarind	0.15	0.4
Teak	0.088	1
Thai village	0.05	1
Mixed crop	0.255	0.4
Upland rice	0.2	0.4

4.3.3 K-factor evaluation results

The results from NDVI analysis is exhibited in Fig4-7. Consistent with the results from NDVI analysis, an abundance of deciduous forest can be sensed in the upstream area of the basin. Furthermore, rice paddy and corn fields can be founded, distributed around residential areas and neighboring areas of the mines.

Since only NDVI analysis is not sufficient in identifying the vegetation types, resulting in the degradation of K-factor precision, secondary data on land use and soil properties (including soil type identification) of the Mae Tao Basin from the LDD were used in association with soil taxonomy and evaluated. The soil type and the K-factor results are exhibited in Table 4-12. Finally, the K-factor values, obtained from the evaluation, were assigned and transformed into a raster layer for calculation, as shown in Figure 4-9.

Figure 4-7 NDVI classification result of the Mae Tao Basin

Table 4-12 K-factor evaluation based on local Thai soil series and soil taxonomy

No	Soil Type (Thai)	Soil Series	Soil Taxonomy						K factor value
			Order	Suborder	Great group	Sub group	Family	Code	
1	31	Wang Hai	Alfisols	Ustalfs	Paleustalfs	Oxyaquic (Ultic)	Fine, mixed, Isohyperthermic	Wi	0.25
		Loi	Oxisols	Ustox	Kandiustox	Typic	Very fine, Kaolinitic, Isohyperthermic	Lo	
2	33	Tapanhin	Alfisols	Ustalfs	Haplustalfs	Ultirc	Fine-silty,Mixed,Isohyperthermic	Tph	
		Dong Yang En	Alfisols	Ustalfs	Haplustalfs	Oxyaquic (Ultic)	Fine-silty,Mixed,Isohyperthermic	Don	
		Kampaeng Petch	Alfisols	Ustalfs	Haplustalfs	Oxyaquic (Ultic)	Fine-silty,Mixed,Isohyperthermic	Kp	
		Lam Sonthi	Alfisols	Ustalfs	Haplustalfs	Oxyaquic (Ultic)	Fine,Mixed,Isohyperthermic	Ls	0.37
		Nam dug	Alfisols	Ustalfs	Paleustalfs	Oxyaquic (Ultic)	Fine-silty,Mixed,Isohyperthermic	Nd	
		Kampaeng Saen	Alfisols	Ustalfs	Paleustalfs	Typic	Fine-silty,Mixed,Isohyperthermic	Ks	
		That Phanom	Alfisols	Ustalfs	Paleustalfs	Ultirc	Fine-silty,Mixed,Isohyperthermic	Tp	
3	55	Chatturat	Alfisols	Ustalfs	Haplustalfs	Typic	Fine,Mixed,Isohyperthermic	Ct	0.24
		Wang sapung	Alfisols	Ustalfs	Haplustalfs	Typic	Fine,Mixed,Isohyperthermic	Ws	
4	60	Well drained	Unclassified	unclassified	unclassified	unclassified	unclassified	unclassified	0.29
5	62	Slope complex	Unclassified	unclassified	unclassified	unclassified	unclassified	unclassified	0.25

Figure 4-8 K factor calculation raster of the Mae Tao Basin area.

4.3.4 LS-factor calculation results

Figure 4-9 to Figure 4-13 displays the slope calculations from the DEM of the Mae Tao Basin. The DEM (Figure 4-9) analyzed and transformed to illustrate the flow direction layer (Figure 4-10) and flow accumulation (Figure 4-11) of the study area. Figure 4-12 demonstrates the differences between the slope calculation results from DEM (degrees vs. percent gradient) which have the similar interval with each other. These layers were combined with the raster calculation to generate the raster layer of the LS factor, as shown in Figure 4-13. Three LS factors from different calculation type, which are different in unit of slope, were calculated based on relative standard deviation analysis and the results are shown in Table 4-13 and Figure 4-11.

Table 4-13 Comparisons of LS-factor values from relative standard deviation analysis

Calculation method	1 (Mitasova et al., 1999)	2 (Presbitero et al., 2003)	3 (Bizuwerk et al., 2003)
Mean	15.16	84.23	12.67
Maximum	1971.9	6740.31	1833.66
Minimum	0	0	0
SD	60.52	287.4	48.01
% RSD	399.21%	341.21%	378.94%

According to the results, the second method (based on Equation3-5) demonstrated the smallest value of %RSD among the selected methods at 341.21%. This result indicates that with only LS factor calculation the second method have more precision and should be selected as the appropriate method for the study area

DEM of the Mae Tao Basin

Legend

Fill

Value

High : 942

Low : 221

Meters
0   1,250   2,500   5,000
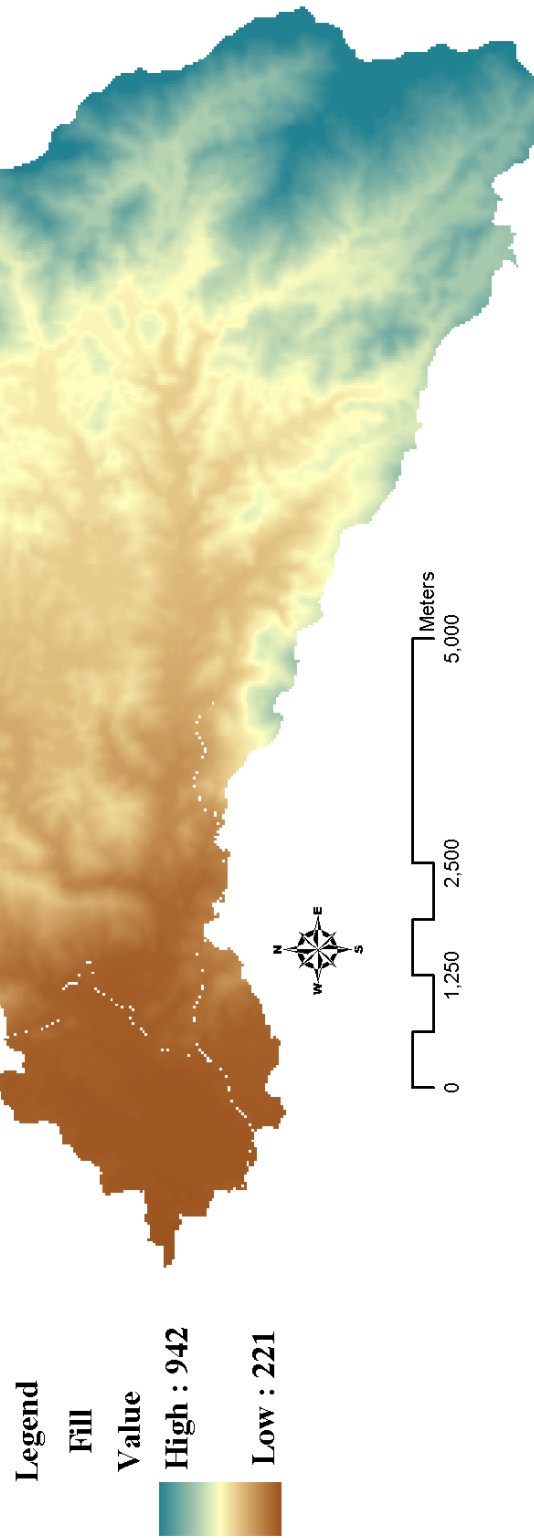
Figure 4-9 Digital Elevation Map (DEM) of the Mae Tao Basin area.

Flow direction
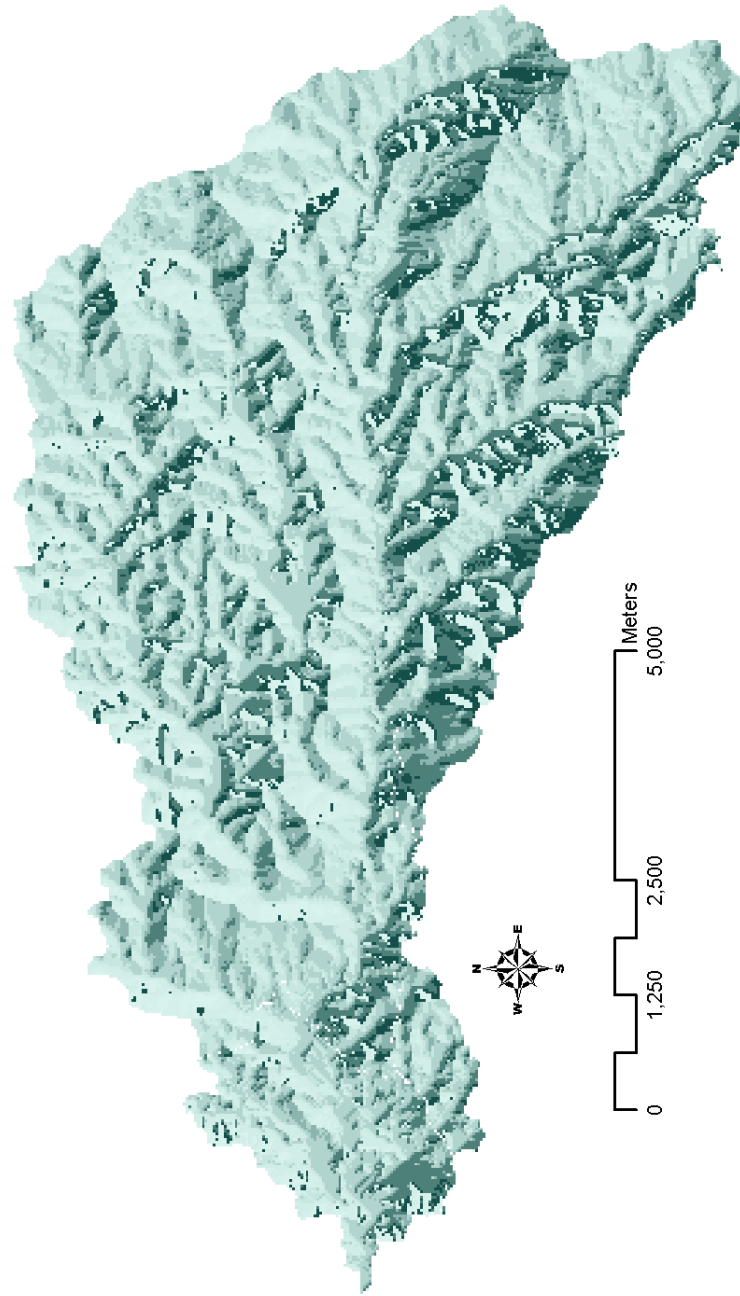
Legend
Flow_D
Value
High : 128

Low : 1

Meters
0   1,250   2,500   5,000
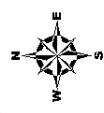
Figure 4-10 Calculated flow direction of the Mae Tao Basin.
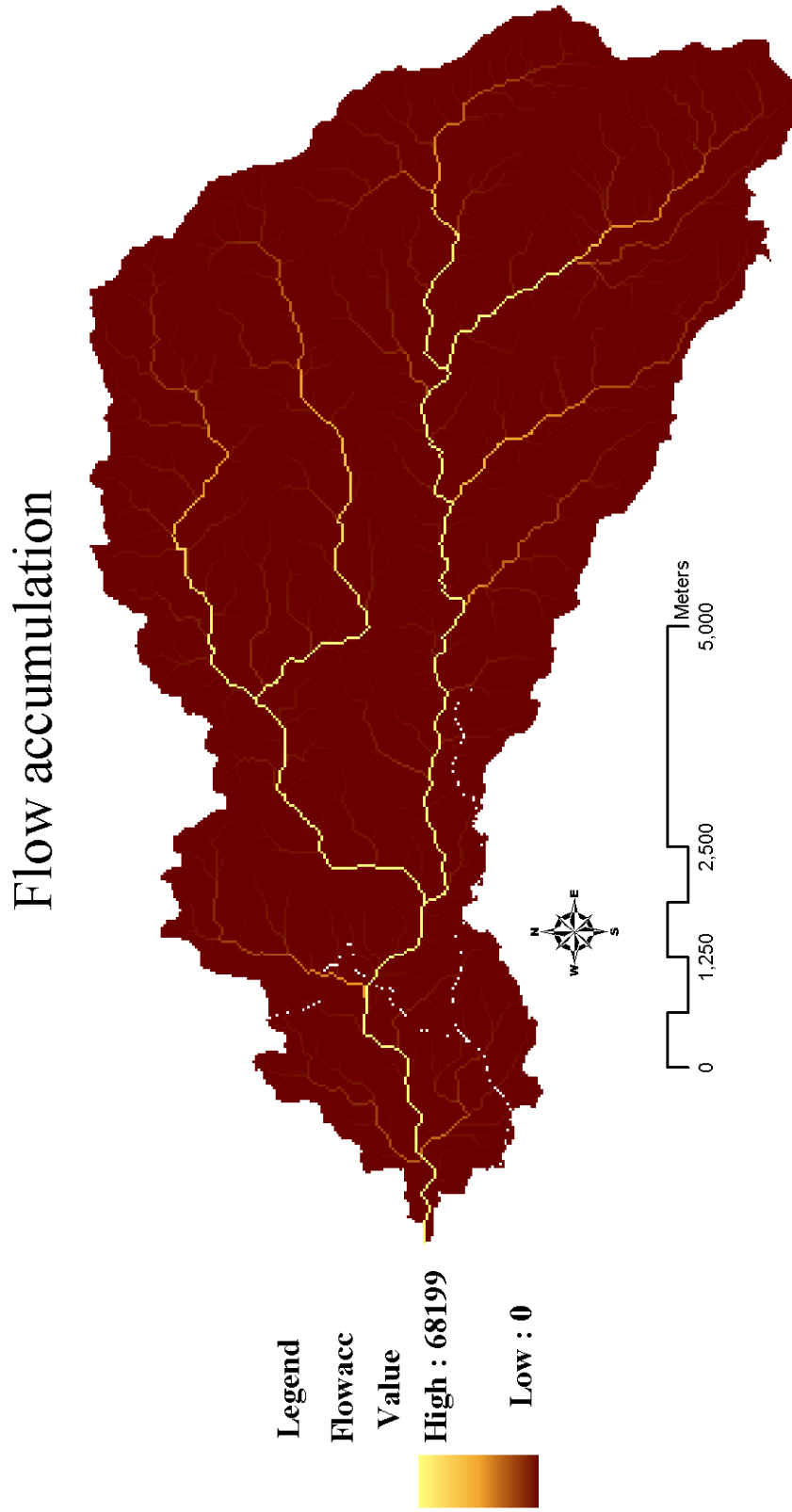
Figure 4-11 Calculated flow accumulation of the Mae Tao Basin.
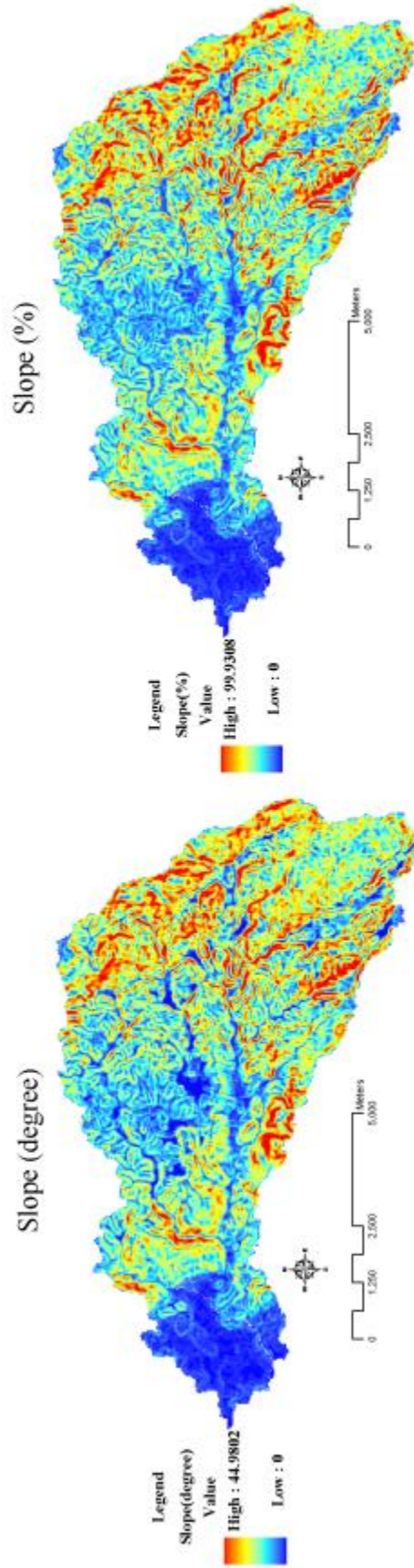
Figure 4-12 The calculated slope results created by the GIS technique: (a) slope of the Mae Tao Basin in degrees. (b) slope of the Mae Tao Basin in percent gradient.
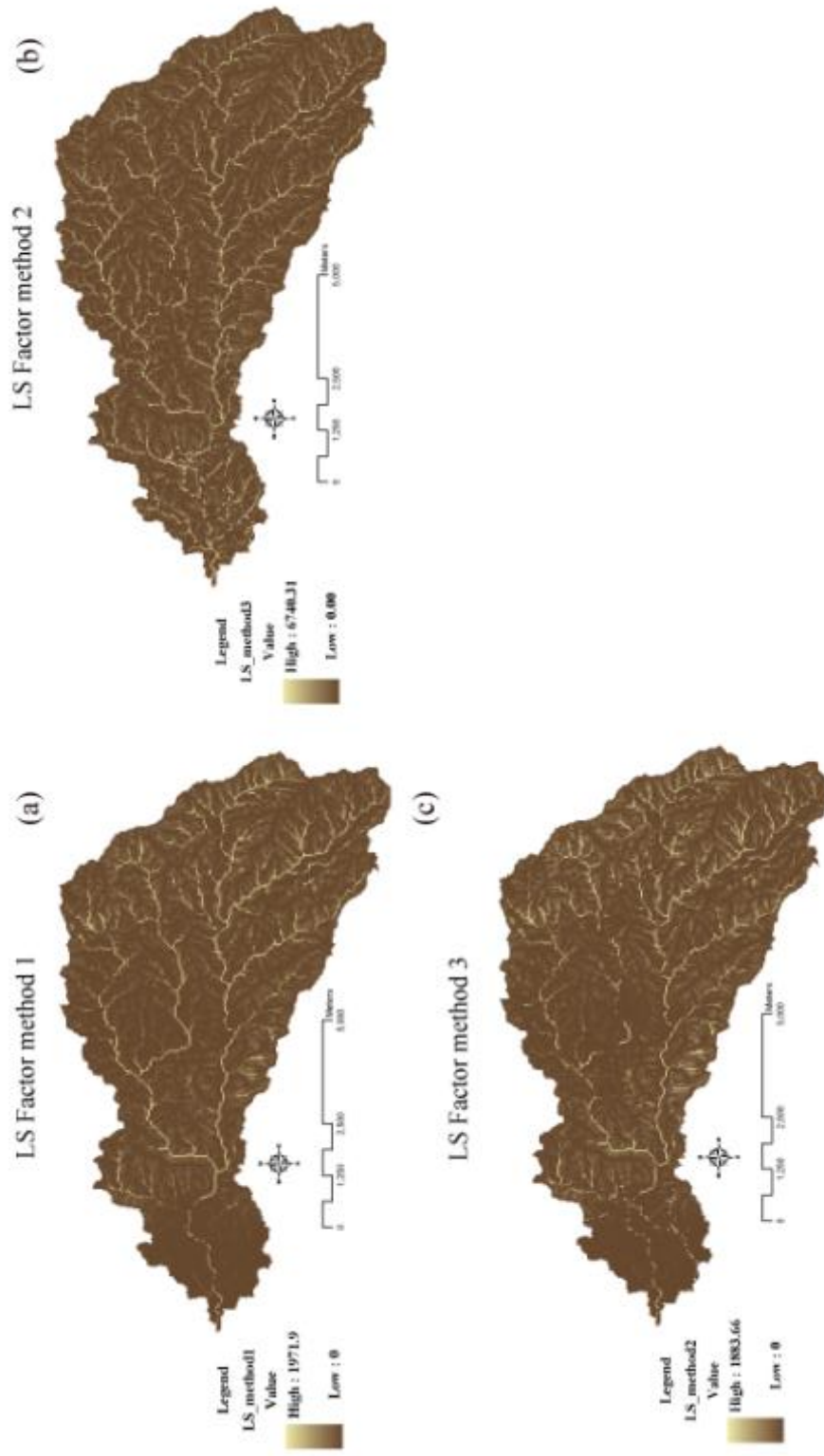
Figure 4-13 LS factors from three different methods: the results indicate the increasing slope in the eastern part of the map as the S part of the factor increased (a) LS calculation method 1 (Mitasova et al., 1999), (b) LS calculation method 2 (Presbitero et al., 2003), (c) LS calculation method 3 (Bizuwerk et al., 2003).

4.3.5 Soil erosion calculation results

After the required factors for RUSLE had been complemented, the raster calculation of those factors in the GIS software was assigned in association with Equation 2-1. The results of the calculations are provided in Figure 4-14. The high values of erosion can be detected at the junction point of the creeks and in the mining production area.

Erosion was found to occur along the banks of the Mae Tao creeks. Moreover, at the upstream area of the basin, moderate erosion potential numbers were found due to the topography.

4.3.6 Potential cadmium flux from erosion estimations

Cadmium concentration contours of the Mae Tao Basin (Figure 4-15) were implemented into the GIS program with the RUSLE results. The contours designate high cadmium concentrations near the conjunction of the two Mae Tao creeks and its branch. The cadmium concentration, found in the basin, ranged from 0 to 200 mg/kg.

Additionally, high cadmium contaminated areas were detected at downstream near the residential area of the Mae Tao Basin. The raster calculation results of the potential cadmium flux from erosion are presented in Figure 4-16 and the result from both RUSLE and potential cadmium flux from erosion is determined in Table 4-14 to Table 4-15.

The results from erosion, obtained from Equation 3-4 and Equation 3-6, have similar ranges. The potential cadmium flux from erosion, obtained using Equation 3-4, ranged from 0 to 1.7 t/ha/y, while the cadmium flux using Equation 3-5 ranged from 0 to 1.85 t/ha/y. in addition, Equation 3-5 results were higher, ranging from 0 to 26.80 t/ha/y. The difference in these results is the effect of the LS factor, especially in Equation 3-5 where it was three times higher than it was in the other equations.
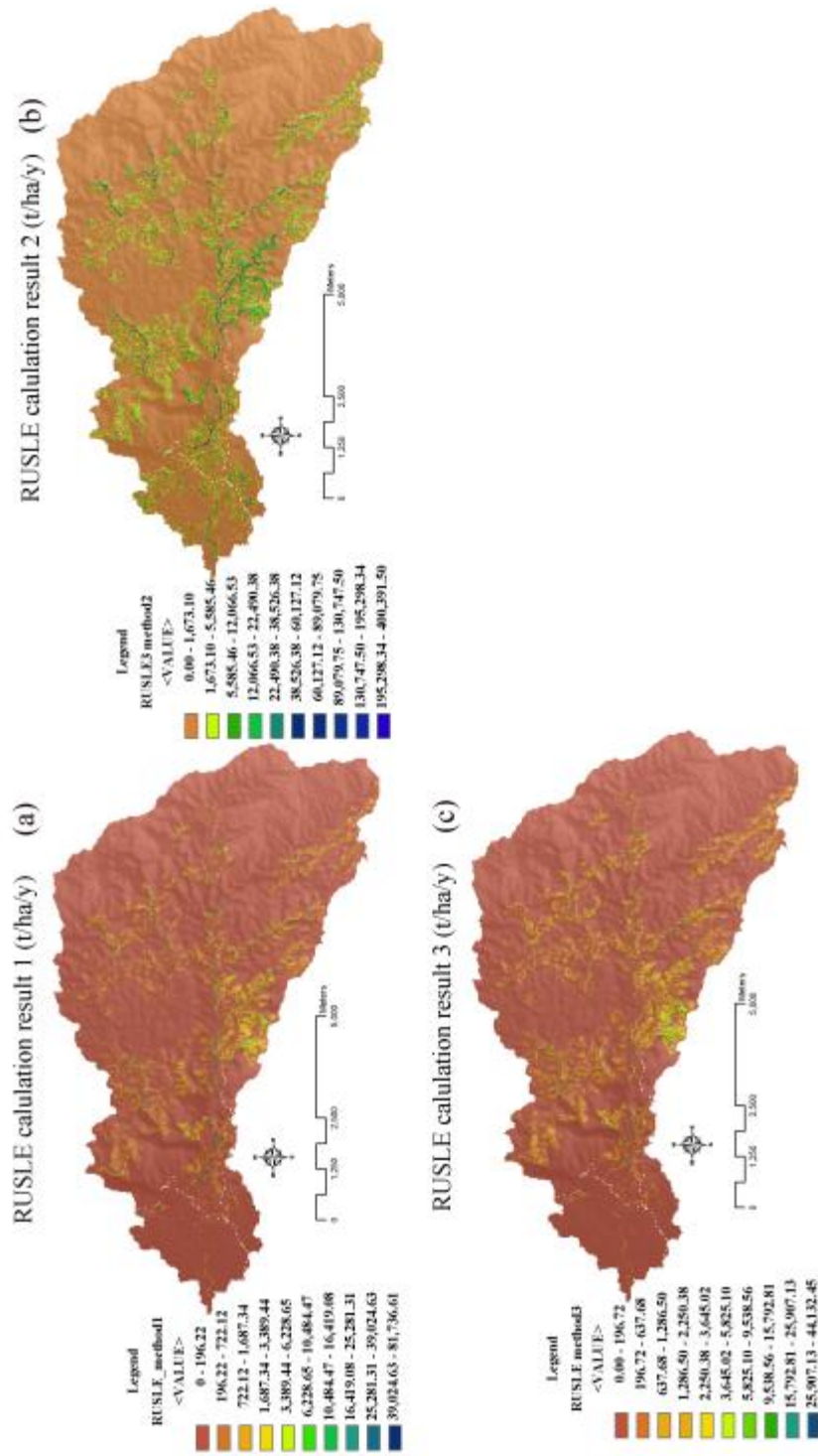
Figure 4-14 Soil erosion potential of the Mae Tao Basin form RUSLE: (a) Calculated result from method 1 (Mitasova et al., 1999), (b) calculated result from method 2 (Presbitero et al., 2003), and (c) calculated result from method 3 (Bizuwerk et al., 2003). All methods show that the mining production area has the highest erosion potential. The second method produced an overestimated result. In addition, high erosion potential was founded at the conjunction of the two Mae Tao creeks.
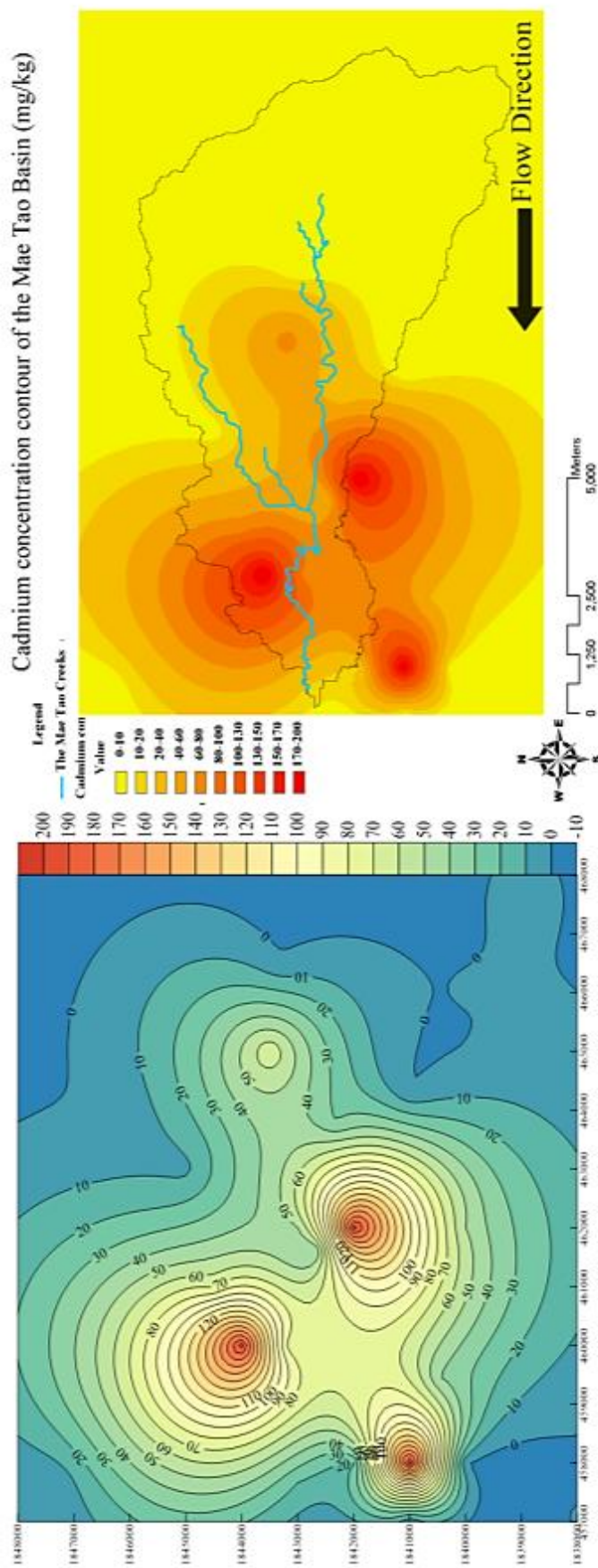
Figure 4-15 Left: The cadmium concentration contours of the Mae Tao Basin, integrated with data from the PCD (2009). Right: The digitized raster layer of the cadmium concentration profile of the Mae Tao Basin. The high concentration area in the map is located in the downstream area of the basin
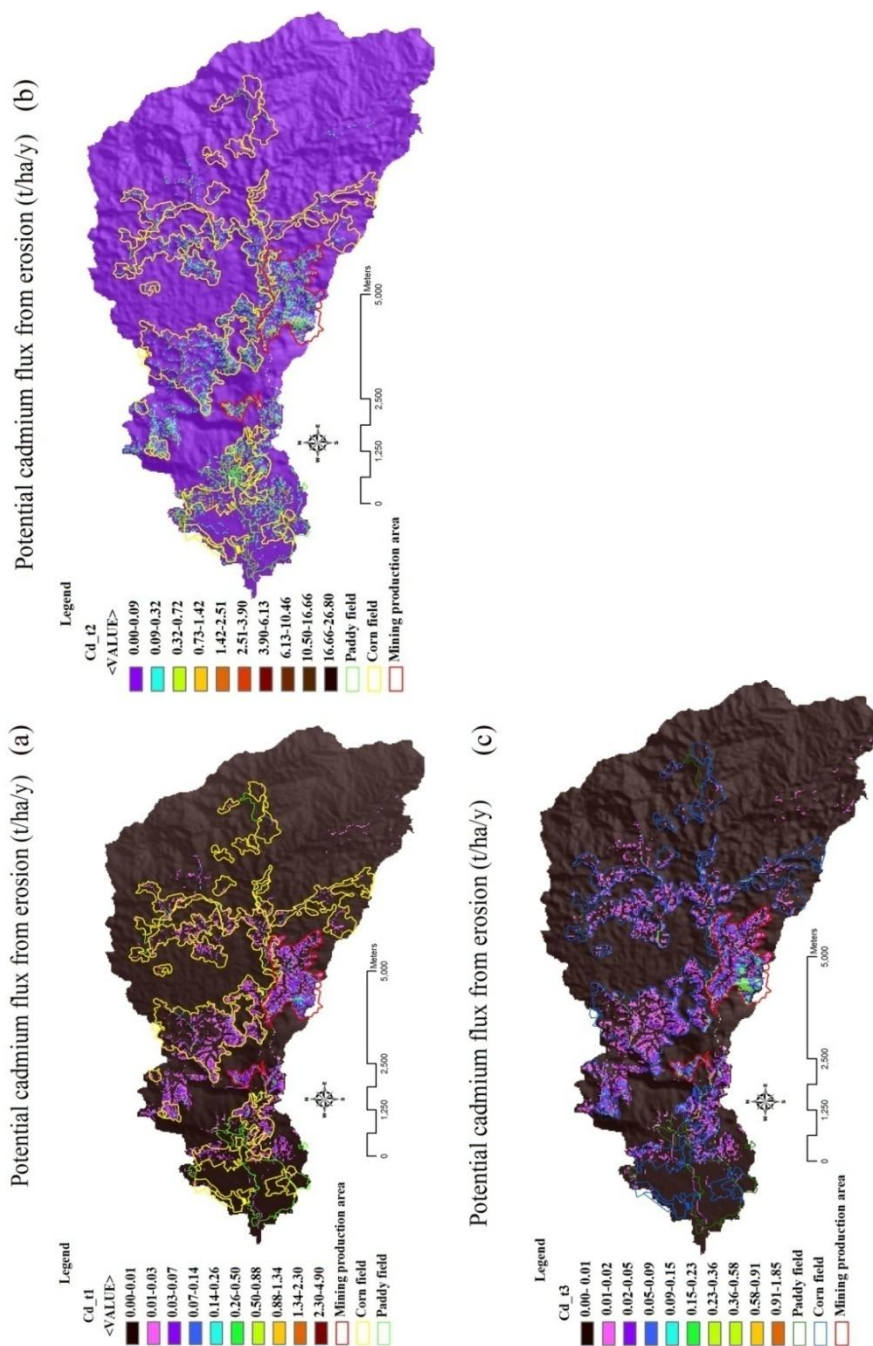
Figure 4-16 The estimated potential cadmium flux from erosion over the Mae Tao Basin: (a) The potential cadmium flux from erosion result of method 1 (Mitasova et al., 1999), (b) the potential cadmium flux from erosion result of method 2 (Presbitero et al., 2003), and (c) the potential cadmium flux from erosion result of method 3 (Bizuwerk et al., 2003).

Table 4-14 Potential cadmium flux from erosion in the Mae Tao Basin based on land utilization

Calculation method	1	2	3	Area (ha)	Area contribution (%)
All areas					
Minimum potential cadmium flux from erosion (t/h/y)	0.000	0.000	0.000	5961.87	100.00%
Maximum potential cadmium flux from erosion (t/h/y)	4.904	26.805	1.854		
mean (t/h/y)	0.006	0.053	0.005		
SD	0.062	0.482	0.032		
RSD (%)	1074%	913%	587%		
Potential cadmium erosion in one year (t)	34.594	314.901	32.195		
Mining production area					
Minimum potential cadmium flux from erosion (t/h/y)	0.000	0.000	0.000	262.53	4.40%
Maximum potential cadmium flux from erosion (t/h/y)	4.904	24.024	1.854		
mean (t/h/y)	0.043	0.263	0.044		
SD	0.177	1.097	0.088		
RSD (%)	415%	417%	201%		
Potential cadmium erosion in one year (t)	11.227	69.123	11.527		
Corn field area					
Minimum potential cadmium flux from erosion (t/h/y)	0.000	0.000	0.000	616.22	10.34%
Maximum potential cadmium flux from erosion (t/h/y)	3.597	26.805	1.324		
mean (t/h/y)	0.015	0.139	0.013		
SD	0.099	0.847	0.049		
RSD (%)	673%	609%	375%		
Potential cadmium erosion in one year (t)	9.02	85.71	8.03		

Table 4-15 Potential cadmium flux from erosion in the Mae Tao Basin based on land utilization (cont.)

Calculation method	1	2	3	Area (ha)	Area contribution (%)
Rice paddy field					
Minimum potential cadmium flux from erosion (t/h/y)	0.000	0.000	0.000	174.33	2.92%
Maximum potential cadmium flux from erosion (t/h/y)	0.961	21.475	0.451		
mean (t/h/y)	0.003	0.122	0.002		
SD	0.027	0.734	0.012		
RSD (%)	924%	600%	595%		
Potential cadmium erosion in one year (t)	0.52	21.32	0.36		
Forest area					
Minimum potential cadmium flux from erosion (t/h/y)	0.000	0.000	0.000	3352.64	56.23%
Maximum potential cadmium flux from erosion (t/h/y)	1.328	7.422	0.517		
mean (t/h/y)	0.001	0.009	0.002		
SD	0.015	0.089	0.011		
RSD (%)	1063%	983%	712%		
Potential cadmium erosion in one year (t)	4.59	30.33	5.24		

method 1:(Mitasova et al., 1999), method2:(Presbitero et al., 2003), method 3 (Bizuwerk et al., 2003).

Potential cadmium flux from erosion (t/ha/y)

Legend

Cd_t3

- 0.00– 0.01
- 0.01-0.02
- 0.02-0.05
- 0.05-0.09
- 0.09-0.15
- 0.15-0.23
- 0.23-0.36
- 0.36-0.58
- 0.58-0.91
- 0.91-1.85
- Paddy field
- Corn field
- Mining production area
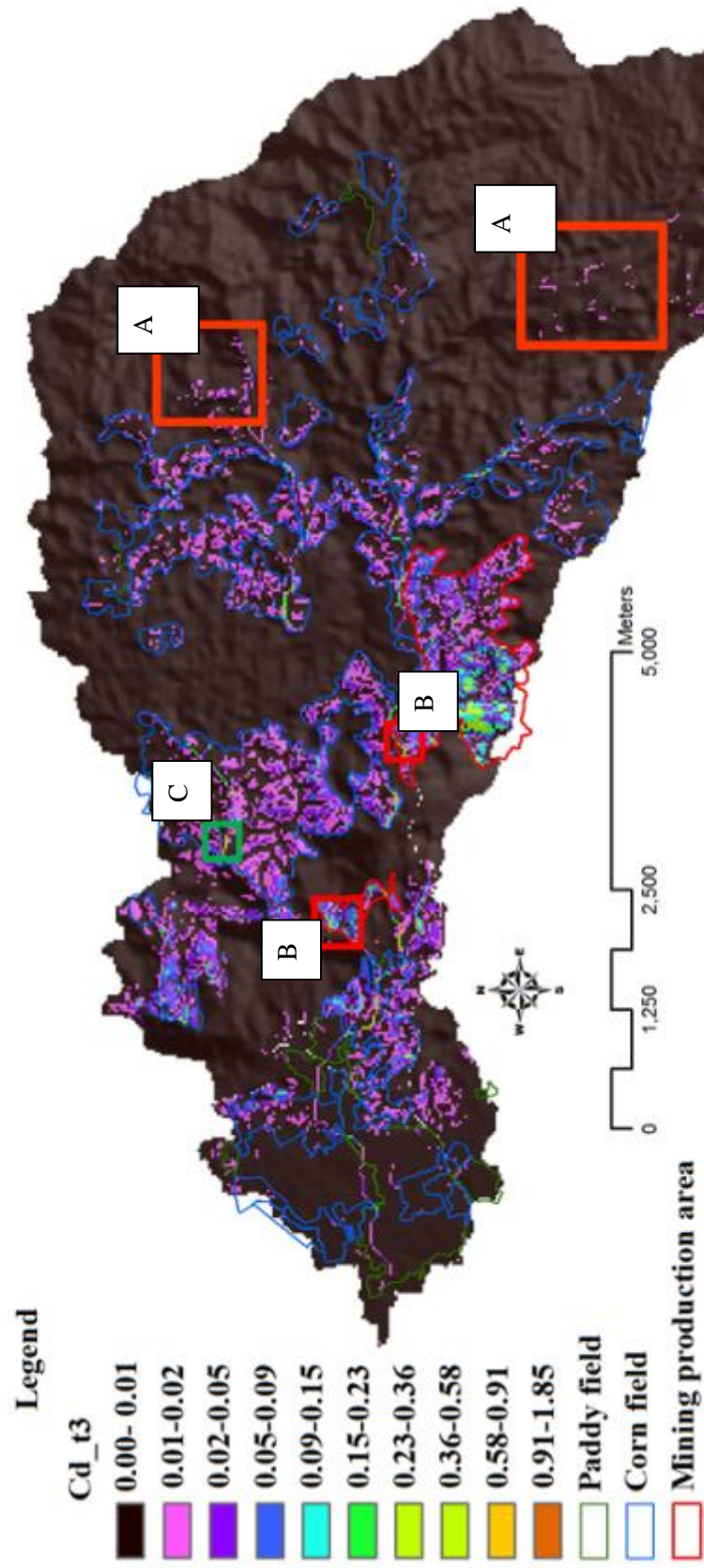
Figure 4-17 Potential cadmium flux from erosion in the Mae Tao Basin

After estimating the potential cadmium flux from erosion, a statistical analysis of the results from each method was performed. According to the Table 4-11, the results of Equation 8 have the least SD and %RSD values in every area of contribution. Since smaller %RSD represents the better value of precision and consistency of the estimation, the third LS calculation method was selected and its results are presented in Figure 4-17.

Based on the %RSD results, the third LS calculation method was selected and its results are presented in Figure 4-17. The map indicates the scattered distribution of cadmium contamination from erosion in many parts of the Mae Tao Basin. The highest value of potential cadmium flux from erosion (1.854 ± 0.088 t/ha/y), was found in the red square area of Figure 4-18.This area is the location where mining production area are operated

Like the mining production area, corn fields, abundantly located in the middle of the basin, have the ability to release high levels of cadmium. The highest value of cadmium flux due to erosion, labeled as green square area in Figure 4-17, was 1.324 ± 0.049 t/ha/y. This value is close to the result obtained from the mining production areas of the Mae Tao Basin.

Although the highest values of potential flux were found in the mining production areas and corn fields, cadmium contamination from erosion can still be found in other areas of the Mae Tao Basin. In some paddy fields downstream, the potential cadmium flux due to erosion was 0.451 ± 0.012 t/ha/y. The existence of a cadmium contamination potential signals the risk of utilizing the soil and water in areas that have accumulated cadmium from an upstream part of the basin.

Moreover, the deciduous forest area, located in an undisturbed upstream area of the basin, had a small proportion of potential flux (0.517 ± 0.002 t/ha/y). The existence of potential flux from erosion in this undisturbed area designates the capability of the area as natural cadmium source with a small proportion, comparing to the entire study area.

As a validation, Table F-4 (Appendix F) demonstrates that the result from empirical estimation foll0w the same trend as the observed data. Thus, the result of some stations in mining production area demonstrates an incongruity between observed and estimated data. This is because of the uncertainty and errors form secondary data, used as model input especially DEM of the study area, resulting in the variation of LS factor.

4.4 Simulation Results

4.4.1 MIKE11And MIKESHE simulation result.

4.4.1.1 Hydrodynamic simulation calibration

Hydrodynamic simulation of the Mae Tao Creek was calibrated, based on the measured water depth at station MT 04 from March 2012 to February 2013. The simulated and measured water level at station MT 04 as shown in Figure 4-18, statistic calculations were generated for estimating the reliability of model calibration were generated for estimating the reliability of model calibration.
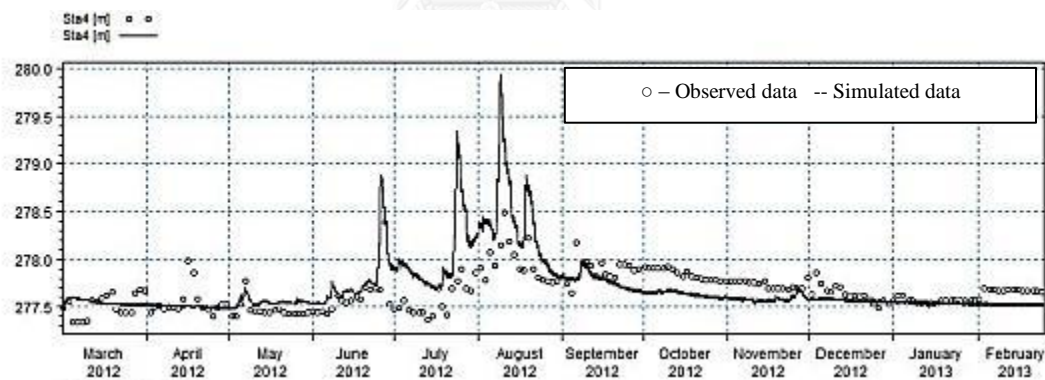
Figure 4-18 Observed and simulated water level at station MT 04 (m)

Correlation coefficient (R) is a measure of linear dependency between simulated and measured values. The closer value to 1.00, the better match for each simulation scenarios are. Root mean square error (RMSE), have a preference to be 0, refers to how perfect match of the observation and simulation are. This study obtained the R value of 0.57and the RMSE value of 0.26 m.

The noise between the simulation results and observation results occurs by the human erros in the monitoring of the water level in the Mae Tao Creeks. Figure 4-19 demonstrates the rainfall intensity data during the study period. According to the high rainfall intensity during the wet season, reaching station MT04 cannot be continuous so that some of the data in the simulation were based on interpolation, causing high uncertainty in the final results of the simulation.
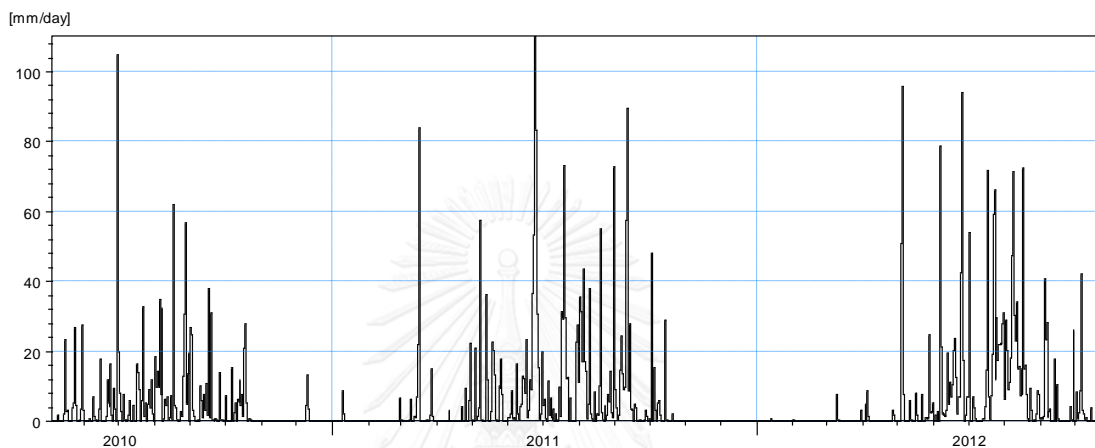
Figure 4-19 Rainfall intensity during the stduy period

4.4.1.2 Hydrodynamics result

MIKE SHE in association with MIKE 11 was applied in order to estimate the hydrodynamic results, including water depth and water discharge. Water depth and water discharge is monitored from 9 stations along the main Mae Tao Creek, Mae Tao Right and Mae Tao Left, except station MT 01 which were assigned as downstream boundary condition. The simulated results indicated that highest rate of water discharge were obtained at the downstream of the main Mae Tao Creek. The water balance flow chart of the Mae Tao subcatchment is demonstrated in Figure 4-20 and 4-21.

According to the simulation's result, the water depth and the water discharge during the wet season of the study period is much higher than the dry season. Most of the high discharge rate were occur during June to July of 2012 where the rainfall intensity was relatively high, resulting in the existence of continuous peaks in the hydrodynamic simulation. Furthermore, the overland flow depth, stored

after the simulation, revealed the significant depth of the overland flow over than 40 m in some area of the Mae Tao Basin.
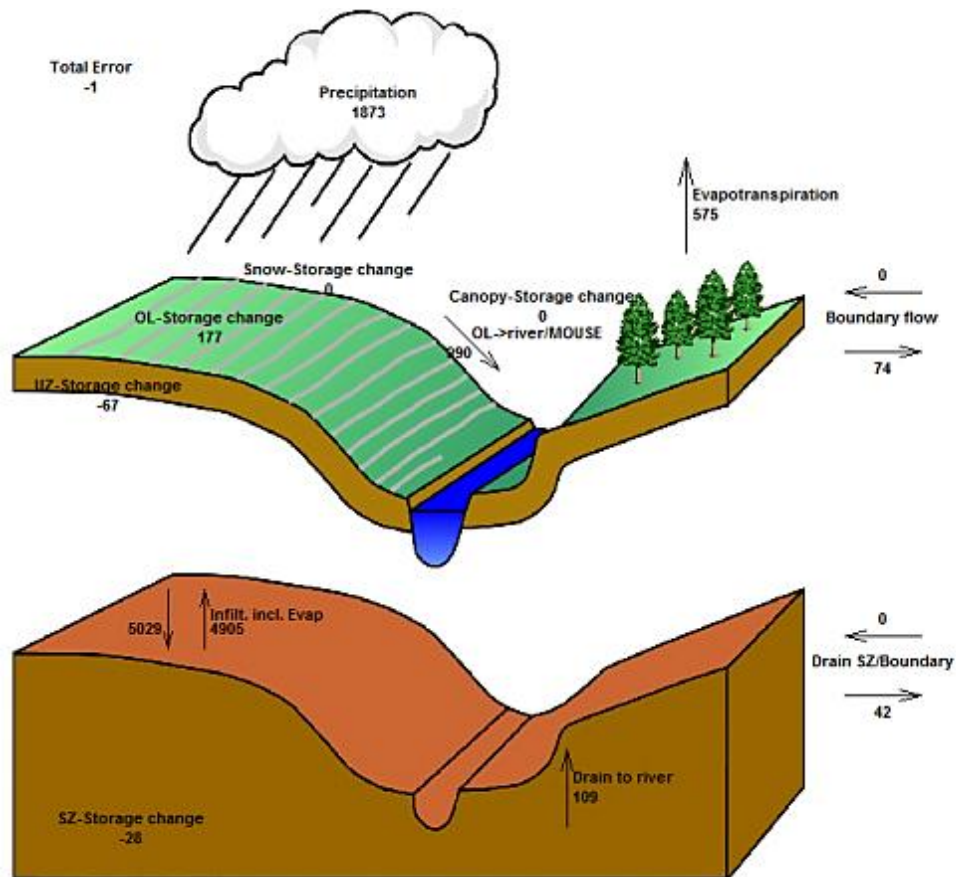
Figure 4-20 Total water balance chart of the Mae Tao subcatchment in wet season
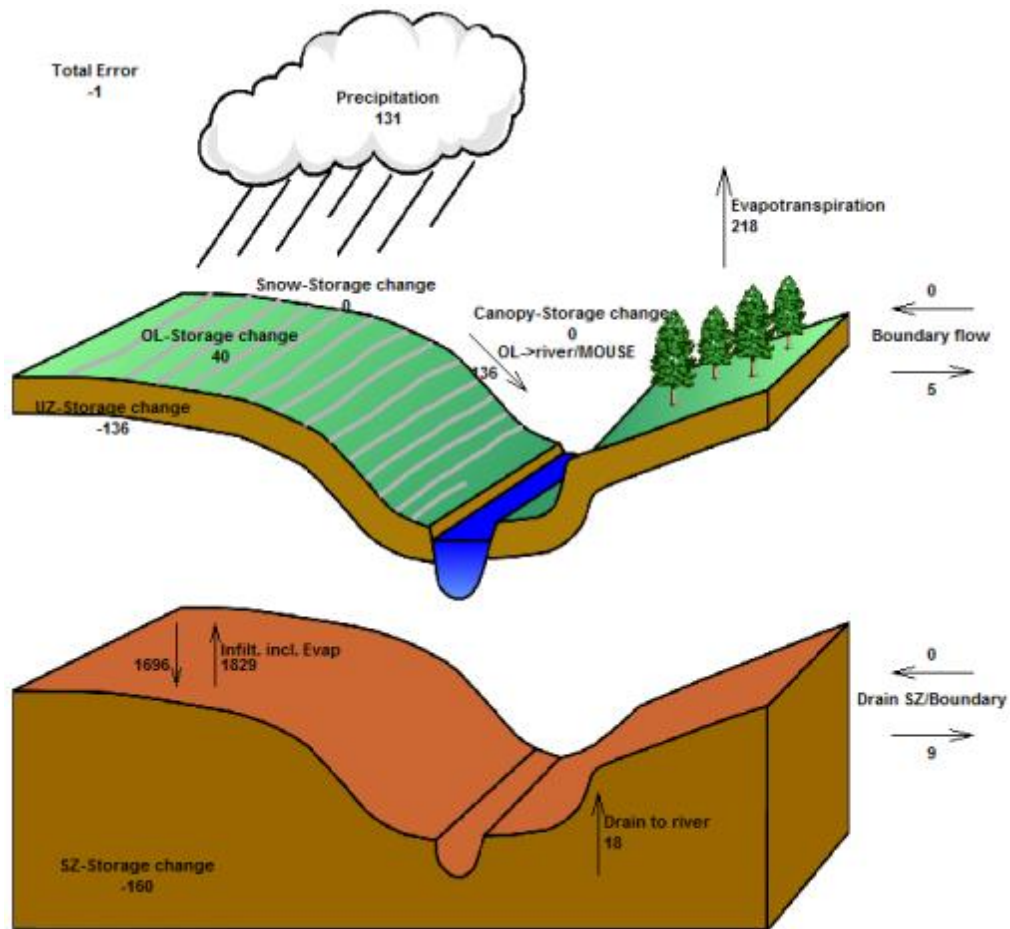
Figure 4-21 Total water balance chart of the Mae Tao subcatchment in wet season

4.4.1.3 Stream sediments transport result

After calibrating the hydrodynamic results from MIKE SHE model, sediment transport module was operated in MIKE 11 with hydrodynamic results for simulating sediment transport. Both wet and dry season, total sediment transport was estimated, classified as suspended sediment and bed load. The study periods were selected from May 2012 to October 2012 as the wet season, and November 2011 to February 2013 as the dry season.

Throughout the wet season, total sediment transport was calculated as 563.76 m^3, transported by 4.82×10^7 m^3 of water discharge, while 4.22 m^3 of the sediment was occurred in the dry season, This amount of sediments was transported by 8.46×10^5 m^3 of water discharge.

The sediment transport was occurred during wet season with 99.23% of total, and 75.48% of total transported sediment is classified as suspended form. The results indicated that sediment transport rate, occurred in the Mae Tao Creeks, is depended on water discharge rate. In accordance with wet season, high water discharge resulting from high rainfall intensity caused the sediment to have high availability in sediment transport along the river system. The small amount of bed load was transported due to the proportion of total sediment in sand-bed channels contained a few availability of bed-transportation (Simons and Senturk, 1977).

4.4.1.3.1 Stream sediment transport during wet season

From May 2013 to October 2013, sediment transport, occurred in the Mae Tao Creek, has a simulation result which can indicate that both suspended sediment had an abundant transport rate during rainfall period. The highest transport rates of sediment of wet season took place in June 2011.

Figure 4-22 demonstrates the suspended sediment which was transported to the downstream of the Mae Tao Creeks. Highest suspended sediment rate obtained from 9th August 2012, which had the highest precipitation. The highest rate was 2.87×10^{-4} m^3/s with 20.68 m^3/s water discharge. The volume of accumulated suspended sediment was determined as 424.75 m^3.

According to Figure 4-23, bed load transport rates at the downstream were presented in the same trend as suspended sediment. The highest bed load transport rate was 1.50×10^{-4} m^3/s and accumulated amount was 139.01 m^3. Therefore, accumulated total sediment transport, consisted of suspended and bed load sediment, was estimated at 563.76 m^3 at downstream during the wet season of 2012, as shown in Figure 4-24.
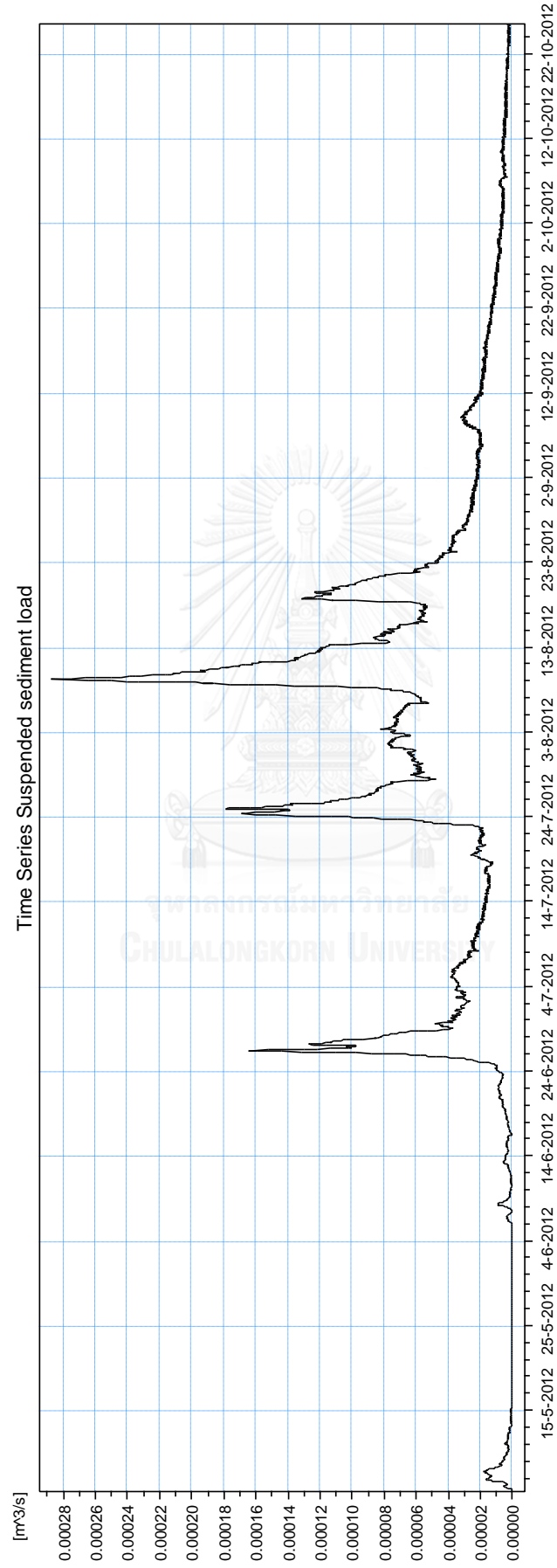
Figure 4-22 Suspended sediment transported to the downstream of the Mae Tao Creeks during wet season
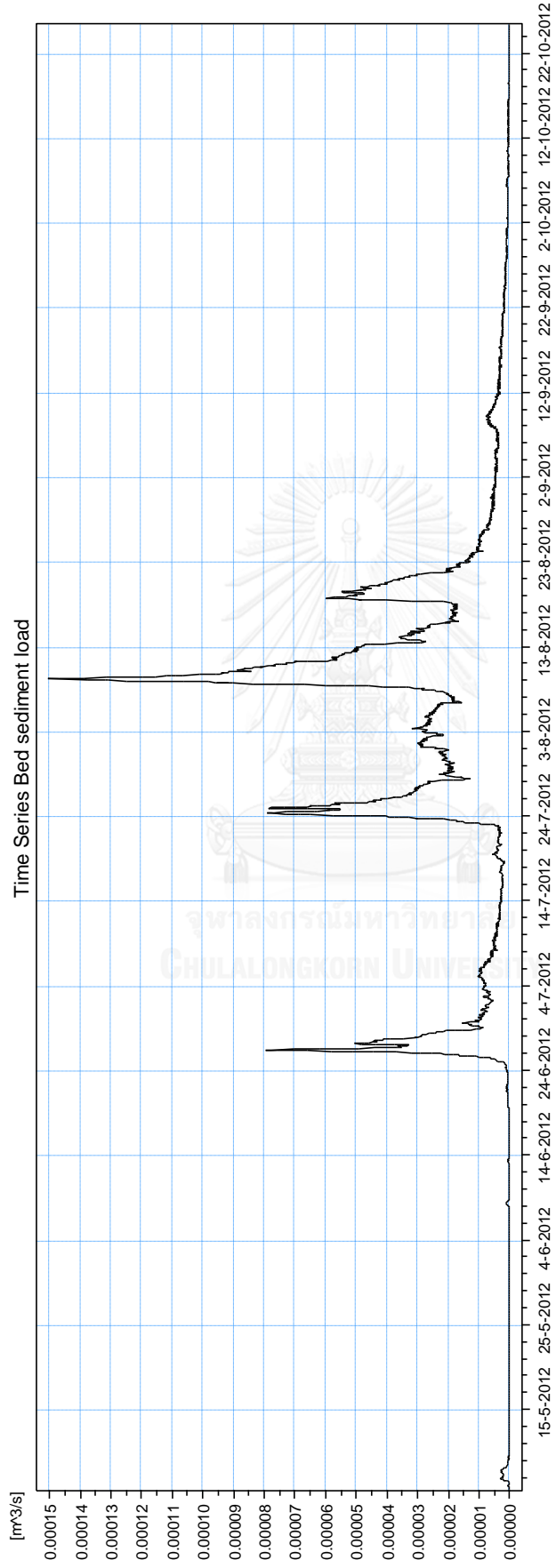
Figure 4-23 Bed load transported to the downstream of the Mae Tao Creeks during wet season
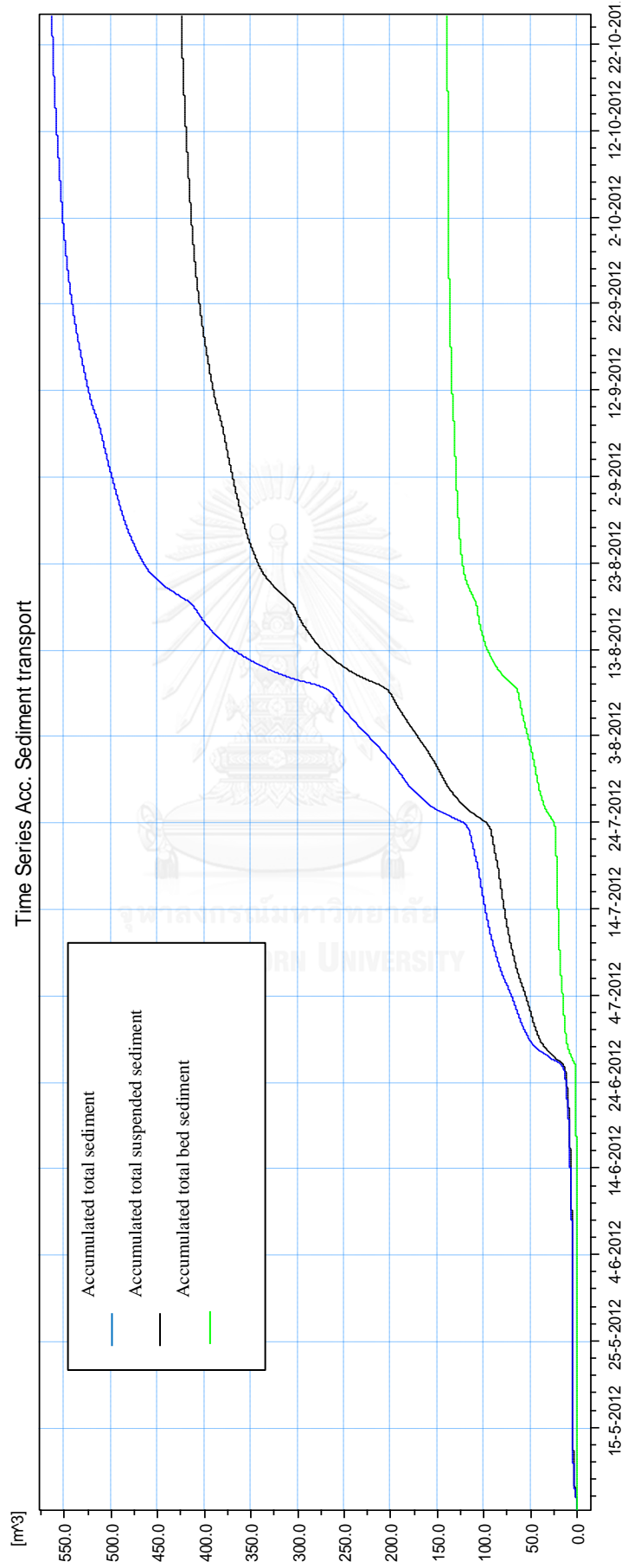
Figure 4-24 Total sediment transported to the downstream of the Mae Tao Creeks during wet season

4.4.1.3.2 Stream sediment transport during dry season

Sediment transport suspended sediment and bed load of dry season were simulated from November 2012 to February 2013.Transport rates of suspended sediment and bed load at downstream are respectively demonstrated in Figure 4-25 to figure 4-26. Highest suspended sediment rate obtained from 26th November 2012 due to the high precipitation rate. The highest rate was 8.92×10^{-6} m^3/s with 1.97 m^3/s water discharge.

Figure 4-27 displayed the total sediment transported downstream in dry season. The accumulated total sediment transport during dry season was 4.22 m^3 which can be divided into 4.04 m^3 of suspended sediment and 0.18 m^3 of bed load transport

Sediment transport rate demonstrated a similar pattern based on the moving of water discharge, as displayed in Figure 4-28. During wet season, the highest peak of sediment transport rate can be inspected in August and the other peaks were scattered shown during June to September of 2012 related to high discharge incident. After storm event, the sediment transport rate gently decreases until the end of the study period. This can be implied that water discharge with high rainfall intensity can varies the rate of sediment transport. Thus, high flow seasonal takes a significant role on total sediment input into downstream of river system.
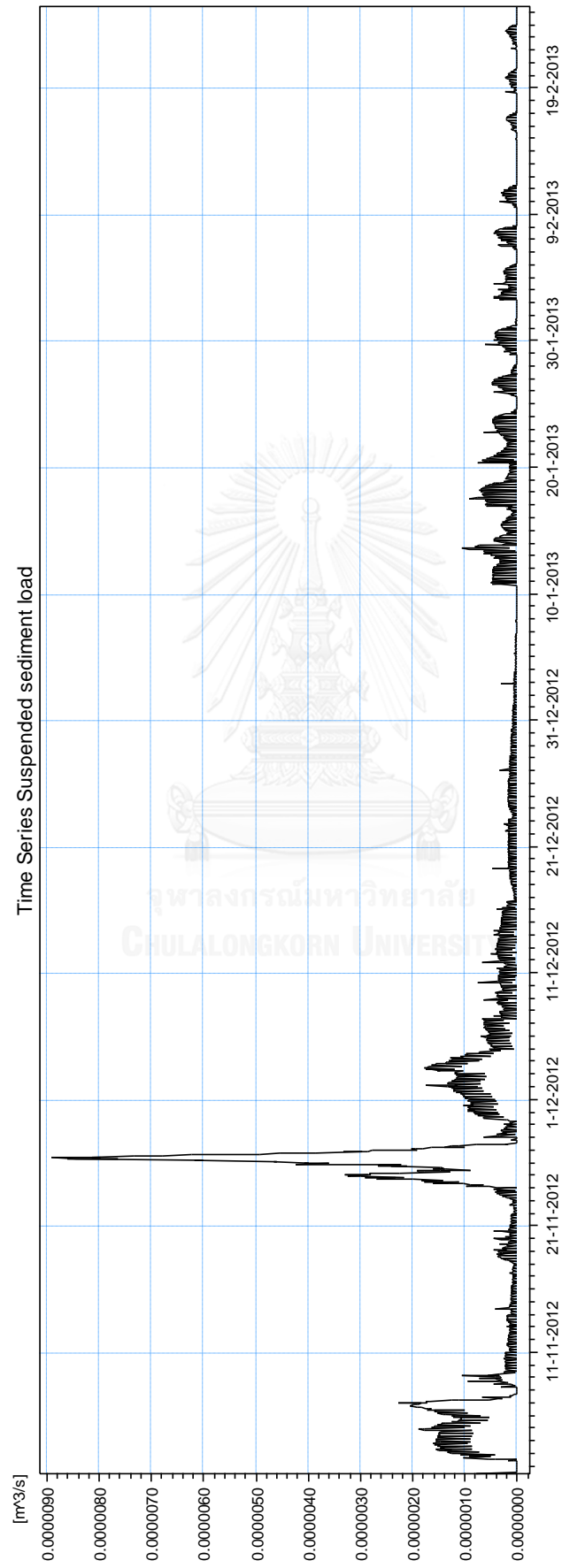
Figure 4-25 Suspended sediment transported to the downstream of the Mae Tao Creeks during dry
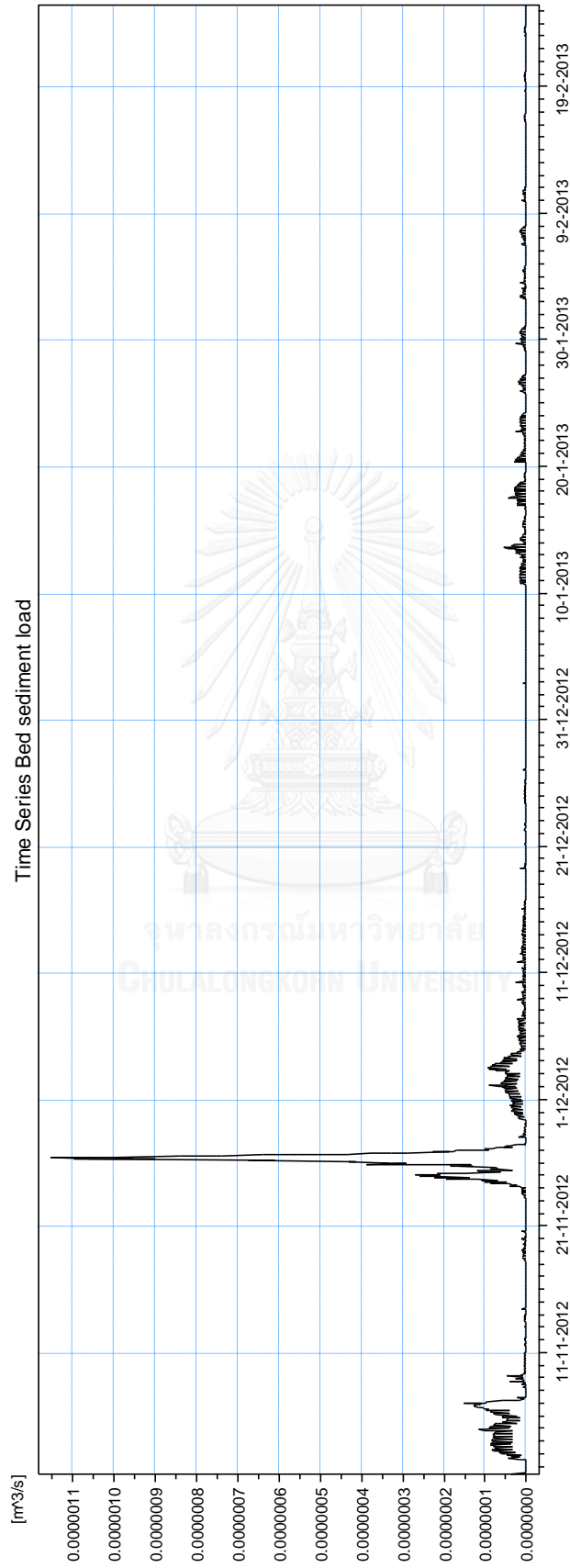
Figure 4-26 Bed load transported to the downstream of the Mae Tao Creeks during dry season
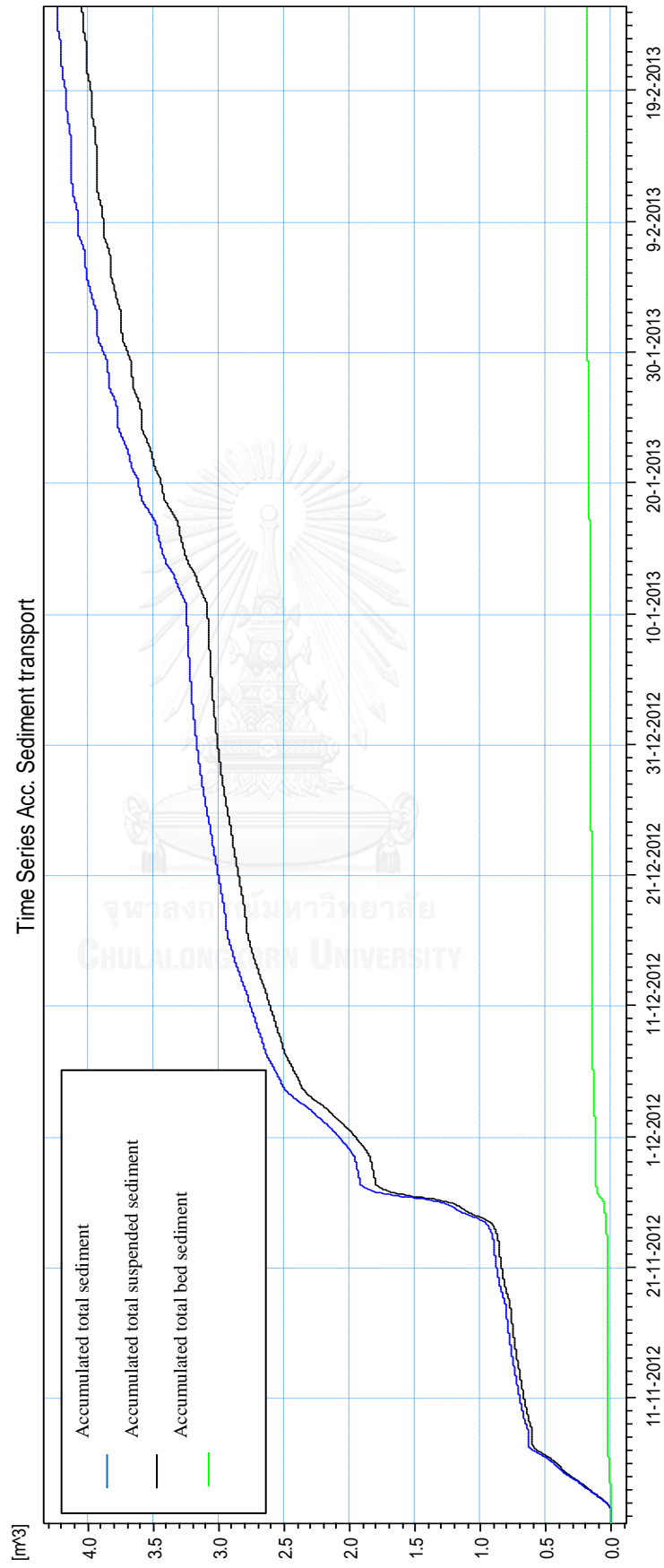
Figure 4-27 Total sediment transported to the downstream of the Mae Tao Creeks during wet season
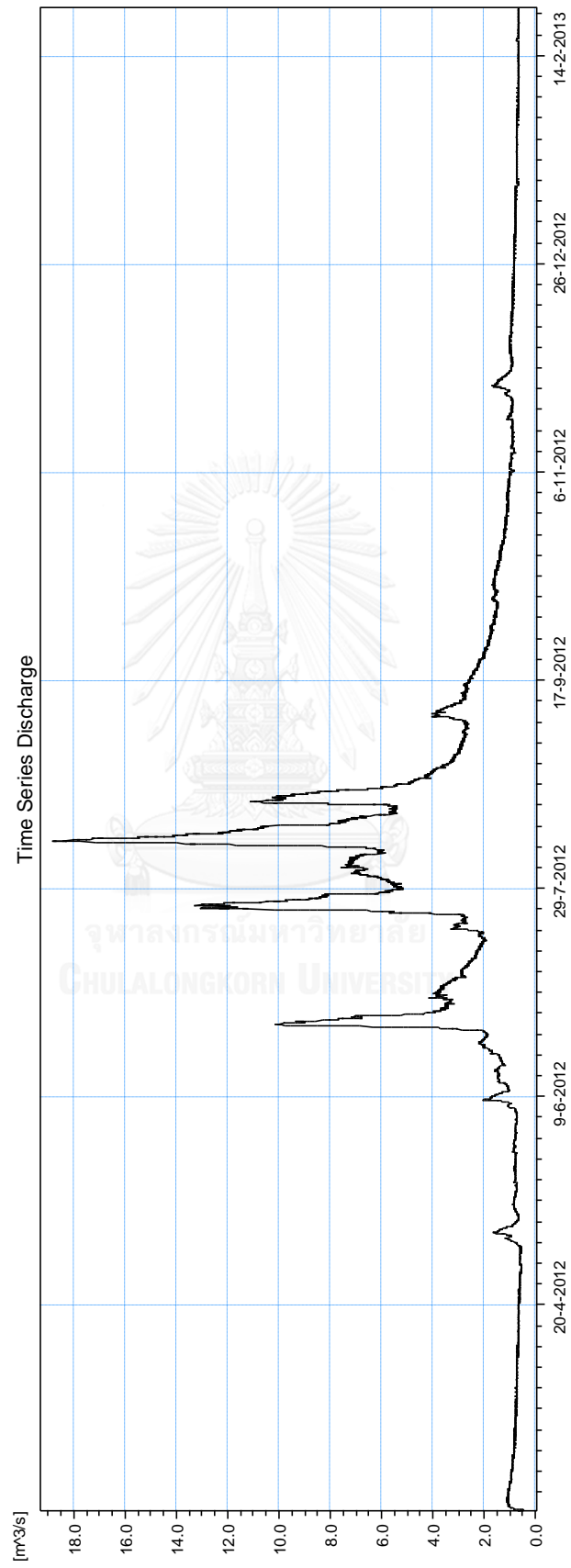
Figure 4-28 Water discharge rate of the study period

4.4.2 OfSET module simulation.

The OfSET module is applied to estimate the cohesive sediment, occurred as result of overland –erosion. According to the laboratory result, high levels of cadmium concentration were significantly detected in sediment samples which are smaller than 200 mesh. Table 4-16 demonstrate the result of the simulation by OfSET module. According to the capability of the module, the flux of the sediment transport and total mass erosion of sediment, smaller than 200 mesh (75 microns), are stored as the result of the simulation.

Table 4-16 Overland flow sediment transport simulation's result

Study period	Simulation result	Minimum	Simulated	Maximum
Wet season	Cohesive sediment discharge (m^3)	363.87	857.41	881.21
	Total cohesive sediment (kg)	269.99×10^3	93.58×10^3	1280.11×10^3
Dry season	Cohesive sediment discharge (m^3)	5.51	12.7	14.68
	Total cohesive sediment (kg)	3.59×10^3	9.05×10^3	14.3×10^3

According to the simulation results, the overland sediment discharge was higher durin the wet season. As in common, the high rainfall intensity can affect the volume discharge from the overland erosion.During the wet season, 91.18% of total overland sediment were transport in to the Mae Tao Creeks with total mass erosion of 93.58 t.These vast amount of the soil erosion is occurred due to the low surface resistance of the Mae Tao Basin Area, represented by the low C and P factor in the empirical estimation.

4.4.2.1 Overland sediment transport

During wet season, the total cohesive sediment from overland-erosion that moved into the Mae Tao Creeks is equal to 2.09×10^5 kg. The highest rate of the sediment transported occurred at 9.78×10^3 kg in May 2013.The highest peak of the overland sediment transport occurs on the highest day of the recorded rainfall intensity level. Additionally, during dry season with low precipitation and rainfall

runoff, total cohesive sediment that moved into the creeks is estimated at 3.60×10^3 kg with the highest rate at 177.86 kg in December 2013. According to the simulation results, the overland sediment is really responsive to the change in the ranfall intensity. Since the rainfall intensity can raise the overland depth, resulting in the high shear stress during erosion incident. The simulation results from the estimation were illustrated in Figure 4-29 to Figure 4-32.

4.5 Statistical Analysis

4.5.1 Sensitivity analysis result of MIKE operation

The sensitivity of model's parameters affecting water discharge was calibrated based on Equation (3.77) and evaluated by sensitivity classes, mentioned in Table 3-4. The result in Table 4-17 indicates that the effect of parameters in overland flow, unsaturated flow and saturated zone to water discharge is different. Sensitivity analysis indicated that hydrodynamic parameters, related to the water discharge of the Mae Tao Creek, are sensitive to the process in saturated zone especially a drainage level of the river, and the Manning number in the process of overland flow to the river. Manning's number affects the flow velocity in the overland flow resulting in the differences in rainfall runoff rate moving into the Mae Tao Creeks.

The drainage level is defined by the saturated layer whereas drained water is extracted. If surface drainage is routed by drain levels, the drainage routing is calculated from the drainage level in each cell. So, the drain flow will continue until crossing a river (Thamjesda 2012).

4.5.2 Sensitivity analysis results of OfSET module

The result from sensitivity analysis of OfSET module's simulation from table 4-17 indicates that the change in soil properties have a high effect on the simulation result, especially density of slurry. Since the slurry content and density can varies based on the soil type of monitoring area, precision in soil type and land use of the study area must be concerned. Soil type and soil properties especially the critical shear stress values can cause a lot of impact to the volume of upland erosion that can

be transported over the Mae Tao Basin. Thus, the density of slurry can refer to the mobility of the eroded sediment that can move during rainfall runoff occur.

For uncertainty analysis the result indicates the range of possible value of the sediment transport which demonstrates in each part of the simulation results. The uncertainty analysis form each simulation procedure demonstrates the wide range of possible value of sediment and cadmium transport over the Mae Tao Basin area. However the simulation results of sediment transport and cadmium transport are concordant with each other. The uncertainty analysis results are demonstrated in consort with each simulation result's table.
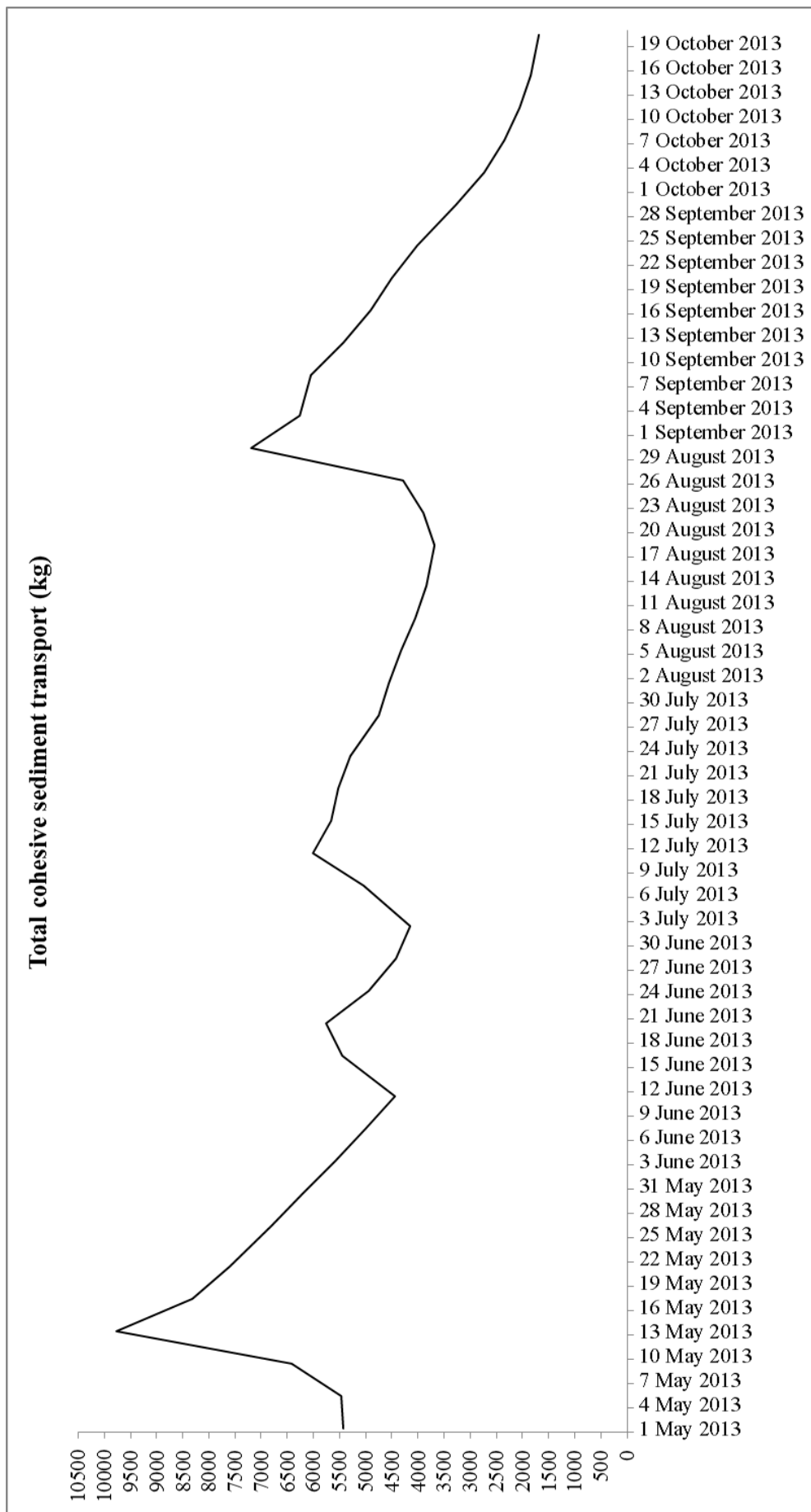
Figure 4-29 Overland sediment transport during wet season
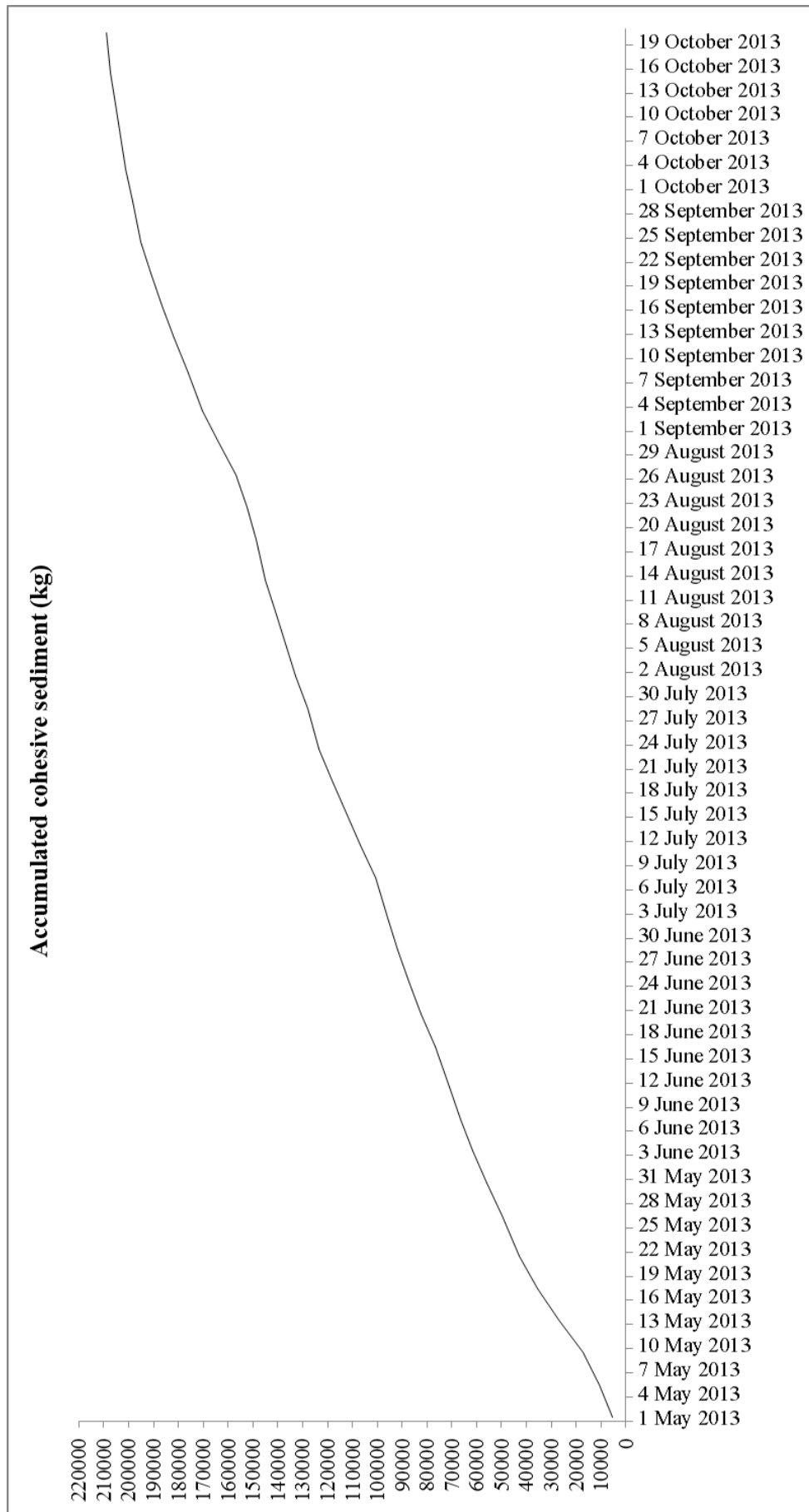
Figure 4-30 Accumulated overland sediment transport during wet season
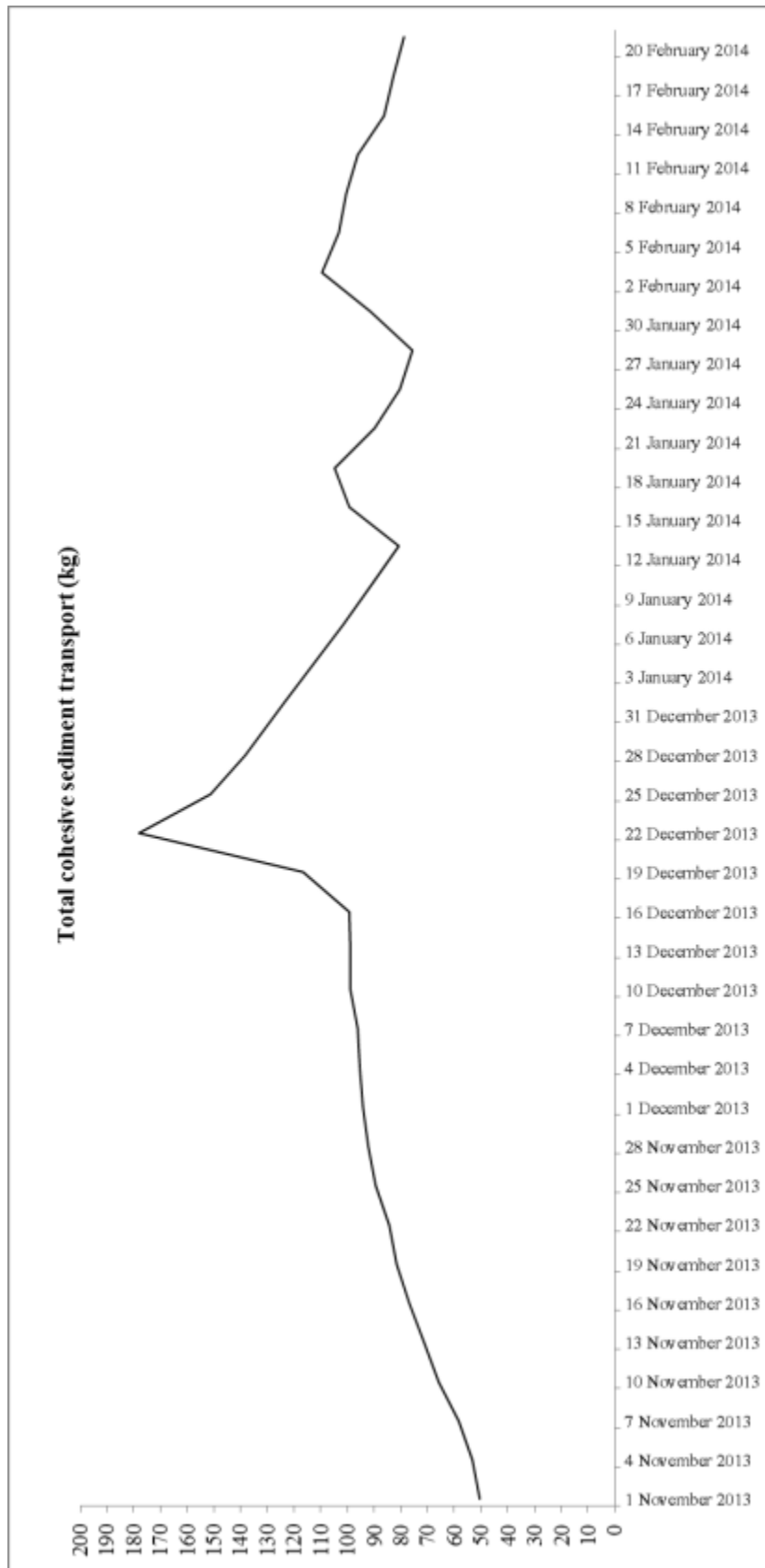
Figure 4-31 Overland sediment transport during dry season
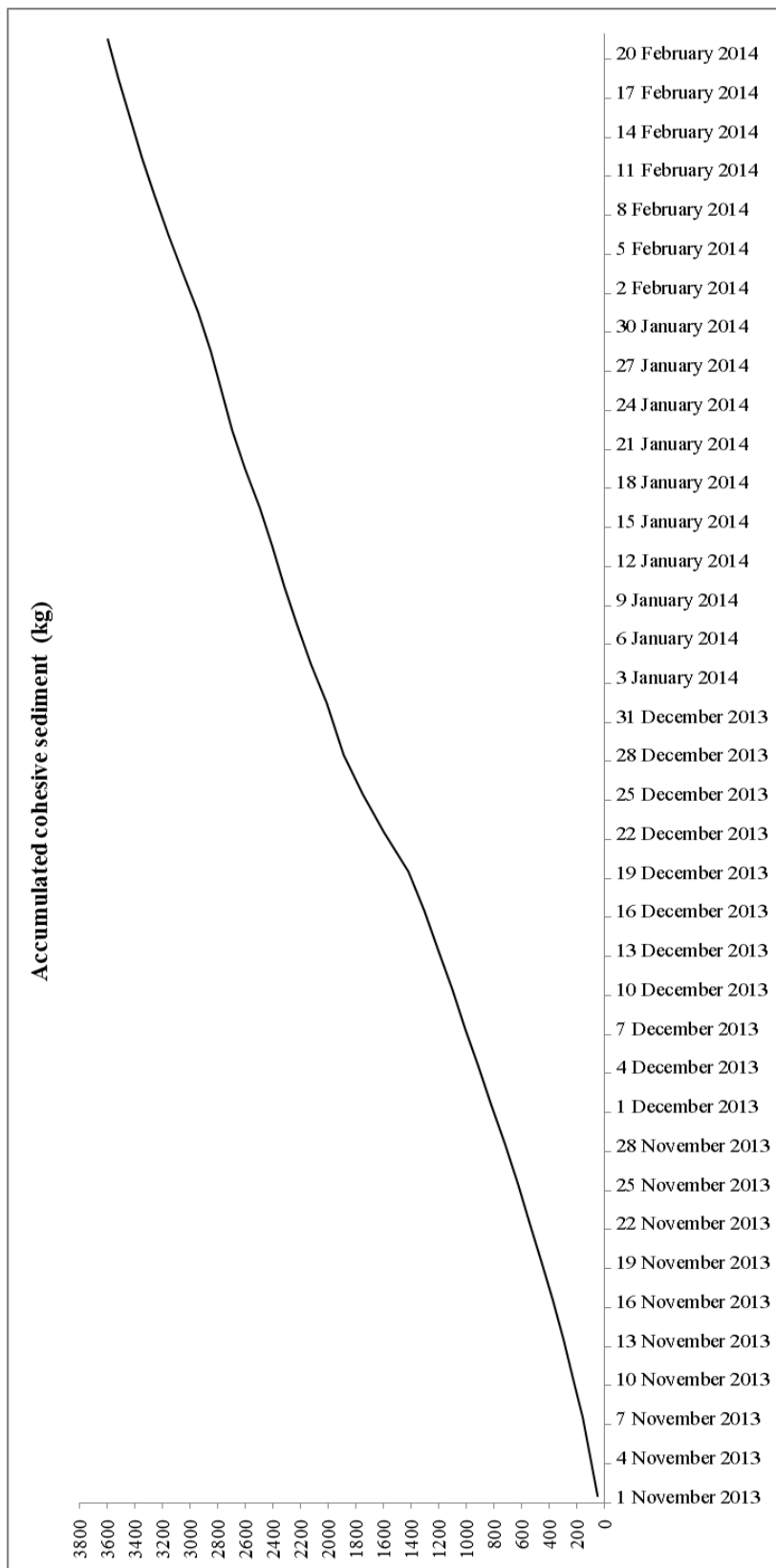
Figure 4-32 Accumulated overland sediment transport during dry season

Table 4-17 Sensitivity of parameters in MIKE SHE

Parameters	Sensitivity index (I)	Sensitivity
Overland flow		
- Manning number	0.08	Medium
- Detention storage	0.01	Small to negligible
Unsaturated Flow		
- Saturated hydraulic conductivity	0.01	Small to negligible
- Groundwater depths used for UZ classification	0.00	
Saturated Zone		
- Lower level	0.01	
- Horizontal Hydraulic Conductivity	0.01	
- Vertical Hydraulic Conductivity	0.00	
- Specific yield	0.00	Small to negligible
- Specific storage	0.03	
- Initial potential head	0.00	
- Drainage level	0.16	Medium
- Drainage time constant	0.00	Small to negligible

Table 4-18 Sensitivity of parameters in OfSET module

Parameter	Sensitivity index	Sensitivity
Bulk Density	0.25	High
Solid content	0.99	High
Density of Slurry	2.18	Very high

4.6 Cadmium transport estimation

4.6.1 Cadmium transport in stream sediment

Cadmium transport in stream sediment was estimated based on Equation 3-95. The results from the estimation are demonstrated in Table 4-19. According to the estimation, the total cadmium transport in the wet season is much higher than dry season due to the high discharge rate of water and sediment in the Mae Tao Creeks. Using sediment density in association with total sediment accumulated volume, the total mass of sediment was estimated at 8230.33×10^3 kg which can be divided into 8215.10×10^3 kg of suspended sediment and 15.22×10^3 kg of bed load for wet season. For dry season, the total of 79.87×10^3 kg stream sediment was transported and 79.52×10^3 kg from total is classified as suspended sediment.

Table 4-19 Possible values of sediment transported in the Mae Tao Creeks due to uncertainty

Study period	Sediment type	Minimum sediment transport (10^3kg)	Simulate sediment transport (10^3kg)	Maximum sediment transport (10^3kg)
Wet season	Suspended sediment	1038.47	8215.10	12472.21
	Bed load	1.92	15.22	23.11
	Total sediment	1040.39	8230.33	12495.32
Dry season	Suspended sediment	10.05	79.52	120.73
	Bed load	0.043	0.34	0.52
	Total sediment	10.09	79.87	121.25

In relation to the mass transport of the sediment, total cadmium contaminant, transported along the Mae Tao Creeks is estimated to be 22.15 kg in wet season and 0.51 kg in dry season as displayed in Table 4-20. This can be suggested that the high discharge rate of water in wet season can emphasize the contamination of cadmium in the Mae Tao Creeks and most of the cadmium transport in the Mae Tao Creek was mainly controlled by suspended sediment transport, especially during the storm event.

Due to high uncertainty of sediment transport simulations, the possible of sediment transport and cadmium transport in hydraulic structure scenarios were estimated from uncertainty analysis as minimum and maximum values of possible cadmium transport.

Table 4-20 Possible values of cadmium transported in the Mae Tao Creeks due to uncertainty

Study period	Sediment type	Minimum cadmium transport (kg)	Simulate cadmium transport (kg)	Maximum cadmium transport (kg)
Wet season	Suspended sediment	2.77	21.93	33.30
	Bed load	0.03	0.22	0.33
	Total cadmium transport	2.80	22.15	33.63
Dry season	Suspended sediment	0.06	0.50	0.76
	Bed load	0.00	0.00	0.01
	Total cadmium transport	0.06	0.51	0.77

4.6.2 Cadmium transport in overland sediment

Cadmium transports by the overland flow of the Mae Tao Basin were estimated based on Equation 3-101.The average cadmium concentration in cohesive sediment of the Mae Tao Basin is estimated as 8.32 mg/kg. The result from OfSET module is established in Table 4-21 to Table 4-22.From the result cadmium transport by the overland flow in wet season was equal to 8.36 kg while 0.08 kg of cadmium was transported during dry season. The results indicate the consistency between sediment transport via channel flow and overland flow that during the wet season with high precipitation rate, sediment and cadmium transport can be greater than the dry season.

Table 4-21 Possible cadmium transport in overland sediment during wet season due to uncertainty

Study period	Wet season		
	Minimum	Average	Maximum
Cohesive sediment discharge (m^3)	363.87	881.21	857.41
Total cohesive sediment (kg)	269.99×10^3	93.58×10^3	1280.111×10^3
Total cadmium transport (kg)	2.41	8.36	11.42

Table 4-22 Possible cadmium transport in overland sediment during dry season due to uncertainty

Study period	Dry season		
	Minimum	Average	Maximum
Cohesive sediment discharge (m^3)	5.51	12.70	14.68
Total cohesive sediment (kg)	3.59×10^3	9.05×10^3	14.3×10^3
Total cadmium transport (kg)	0.03	0.08	0.13

4.7 Potential cadmium contributor of the natural deposition evaluation.

To assess the potential of being a cadmium contributor of cadmium deposition (natural source), the comparison of potential cadmium transport between each potential sources must be accomplished. Total sediment, transported by the river system, can represent the accumulated sediment from all contaminant sources in the catchment area. For wet season, the high rainfall runoff rate can raised the contamination level, transported by river system. Thus, the identification of the contamination sources is merely impossible because the complexity in sediment transport phenomena.

Table 4-23 Cadmium potential contributor assessment of the cadmium deposition in dry season of the Mae Tao Basin

Simulation type	Dry Season			Wet Season		
	Simulation result	Total Cd transport (kg)	Cd contribution (%)	Simulation result	Total Cd transport (kg)	Cadmium contribution (%)
MIKE application	Stream sediment	0.5	100.00	Stream sediment	21.93	100.00
OfSET' Module	Overland sediment	0.08	16.00	Overland sediment	8.36	38.12
	unknown sources	0.42	84.00	unknown sources	13.57	61.88

Conversely, in dry season with low precipitation rate, few sediment transports by hydrological activity take place, so that the assessment for cadmium contamination sources can be assessed.

Since MIKE application is capable for simulating sediment transport in channel flow, the result of the accumulated sediment from dry season can be implied as the total sediment from both overland flow and stream flow that move to the residential area of the Mae Tao Basin. The comparison between cadmium transported in overland sediment (cadmium from natural source) and stream sediment (total cadmium transport from all sources) based on Equation 3-100 can assess the potential in being cadmium contributor of the natural deposition of the Mae Tao Basin. Table 4-23 demonstrates the comparison between cadmium transports from both simulation techniques.

During dry season of 2012-2013, with lowest interference of other sediment transport phenomenon, the area source of the Mae Tao Basin which is the natural deposition of zinc-cadmium mineral composite can approximately contribute 18.00% of total cadmium flux , while 38.12 % cadmium contribution were estimated from the wet season. The cadmium transport result from both stream sediment and overland sediment indicate that natural deposition of cadmium in the Mae Tao Basin is one of significant contributors of cadmium contamination in the Mae Tao Creeks.. Nevertheless, there are some unknown sources of cadmium contamination in the Mae

Tao Basin which requires further information or observation to clarify the main sources of cadmium over the Mae Tao Basin area.

CHAPTER 5

Conclusion and suggestion

5.1 Discussion and Conclusions

The Mae Tao Basin is specified as the cadmium contaminated area which has been supported by many studies, related to the contamination by utilizing the main water resources named as the Mae Tao Creek. More than the creek, the contamination in the Mae Tao Basin can be detected in the agricultural area, utilizing the water from the creek. According to those founding, the hypothesis that the area sources of the Mae Tao Basin, which is the natural deposition of zinc-cadmium composite mineral, can be one of the main contributor of the cadmium in the study area. The potential of being cadmium contributor of natural deposition of zinc mineral in association with cadmium composite was assesses using both empirical and hypothetical procedure as can be seen in Figure 5.1.
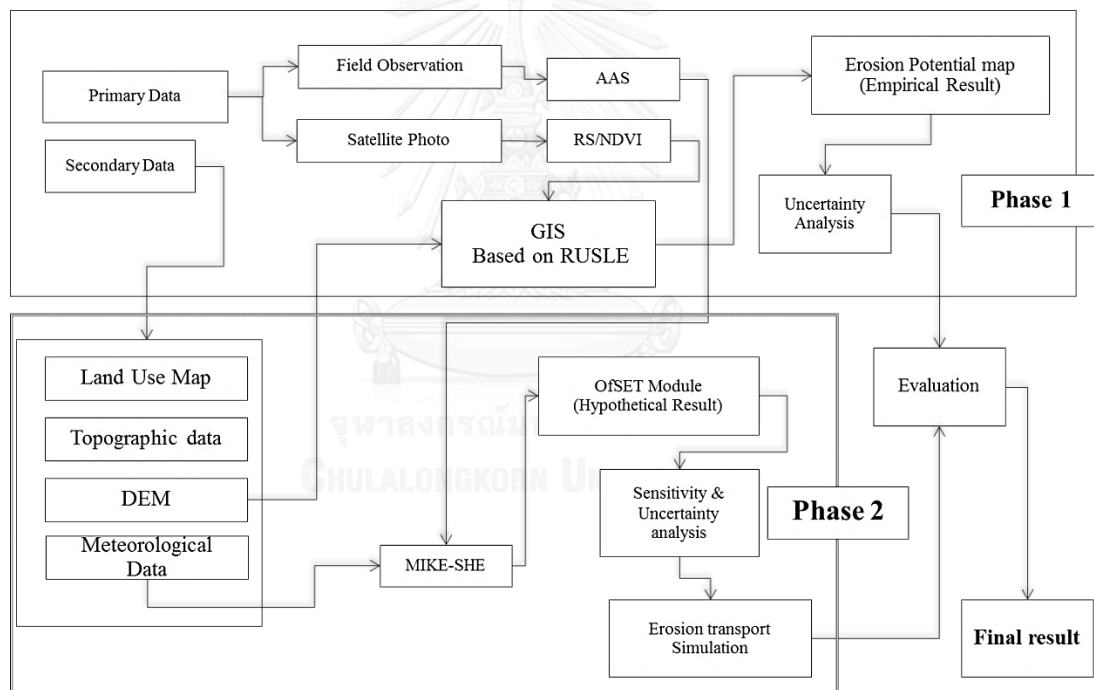
Figure 5-1 Summary of the study framework

For empirical assessment (Phase 1), in order to roughly estimate the possibility of the area as the contributor of cadmium, Revised Universal Soil Loss Equation (RUSLE) was applied to estimate the potential erosion flux of the Mae Tao Basin. The integrated cadmium concentration map and secondary data analysis were take part in calculating the potential cadmium flux from erosion during the rainfall incident.

The estimation results show that the mining areas contribute a large portion of the contaminant at 1.854 ± 0.088 t/ha/. There is an evidence of contamination in the left branch of the Mae Tao creeks, especially the area that passes through an active mine. The results from also designate some other areas with high contamination potential due to being natural sources and having high soil erosion capabilities.

In proportion to the result, corn silage fields can release some portion of cadmium contamination from erosion at 1.324 ± 0.049 t/ha/y. These dense corn fields, located in an area of natural zinc reservoirs, also release cadmium downstream. The combination between the effects of low erosion resistance and being situated in a mountainous area with mining activities results in the area's high cadmium erosion potential, evidently shown by the cadmium concentrations in the upstream area of the Mae Tao creeks

The monitoring check dam were setup during July to October 2014, covering the significant area that high potential of cadmium flux from erosion are existed with the purpose of comparing the cadmium flux result between the estimation and the real erosion sediment. According to the results, the estimation and field observation is not conterminous. The field observation's result indicated a lower erosion flux of cadmium transportation due to erosion.

These inaccuracies in the estimation were the effects of the initial error of each parameters applied in the estimation procedure. However, in the mining production area with high value of LS factor, the potential cadmium flux from the estimation and the observation demonstrates a same trend at 1.75 t/ha/year and 1.854 t/ha/year respectively.

This can be determined that the estimation based on RUSLE can only illustrate the significant potential area that can release cadmium during rainfall incident, thus the total amount of cadmium that move into the Mae Tao Creeks, which is the sources of cadmium are still indistinct. In the area, in which uncomplicated cover practice area are defined, RUSLE can effectively applied to use as a primary tool to estimate the potential contaminated area effected by rainfall erosion.

The hypothetical part of the study is the complement of the assessment in being a significant cadmium contributor of the natural source of the Mae Tao Basin. Since RUSLE can estimate only the potential cadmium flux without the transportation of the contamination, the mathematical modeling was applied to estimate the sediment and contamination transport from both rainfall erosion in the overland flow and the river system of the Mae Tao Basin.

The significant contamination media in the Mae Tao Creek was found to be suspended sediment which can be classified as small size particle and the bed particle smaller than 75 microns. As stated by these founding, the movement of small size particle over the surface of the study area to the Mae Tao creeks was simulated based on MIKE11 and MIKE SHE application binding with Overland flow Sediment Transport module (OfSET).

During May 2012 till the end of February 2013, Cadmium contaminated sediment transport in the Mae Tao Basin was estimated by the simulation of MIKE SHE coupled with MIKE 11 model to simulate hydrodynamic and sediment transport results in the Mae Tao Creeks. While the sediment transport in the creeks was simulated the overland flow depth, overland flow volume in x and y axis were exported to the Overland flow Sediment Transport module (OfSET) to estimate the overland erosion of the Mae Tao Basin.

The assessment of hydrodynamics in the Mae Tao Creek was calibrated with the observed water depth at station MT 04. The performances of the simulated hydrodynamic results were based on correlation coefficient (R) and root mean square error (RMSE). The values of R and RMSE were generated with 0.57 and 0.26 m, respectively which means that the performance of the simulation is acceptable based on limitation of rainfall data.

According to the simulation, wet season cause higher water depth and discharge than dry season due to the differences in precipitation rate. Water discharge was detected to have highest value at downstream. Moreover, as a result of sensitivity analysis, a drainage level in the saturated zone and the process in overland flows to the river were majorly affected the water discharge.

Size distribution of bed sediment was conduct and the results shows that almost all of bed particle is sand size. According to analysis result, non-cohesive sediment transport module in MIKE 11 was applied to assess a sediment transport. The sediment transport had been simulated from May 2012 to October 2012 as wet season, while the rest period of November 2012 to February 2013 was assigned as dry season

.   Total sediment transport was divided into suspended sediment and bed load. During wet season, the total accumulated sediment transport was simulated to 563.76 m^3, which obviously occurred in the wet season by 99.23 due to the greater rainfalls than the dry season, contributing to high availability of sediment transport in the Mae Tao Creeks.

According to field observation, the cadmium contaminated contains higher concentrations in wet season for both suspended sediment and bed load. Station MT 02 located at downstream before entering the residential area was assigned as monitoring spot to estimate cadmium transport. Cadmium concentrations in suspended sediment were found exceed the standard at 6.29 mg/kg and 2.67 mg/kg for wet and dry season, respectively. Bed load contained cadmium values with 16.01 mg/kg and 14.39 mg/kg for wet and dry season.

In addition field observation on cadmium contamination and size distribution of overland sediment were conducted. The results indicate that high concentration of cadmium can be found in mining production area at 303.49 mg/kg; however, this concentration was collected at the water management HQ where the treatment of contaminated soil is operated. The average cadmium concentration of the overland cohesive sediment in the Mae Tao Basin area was estimated as 8.32 mg/kg.

The distribution of cadmium contaminated via sediment transport in the Mae Tao Creek mainly occurred in the wet season. In relation to high transport capacity of suspended sediment, the cadmium transport was dominant by suspended sediment transport. From May 2011 to February 2012, cadmium was transported out of the Mae Tao Creek about 22.15 kg by adsorbing in the sediment of wet season with 21.93 kg and in dry season with 0.22 kg.

For the overland sediment transportation, wet season with high precipitation rate can dominate the total cadmium transport. During wet season 8.36 kg of cadmium were transported into the Mae Tao creeks, while 0.08 kg of cadmium was transported during dry season.

Since cohesive sediment, which is smaller than 75 microns, is the dominant particle size that induces the contamination of cadmium in the Mae Tao Basin Area. During dry season with lowest precipitation rate, the comparison between total cadmium transport by stream sediment and overland sediment can complete the assessment of being a contributor of the natural sources. With 16% of cadmium contribution, the zinc-cadmium deposits in the Mae Tao basin area is one but not significant contributor of the contamination in the Mae Tao Basin area.

From the study result, it can be concluded that this set of methodology frame work can signify the contributor of the contamination of the remote area whereas the main transporter of the contaminant are water and sediment. The combination between empirical and hypothetical techniques is the key to incredulous the difficulties in direct field observation of the remote contaminated area.

5.2 Suggestions

To accomplish the investigation of cadmium transport via suspended sediment and bed load, cadmium concentration was a key factor to define the transport. Cadmium transport in the Mae Tao Creek was evaluated in two seasons which are dry and wet season. However, the accessibility to sediment collection during wet season had limitation from the extensive flood occurrence.

According to the important of cadmium concentration, more of sediment samples should be collected in each season. Additionally, the cadmium concentrations would be collected from the agricultural area receiving water from the Mae Tao Creek to more understanding on source and cadmium contamination in the area. In accordance with the assessment impacts of land use, leaf area index of each crop was defined by basing on literature.

The leaf area index should be measured at the study area to obtain more reliable simulated results. The sediment density was obtained from literature reviews that caused the high uncertainty in this study. To improve the cadmium transport result, more effort should be focused on estimating accurate density of sediment both in suspended sediment and bed load to be used in cadmium transport estimation. Moreover, other eatable crop type in study area would be taken into account for further discussion.

As result from this study found that weir in the Mae Tao Creek may reduce a lot of contaminate sediment to downstream which is the more dense resident area. It would be worth to do more study on using such structure to manage cadmium contaminate.Sincr hydrologic structure is capable for reducing the sediment prenatrating the downstream area, the effect of the wier to smaller size of sediment especially sand and mud particle in the Mae Tao Creek should be extended.

As can be seen in the estimation results, OfSET module still requires a complemention in its capability in estimating the size distribution of the overland sediment especially in the non-cohesive sediment size particle.

In case of having suffiecient data for other parameters, other 2d overland model with more detail in sediment transport for heavy metal process should be appliedfor better description of the overland sediment transpot incident over the Mae To Basin area. For instance, MIKE21 binding with sediment transport and mud transport module could be one of the alternatives in this case of estimation.

More extensive field survey at structure may require refining and validating the simulation result. Further recommend for future study is extended to ECOLab model in MIKE 11 that would be taken into simulation to describe heavy metal transport with sediment and river flow.

Even though a high potential of cadmium from erosion was detected, practices to diminish the outflow from the mine were found to be in place. To enhance the efficiency with which the mine manages its outflow, a study on the relationship

between the quantity of outflow from the mine and the capacity of the tailing dam should be performed.

Strip cropping performed against the flow path of the mountainside area can reduce the erosion rate by increasing the value of the supporting practice factor. Therefore, developments in vegetation planning like strip cropping must be promoted. However, in areas that are already contaminated, subsidies must be put in places that successfully persuade rice farmers to plant other kinds of crops or vegetation.

For applying this study framework to another similar contaminated site, the field observation for the input parameter in the simulation must be accomplished as much as possible in order to gain less uncertainty in the simulation result. Nevertheless, for the contamination site where the filed observation can be merely accomplished this study framework can be one of recommended alternative to signify the contamination contributor in the area.
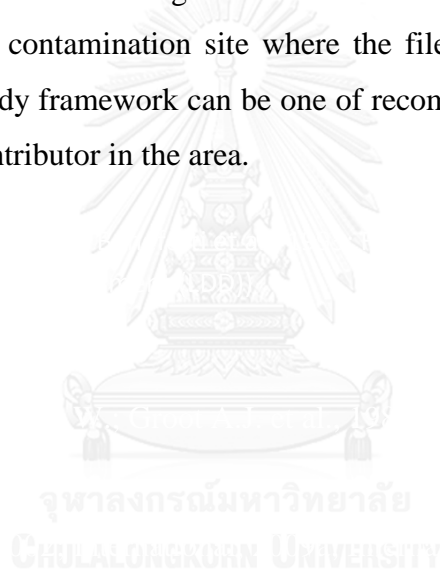
REFERENCES

A., R., and Kjelds J. Mike She Groundwater Model Selected as Best Management Tool in Us. 2001. Available: http://www.dhigroup.com/News/NewsArchive/2001/MIKESHEGroundwater. MAY 1 2012.

Akkajit P., and Tongcumpou C. Fractionation in Cadmium Contaminated Soil: Relation and Effect on Bioavailable Cadmium. Geoderma 156 (2010): 126-132.

Almas M. , and Jamal T. . Use of Rusle Soil Loss Prediction During Different Growth Periods. Pakistan Journal of Biological Sciences 3 1 (2000): 118-221.

Ariathurai R . , and Arulanandan K. . "Erosion Rates of Cohesive Soils." the ASCE: Jounal of the Hydraulics Division,, 1978. 279-283. Vol. 104.

Arnason J. G. , and Fletcher B. A. 40+ Year Record of Cd, Hg, Pb, and U Deposition in Sediments of Patroon Reservoir, Albany County, Ny, USA. Environmental Pollution 123 (2003): 383-391.

Asrar G. , Fuchs M. , Kanemasu E.T., and Hatfield J.L. Estimating Absorbed Photosynthetic Radiation and Leaf Area Index from Spectral Reflectance in Wheat. Agron 76 (1984): 300-307.

Benefetti, Roberto, and Paolo R. . On the Use of Ndvi Profiles as a Tool for Agricultural Statistics: The Case Study Ofwheat Yield Estimates and Forecast in Emilia Romagna. Remote Sensing of the Environment 45 (1993): 311-326.

Bizuwerk A. , Taddese G. , and Getahun Y. . Application of Gis for Modeling Soil Loss Rate in a Wash Basin, Ethiopia: International Livestock Research Institute (ILRI), 2008.

Breda N.J. Ground-Based Measurements of Leaf Area Index: A Review of Methods, Instruments and Current Controversies. Journal of Experimental Botany. . 54 (2003): 2403-2417.

Bryan G. (2012) Flame Atomic Absorption Spectroscopy Demonstration. https://www.youtube.com/watch?v=_KZjb9G3hB8. Accessed 9/07/2015 2015

Burt T. N. "Cohesive Sediment and Physical Models,." Int. Con5 on Phys. Modeling of Transport. MIT: Cambridge, Massachusetts, 1990.

Butt M. B., Payne J.T., and Overgaard J. "Improving Streamflow Simulations and Firecasts with Multimodel Ensembles." The 6th International Conference on Hydroinformatics. Eds. Liong, Phoon and Babovic, 2004. 1189-1196.

CCME. "Recommended Canadian Soil Quality Guidelines." 2002.

Chen C.W., Kao C.M., and Dong C.D. Distribution and Accumulation of Heavy Metals in the Sediments of Kaohsiung Harbor, Taiwan. Chemosphere 66 (2007): 1431-1440.

Codex Alimentarius Commission Report of the 34th Session of the Codex Committee on Food Additives and Contaminants (Ccfac). Rotterdam, 2002.

Deering D. W. , and Haas R.H. Using Landsat Digital Data for Estimating Green Biomass. Greenbelt, MD 1980.

Demattê* J.A.M., Fioriob P.R., and Ben-Dorc E. . Estimation of Soil Properties by Orbital and Laboratory Reflectance Means and Its Relation with Soil Classification The Open Remote Sensing Journal, 2 (2009): 12-23.

Department of Primary Industries and Mines (DPIM). "Report of Water Quality and Stream Sediment Monitoring at Doi Padaeng Zinc Mining in Mae Sot District, Tak Province. ." Ed. M. o. I. Department of Primary Industries and Mines. Bangkok, Thailand: Office of Primary Industries and Mines Khet 3 (Northern part), 2009.

DHI Water Environment Health. Mike 11 Reference Manual. Hørsholm, Denmark: DHI, 2011a.

DHI Water Environment Health. Mike 11 Short Introduction Tutorial Version 2010. Hørsholm, Denmark: DHI, 2011b.

DHI Water Environment Health. Mike 11 User Guide. Hørsholm, Denmark: DHI, 2011c.

Dymond J.R. , Stephens P.R. , Newsome P.F., and Wilke R.H. Percentage Vegetation Cover of a Degrading Rangeland from Spot. International Journal of Remote Sensing 13,11 (1992): 1999-2007.

Erskine W.D., Mahmoudzadeh A. , and Myers C. . Land Use Effects on Sediment Yields and Soil Loss Rates Insmall Basins of Triassic Sandstone near Sydney, Nsw, Australia. . Catena 49 (2002): 271-278.

ESRI.   Arcgis   Desktop   Help   9.3.   2015.   Available: http://webhelp.esri.com/arcgisdesktop/9.3/index.cfm?TopicName=welcome. Feb 2 2015.

European Economic Commission (EEC). Council Directive 86/278/Eec on the Protection of the Environment, and in Particular of the Soil, When Sewage Sludge Is Used in Agriculture, 1986.

Forstner U., and Salomons W. Trace Metal Analysis on Polluted Sediments Part I: Assessment of Sources and Intensities. Environ. Technol. Lett. 1 (2003): 494-505.

GCOS. . Implementation Plan for the Global Observing System for Climate in Support of the Unfccc, 2004.

Groot A.J., Zschuppe K.H., and Salomons W. Standardization of Methods of Analysis for Heavy Metals in Sediments. Hydrobiologia 92 (1982): 689-665.

Hayter E.J. Prediction of Cohesive Sediment Movement in Estuarial Waters,. Ph.D., University of Florida, 1983.

Hayter E.J., et al. Hsctm-2d, a Finite Element Model for Depth-Averaged Hydrodynamics, Sediment and Contaminant Transport,. Athens, Georgia. : National Exposure Research Laboratory, Office of Research and Development, U.S. EPA, 1999.

Hoffer R.M. Biological and Physical Considerations in Applying Computer-Aided Analysis Techniques to Remote Sensor Data, in Remote Sensing: The Quantitative Approach. Eds. PH Swain and SM Davis: McGraw-Hill Book Company, 1998.

Honda R. . Cadmium Induced Renal Dysfunction among Residents of Rice Farming Area Downstream from a Zinc-Mineralized Belt in Thailand.Toxicology Letters 198 (2010): 26-32.

Hwang K.N., and Mehta A.J. <u>Fine Sediment Erodibility in Lake Okeechobee</u>. Gainesville, Florida.: Coastal and Oceanographic Engineering Dept. , Univ. of Florida,, 1989.

IARC. <u>Cadmium and Cadmium Compounds. Beryllium, Cadmium, Mercury and Exposures in the Glass Manufacturing Industry</u>, 1993.

International, A. S. f. T. a. M. <u>Astm C136 - 06 Standard Test Method for Sieve Analysis of Fine and Coarse Aggregates</u> 2009a. Available: http://www.astm.org/Standards/C136.html. 2012,May 1.

International, A. S. f. T. a. M. "Astm D422 - 63(2007) Standard Test Method for Particle-Size Analysis of Soils." 2009b.

International Cadmium Association (ICDA). <u>Cadmium</u>. 2009. Available: http://www.cadmium.org. Jan 23 2015.

International Programme on Chemistry Safety (IPCS) "Environmental Health Criteria 135: Cadmium: Environmental Aspect." Ed. W. H. O. (WHO). Geneva, Switzerland., 1992.

Design of an Environmental Information System for Yonezawa City in Japan 2006.

Jain C.K. Metal Fractionation Study on Bed Sediments of River Yamuna,. <u>India Water Research.</u> 38 (2014): 569-578.

Joe R. Galetovic. "Guidelines for the Use of the Revised Universal Soil Loss Equation(Rusle) Version 1.06 on Mined Lands, Construction Sites ,and Reclaimed Land." Ed. T. O. o. T. T. W. R. C. C. O. o. S. Mining: Broadway, Suite 3320Denver, 1999.

Joint FAO/WHO Expert Committee on Food Additives (JECFA) <u>Report of the 61st Session of Jecfa, 10-19 June</u>. Rome: JECFA, 2003.

Joint FAO/WHO Expert Committee on Food Additives (JECFA) "Report of the 64th Meeting of the Jecfa, 8-17 February.". Rome, 2005.

Jonckheere I. Review of Methods for in Situ Leaf Area Index Determination Part I. Theories, Sensors and Hemispherical Photography..<u>Agricultural and Forest Meteorology.</u> 121 (2004): 19-35.

José L G.R., and Martín C. GS. Historical Review of Topographical Factor, Ls, of Water Erosion Models. <u>Aqua-LAC</u> 2,2 (2010): 56-61.

Julien P.Y., Saghafian B., and Ogden F.L. Raster-Based Hydrologic Modeling of Spatially-Varied Surface Runoff. <u>Water Resources Bulletin</u> 31,3 (1995): 523-536.

Kamel A.H. Application of a Hydrodynamic Mike 11 Model for the Euphrates River in Iraq. <u>Slovak Journal of Engineering.</u> 2 (2008): 1-7.

Karoonmakphol P. <u>Evaluation of Cadmium Contamination Due to Sediment Transport in Mae Tao Creek, Mae Sot District, Tak Province</u>. Master, Graduate Schoo Chulalongkorn University., 2009.

Karoonmakphol P., and Chaiwiwatworakul P. "Evaluation of Cadmium Contamination Due to Bed Load Sediment Transport in Mae Tao Creek, Mae Sot District, Tak Province, Thailand." <u>Chemistry and Chemical Engineering (ICCCE), 2010 International Conference</u>. Kyoto, 2010. 114-118.

Krige D.G. <u>A Statistical Approach to Some Mine Valuations and Allied Problems at the Witwatersrand,</u>. Master, the University of Witwatersrand, 1951.

Krige D.G. , and Assibey-Bonsu W. New Developments in Borehole Valuations for News Gold Mines and Unddeveloped Sections of Existing Mines. Journal of the South African Institute of Mining and Metallurgy 9,3 (1992): 71-78.

Krissanakriangkrai O. Assessment on Environmental Impact and Health Risk from Aquatic Animals in Cadmium Contaminated Area in Mae Sot District, Tak Province.: Naresuan University, 2007.

Kristensen K. J., and Jensen S.E. . A Model for Estimating Actual Evaprotranspiration from Potential Evaprotranspiration. Nordic Hydrology 6,3 (1975): 170–188.

Krone R.B. Flume Studies of the Transport of Sediment in Estuarial Shoaling Processes. Berkeley California.: Hydraulic Engineering Laboratory, University of California, 1962.

Land Development Department (LDD). "Annual Report 2003." Ed. M. o. A. a. c. Land Development Department. Bangkok, Thailand, 2003.

Land Development Department (LDD). "Assessment of Soil Loss Using the Equation of Soil Loss." Ed. M. o. A. a. c. Land Development Department. Bangkok, Thailand, 2002. 26.

Land Development Department (LDD). "Group of Soil Series for Economic Crops of Thailand." Ed. M. o. A. a. c. Land Development Department. Bangkok,Thailand: Office of Soil Survey and Landuse Planning, 2005.

Land Development Department (LDD). "Soil Erosion in Thailand." Soil Loss Map of Thailand Ed. M. o. A. a. c. Land Development Department. Bangkok, Thailand, 2000. 266.

Lenhart T., Eckhardt K., Fohrer N.H., and Frede H.G. Comparison of Two Different Approaches of Sensitivity Analysis. Physics and Chemistry of the Earth 27 (2002): 645-654.

Mahidol University. Specification of Pollution Standard and Environmental Management of Miningindustry and Metallurgy of Zinc, Tak Province. Bangkok, Thailand: Faculty of Environment and Resource Studies, 2006.

Maneewong P. Cadmium Distribution in Stream Sediment and Suspended Solids Along Huai Mae Tao and Huai Mae Ku, Mae Sot District, Tak Province. Master's, Graduate School Chulalongkorn University., 2005.

Mitasova H. , Mitas L, Brown WM, and Johnston D. Terrain Modeling and Soil Erosion Simulations for Fort Hood and Fort Polktest Areas. Illinois: Geographic Modeling and Systems Laboratory, University of Illinois, Urbana-Champaign, Illinois, 1999.

Mitchener H., and Torfs H. Erosion of Mud/Sand Mixtures. Journalof Coastal Engineering 29 (1996): 1-25.

National Toxicology Program. Report on Carcinogens: Department of Health and Human Services, 2011.

NEPC. National Environment Protection (Assessment of Site Contamination) Measure Schedule B (1) Guideline on the Investigations Levels for Soil and Groundwater: National Environment Protection Council ,Australia,, 1999.

Nichanon K. Management Issues Affecting the Health of the Environment: Cadmium in Mae Sot District of Tak Province 2005. Available: http://advisor.anamai.moph.go.th/283/28305.htmlApril 2011.

Nogawa K., and Kido T. Biological Monitoring of Cadmium Exposure in Itai-Itai Disease Epidemiology. . International Archives of Occupational and Environmental Health 63 (1993): 43-46.

Oil Spill Prevention Administration and Response (OSPAR) Commission " Ospar Background Document on Cadmium.", 2002.

Oliver M.A. , and Webster R. Kriging: A Method of Interpolation for Geographical Information System. INT. J. Geographical Information Systems 4,3 (1990): 313-332.

Padaeng Industry Public Company Limited. The Report of Environmental Impact Assessment and Environmental Quality Monitoring on Zinc Mining Project 2/2552 During July-December 2552. Bangkok, Thailand: Padaeng Industry Public Company Limited, 2009.

Partheniades E. A Study of Erosion and Deposition of Cohesive Soils in Sult Water. University of California, 1962.

Phaenark C., Pokethitiyook P., Kruatrachue M., and Ngernsansaruay C. Cd and Zn Accumulation in Plants from the Padaeng Zinc Mine Area. . International Journal of Phytoremediation 11 (2009): 479-495.

Pollution Control Department (PCD). "Survey and Assessment of Cadmium Distribution and Sources of Contamination in Mae Tao River Basin, Mae Sod District, Tak Province." Ed. M. o. N. R. a. E. Pollution Control Department. Bangkok, Thailand, 2011.

Pollution Control Department (PCD). Thai Environment Regulations. . 2009. Ministry of Natural Resources and Environment. Available: http://www.pcd.go.th/info_serv/en_regulation.html

Presbitero A.L. . Soil Erosion Studies on Steep Slopes of Humid-Tropic Philippines. Australia: School of Environmental Studies, Nathan Campus, Griffith University 2003.

Pryseley, et al. Estimating Precision, Repeatability, and Reproducibility from Gaussian and Non- Gaussian Data: A Mixed Models Approach. Journal of Applied Statistics 37,10 (2010): 1729-1747.

Refsgaard J.C. An Integrated Model for the Danubian Lowland -Methodology and Applications. Water Resources Management. 12 (1998): 433-465.

Rosalía R.S. Gis-Based Upland Erosion Modeling, Geovisualization and Grid Size Effects on Erosion Simulations with Casc2d-Sed Ph.D., Department of Civil Engineering Colorado State University, 2002.

Rouse J.W., Haas R.H., Deering, D. W., and Sehell, J. A. Monitoring the Vernal Advancement and Retro Gradation (Green Wave Effect) of Natural Vegetation: Remote Sensing Center,, 1974.

Sadeghi S.H. . "Application of Musle in Prediction of Sediment Yield in IranianConditions " ISCO2004-13th International Soil Conservation Organization Conference-Brisbane. Ed. T. M. U. Natural Resources College. Brisbane, 2004.

Salomons M. Biochemical Processes Affecting Metal Concentrations in Lake Sediments (Ijsselmeer, the Netherlands). Science of the Total Environment. 16 (1980): 217-229.

Shamshad A., Azhari M.N., Wan WMA. , and Parida B.P. Development of an Appropriate Procedure for Estimation of Rusle Ei30index and Preparation of Erosivity Maps for Pulau Penang in Peninsular Malaysia. Catena 72 (2008): 423-433.

Simmons R.W., Noble A.D., Pongsakul P., Sukreeyapongse O., and Chinabut N. "Analysis of Field-Moist Cd Contaminated Paddy Soils During Rice Grain Fill Allows Reliable Prediction of Grain Cd Levels. Plant Soil.". Bangkok, Thailand, 2008. 125-128.

Simmons R.W., Sukreeyapongse O., Noble A.D., and Chinabut N. "Report of Ldd-Iwmi Land Zoning and Cd Risk Assessment Activities Undertaken in Phatat Pha Daeng and Mae Tao Mai Sub-Districts, Mae Sot, Tak Province, Thailand." Ed. M. o. A. a. c. Land Development Department. Bangkok, Thailand, 2005.

Somboon P. Distribution of Cadmium and Zinc in Soil from Zinc Mining Activitiy: A Case Study of Zinc Mine, Mae Sot District, Tak Province,. Master, Department of Technology of Environmental Planning for Rural Development,Faculty of Science, Mahidol University., 1999.

Soo H.T. Soil Erosion Modeling Using Rusle and Gis on Cameron Highlands, Malaysia for Hydropower Development. Master, The School for Renewable Energy Science University of Iceland 2011.

Sriprachot A. Distribution of Cadmium in Contaminated Soil. . Master, Graduate School Kasetsart University, 2006.

Supakij N., and Burin C. Internet Gis, Based on Usle Modeling, for Assessment of Soil Erosion in Songkhram Watershed, Northeastern of Thailand. Kasetsart J. (Nat. Sci.) 46 (2012): 272-282.

T.O., L. Cadmium (Materials Flow), : U.S. Department of Interior, Bureau of Mines., 1994.

Thamjesda T. Effects of Agricultural Land Use on the Transport of Cadmium in the Mae Tao Creek, Thailand. Master, Graduate School of Chulalongkorn University Chulalongkorn University, 2012.

Tharathammathigorn W. Transport Modeling of Cadmium Contaminated Suspended Sediment and Bed Load in Mae Tao Creek, Thailand. Master, Graduate School of Chulaongkorn University Chulalongkorn Unversity, 2010.

Tucker C.J. Red and Photographic Infrared Linear Combinations for Monitoring Vegetation. Remote Sensing of the Environment 8 (1979): 127-150.

U.S. Geological Survey (USSG). Frequently Asked Questions About the Landsat Missions: What Are the Best Spectral Bands to Use for My Study? (Utilization). 2012. Available: http://landsat.usgs.gov/best_spectral_bands_to_use.php December 2012.

Unhalekhaka U., and Kositanont C. Distribution of Cadmium in Soil around Zinc Mining Area. . Thai Journal Toxicology 23 (2008): 170-174.

Van Rijn L.C. Sediment Transport, Part I: Bed Load Transport. Journal of Hydraulic Engineering 110 (1984a): 1434-1456.

Van Rijn L.C. Principles of Sediment Transport in Rivers, Estuaries and Coastal Seas. Amsterdam, The Netherlands: Aqua Publications, 1993.

Van Rijn L.C. . Sediment Transport, Part Ii: Suspended Load Transport. . Journal of Hydraulic Engineering,110 (1984b): 1613-1641.

Wanjura D.F., and Hatfield J.L. Sensitivity of Spectral Vegetation Indices to Crop Biomass. ASAC,30 (1987): 810-816.

Whitlock W., and Rumpus A. Gis—Guided Independent Study: A Brief Guide 2010. Available:
https://www.westminster.ac.uk/__data/assets/pdf_file/0003/48387/wex_GIS_brief_guide.pdf. March 2010 March 2010

WHO. International Programme on Chemical Safety. 2014. Available: http://www.who.int/ipcs/assessment/public_health/cadmium/en/. 15/02/1014 2014.

Yunus K. Heavy Metal Concentration in the Surface Sediment of Tanjung Lumpur Mangrove Forest, Kuantan, Malaysia. Sains Malaysiana 40,2 (2011): 89-92.

Zhang M., Rudi G., and L Daels. Application of Satellite Remote Sensing to Soil and Land Use Mapping in the Rolling Hilly Areas of Nanjing Eastern China ,. ADVANCES IN REMOTE SENSING 2,3 (1993): 11.

APPENDICES

APPENDIX A

Additional input data of simulation
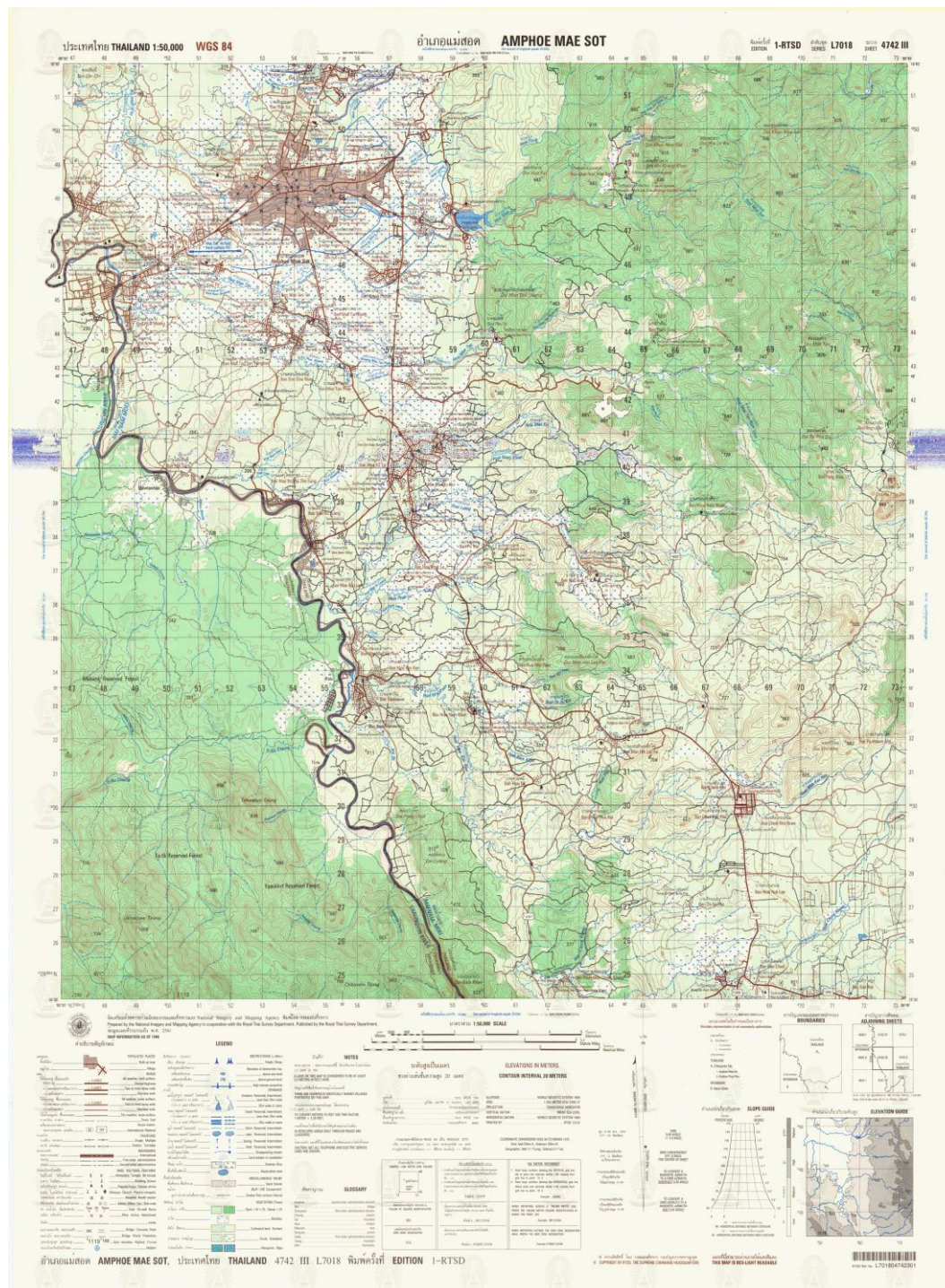
Figure AP 1 The topographic map 1:50,000 scale, sheet 4742III, series L7018, and edition 1-RTS

Table A 1 Land use classification (Land Development Department, 2007)

Code	Land use classification
A101	Rice paddy
A202	Corn
A301	Mixed perennial
A401	Mixed orchard
A412	Tamarind
A413	Longan
A602	Corn
A616	Upland rice
F100	Disturbed evergreen forest
F200	Disturbed deciduous forest
F201	Dense deciduous forest
M301	Mine
M403	Rock out crop
M405	Landfill
U201	Village
U405	Road
U502	Factory
W101	River, Canal
W102	Lake
W202	Farm pond

APPENDIX B

Rainfall intensity and evapotranspiration rate during 2010-2013
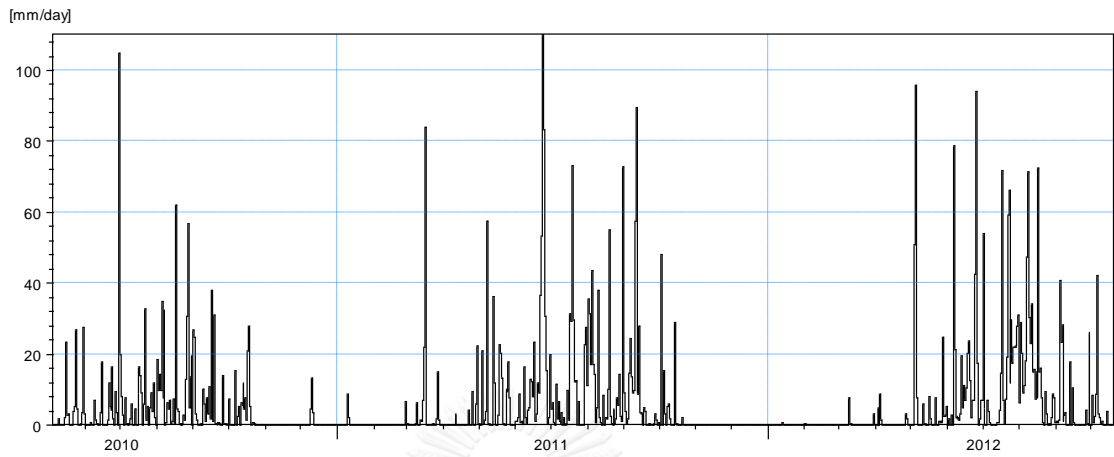
Figure AP 2 Rainfall intensity during 2010-2013 in simulation calibration
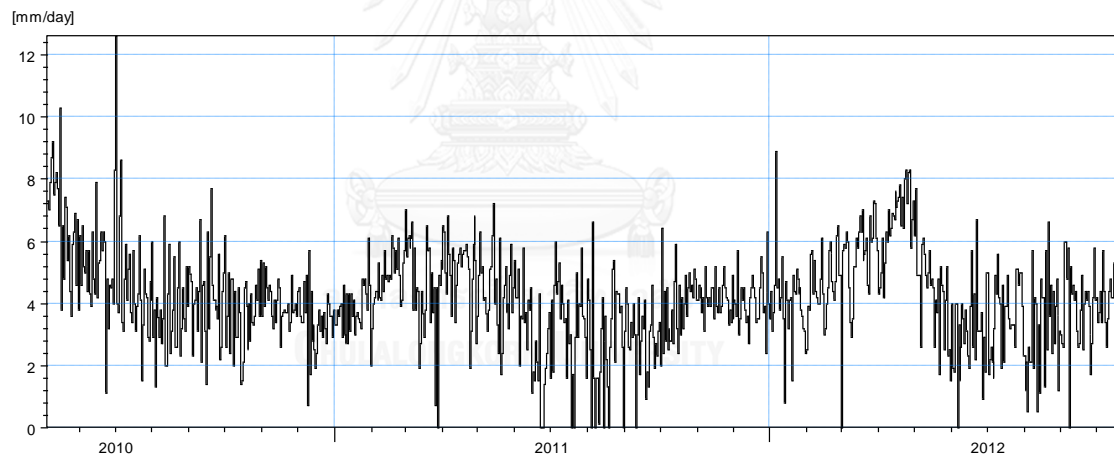
Figure AP 3 Reference evapotranspiration during 2010-2013 in simulation calibration
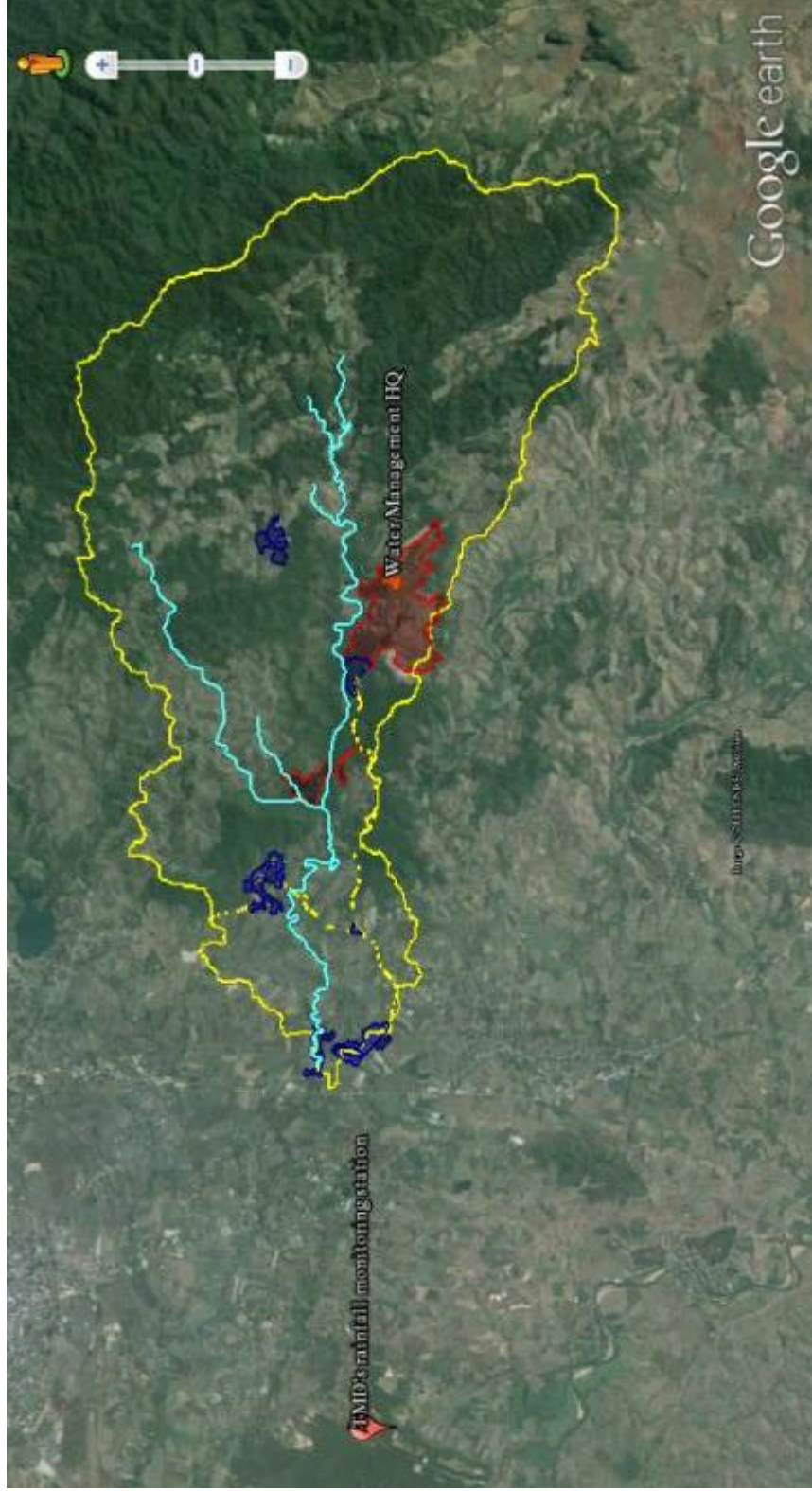
Figure AP4 Rainfall monitoring station of Thai Meteolrological Department

APPENDIX C

Additional Field observation results

Table C-1 Rainfall intensity from the Mae Sot monitoring station

Year	Month	Total rain	Rainy day	MaxRain24hrs
2010	1	11.5	4	9.1
2010	2	0	0	0
2010	3	0	0	0
2010	4	0	0	0
2010	5	104.1	12	27.4
2010	6	87.9	16	17.8
2010	7	281.4	23	104.8
2010	8	368.3	28	62
2010	9	182.9	22	38.1
2010	10	121.6	15	27.7
2010	11	0	0	0
2010	12	21.1	3	13.2
2011	1	10.8	2	8.8
2011	2	0	0	0
2011	3	147.7	13	84
2011	4	45	5	22.3
2011	5	237.3	19	57.6
2011	6	463.4	29	110.1
2011	7	314.4	23	73.1
2011	8	355.5	28	55
2011	9	374.1	23	89.5
2011	10	113.8	12	48.1
2011	11	0	0	0
2011	12	0	0	0
2012	1	0.6	1	0.6
2012	2	0.2	1	0.2
2012	3	11.2	3	7.5
2012	4	20.1	5	8.7
2012	5	211.8	15	95.8
2012	6	409.2	26	94.2
2012	7	480.8	24	71.6
2012	8	535.4	28	72.6
2012	9	163.2	16	40.9
2012	10	93.9	11	42
2012	11	126.2	8	73.1
2012	12	0	0	0

Table C-2 Zinc concentration from monitoring check dam

Station	Location	Sieve Size	14/7/2014	25/7/2014	8/8/2014	22/8/2014	5/9/2014
			Zn, ppm	Zn, ppm	Zn, ppm	Zn, ppm	Zn, ppm
SED_OB1	Downstream (MT02)	10 -70 mesh	182	No Data	227	211	217
		70- 100 mesh	114		66	69	75
		100-140 mesh	109		92	140	59
		140-200 mesh	65		72	95	70
		< 200 mesh	199		191	209	293
SED_OB2	Heavy Equipment plant	10 -70 mesh	No Data	2,431	1,816	661	644
		70- 100 mesh		815	690	264	229
		100-140 mesh		785	506	275	261
		140-200 mesh		723	510	304	276
		< 200 mesh		2,955	1,771	2,021	1,344
SED_OB3	Active Mining zone	10 -70 mesh	6,652	6,469	5,553	10,189	8,793
		70- 100 mesh	3,827	3,125	3,399	7,730	3,749
		100-140 mesh	4,218	4,496	4,341	9,833	4,176
		140-200 mesh	6,810	8,596	6,837	12,408	5,974
		< 200 mesh	13,066	13,600	12,113	16,072	10,458
SED_OB4	Green Mining zone	10 -70 mesh	2,691	2,843	4,491	3,130	1,567
		70- 100 mesh	1,695	1,780	3,852	3,422	1,382
		100-140 mesh	2,545	2,094	6,343	2,622	1,642
		140-200 mesh	4,103	3,476	9,982	3,795	2,708
		< 200 mesh	9,424	5,244	9,297	3,421	3,717
SED_OB5	Water Management HQ office	10 -70 mesh	No Data	5,109	3,511	9,677	9,316
		70- 100 mesh		5,125	3,112	12,636	8,805
		100-140 mesh		6,406	3,029	9,396	8,593
		140-200 mesh		8,488	3,303	10,192	7,369
		< 200 mesh		9,327	11,513	13,043	12,778

Table C-2 Zinc concentration from monitoring check dam (continued)

SED_OB6	Overburden Dump Site	10 -70 mesh	5,214	3,328	3,167	2,848	2,812
		70- 100 mesh	1,705	1,181	1,102	1,390	1,206
		100-140 mesh	1,726	1,362	1,397	1,646	1,395
		140-200 mesh	2,590	2,073	2,280	2,282	2,118
		< 200 mesh	4,706	5,918	5,414	4,588	4,608
SED_OB7	Sediment Pawn (E1)	10 -70 mesh	1,413	1,223	1,005	1,005	985
		70- 100 mesh	952	956	934	855	929
		100-140 mesh	794	859	677	643	710
		140-200 mesh	744	685	526	552	628
		< 200 mesh	1,052	938	698	728	716
SED_OB8	Bench (Overburden Dump site 1)	10 -70 mesh	No Data	541	819	334	643
		70- 100 mesh		469	336	345	506
		100-140 mesh		381	283	308	380
		140-200 mesh		402	239	273	345
		< 200 mesh		642	506	583	602
SED_OB9	Bench (Overburden Dump site 3)	10 -70 mesh	No Data	541	344	343	447
		70- 100 mesh		415	524	377	347
		100-140 mesh		482	592	401	395
		140-200 mesh		498	734	324	421
		< 200 mesh		897	555	663	615
SED_OB10	Upstreame (MT07)	10 -70 mesh	777	844	882	No Data	No Data
		70- 100 mesh	703	662	653		
		100-140 mesh	632	545	580		
		140-200 mesh	592	483	672		
		< 200 mesh	1,101	971	1,192		

APPENDIX D

Parameter values in MIKE SHE

Table D-1 The values of parameter in each compartment of MIKE SHE

Parameters in MIKE SHE	Value
<u>Overland flow</u>	
- Manning number	$10 \text{ m}^{1/3}/\text{s}$
- Detention storage	0.01 mm
<u>Unsaturated Flow</u>	
- Saturated hydraulic conductivity	10^{-8} m/s
- Groundwater depths used for UZ classification	3 m
<u>Saturated Zone</u>	
- Lower level	-27 m
- Horizontal hydraulic conductivity	10^{-8} m/s
- Vertical hydraulic conductivity	10^{-4} m/s
- Specific yield	0.8 %
- Specific storage	10^{-4} m^{-1}
- Initial potential head	-3 m
- Drainage level	-1.5 m
- Drainage time constant	10^{-6}s^{-1}

Table D-2 Vegetation setup for land use compartment in MIKE SHE

Vegetation	End day	LAI	Root	Kc
Rice	0	1.5	200	1
	15	1.5	200	1
	30	4	600	1
	60	5	800	1.1
	80	5	1000	1
	120	4	1000	1
Sugarcane	0	2	500	1
	75	4	1000	1
	95	6	600	1.5
	145	6	1500	1.4
	250	6	1500	1.2
	300	3	1500	1
	366	1	1500	1
Corn	0	0.5	500	1
	30	0.5	500	1
	75	5	1000	1
	105	5	1000	1.1
	125	5	1000	1.1
	175	5	1000	1
Forest	0	6	800	1
	100000	6	800	1

Table D-3 The values of parameters in hydrodynamic module of MIKE 11

Hydrodynamics parameters (HD)		Value	Unit
Initial conditions	Water level	5	meter
	Discharge	1.4	m^3/s
Bed Resistance	Resistance Number	0.01	$s/m^{1/3}$
Default Values	Delta	0.85	-
	Delhs	0.01	-
	Delh	0.1	-
	Alpha	1	-
	Theta	1	-
	Eps	0.0001	-
	Dh Node	0.01	-
	Zeta Min	0.1	-
	Struc Fac	0	-
	Inter1 Max	10	-
	Nolter	1	-
	MaxlterSteady	100	-
	FroudeMax	-1	-
	FroudeExp	-1	-

Table D-4 The values of parameters in sediment transport module of MIKE 11

Sediment transport parameter (ST)		Value	Unit
Sediment Grain Diameter	Global Grain Diameter	0.001	meter
	St. Deviation	1	meter
Transport Model	Model Parameters:		
	-Rel. density	2.65	-
	-Kin. Viscosity	10^{-6}	m^2/s
Bed Shear Stress	Manning (M):		
	- Minimum	20	$m^{1/3}/s$
	- Maximum	40	$m^{1/3}/s$
	- Omega	1	$m^{1/3}/s$
Non Scouring Bed Level	Thickness of active layer	0.1	meter
	Non scouring bed level	-1.5	meter
Calibration Factors	Factor	0.117	-
Data for Graded ST	Min. depth of active layer	0.1	meter
	Init. Depth of passive layer	1	meter

Table D-5 The bulk density applied in OfSET simulation

Land Use Type	Average bulk density	Standard deviation
Forrest	1.19	0.13
Grassland	1.26	0.11
Degrade forest	1.28	0.12
Corn Field	1.3	0.1
Orchard	1.31	0.09
Natural vegetation	1.24	0.13
agricultural	1.3	0.09

APPENDIX E

Calculation method

Laboratory results

1. Grain size distribution of bed load

- **Loss (g)**

Loss weight of bed load samples after sieving is calculated from the difference between weight before sieving (g) and total weight after sieving (g). The bed load weight at each were displayed in Chapter IV, Table 4-3 for the dry season and in Chapter IV, Table 4-5 for the wet season.

Loss = Sample weight before sieving (g) – Total sample weight after sieving (g)

- **Loss (%)**

After the loss weight of bed load samples after sieving was calculated, percent loss of bed load in each station after sieving can be computed from the ratio of the loss weight (g) per sample weight before sieving (g). The bed load weight at each were displayed in Chapter IV, Table 4-3 for the dry season and in Chapter IV, Table 4-5 for the wet season.

$$\text{Loss (\%)} = \frac{\text{Loss (g)}}{\text{Sample weight before sieving (g)}} \times 100$$

- **% Passing Sieve No. 200**

The amount of bed load passing sieve no. 200 is estimated from sample weight on receiver (g) per sample weight before sieving (g). The bed load weight at each mesh sieve in ten sampling station were displayed in Chapter IV, Table 4-3 for the dry season and in Chapter IV, Table 4-5 for the wet season.

$$\text{\% Passing Sieve No. 200} = \frac{\text{Sample weight on receiver (g)}}{\text{Sample weight before sieving (g)}} \times 100$$

- **Mean Diameter (mm)**

Mean diameter of bed load samples in each station was calculated from the pooled data of bed load from sieves No. 3/4'', 3/8'', 4, 10, 20, 35, 65, 100, 150, and 200. The mean size of each mesh and sample weight on each mesh were displayed in Chapter IV, Table 4-3 for the dry season and in Chapter IV, Table 4-5 for the wet season.

$$\text{Mean Diameter (mm)} = \frac{X_{3/4"}W_{3/4"} + X_{3/8"}W_{3/8"} + \ldots + X_{receiver}W_{receiver}}{\text{Sample weight after sieving (g)}}$$

Where   X   =   Mean size of each mesh

            W   =   Sample weight on each mesh

2 .Cadmium concentration

- **Cadmium concentration of suspended sediment and bed load**

Cadmium concentration for suspended sediment and bed load were computed from cadmium concentration result from the ratio of atomic absorption spectrometry (μg/L) and volume of digested sample (L) per weight of digested sample (g)

$$\text{Cadmium concentration (mg/kg)} = \frac{\text{AAS result (μg/L) x digested sample vol. (L)} \times 10^{-3}}{\text{Weight of digested sample (g)}}$$

- **Total cadmium concentration of bed load**

From bed load samples which were sieved with sieve No. 65, 100, 150 and 200, the total cadmium concentration is calculated by weighted average in which each quantity to be averaged is assigned a weight. Cadmium concentration of bed load in sieve No. 65, 100, 150 and 200 showed in Chapter IV, Table 4-1, and weight of bed load samples in sieve No. 65, 100, 150 and 200 displayed in Chapter IV, Table 4-3 for the dry season and in Chapter IV, Table 4-5 for the wet season.

Total cadmium concentration (mg/kg)

$$= \frac{C_{\#65}W_{\#65} + C_{\#100}W_{\#100} + X_{\#150}W_{\#150} + X_{\#200}W_{\#200}}{W_{\#65} + W_{\#100} + W_{\#150}W_{\#200}}$$

Where   C   =   Cadmium concentration of each mesh

W   =   Bed load weight on each mesh

- **Standard deviation from several cadmium measurement in bed load**

    Just as several means may be combined to obtain a grand average, standard deviations also can be combined to obtain a single estimate. Pooled standard deviation is calculated from standard deviation of separate sets of cadmium measurement in sieve No. 65, 100, 150 and 200.

Pooled standard deviation $= \sqrt{\dfrac{s_{\#65}^2(n_{\#65}-1)+s_{\#100}^2(n_{\#100}-1)+s_{\#150}^2(n_{\#150}-1)+s_{\#200}^2(n_{\#200}-1)}{(n_{\#65}-1)+(n_{\#100}-1)+(n_{\#150}-1)+(n_{\#200}-1)}}$

Where   S   =   Standard deviation

n   =   Number of measurements

Simulation results

1. Sensitivity Analysis

    The sensitivity index (*I*) was calculated to determine the sensitivity of input parameter in MIKE SHE model that effected water discharge (see parameter values in Appendix D, Table D-1). For example, the Manning' M used input value (x_0) equal to 10, then x_1 and x_2 were calculated equal to 5 and 15, respectively. The output (*y*) is water discharge in 26 June 2011due to the highest rainfall rate occurred in this period.

$$I = \frac{(y_2-y_1)/y_0}{2\Delta x/x_0}$$

$$\Delta x = x_0 - x_1$$

$$\Delta x = x_2 - x_0$$

Where *I*   =   sensitivity index (dimensionless),

     x_0 =   initial value of parameter *x*,

     y_0 =   model output calculates with x_0,

     y_1 =   model output calculates with x_1, and

     y_2 =   model output calculates with x_2

2.Sediment transport in stream sediment (kg)

The sediment transport (kg) at downstream of the Mae Tao Creek is computed from the accumulated sediment (m^3) that simulated from model and density of sediment (kg/m^3).

Sediment transport = Accumulated sediment (m^3) x Sediment density (kg/m^3)

3.Cohesive sediment transport in overland sediment (kg)

The cadmium transport in overland sediment was computed by the percentage of sand and silt partition in the sediment slurry (see Chapter 4, Table 4-)

Slurry density can be computed from

$$\rho_m = 100/[C_w/\rho_s + [100 - C_w/\rho_l]$$

Where

     ρm =   density of slurry (lb/ft3, kg/m3)
     Cw   =   concentration of solids by weight in the slurry (%)
     ρs =   density of the solids (lb/ft3, kg/m3)
     ρl =   density of liquid without solids (lb/ft3, kg/m3)

Overland sediment transport = Density of slurry (kg/m^3) x Accumulated sediment (m^3)

4.Cadmium transport in sediment (mg)

After sediment transport amount value was computed, the cadmium transport could be estimated. The amount of cadmium transport (mg) is calculated from sediment transport (kg) and observed cadmium concentration from field observation (mg/kg), as shown in Chapter IV.

Cadmium transport (mg)

= Sediment transport (kg) x Observed cadmium concentration (mg/kg)

5. Summary of the significant equation

No.	Equation	Equation name	Page
1	$A = R \times K \times Ls \times C \times P$	RUSLE	30
2	$NDVI = \dfrac{NIR - VIS}{NIR + VIS}$	NDVI analysis	37
3	$Fi_x = \dfrac{M_x^2}{P_y}$	Fourier index of rainfall	
4	$Ei_{30,x} = kFi_x^{0.584}$	Maximum intensity rainfall energy	64
5	$R = \dfrac{1}{n}\sum_{x=1}^{n} Ei_{30,x}$	Rainfall/runoff erosivity	
6	$LS = (\dfrac{Flowacc \cdot resolution}{2213})^m (65.41\sin^2\theta + 4.56\sin\theta + 0.0654)$	LS factor calculation	66
7	$Cd_{erosion} = cA \times 10^6$	Petental cadmium flux from ersion	70
	$q_b = u_b \delta_b c_b$	Bed load transport rate (m3/s)	90
9	$q_s = \int_a^D cudy$	Sedimenttransport rate (m3/s)	94
10	$Q_{se} = \begin{cases} M_{se}\dfrac{\tau - \tau_{se}^c}{\tau_{se}^c}; \tau \geq \tau_{se}^c \\ 0; \tau < \tau_{se}^c \end{cases}$	Surface erosion rate (kg/m2s)	99
11	$Q_{se\_out} = \dfrac{0.37 Q_{se} w^2 dt}{1000}$	Total volume of sediment coming from a cell (m3/s)	101
12	$Cadmiumtransport = S_{bd}\rho_{bd}[Cd]_{bd} + S_{ss}\rho_{ss}[Cd]_{ss}$	Total cadmium transport by stream flow (kg)	101
13	$Cd_{total} = \sum_{i=1}^{3}[(Cd_i)(OfVol_i)]$	Total cadmium transport by overland flow (kg)	102
14	$J_{Creek}^C = J_{Area}^C + J_{point\,source}^C$	Flux of total contaminants transported into receiving water	107

APPENDIX F

Monitoring Check Dam

Monitoring check dam assembly
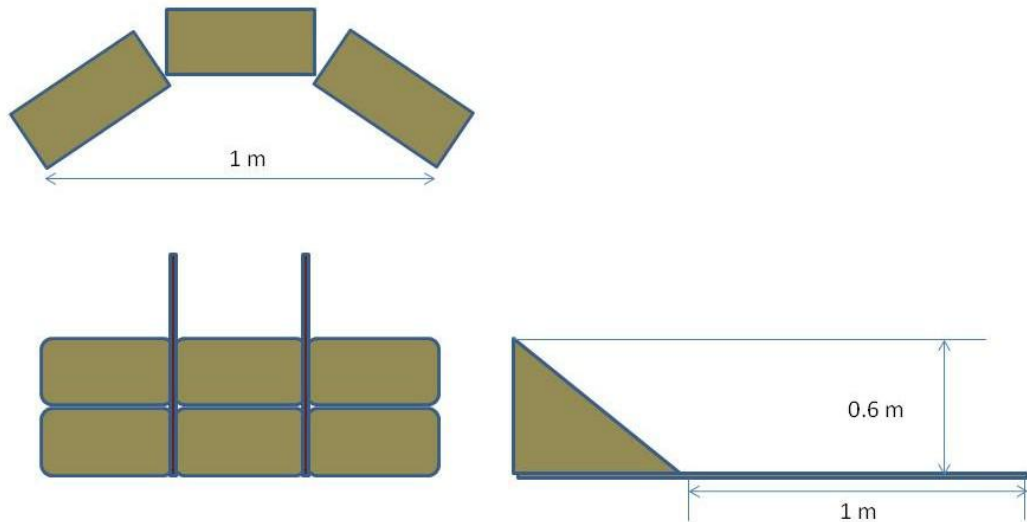
Figure AP-4 Assembly of the monitoring check dam

Figure AP-5 Applied monitoring check dam in mining production area

Figure AP-6 The monitoring check dam near the agricultural area at OB_SED 10

Figure AP-7 Agricultural area of the Mae Tao Basin during wet season (2014)

APPENDIX G

OfSET's source code (Based on C++ Language)

Overal Process

MIKE SHE result time series disintegration

```csharp
using System;
using System.Collections.Generic;
using System.Linq;
using System.Text;
using System.IO;

namespace ConsoleApplication1
{
    class Program
    {
        static void Main(string[] args)
        {
            string filePath = @"D:\work\casc2d\Final_dry_kom\wet\Overland.txt";
            Console.WriteLine("read file from {0}", filePath);
            string[] item = {"OverlandDepth","FlowX","FlowY"};

            int maxRow = 81;
            //if (string.IsNullOrEmpty(filePath))
            {
                using (StreamReader sr = new StreamReader(filePath))
                {
                    String line;
                    while ((line = sr.ReadLine()) != null)
                    {
                        //FormatData(line);
                        if (line.Contains("\"tstep\""))
                        {
                            Console.WriteLine(line);
                            var parts = line.Split(' ');
                            string fileName = filePath.Replace(".txt", "_") +
                            item[Convert.ToInt32(parts[3]) - 1] + "." + parts[1];


                            using (System.IO.StreamWriter file = new
System.IO.StreamWriter(fileName))
                            {
                                file.WriteLine("ncols        141");
                                file.WriteLine("nrows         81");
                                file.WriteLine("xllcorner     457142.79741662");
                                file.WriteLine("yllcorner     1838702.9240394");
                                file.WriteLine("cellsize      100");
                                file.WriteLine("NODATA_value  -1E-035");
                                // ignore first line to fit the grid line
                                line = sr.ReadLine();
                                line = sr.ReadLine();
```

```
                    // start copy
                    // limit row
                    //while ((line = sr.ReadLine()) != null)
                    for(int i = 0; i<maxRow; i++)
                    {
                      line = sr.ReadLine();
                      if (line == null || line.Equals(""))
                        break;

                      file.WriteLine(line);
                    }

                    while ((line = sr.ReadLine()) != null)
                    {
                      if (line.Equals(""))
                        break;
                    }

                }

              }
            }
          }
        }
      }
    }
}
```

OfSET's Control files Reading

/********************************/

/*   ReadControlFile.c   */

/********************************/

```
#include "all.h"

extern void ReadControlFile()

{

        int i,j,l;
```

```
printf("Reading CONTROL file \n");


fprintf(Summ_file_fptr,"\nCONTROL Input Data \n");

fprintf(Summ_file_fptr,          "================= \n");

fprintf(Summ_file_fptr,          "Control file : %s\n", control_file);


fscanf(control_file_fptr,"%f %ld %ld %ld %ld",

                       &dt,&niter,&nitrn,&nprn,&nplt);


fprintf(Summ_file_fptr,

"DT = %2.2f sec NITER= %ld NITRN = %ld NPRN = %ld NPLT = %ld\n\n",

                       dt,niter,nitrn,nprn,nplt);


fprintf(Summ_file_fptr,"Overland outlet cell: \n");

fscanf(control_file_fptr,"%ld %ld %f",&jout,&kout,&sovout);

fprintf(Summ_file_fptr,"JOUT = %ld KOUT = %ld SOVOUT = %g
\n\n",jout,kout,sovout);

fscanf(control_file_fptr,"%i",&chancheck);

fprintf(Summ_file_fptr,"CHANCHECK= %i \n",chancheck);


fscanf(control_file_fptr,"%f",&elconv);

fprintf(Summ_file_fptr,"ELCONV = %.2f\n",elconv);


fprintf(Summ_file_fptr,"\nRainfall Data \n");
```

```c
fprintf(Summ_file_fptr,          "============ \n");


fscanf(control_file_fptr,"%ld ",&irain);

fprintf(Summ_file_fptr,"IRAIN = %ld \n",irain);


if(irain == 0)

{

 fscanf(control_file_fptr,"%f ",&crain);

 fprintf(Summ_file_fptr,"CRAIN = %.3f (mm/h)\n",crain);

}

else

{

 fprintf(Summ_file_fptr,"Rainfall file: %s \n",rain_file);

 fscanf(control_file_fptr,"%ld %ld ",&nrg,&nread);

 fprintf(Summ_file_fptr,"NRG = %ld NREAD = %ld \n",nrg,nread);


 xrg = (float*) malloc((nrg+1)*sizeof(float));

 yrg = (float*) malloc((nrg+1)*sizeof(float));

 rrg = (float*) malloc((nrg+1)*sizeof(float));


 for(l=1;l<=nrg;l++)

 {

        fscanf(control_file_fptr,"%f %f ",&xrg[l],&yrg[l]);

        fprintf(Summ_file_fptr,"XRG[%ld] = %8.6f\tYRG[%ld] = %8.6f \n",
```

```
l,xrg[l],l,yrg[l]);

 }

}


fprintf(Summ_file_fptr,"\nLand Use Parameters \n");

fprintf(Summ_file_fptr,          "=================== \n");


/* Allocate memory for the variables derived from the landuse            */

pman = (float*) malloc((nman+1)*sizeof(float));

retention = (float*) malloc((nman+1)*sizeof(float));

cfactor = (float*) malloc((nman+1)*sizeof(float));

pfactor = (float*) malloc((nman+1)*sizeof(float));


fscanf(control_file_fptr," %ld %ld ",&nman,&indexsdep);

fprintf(Summ_file_fptr,"NMAN = %ld INDEXSDEP = %ld \n\n",


nman,indexsdep);

fprintf(Summ_file_fptr,"\tIndex\tManning    Intercept.\tCusle\tPusle\n");

fprintf(Summ_file_fptr,"\t-----\t-- n --    -- [mm] --\t-----\t-----\n");


for(i=1;i<=nman;i++)

{

 fscanf(control_file_fptr,"%f %f %f %f",
```

```
                                        &pman[i],
&retention[i],&cfactor[i],&pfactor[i]);

        fprintf(Summ_file_fptr,

                "\t%3ld%11.3f\t%10.3f\t%5.3f\t%5.3f\n",

                        i,pman[i],retention[i],cfactor[i],pfactor[i]);

        }


        fprintf(Summ_file_fptr,"\nSoil type Parameters \n");

        fprintf(Summ_file_fptr,        "=================== \n");


        fscanf(control_file_fptr,"%i %i %i",&indexinf,&indexeros,&nsoil);

        fprintf(Summ_file_fptr,"INDEXINF= %i INDEXEROS= %i NSOIL= %i \n",

        indexinf,indexeros,nsoil);


        fprintf(Summ_file_fptr,

                "\n    Index    Ks      G      Md    %%Sand    %%Silt    %%Clay
Kusle\n");

        fprintf(Summ_file_fptr,

                "    -----  [cm/h]   [cm]   -----   -----   -----   -----   -----\n");

        if(indexinf == 1)

        {

        pinf = floatMemAlloc2d(nsoil,8);


        /* Read values from the CONTROL file */

        for(i=1;i<=nsoil;i++)
```

```c
{
        fprintf(Summ_file_fptr,"%10i",i);

        for(j=1;j<=7;j++)

        {
                fscanf(control_file_fptr,"%g ",&pinf[i][j]);

                fprintf(Summ_file_fptr,"%10.3f",pinf[i][j]);

                /* Converts Ks: cm/h -> m/s
                                                                */

                if(j ==1) pinf[i][j] = pinf[i][j]/3600/100;

                /* Converts G:  cm -> m
        */
                if(j ==2) pinf[i][j] = pinf[i][j]/100;

        }


        fprintf(Summ_file_fptr,"\n");

}
}


fprintf(Summ_file_fptr,"\nInternal Gages Data \n");

fprintf(Summ_file_fptr,          "------------------- \n");


fscanf(control_file_fptr,"%ld %ld %i",&indexdis,&ndis, &unitsQ);

fprintf(Summ_file_fptr,

                "INDEXDIS = %ld  NDIS = %ld  Q_units = %i \n",

                indexdis,ndis, unitsQ);
```

```
if(indexdis == 1)

{

 fprintf(Summ_file_fptr,"\n      Gage    Row    Column    Area\n");

      fprintf(Summ_file_fptr,"      ----    ---    ------    [has]\n");

      iq = intMemAlloc2d(ndis,2);

      areaQ = (float*) malloc((ndis+1)*sizeof(float));


      for (i=1;i<=ndis;i++)

      {

       fprintf(Summ_file_fptr,"      %2i",i);

       for (j=1;j<=2;j++)

       {

            fscanf(control_file_fptr,"%ld ",&iq[i][j]);

            fprintf(Summ_file_fptr,"%10i",iq[i][j]);

       }

       fscanf(control_file_fptr,"%f", &areaQ[i]);

       fprintf(Summ_file_fptr,"%14.3f\n", areaQ[i]);

      }

}


fprintf(Summ_file_fptr,"\nInternal Sediment Gages Data \n");

fprintf(Summ_file_fptr,      "--------------------------- \n");


fscanf(control_file_fptr,"%ld %ld %i",&indexsed,&nsed, &unitsQs);
```

```
        fprintf(Summ_file_fptr,

"INDEXSED = %ld  NSED = %ld Qs_Units = %i\n",

                                        indexsed,nsed,
unitsQs);


        if(indexsed == 1)
        {
                fprintf(Summ_file_fptr,"\n     Gage    Row    Column    Area\n");
                fprintf(Summ_file_fptr,"     ----    ---    ------    [has]\n");
                ised = intMemAlloc2d(nsed,2);
                areaQs = (float*) malloc((nsed+1)*sizeof(float));


                for(i=1;i<=nsed;i++)
                {
                 fprintf(Summ_file_fptr,"     %2i",i);
                 for (j=1;j<=2;j++)
                 {
                        fscanf(control_file_fptr,"%ld ",&ised[i][j]);
                        fprintf(Summ_file_fptr,"%10i",ised[i][j]);
                 }
                 fscanf(control_file_fptr,"%f", &areaQs[i]);
                 fprintf(Summ_file_fptr,"%14.3f\n",areaQs[i]);
                }
        }
```

```
        printf("Successfully Read All CONTROL Information \n");

        fclose(control_file_fptr);



        /* Allocate memory for the vector that holds the flow
                        */
        /* dicharge and sediment discharge at each of those locations            */

        q =  (float*) malloc((ndis+1)*sizeof(float));

        qsed = (float*) malloc((nsed+1)*sizeof(float));



}
```

Overland depth import

```
                                /*****************************/

                                /*       OvrlDepth.c       */

                                /*****************************/



#include "all.h"



extern void OvrlDepth( )

{

        char fn[128];

        int j,k,l,rindex,icall;

        float hov;


                /* Variables that will hold the ASCII grids header information      */
```

```
char nrows_label[15], ncols_label[15], xllcorner_label[15],

        yllcorner_label[15], cellsize_label[15], nodatavalue_label[15],

        h_label[7][80];

int  head;


float overland_depth;



/*********************************************/

/*   Updating overland depth (water balance) */

/*********************************************/



/* Applying the Rainfall to each Grid Cell within the Watershed */



sprintf(fn,"Input/Overland_OverlandDepth.%i",iter);


if((overland_depth_fptr=fopen(fn,"r"))==NULL)

{

        printf("Can't open Output PRN File : %s \n",fn);

        exit(EXIT_FAILURE);

}


fscanf(overland_depth_fptr,"%s %i",&ncols_label, &n);

fscanf(overland_depth_fptr,"%s %i",&nrows_label, &m);

fscanf(overland_depth_fptr,"%s %f",&xllcorner_label, &xllcorner);

fscanf(overland_depth_fptr,"%s %f",&yllcorner_label, &yllcorner);
```

```c
        fscanf(overland_depth_fptr,"%s %f",&cellsize_label, &w);

        fscanf(overland_depth_fptr,"%s %f",&nodatavalue_label, &nodatavalue_ovl);

        //row

        for(j=1;j<=m;j++)

        {

                //col

                for(k=1;k<=n;k++)

                {



                        fscanf(overland_depth_fptr,"%f ",&overland_depth);



                        if ((overland_depth != nodatavalue_ovl)/*||(ishp[j][k] !=
nodatavalue)*/)

                        {

                                h[j][k] = overland_depth;
                                /*

                                if(overland_depth != nodatavalue_ovl)

                                        printf("***** overland depth
%f",overland_depth);*/

                        }

                }

        }

        fclose(overland_depth_fptr);

}
```

Overland flow routing process
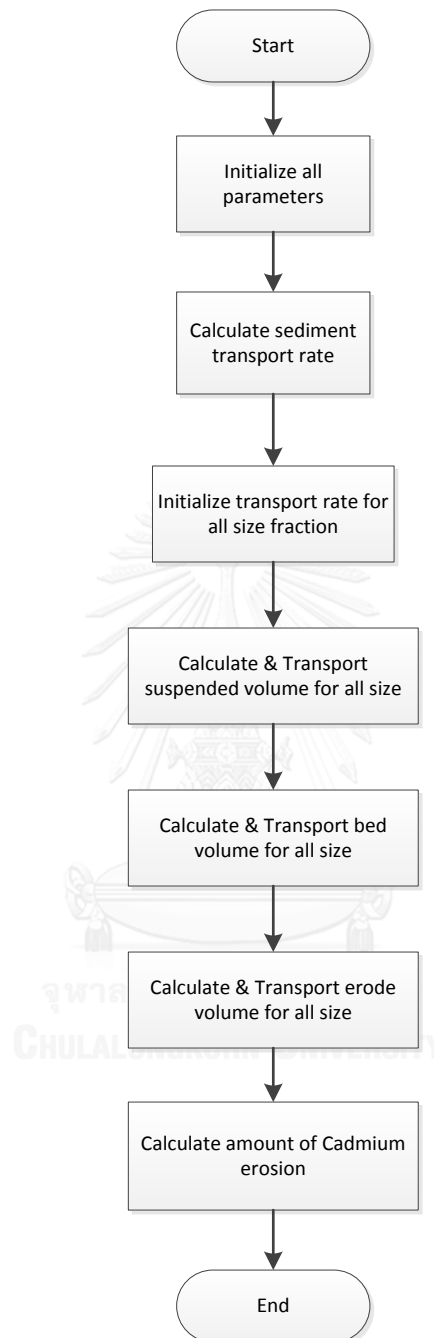
Overland flow routing calculation

```
/*****************************/

                              /*          OvrlRout.c
*/

/*****************************/


                              /********************************/
                      /*      FUNCT: OvrlRout        */
                              /********************************/


#include "all.h"


extern void OvrlRout()

{

                int j,k,jj,kk,l;

                char fn[128];

                int  head;

                float  nodatavalue_flow;

                /* Variables that will hold the ASCII grids header information
                */

                char nrows_label[15], ncols_label[15], xllcorner_label[15],

                        yllcorner_label[15], cellsize_label[15],
nodatavalue_label[15],

                        h_label[7][80];


                float flow;
```

```
//OfSET : read overland flow data provided files

sprintf(fn,"Input/Overland_FlowX.%i",iter);
if((overland_flow_x_fptr=fopen(fn,"r"))==NULL)
{
        printf("Can't open overland flow x : %s \n",fn);
        exit(EXIT_FAILURE);
}


sprintf(fn,"Input/Overland_FlowY.%i",iter);
if((overland_flow_y_fptr=fopen(fn,"r"))==NULL)
{
        printf("Can't open overland flow y : %s \n",fn);
        exit(EXIT_FAILURE);
}
//NKK

fscanf(overland_flow_x_fptr,"%s %i",&ncols_label, &n);
fscanf(overland_flow_x_fptr,"%s %i",&nrows_label, &m);
fscanf(overland_flow_x_fptr,"%s %f",&xllcorner_label,
&xllcorner);
fscanf(overland_flow_x_fptr,"%s %f",&yllcorner_label,
&yllcorner);
fscanf(overland_flow_x_fptr,"%s %f",&cellsize_label, &w);
fscanf(overland_flow_x_fptr,"%s %f",&nodatavalue_label,
&nodatavalue_flow);
```

```
fscanf(overland_flow_y_fptr,"%s %i",&ncols_label, &n);

fscanf(overland_flow_y_fptr,"%s %i",&nrows_label, &m);

fscanf(overland_flow_y_fptr,"%s %f",&xllcorner_label,
&xllcorner);

fscanf(overland_flow_y_fptr,"%s %f",&yllcorner_label,
&yllcorner);

fscanf(overland_flow_y_fptr,"%s %f",&cellsize_label, &w);

fscanf(overland_flow_y_fptr,"%s %f",&nodatavalue_label,
&nodatavalue_flow);


for(j=1;j<=m;j++)
{
 for(k=1;k<=n;k++)
 {
        //if(ishp[j][k] != nodatavalue)
        {
                fscanf(overland_flow_x_fptr,"%f ",&flow);

                dqovx[j][k] = flow;

                fscanf(overland_flow_y_fptr,"%f ",&flow);

                dqovy[j][k] = flow;
        }
 }
}


for(j=1;j<=m;j++)
{
 for(k=1;k<=n;k++)
```

```
                    {

                        if(ishp[j][k] != nodatavalue)

                        {

                                for(l=-1;l<=0;l++)

                                {

                                        jj=j+l+1;

                                        kk=k-l;


                                        if(jj <= m && kk <=n && ishp[jj][kk]
!= nodatavalue)

                                        {

                                                ovrl(j,k,jj,kk);

                                        }

                                }

                        }

                    }

                }


                fclose(overland_flow_x_fptr);

                fclose(overland_flow_y_fptr);

        }



                                /********************************/

                                /*      FUNCT: Ovrl          */

                                /********************************/
```

```
extern void ovrl( int j,int k, int jj, int kk)

{

                        int jfrom,kfrom,jto,kto;


                        float a=1.0;


                        float vel = 0.0;


                        float so,sf,dhdx,hh,/*rman,*/alfa,dqq,stordepth;


                        float shearStress=0, criticalShearStress=0, bulkDen=0;

                        float Msc = 1;

                        const float ksConstant = 0.84;

                        double test =0;

                        ksErosionRate = 0;


                        //OfSET : read from DEM (hieght) how it translate for raw

slope

                        so = (e[j][k] - e[jj][kk])/w;


                        dhdx = (h[jj][kk] - h[j][k])/w;


                        sf = so - dhdx +(float)(1e-30);


                        // hh = overland depth

                        hh = h[j][k];
```

```
if(j == 10 && k == 37 && hh != nodatavalue_ovl)

{

        printf("slove : %f",so);

        printf("hh : %f",hh);

}


//rman = pman[iman[j][k]];

bulkDen = bulk_dens[j][k];


//OfSET : convert from g/cm3 --> kg/m3, g/l

bulkDen = bulkDen* 1000;

//bulkDen = bulkDen;

//OfSET : calculate shear stress and critical shear stress here.

shearStress = fabs(so) * hh * Water_Density;

//OfSET : change rman to bulk density read from file

if(bulkDen < Water_Density)

{

        criticalShearStress = 0;

        ksErosionRate = 0;

}

else

{

        criticalShearStress = 0.015* pow((bulkDen -
Water_Density) ,ksConstant);

                //OfSET : replace KRcap with this

                Msc = 0.55*pow((bulkDen/Water_Density),3);
```

```
                    ksErosionRate = Msc * ((shearStress -
criticalShearStress)/criticalShearStress);

                    if(ksErosionRate < 0)

                    {

                            ksErosionRate = 0;

                    }

                }


                if(chancheck == 1 && link[j][k] > 0)

                {

                        if(sdep[j][k] > chp[link[j][k]][node[j][k]][3])

                        {

                                stordepth = sdep[j][k] -
chp[link[j][k]][node[j][k]][3];

                        }
                        else

                        {

                                stordepth = 0.0;

                        }

                }

                else

                {

                        stordepth = sdep[j][k];

                }


                if(sf < 0)
```

```
{
        hh = h[jj][kk];

        //rman = pman[iman[jj][kk]];


        if(chancheck == 1 && link[jj][kk] > 0)
        {
                if(sdep[jj][kk] >
chp[link[jj][kk]][node[jj][kk]][3])
                {
                        stordepth = sdep[jj][kk] -
chp[link[jj][kk]][node[jj][kk]][3];
                }
                else
                {
                        stordepth = 0.0;
                }
        }
        else
        {
                stordepth = sdep[jj][kk];
        }
}


if(hh >= stordepth)
{
        //alfa = (float)((pow(fabs(sf),0.5))/rman);
```

```
/*      Note : The variable "a" represents the sign of the
           */

/*      Friction Slope (Sf)      Computing Overland
Flow                                                   */


if(sf >= 0) a = 1.0;



if(sf < 0) a = -1.0;



//dqq = (float)(a*w*alfa*pow((hh-stordepth),1.667));
if (j != jj)
{
        dqq = dqovx[j][k];
        OfSETDqq = 1; // dqq = x, used to determine the
RoutOutlet qoutov

}
else if(k != kk)

{

        dqq = dqovy[j][k];
        OfSETDqq = 2; // dqq = y

}


dqov[j][k] = dqov[j][k] - dqq;



dqov[jj][kk] = dqov[jj][kk] + dqq;
```
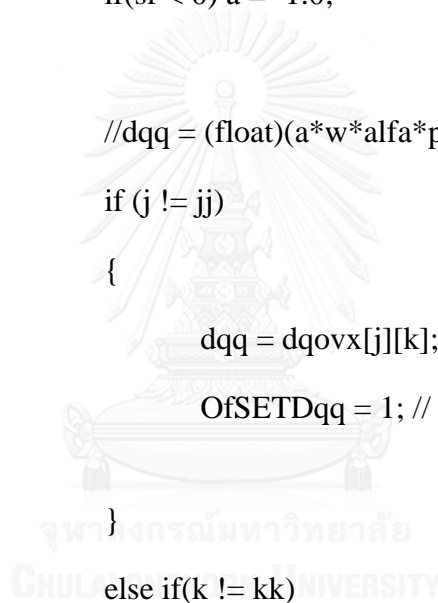
```
                              /* Compute overland sediment flow and
erosion/deposition                  */



              if(indexeros == 1 && dqq != 0.0)

              {

                     if(a > 0)       /* (J,K) to (JJ,KK) */

                     {

                            jfrom = j;

                            kfrom = k;

                            jto = jj;

                            kto = kk;

                     }
                     else           /* (JJ,KK) to (J,K) */

                     {

                            jfrom = jj;

                            kfrom = kk;

                            jto = j;

                            kto = k;

                     }


                     if (ishp[jfrom][kfrom] == 1)

                     {

              RoutSedOvrl(dqq,sf,jfrom,kfrom,jto,kto);
```

```
                    }

                  }


              }      /* End of HH >= STORDEPTH */



}  /* End of OVRL */
```

Stream Chanel determination

```
                    /*****************************/

                                      /*      ReadChannFile.c
*/

                    /*****************************/


#include "all.h"


extern void ReadChannFile()

{

              char ch;

              int j,k;


              printf("Reading Channel Data \n");


              do{

               ch=fscanf(chn_file_fptr,"%ld",&nchan_link);

               ch=fscanf(chn_file_fptr,"%ld",&nchan_node[nchan_link]);
```

```c
                            for(k=1;k<=nchan_node[nchan_link];k++)

                    {

                            for(j=1;j<=6;j++)

                            {

                                    ch=fscanf(chn_file_fptr,"%f
",&chp[nchan_link][k][j]);

                            }

                    }


                    } while(ch!=EOF);


                    maxlink = nchan_link;


                    /* Writing Channel Information to Output Summary File
                                            */


/*                  fprintf(Summ_file_fptr,"\n Channel Input Data \n");

                    fprintf(Summ_file_fptr," ----------------- \n");

                    for(i=1;i<=maxlink;i++)

                    {

                            for(k=1;k<=nchan_node[i];k++)

                            {

                                    for(j=1;j<=6;j++)

                                    {

                    fprintf(Summ_file_fptr,"CHP[%ld][%ld][%ld] = %f ",
```

```
                    i,k,j,chp[i][k][j]);

                              }

                              fprintf(Summ_file_fptr,"\n");

                    }

          }
*/


          printf("Successfully Read Channel Data \n");

          fclose(chn_file_fptr);



}
```

Precipitation Determination

```
/******************************/
                              /*        rain.c        */
/******************************/



#include "all.h"


extern void rain(int j,int k)

{

          float totdist = 0.0;

          float totrain = 0.0;
```

```
float xc,yc,dist,xul,yul;

int l;


rint[j][k] = -999.0;


xul = xllcorner;

yul = yllcorner + m * w;


if(nrg == 1)

{

        rint[j][k] = rrg[1];

}

else

{

    for(l=1;l<=nrg;l++)

        {

                yc = (float)(yul - j * w + w / 2.0);

                xc = (float)(xul + k * w - w / 2.0);


                dist = (float)(sqrt(pow((yc-yrg[l]),2.0) +
pow((xc-xrg[l]),2.0)));

                if(dist < 1e-5)

                {

                        rint[j][k] = rrg[l];

                }
```

```
                              else

                              {

                                      totdist = (float)(totdist +
1.0/pow(dist,2.0));

                                      totrain = (float)(totrain +
rrg[l]/pow(dist,2.0));

                              }

                      }

              }


              if(rint[j][k] == -999.0)

              {

                      rint[j][k] = totrain / totdist;

              }


/* Changing Units from inches/hour to meters/second */


              rint[j][k] = (float)(rint[j][k] * 0.0254 / 3600.);


              /* Rainfall rate is reduced until interception is satisfied */


              if (ret[j][k] != 0)

              {

                      intercept(j,k);

              }
```

}

Rainfall intensity period

```
/*****************************/

                                    /*        RunTime.c
*/

/*****************************/


#include "all.h"


extern void             RunTime(clock_t finish)

{

        double elapsedTime;

        fprintf(Summ_file_fptr,

                "\nProgram stops at simulation minute:%10.2f\n",(iter-
1)*dt/60);


        elapsedTime = (double)(finish -
startTime)/CLOCKS_PER_SEC;


        fprintf(Summ_file_fptr,

                "\nCASC2D RUNNING TIME:%10.2f minutes\n",
elapsedTime/60);
```

```
                    fclose(Summ_file_fptr);

}
}
```

Water outlet calculation

```
                    /*****************************/

                                        /*      RoutOutlet.c
*/

                    /*****************************/

#include "all.h"

extern void RoutOutlet()

{
                    int ill;
                    float hout, alfa,qoutch;


                    qoutov = 0.0;

                    qoutch = 0.0;



                    /* FIRST:calculate the flow going out from the overl. portion
                        */


                    //alfa = (float)(sqrt(sovout)/pman[iman[jout][kout]]);
```

/* Discharge from overland flow. NOTE: because the water from */

/* this part of the outlet overland cell was already "poured"   */

/* into the channel when updating the channel depth (channDepth)*/

/* qoutov = 0 when the channel routing is selected   */

```
if(h[jout][kout] > sdep[jout][kout])
{
        //qoutov = (float)(w*alfa*pow((h[jout][kout]-sdep[jout][kout]),1.667f));
        float dqx2 = powf(dqovx[jout][kout],2);
        float dqy2 = powf(dqovy[jout][kout],2);
        qoutov = sqrtf(dqx2 + dqy2);
}
```

/* Overland water depth at outlet cell is reduced after taking */

/* the outflow out of the cell   */

```
h[jout][kout] = (float)(h[jout][kout] - qoutov*dt/(pow(w,2.0f)));
```

/* SECOND:calculate the flow going out from the channel portion   */

```
if(chancheck == 1 && hch[jout][kout] > sdep[jout][kout])

{

        hout = hch[jout][kout] - sdep[jout][kout];


        qoutch =
chnDischarge(hch[jout][kout],hout,wchout,dchout,

sdep[jout][kout],rmanout,1,sout,sfactorout);


        dqch[jout][kout] = dqch[jout][kout] - qoutch;

}


/* The total outflow at the basin's outlet is given by adding
*/

/* the outflow from the overland & channel portion of the cell
*/


qout = qoutov + qoutch;


/* Keeping Track of the Total Outflow Volume
                                                            */


vout = vout + qout*dt;


/* Checking to see if the Peak Flow has been reached
                              */
```

```
if(qout > qpeak)

{

 qpeak = qout;

 tpeak = (float)( iter*dt/60.0);

}



/* Populating the Output Flows at the Watershed Outlet
                        */



for(ill = 1;ill <= ndis; ill++)

{

 if(jout == iq[ill][1] && kout == iq[ill][2])

 {

        q[ill] = qout;

 }

}
```

}

Overland sediment routing simulation

```
/*******************************/

                                /*      RoutSedOvrl.c

*/

                    /*******************************/
```

```
#include "all.h"

extern void RoutSedOvrl(float dqq, float sf,int jfrom,int kfrom,int jto,int kto)
{

                float V, qsSUS[4],qsADV[4],qsSUStot,SUStot,
DEPtot,qsBM[4],

                                totXSScap,capacity[4],RESIDcap,
qsBMtot,

                qsEROS[4],qsEROStot,percent[4],qs[4],qsKR;

                int SizeFr,SoilType;
                // OfSET
                const float MILLION = 1000000.0f;
                // OfSET : some equation must be derived later.
                // all soil density (kg per m3)
                const float SOIL_DENSITY = 656;
                // OfSET : do not use KR capapcity calculation of CASC2D
alogrithm
                //qsKR = KRcap(KRov,dqq,w,sf,jfrom,kfrom);
                // OfSET : Fixed percent of sand, silt, and clay in soil
                percent[1] = 0.0; //sand
                percent[2] = 0.007; //silt
                percent[3] = 0.055; //clay


                /* SizeFr: Soil size fraction:    1: sand; 2: silt; 3: clay    */
```

```
/* Outgoing cell : (jfrom, kfrom)                    */

/* Receiving cell: (jto, kto)                    */


/* Flow velocity [m/s]                    */

V = (float)(fabs(dqq)/(w * h[jfrom][kfrom]));

if(dqq > 0.0)

{

    int x = 0;

}
/* Initialize sediment volumes to zero               */

qsSUStot = 0;    /* Total transported suspended volume

*/

qsBMtot = 0;     /* Total transported bed material volume

*/

qsEROStot = 0;   /* Total transported eroded material volume

*/

SUStot = 0;    /* Total susp. volume in outgoing cell       */

DEPtot = 0;    /* Total deposited volume in outgoing cell

*/



/* Finds soil type for the outgoing overland cell          */

SoilType = isoil[jfrom][kfrom];



/* Transport Capacity using the Kilinc-Richardson equation

*/



// OfSet : calculate KR capacity
```

```
// erosion = (0.5) Q (w^2) dt

if(bulk_dens[jfrom][kfrom] > 0){

        qsKR = (0.5f * ksErosionRate * w * h[jfrom][kfrom] *
dt ) / (bulk_dens[jfrom][kfrom] * 1000); // m3

}else{

    qsKR = 0;

}




/* Initialize transport volumes by size fraction to zero      */

for(SizeFr=1;SizeFr<=3;SizeFr++)

{              /* For size fraction SizeFr:            */

        qsSUS[SizeFr] = 0;  /* transported volume from
suspension     */

        qsBM[SizeFr] = 0 ;  /* transported volume from
deposition     */

        qsEROS[SizeFr] = 0; /* transported volume from parent
material*/

        qs[SizeFr] = 0;     /* total transported volume            */

        /* Outgoing cell total suspended and deposited sediment
*/

        SUStot += qovs[SizeFr][jfrom][kfrom]; //suspend vol

        DEPtot += vols[SizeFr][jfrom][kfrom]; //deposited vol



}



for(SizeFr=1;SizeFr<=3;SizeFr++) /* For each size fraction
*/
```

```
                    {

                              /* Is this size fraction present in suspended portion ?
*/

                              if(qovs[SizeFr][jfrom][kfrom] > 0)

                              {

                                    if(qsKR < SUStot) /* Transport capacity is <
total suspended*/

                                    {

                                          /* Volume that can be transported using
the KR equation   */

                                          capacity[SizeFr] = qsKR *
qovs[SizeFr][jfrom][kfrom]/SUStot;

                                          /* Volume that can be transported by
advective processes  */

                                          qsADV[SizeFr] =
qovs[SizeFr][jfrom][kfrom] * V * dt / w;

                                          /* Transport the maximum between the
last two quantities  */

                                          qsSUS[SizeFr] =
(float)(MAX(capacity[SizeFr],qsADV[SizeFr]));

                                    }

                                    else /* If transport capacity is > total suspended
sediment */

                                    {

                                          /* Transport all the suspended sediment
for this size fr. */

                                          qsSUS[SizeFr] =
qovs[SizeFr][jfrom][kfrom];

                                    }
```

/* Transfers the volume qsSUS[SizeFr] of sediment size   */

/* fraction, SizeFr, in suspension in the outgoing cell   */

/* to the suspended portion of the receiving cell */

```
TransferSed(SizeFr,qovs,qsSUS[SizeFr],jfrom,kfrom,jto,kto);
```

/* Keeps track of the total volume of sediment coming from */

/* the suspended material portion of the outgoing cell   */

```
        qsSUStot += qsSUS[SizeFr];
    }
}
```

/* Reduces the transport capacity by the volume that has already*/

/* been transported from the outgoing cell to get the total   */

/* excess capacity   */

```
totXSScap = (float)(MAX(0,qsKR - qsSUStot));
```

/* If there is an excess transport capacity, and provided that */

/* the outgoing cell has previously deposited material, we use */

/* this capacity to put this sediment in suspension and move it */

/* to the suspended portion of the receiving cell   */

```c
if(totXSScap > 0 && DEPtot > 0)
{
    for(SizeFr=1;SizeFr<=3;SizeFr++)
    {
        /* Is this size fraction present in deposited portion ? */

        if(vols[SizeFr][jfrom][kfrom] > 0)
        {
            /* Excess transport capacity is < total deposited sediment*/

            if(totXSScap < DEPtot)
            {
                /* Volume that can be transported for this size     */

                /* fraction is proportional to its percentage in the   */

                /* total deposited sediment     */

                qsBM[SizeFr] = totXSScap * vols[SizeFr][jfrom][kfrom] / DEPtot;
            }
            else /* If transport capacity is > total deposited sed.  */
            {
                /* Transport all the deposited sed. for this size fr.  */

                qsBM[SizeFr] = vols[SizeFr][jfrom][kfrom];
            }
```

/* Transfers the volume qsBM[SizeFr] of sediment size */

/* fraction, SizeFr, in deposition in the outgoing cell */

/* to the suspended portion of the receiving cell */

```
TransferSed(SizeFr,vols,qsBM[SizeFr],jfrom,kfrom,jto,kto);
```

/* Keeps track of the total volume of sediment leaving */

/* the deposited material portion of the outgoing cell */

```
                qsBMtot += qsBM[SizeFr];

            }
        }
    }
```

/* Reduces the excess transport capacity by the total volume */

/* of sediment, qsBMtot,that has alrady been transported */

/* from the deposited portion of the outgoing cell */

```
RESIDcap = (float)(MAX(0,totXSScap - qsBMtot));
```

/* Any residual transport capacity is used to erode the parent */

/* material. Erosion by size fraction is proportional to its */

```
/* percentage in the parent material                    */

if(RESIDcap >0)

{

        for(SizeFr=1;SizeFr<=3;SizeFr++)

        {

                /* Volume of eroded parent material

corresponding to size   */

                /* fraction SizeFr                        */

                qsEROS[SizeFr] = RESIDcap * percent[SizeFr];

                /* Keeps track of the total volume of sediment

coming from  */

                /* the parent material portion of the outgoing

cell        */

                qsEROStot += qsEROS[SizeFr];

                /* Transfers the volume qsEROS[SizeFr] of

sediment size    */

                /* fraction, SizeFr from the outgoing cell parent

material  */

                /* to the suspended portion of the receiving cell

*/

        TransferSed(SizeFr,ssoil,qsEROS[SizeFr],jfrom,kfrom,jto,kto
);

        }
}


        /* Keeps track of the total sediment volume leaving the         */
```

```
                    /* outgoing cell (coming from all 3 sources)              */

                    qss[jfrom][kfrom] += qsSUStot + qsBMtot + qsEROStot;


                    // OfSET
                    /* Keeps track of the total Cadmium sediment mass leaving
the         */
                    /* outgoing cell (coming from all 3 sources)              */


                    mass_cd[jfrom][kfrom] += ((qsSUStot + qsBMtot +
qsEROStot) * SOIL_DENSITY * Cd_conc[jfrom][kfrom] / MILLION); // change
unit ppm


                    for(SizeFr=1;SizeFr<=3;SizeFr++)
                    {
                            /* Total sediment volume leaving the outgoing cell by
size   */
                            /* fraction                                       */
                            qs[SizeFr] = qsSUS[SizeFr] + qsBM[SizeFr] +
qsEROS[SizeFr];


                            /* Keeps track of the sediment flux [m3/s] by size
fraction   */
                            /* out of the outgoing cell                       */
                            SedFluxOut[SizeFr][jfrom][kfrom] += qs[SizeFr] / dt;
                    }
                    if(ishp[jfrom][kfrom] == 1 && ishp[jto][kto] == 2)
                    {// from land to channel
```

// Keeps track of the total sediment volume (ton) leaving from land to channel

outLetSum += qsEROStot;

outLetCdSum += qsEROStot * SOIL_DENSITY * Cd_conc[jfrom][kfrom] / MILLION;

}

/* Calls the function findMFAC to find the maximum flux */

/* averaged concentration out of the outgoing cell   */

findMFAC(jfrom,kfrom,qsKR,dqq,qs);

Land to water sediment discharge simulation

```
/*****************************/

                                    /*      RoutSedOut.c    */

/*****************************/



#include "all.h"


extern void RoutSedOut()


{

                if(ishp[jout][kout] == 2 )  /* Case of a channel cell        */
```

```
                {

                        if(hch[jout][kout] != 0)

                        {

RoutSedChn(qout,sout,jout,kout,1,1,wchout,hch[jout][kout]);

                        }

                }


                else /* case of an overland cell                    */

                {

                        if(h[jout][kout] != 0)

                        {

                                RoutSedOvrl(qoutov,sovout,jout,kout,1,1);

                        }

                }

        }
```

<u>Sediment status determination</u>

```
/*      SedStats.c      */

                /*****************************/



#include "all.h"
```

```c
extern void SedStats()

{
                    int j,k, SizeFr;

                    float totdepv,totscourv;


                    for(j = 1;j <= m; j++)

                    {

                        for(k = 1;k <= n; k++)

                        {

                            if(ishp[j][k] != nodatavalue)

                            {

                                totdepv = 0.0;

                                totscourv = 0.0;

                                totsus[j][k] = 0.0;


                                for(SizeFr=1;SizeFr<=3;SizeFr++)

                                {

                                    /* Total (sand+silt+clay)
deposited sed. volume (m3)               */


                                    totdepv += vols[SizeFr][j][k];


                                    /* Total (sand+silt+clay) scoured
sed. volume (m3)               */


                                    totscourv += ssoil[SizeFr][j][k];
```

/* Total (sand+silt+clay) suspended sed. volume (m3)   */

```
                                       totsus[j][k] += qovs[SizeFr][j][k];

                                   }


                                   /* Net (deposited - eroded) sediment volume (mm)                */

                                   totnetv[j][k] = (totdepv + totscourv) * 1000 / (w*w);


                                   /* Min. and Max. net erosion/depostion volume (m3)          */

                                   aminnetv = MIN((double)(totnetv[j][k]) , aminnetv);

                                   amaxnetv = MAX(totnetv[j][k] , amaxnetv);


                                   /* Absolute max. flux conc., susp. volume and suspended         */

                                   /* conc. at any time step and at any overland cell              */


                                   if(ishp[j][k] == 1)

                                   {
```

amaxFluxCoutOv = MAX(MaxFluxCout[j][k],amaxFluxCoutOv);

amaxSusOv = MAX(totsus[j][k],amaxSusOv);

/* Limiting the mim. water depth to 0.5mm will reduce   */

/* very high concentration calculations   */

if(h[j][k] > 5E-4)

{

    SusC[j][k] = totsus[j][k] / (h[j][k]*w*w);

    amaxSusCov = MAX(amaxSusCov,SusC[j][k]);

}

else

{

    SusC[j][k] = 0;

}

}

/* Absolute max. flux conc., susp. volume and suspended   */

/* conc. at any time step and at any channel cell   */

if(ishp[j][k] == 2)

{

```
                                        amaxFluxCoutCh =
MAX(amaxFluxCoutCh,MaxFluxCout[j][k]);

                                        amaxSusCh =
MAX(amaxSusCh,totsus[j][k]);


                                        if(hch[j][k] > 5E-4)

                                        {

                                                SusC[j][k] = totsus[j][k] /

                (hch[j][k]*w*chp[link[j][k]][node[j][k]][2]);


                                                amaxSusCch =
MAX(amaxSusCch,SusC[j][k]);

                                        }
                                        else
                                        {

                                                SusC[j][k] = 0;

                                        }
                                }
                        }
                }
        }
}
```

Sediment transport volume estimation

```
/*****************************/

                                        /*      SedVolumes.c
*/

                    /*****************************/


/* Calculates at the end of the simulation the volume of      */

/* suspended, deposited and (suspended+deposited) sediment      */

/* by size fraction remaining in the overland or the channels     */

#include "all.h"


extern void          SedVolumes()

{

            int j,k,SizeFr;


            for(j=1;j<=m;j++)

            {

                  for(k=1;k<=n;k++)

                  {

                        if(ishp[j][k] != nodatavalue)

                        {

                              /* Total eroded sediment by size fraction
*/

                              for(SizeFr =1;SizeFr<=3;SizeFr++)
```

tot_eroded[SizeFr] +=

ssoil[SizeFr][j][k];

if(ishp[j][k] == 1) /* for the overland
cells   */

{

　　for(SizeFr
=1;SizeFr<=3;SizeFr++)

　　{

　　　/* Total suspended

volume by size fraction   */

　　　sus_ov[SizeFr] +=

qovs[SizeFr][j][k];

　　　/* Total deposited volume

by size fraction   */

　　　dep_ov[SizeFr] +=

vols[SizeFr][j][k];

　　　/* Total suspended and

deposited volume by size fract.*/

　　　tot_ov[SizeFr] +=

qovs[SizeFr][j][k] +

　　　vols[SizeFr][j][k];

　　}

}

if(ishp[j][k] == 2) /* for the channel
cells   */

```
                                                {

                                                    for(SizeFr
=1;SizeFr<=3;SizeFr++)

                                                    {

                                                        /* Total suspended
volume by size fraction          */

                                                        sus_ch[SizeFr] +=
qovs[SizeFr][j][k];


                                                        /* Total deposited volume
by size fraction         */

                                                        dep_ch[SizeFr] +=
vols[SizeFr][j][k];


                                                        /* Total suspended and
deposited volume by size fract.*/

                                                        tot_ch[SizeFr] +=
qovs[SizeFr][j][k] +
                                                        vols[SizeFr][j][k];

                                                    }

                                                }

                                            }

                                        }

                                    }

}
```

Simulation grid result display
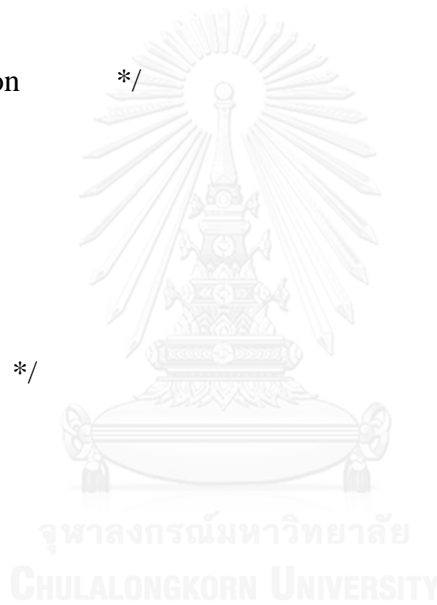
```
/*****************************/

                                              /*        WriteGrids.c
*/

                        /*****************************/



#include "all.h"


extern void WriteGrids()

{

                int j1,k1;


                float **WatDep;


                char wr_rname[80],wr_vinfname[80],wr_dname[80],

                    wr_cname[80],wr_susname[80],wr_erosdepname[80],

                    wr_sandfluxname[80],wr_siltfluxname[80],

                    wr_clayfluxname[80],wr_totalfluxname[80],

                    wr_sandMFACname[80],wr_siltMFACname[80],

                    wr_clayMFACname[80],wr_totalMFACname[80];

                //OfSET

                char wr_totalfluxCdname[80];

                FILE *wr_totalfluxCdname_h = NULL;


                FILE *wr_dname_h = NULL;
```

```
FILE *wr_erosdepname_h = NULL;

FILE *wr_rname_h = NULL;

FILE *wr_sandfluxname_h = NULL;

FILE *wr_siltfluxname_h = NULL;

FILE *wr_clayfluxname_h = NULL;

FILE *wr_totalfluxname_h = NULL;

FILE *wr_sandMFACname_h = NULL;

FILE *wr_siltMFACname_h = NULL;

FILE *wr_clayMFACname_h = NULL;

FILE *wr_totalMFACname_h = NULL;

FILE *wr_cname_h = NULL;

FILE *wr_vinfname_h = NULL;

FILE *wr_susname_h = NULL;


WatDep = floatMemAlloc2d(m,n);



if(ipcount == nplt)

{

        printf("Writing Output Grids, IFCOUNT = %ld  Time =
%.2f \n",



                                ifcount,iter*dt/60.);



        /* SusC: grid holds the values of total suspended
sediment              */
```

```
                        /* WatDep: water depth in basin's overland or channel
cells                   */


                        for(j1=1; j1<=m; j1++)

                        {

                                for(k1=1; k1<=n; k1++)

                                {

                                        if (ishp[j1][k1] != nodatavalue)

                                        {

                                                if(ishp[j1][k1] == 1)

                                                {

                                                        WatDep[j1][k1] =
h[j1][k1];

                                                }
                                                else
                                                {

                                                        WatDep[j1][k1] =
hch[j1][k1];

                                                }
                                        }
                                }
                        }


                        /* Writing time series grids

                                */
```

```
/* Water depth in meters

                                        */

write2dTS(dname, wr_dname,wr_dname_h,WatDep,1);


/* Rainfall intensity in mm/h

                        */

write2dTS(rname,
wr_rname,wr_rname_h,rint,3600000);


/* Infiltrated volume in mm

                            */

write2dTS(vinfname,wr_vinfname,wr_vinfname_h,vinf,1000)
;


/* Suspended sediment concentration in m3/m3
                                        */
write2dTS(cname,wr_cname,wr_cname_h,SusC,1);


/* Total suspended sediment in mm

                */

write2dTS(susname,wr_susname,wr_susname_h,totsus,1000/(
w*w));


/* Erosion and deposition in mm

                */
```

```
                    write2dTS(erosdepname,wr_erosdepname,wr_erosdepname_h
,
                    totnetv,1);


          /* Sediment fluxes are in (m3/s)

                    */


          write3dTS(sandfluxname,wr_sandfluxname,wr_sandfluxname
_h,
                    1,
SedFluxOut);


          write3dTS(siltfluxname,wr_siltfluxname,wr_siltfluxname_h,
                    2,
SedFluxOut);


          write3dTS(clayfluxname,wr_clayfluxname,wr_clayfluxname_
h,
                    3,
SedFluxOut);


          write2dTS(totalfluxname,wr_totalfluxname,wr_totalfluxname
_h,
                    qss,(1/dt));
          // OfSET : Write total flux of cadmium to file


          write2dTS(totalfluxCdname,wr_totalfluxCdname,wr_totalflux
Cdname_h,

          mass_cd,(1/dt));
```

```
                                /* Sediment concentrations are in m3 sed/ m3 mixture
                                              */


                        write3dTS(sandMFACname,wr_sandMFACname,wr_sandMF
ACname_h,

                                                    1, MFAC);


                        write3dTS(siltMFACname,wr_siltMFACname,wr_siltMFACn
ame_h,

                                                    2, MFAC);


                        write3dTS(clayMFACname,wr_clayMFACname,wr_clayMF
ACname_h,

                                                    3, MFAC);


                        write2dTS(totalMFACname,wr_totalMFACname,wr_totalMF
ACname_h,


                MaxFluxCout,1);


                                /* Incrementing counters

                                                        */


                        ifcount++;

                        if (iter == 1) ipcount++;

                        if (iter != 1) ipcount = 1;

        }

        else
```

```
        {

                        ipcount++;

        }


                        /* Freeing memory

                                                              */


                        fMemFree2d(WatDep, m,n);
}




                        /***********************************/
                        /*      FUNCT: write2dTS       */
                        /***********************************/


extern void write2dTS(char *name, char *wr_name,FILE *wr_name_h,

                                                              float
**ParamValue, float UnitsConv)

{
                int j1,k1;


                if(name[0] != '\0')
                {
                        strncpy(wr_name,name,21);
```

```c
sprintf(wr_name,"%s.%ld",name,ifcount);
if((wr_name_h=fopen(wr_name,"w"))==NULL)
{
        printf("Can't open time-series file : %s
\n",wr_name);

        exit(EXIT_FAILURE);
}
fprintf(wr_name_h,"%s",header);


for(j1=1; j1<=m; j1++)
{
        for(k1=1; k1<=n; k1++)
        {
                if (ishp[j1][k1] != nodatavalue)
                {
                        fprintf(wr_name_h,"%10.5f
",ParamValue[j1][k1]*UnitsConv);
                }
                else

                        fprintf(wr_name_h,"%i
",nodatavalue);

        }
        fprintf(wr_name_h,"\n");
}


fclose(wr_name_h);
}
```

```
                          return;


}




                              /*********************************/

                              /*        FUNCT: write3dTS       */

                              /*********************************/


extern void write3dTS(char *name, char *wr_name,FILE *wr_name_h,

                                                    int layer,
float **ParamValue[])

{
                  int j1,k1;


                  if(name[0] != '\0')

                  {
                          strncpy(wr_name,name,21);

                          sprintf(wr_name,"%s.%ld",name,ifcount);
```

```c
if((wr_name_h=fopen(wr_name,"w"))==NULL)
{
    printf("Can't open time-series file : %s
\n",wr_name);

    exit(EXIT_FAILURE);
}
fprintf(wr_name_h,"%s",header);


for(j1=1; j1<=m; j1++)
{
    for(k1=1; k1<=n; k1++)
    {
        if (ishp[j1][k1] != nodatavalue)
        {
            fprintf(wr_name_h,"%10.5f
",ParamValue[layer][j1][k1]);
        }
        else

            fprintf(wr_name_h,"%i
",nodatavalue);
    }
    fprintf(wr_name_h,"\n");
}


fclose(wr_name_h);
}
return;
```

}

Sediment outflow grid display

/********************************/

/*   WriteOutflows.c

*/

/*****************************/

#include "all.h"

extern void WriteOutflow()

{

int ill,ils,jsed,ksed,i;

/****************************/

```c
/*   write results to screen   */
/*****************************/
if(chancheck == 1)
{
        printf(
        "Time (Min) = %7.2f\tQ (m3/s)= %7.2f\tChan.
Depth(m) = %7.3f \n"

                            ,iter*dt/60.0, qout,hch[jout][kout]);
}
else
{
        printf(
        "Time (Min) = %7.2f\tQ (m3/s) = %7.2f\tOver.
Depth(m) = %7.3f\n"

                            ,iter*dt/60.0,qout,h[jout][kout]);
}


/***************************************************
*****/
/*   write outflow and sediment flow to output files */
/***************************************************
*****/


if(iter==1)
{
        fprintf(dis_out_file_fptr," Time_(min) ");
```

```
                        if(indexeros == 1)fprintf(sed_out_file_fptr,"Time_(min)
");

                        for (i=1;i<=ndis;i++)

                        {

                                fprintf(dis_out_file_fptr,"Row%iCol%i
",iq[i][1],iq[i][2]);

                                if(indexeros == 1)

        fprintf(sed_out_file_fptr,"Row%iCol%i ",ised[i][1],ised[i][2]);

                        }

                        fprintf(dis_out_file_fptr,"\n");

                        if(indexeros == 1)fprintf(sed_out_file_fptr,"\n");

                }


        if(icount == nprn)

        {

                /* Write outflow discharge at selected locations
                                                */



                        fprintf(dis_out_file_fptr,"%.2f",iter*dt/60.0);


                        for(ill=1; ill<=ndis; ill++)

                        {

                         switch(unitsQ)

                                {
```

```
                                          case 1: /* Discharge in m3/s */

                                                  fprintf(dis_out_file_fptr,"%15.3f
",q[ill]);

                                                  break;



                                          case 2: /* Discharge in cfs */

                                                  fprintf(dis_out_file_fptr,"%15.3f
",

                                                          q[ill]* pow(3.28084,3));

                                                  break;



                                          case 3: /* Discharge in mm/h */

                                                  fprintf(dis_out_file_fptr,"%15.3f
",

                                                          q[ill] / areaQ[ill] * 360);

                                                  break;
                                  }
                          }


                  fprintf(dis_out_file_fptr,"\n");


                  /* Writing outflow sediment Data at selected locations
                          */


                  if(indexeros == 1 && sed_out_file[0] != '\0')

                  {
```

```
                            fprintf(sed_out_file_fptr,"%.2f",iter*dt/60.0);


                            for(ils=1; ils<=nsed; ils++)
                            {
                                    jsed = ised[ils][1];

                                    ksed = ised[ils][2];



                                    qsed[ils] = qss[jsed][ksed]/dt;



                                    switch(unitsQs)
                                    {
                                            case 1: /* Sediment discharge in
m3/s */

                            fprintf(sed_out_file_fptr,"%15.5f ", qsed[ils]);

                                            break;
                                            case 2: /* Sediment discharge in
tons/ha/day */

                            fprintf(sed_out_file_fptr,"%15.5f ",

                    qsed[ils] / areaQs[ils] * ROs * 86400);

                                            break;
                                    }
                            }
                            fprintf(sed_out_file_fptr,"Total sed,Cadmium
from land to channel (ton) %15.5f , %15.5f ",outLetSum, outLetCdSum);
```

```
                        fprintf(sed_out_file_fptr,"\n");


                        fprintf(debug,"%.2f \t %g \t %g \t %g
\n",iter*dt/60,

                SedFluxOut[1][jout][kout],SedFluxOut[2][jout][kout],

                        SedFluxOut[3][jout][kout]);
        }
        //reset outllet sum
        outLetSum = 0;
        outLetCdSum = 0;
        icount = 1;
}


else
{

        icount = icount + 1;
}


}
```

Simulation Summary

```
/*******************************/

                                    /*      WriteSummFlow.c
*/

                    /*******************************/



#include "all.h"


extern void WriteSummFlow()

{


                double
PercentFlow,InitialVol,FinalVol,InVolume,OutVolume;


                InitialVol = init_ch_vol   +  init_ov_vol;

                FinalVol   = final_ch_vol  +  final_ov_vol;

                InVolume   = InitialVol + vin;

                OutVolume = vinftot + vout + FinalVol;
```

PercentFlow =   100.0 * (InVolume - OutVolume) /
InVolume;

```c
/* ... summary of Output Flow */

fprintf(Summ_file_fptr,

                              "\nSUMMARY OF FLOW
OUTPUT\n");
         fprintf(Summ_file_fptr,"====================\n\n");

         fprintf(Summ_file_fptr,
             "Peak Discharge (m3/s)....................=");
         fprintf(Summ_file_fptr,"%15.2f \n",qpeak);

         fprintf(Summ_file_fptr,
             "Time to Peak (min)......................=");
         fprintf(Summ_file_fptr,"%15.2f \n",tpeak);

         fprintf(Summ_file_fptr,
             "Initial Surface Volume (m3)..............=");
         fprintf(Summ_file_fptr,"%15.2f \n",InitialVol);

         fprintf(Summ_file_fptr,
             "Volume of Rainfall - retention (m3)......=");
         fprintf(Summ_file_fptr,"%15.2f \n",vin);
```

```c
fprintf(Summ_file_fptr,

        "Volume leaving the Watershed
(m3).........................=");
        fprintf(Summ_file_fptr,"%15.2f \n",vout);


        fprintf(Summ_file_fptr,

        "Percentage of Vout to Vin.................................=");
        fprintf(Summ_file_fptr,"%15.2f \n",(vout/vin)*100.0);


        fprintf(Summ_file_fptr,

        "Final Surface Volume (m3).................................=");
        fprintf(Summ_file_fptr,"%15.2f \n",FinalVol);


        fprintf(Summ_file_fptr,

        "Volume Infiltrated (m3).................................=");
        fprintf(Summ_file_fptr,"%15.2f \n",vinftot);


        fprintf(Summ_file_fptr,

        "Percentage of Vinftot to Vin..............................=");
        fprintf(Summ_file_fptr,"%15.2f \n",(vinftot/vin)*100.0);


        fprintf(Summ_file_fptr,

        "Percent Mass Balance...................................... =");
        fprintf(Summ_file_fptr,"%15.2f\n",PercentFlow);
```

```
fprintf(Summ_file_fptr,

        "\nHYDROLOGICAL VARIABLES MINIMUM AND
MAXIMUM VALUES\n");

        fprintf(Summ_file_fptr,


        "=======================================
======\n\n");


        fprintf(Summ_file_fptr,

        "Min. Rainfall Intensity (mm/hr)...........................=");
        fprintf(Summ_file_fptr,"%15.2f \n",aminrain*3600.*1000);


        fprintf(Summ_file_fptr,

        "Max. Rainfall Intensity (mm/hr)...........................=");
        fprintf(Summ_file_fptr,"%15.2f \n",amaxrain*3600.*1000);


        fprintf(Summ_file_fptr,

        "Min. Infiltration Depth (mm)..............................=");
        fprintf(Summ_file_fptr,"%15.2f \n",aminvinf*1000);


        fprintf(Summ_file_fptr,

        "Max. Infiltration Depth (mm)..............................=");
        fprintf(Summ_file_fptr,"%15.2f \n",amaxvinf*1000);


        fprintf(Summ_file_fptr,

        "Min. Overland Depth (m)...................................=");
        fprintf(Summ_file_fptr,"%15.2f \n",amindepth);
```

```
fprintf(Summ_file_fptr,

    "Max. Overland Depth (m)....................................=");

fprintf(Summ_file_fptr,"%15.2f \n",amaxdepth);


fprintf(Summ_file_fptr,

    "Min. Channel Depth (m)....................................=");

fprintf(Summ_file_fptr,"%15.2f \n",amincdepth);


fprintf(Summ_file_fptr,

    "Max. Channel Depth (m)....................................=");

fprintf(Summ_file_fptr,"%15.2f \n\n",amaxcdepth);


}


/*****************************/

                                        /*      WriteSummSed.c
*/


            /*****************************/




#include "all.h"


extern void WriteSummSed()

{
```

```
                double
PercentSed,TotRemOvr,TotRemChn,TotEroded,TotLeaving,

                TotSusRemOvr,TotDepRemOvr,TotSusRemChn,TotDepRem
Chn;

                struct gstats totnetv_stats;

                totnetv_stats = gridstats(totnetv);

                TotEroded    =
fabs(tot_eroded[1]+tot_eroded[2]+tot_eroded[3]);

                TotSusRemOvr = sus_ov[1] + sus_ov[2] + sus_ov[3];

                TotDepRemOvr = dep_ov[1]+dep_ov[2]+dep_ov[3];

                TotRemOvr    = tot_ov[1]+tot_ov[2]+tot_ov[3];

                TotSusRemChn = sus_ch[1]+sus_ch[2]+sus_ch[3];

                TotDepRemChn = dep_ch[1]+dep_ch[2]+dep_ch[3];

                TotRemChn    = tot_ch[1]+tot_ch[2]+tot_ch[3];

                TotLeaving   = sed_out[1]+sed_out[2]+sed_out[3];

                PercentSed = 100.0 * (TotLeaving + TotRemOvr +
TotRemChn

                        - TotEroded) / TotEroded ;

                /* ... summary of output sediment

                        */
```

```c
fprintf(Summ_file_fptr,

        "\nSUMMARY OF SEDIMENT OUTPUT : Volume in
Cubic Meters\n");

fprintf(Summ_file_fptr,

        "(Percentages from the total eroded \n");

fprintf(Summ_file_fptr,


        "=========================================
========\n\n");


fprintf(Summ_file_fptr,

        "Total Volume of Sand Eroded...............................=");
fprintf(Summ_file_fptr,"%15.2f \n",fabs(tot_eroded[1]));


fprintf(Summ_file_fptr,

        "Total Volume of Silt Eroded...............................=");
fprintf(Summ_file_fptr,"%15.2f \n",fabs(tot_eroded[2]));


fprintf(Summ_file_fptr,

        "Total Volume of Clay Eroded...............................=");
fprintf(Summ_file_fptr,"%15.2f \n",fabs(tot_eroded[3]));


fprintf(Summ_file_fptr,

        "Total Volume of Material Eroded...........................=");
fprintf(Summ_file_fptr,"%15.2f \n\n", TotEroded);
```

```
                        fprintf(Summ_file_fptr,

                                "Volumes of Eroded Sediment Remaining on the
Overland:\n");


                        fprintf(Summ_file_fptr,

                                "------------------------------------------------\n");


                        fprintf(Summ_file_fptr,

                                "Total Volume of Suspended
Sand...........................=");
                        fprintf(Summ_file_fptr,"%15.2f -> %5.2f %% \n",

                                sus_ov[1],fabs(sus_ov[1]/tot_eroded[1]*100));


                        fprintf(Summ_file_fptr,

                                "Total Volume of Suspended Silt...........................=");
                        fprintf(Summ_file_fptr,"%15.2f -> %5.2f %% \n",

                                sus_ov[2],fabs(sus_ov[2]/tot_eroded[2]*100));


                        fprintf(Summ_file_fptr,

                                "Total Volume of Suspended
Clay...........................=");
                        fprintf(Summ_file_fptr,"%15.2f -> %5.2f %% \n",

                                sus_ov[3],fabs(sus_ov[3]/tot_eroded[3]*100));
```

```
fprintf(Summ_file_fptr,

        "Total Volume of Suspended

Sediment.........................=");

        fprintf(Summ_file_fptr,"%15.2f -> %5.2f %% \n\n",

        TotSusRemOvr,fabs(TotSusRemOvr/TotEroded*100));


        fprintf(Summ_file_fptr,

            "Total Volume of Deposited Sand.............................=");

        fprintf(Summ_file_fptr,"%15.2f -> %5.2f %% \n",

            dep_ov[1],fabs(dep_ov[1]/tot_eroded[1]*100));


        fprintf(Summ_file_fptr,

            "Total Volume of Deposited Silt............................=");

        fprintf(Summ_file_fptr,"%15.2f -> %5.2f %% \n",

            dep_ov[2],fabs(dep_ov[2]/tot_eroded[2]*100));


        fprintf(Summ_file_fptr,

            "Total Volume of Deposited Clay............................=");

        fprintf(Summ_file_fptr,"%15.2f -> %5.2f %% \n",

            dep_ov[3],fabs(dep_ov[3]/tot_eroded[3]*100));


        fprintf(Summ_file_fptr,

            "Total Volume of Deposited

Sediment.........................=");
```

```
                                fprintf(Summ_file_fptr,"%15.2f -> %5.2f %% \n\n",

                                TotDepRemOvr,fabs(TotDepRemOvr/TotEroded*100));


                                fprintf(Summ_file_fptr,

                                        "Total Volume of Sand Remaining on the
Overland.............=");

                                fprintf(Summ_file_fptr,"%15.2f -> %5.2f %% \n",

                                        tot_ov[1],fabs(tot_ov[1]/tot_eroded[1]*100));


                                fprintf(Summ_file_fptr,

                                        "Total Volume of Silt Remaining on the
Overland.............=");

                                fprintf(Summ_file_fptr,"%15.2f -> %5.2f %% \n",

                                        tot_ov[2],fabs(tot_ov[2]/tot_eroded[2]*100));


                                fprintf(Summ_file_fptr,

                                        "Total Volume of Clay Remaining on the
Overland.............=");

                                fprintf(Summ_file_fptr,"%15.2f -> %5.2f %% \n",

                                        tot_ov[3],fabs(tot_ov[3]/tot_eroded[3]*100));


                                fprintf(Summ_file_fptr,

                                        "Total Volume of Eroded Material Remaining on the
Overland..=");

                                fprintf(Summ_file_fptr,"%15.2f -> %5.2f %% \n\n",
```

```
                    TotRemOvr,fabs(TotRemOvr/TotEroded*100));



          fprintf(Summ_file_fptr,

                    "Volumes of Eroded Sediment Remaining in the
Channels:\n");

          fprintf(Summ_file_fptr,

                    "-------------------------------------------------\n");



          fprintf(Summ_file_fptr,

                    "Total Volume of Suspended
Sand............................=");

          fprintf(Summ_file_fptr,"%15.2f -> %5.2f %% \n",

                    sus_ch[1],fabs(sus_ch[1]/tot_eroded[1]*100));



          fprintf(Summ_file_fptr,

                    "Total Volume of Suspended Silt............................=");

          fprintf(Summ_file_fptr,"%15.2f -> %5.2f %% \n",

                    sus_ch[2],fabs(sus_ch[2]/tot_eroded[2]*100));



          fprintf(Summ_file_fptr,

                    "Total Volume of Suspended
Clay............................=");

          fprintf(Summ_file_fptr,"%15.2f -> %5.2f %% \n",

                    sus_ch[3],fabs(sus_ch[3]/tot_eroded[3]*100));
```

```
fprintf(Summ_file_fptr,

    "Total Volume of Suspended

Sediment........................=");

    fprintf(Summ_file_fptr,"%15.2f -> %5.2f %% \n\n",

    TotSusRemChn,fabs(TotSusRemChn/TotEroded*100));

    fprintf(Summ_file_fptr,

        "Total Volume of Deposited Sand............................=");
    fprintf(Summ_file_fptr,"%15.2f -> %5.2f %% \n",

     dep_ch[1],fabs(dep_ch[1]/tot_eroded[1]*100));

    fprintf(Summ_file_fptr,

        "Total Volume of Deposited Silt...........................=");
    fprintf(Summ_file_fptr,"%15.2f -> %5.2f %% \n",

        dep_ch[2],fabs(dep_ch[2]/tot_eroded[2]*100));

    fprintf(Summ_file_fptr,

        "Total Volume of Deposited Clay............................=");
    fprintf(Summ_file_fptr,"%15.2f -> %5.2f %% \n",

        dep_ch[3],fabs(dep_ch[3]/tot_eroded[3]*100));

    fprintf(Summ_file_fptr,
```

```
                              "Total Volume of Deposited
Sediment........................=");

                   fprintf(Summ_file_fptr,"%15.2f -> %5.2f %% \n\n",


                   TotDepRemChn,fabs(TotDepRemChn/TotEroded*100));



                   fprintf(Summ_file_fptr,

                        "Total Volume of Sand Remaining in the
Channels.............=");

                   fprintf(Summ_file_fptr,"%15.2f -> %5.2f %% \n",


                        tot_ch[1],fabs(tot_ch[1]/tot_eroded[1]*100));



                   fprintf(Summ_file_fptr,

                        "Total Volume of Silt Remaining in the
Channels.............=");

                   fprintf(Summ_file_fptr,"%15.2f -> %5.2f %% \n",

                        tot_ch[2],fabs(tot_ch[2]/tot_eroded[2]*100));



                   fprintf(Summ_file_fptr,

                        "Total Volume of Clay Remaining in the
Channels.............=");

                   fprintf(Summ_file_fptr,"%15.2f -> %5.2f %% \n",


                        tot_ch[3],fabs(tot_ch[3]/tot_eroded[3]*100));



                   fprintf(Summ_file_fptr,
```

```
                                    "Total Volume of Eroded Material Remaining in the
Channels..=");

                    fprintf(Summ_file_fptr,"%15.2f -> %5.2f %% \n\n",

                    TotRemChn,fabs(TotRemChn/TotEroded*100));

                    fprintf(Summ_file_fptr,

                                    "Volumes of Eroded Sediment Leaving the
Watershed:\n");

                    fprintf(Summ_file_fptr,

                                    "----------------------------------------------------\n");

                    fprintf(Summ_file_fptr,

                                    "Total Volume of Eroded Sand Leaving the
Watershed..........=");

                    fprintf(Summ_file_fptr,"%15.2f -> %5.2f %% \n",

                    sed_out[1],fabs(sed_out[1]/tot_eroded[1]*100));

                    fprintf(Summ_file_fptr,

                                    "Total Volume of Eroded Silt Leaving the
Watershed..........=");

                    fprintf(Summ_file_fptr,"%15.2f -> %5.2f %% \n",

                    sed_out[2],fabs(sed_out[2]/tot_eroded[2]*100));

                    fprintf(Summ_file_fptr,
```

```
                              "Total Volume of Eroded Clay Leaving the
Watershed..........=");

                    fprintf(Summ_file_fptr,"%15.2f -> %5.2f %% \n",

                    sed_out[3],fabs(sed_out[3]/tot_eroded[3]*100));


                    fprintf(Summ_file_fptr,

                              "Total Volume of Eroded Material Leaving the
Watershed......=");

                    fprintf(Summ_file_fptr,"%15.2f -> %5.2f %% \n\n",

                              TotLeaving,fabs(TotLeaving/TotEroded*100));


                    fprintf(Summ_file_fptr,

                        "Percent Mass Balance......................................=");
                    fprintf(Summ_file_fptr,"%15.2f \n\n", PercentSed);




                    /* ... Minimum and Maximum Values for Various Variables
                                          */



                    fprintf(Summ_file_fptr,

                              "\nSEDIMENT VARIABLES MINIMUM AND
MAXIMUM VALUES\n");

                    fprintf(Summ_file_fptr,


"========================================\n\n");
```

```
fprintf(Summ_file_fptr,

        "Max. Flux Conc. Overland
(m3/s/m3/s)......................=");

        fprintf(Summ_file_fptr,"\t%g \n", amaxFluxCoutOv);


        fprintf(Summ_file_fptr,

        "Max. Flux Conc. Channels
(m3/s/m3/s)......................=");

        fprintf(Summ_file_fptr,"\t%g \n", amaxFluxCoutCh);


        fprintf(Summ_file_fptr,

        "Max. Suspended Sediment in Overland
(mm)..................=");

        fprintf(Summ_file_fptr,"\t%g \n", amaxSusOv*1000/(w*w));


        fprintf(Summ_file_fptr,

        "Max. Suspended Sediment in Channels
(mm)..................=");

        fprintf(Summ_file_fptr,"\t%g \n", amaxSusCh*1000/(w*w));


        fprintf(Summ_file_fptr,

        "Max. Concentration on Overland
(m3/m3)....................=");

        fprintf(Summ_file_fptr,"\t%g \n", amaxSusCov);


        fprintf(Summ_file_fptr,

        "Max. Concentration in Channels
(m3/m3)....................=");
```

```c
fprintf(Summ_file_fptr,"\t%g \n", amaxSusCch);


fprintf(Summ_file_fptr,

        "Total Net Volume (mm) at the End of the Simulation:
\n");


fprintf(Summ_file_fptr,

        "   Minimum vValue ......................................=");
fprintf(Summ_file_fptr,"%15.3f \n", totnetv_stats.min );


fprintf(Summ_file_fptr,

        "   Maximum Value .....................................=");
fprintf(Summ_file_fptr,"%15.3f \n",totnetv_stats.max );


fprintf(Summ_file_fptr,

        "   Mean ............................................=");
fprintf(Summ_file_fptr,"%15.3f \n",totnetv_stats.mean );


fprintf(Summ_file_fptr,

        "   Standard Deviation ..................................=");
fprintf(Summ_file_fptr,"%15.3f \n",totnetv_stats.stdev );


}
```

VITA

Mr Komsoon Somprasong was born on February 16 th, 1984 in Nakornratchasima province, Thailand. He graduated with Bachelor's degree and Master's degree in Georesources Engineering from the Department of Mining and Petroleum Engineering, Faculty of Engineering, Chulalongkorn University in 2006 and 2009 respectively. He was once an executive officer of planning and development of the Democrat Party of Thailand. Thereafter, he has carried out this research as a part of studied for the Doctoral degree in Environmental Management at graduate school, Chulalongkorn University under the management of Center of Excellence on Hazardous Substance Management.